VELAMMAL MEDICAL COLLEGE
HOSPITAL AND RESEARCH INSTITUTE
MADURAI - 625009

Details of papers published in the journals notified on UGC – CARE list in the UGC website 2020

S.N	UGC website/Scopus/ Web of Science/ PubMed	Publication type	Publication title	Author name	Journal name	Year
1.	Scopus	Original article	Effect of Withaferin-A on aging induced behavioral and non-enzymatic antioxidant impairment in Wistar albino rat	Banu, Mohammad Raziya; Ibrahim, Muhammed; Prabu, K.; Rajasankar, Srinivasagam	Drug Invention Today	2020
2.	31982873	Original article	Withaferin-A Protects the Nigral Dopamine Neuron and Recovers Motor Activity in Aged Rats	Raziya Banu M, Ibrahim M, Prabhu K, Rajasankar S.	Cells Tissues Organs	2020
3.	Scopus	Original article	Aromatic spice Nutmeg attenuates memory deficits in Rotenone modelof Parkinson's disease	Muthuvel V K, Prabhu K, Rajasankar S.	International Journal of Research in Pharmaceutical Sciences	2020
4.	Scopus	Original article	Myristicafragrans seeds alleviate motor behavioural changes in rotenone model of parkinsons disease	Muthuvel Kanagasabapathy, Prabhu Kaliyaperumal, Rajasankar Srinivasagam	International Journal of Pharmaceutical Research	2020
5.	Scopus	Original article	MyristicaFragrans seeds extract mitigate non-	Muthuvel Vijayan kanagasabapat	International Journal Of Pharmaceut	2020

Dean
Velammal Medical College Hospital
and Research Institute
'Velammal Village'
Madurai-Tuticorin Ring Road
Anuppanadi, Madurai (TN) 625 009

			motor behavioural deficits and oxidative stress in Rotenone model of Parkinson's disease	hy, Sumana Radhakrishnan, Prabhu K, Rajasankar Srinivasagam	ical Research	
6.	31065956	Original article	Comprehensive treatment algorithm for management of thoracic and lumbar tubercular spondylodiscitis by single stage posterior transforaminal approach	Subbiah M, Shiromi S, Yegumuthu K	Musculoskeletal surgery	2020
7.	32963437	Original article	Impact of Care Bundle Implementation on Incidence of Catheter-associated Urinary Tract Infection: A Comparative Study in the Intensive Care Units of a Tertiary Care Teaching Hospital in South India	Soundaram GV, Sundaramurthy R, Jeyashree K, Ganesan V, Arunagiri R, Charles J	Indian Journal of Critical Care Medicine	2020
8.	32127102	Original article	Financial support to the poor for the detection of smear-negative pulmonary and extra-pulmonary TB in Bangladesh	Munim IMS, Shewade HD, Jeyashree K, Islam S, Rifat IA, Patwary FK, Begum I, Sarkar MK, Mahmud R, Islam MS, Islam MA	The International Journal of Tuberculosis and Lung Disease	2020

Dean
Velammal Medical College Hospital
and Research Institute
'Velammal Village'
Madurai-Tuticorin Ring Road
Anuppanadi, Madurai (TN)-625 009

9.	32549146	Original article	App-based tracking of smartphone use and its association with perceived stress and sense of coherence among undergraduate medical students in Southern India	eyashree K, Sathiavadivu JS, Suliankatchi A	International Journal of Adolescent Medicine and Health	2020
10.	32114470	Original article	Household food insecurity among patients with pulmonary tuberculosis and its associated factors in South India: a cross-sectional analysis	Ayiraveetil R, Sarkar S, Chinnakali P, Jeyashree K, Vijayageetha M, Thekkur P, Lakshminarayanan S, Knudsen S, Hochberg NS, Horsburgh CR, Ellner J, Roy G	BMJ open	2020
11.	SCOPUS, Web of Science	Review article	Advances in spondyloarthritis : Update 2020	Nallasivan S, Ravindran V	Indian Journal of Rheumatology	2020
12.	33681032	Original article	Risk factors for alcohol use relapse after abstinence in patients with alcoholic liver disease	Arun AC, Ilangovan N, Rajma J	Journal of family medicine and primary care	2020
13.	33149525	Original article	Fracture Resistance of Titanium, chrome-cobalt & Gold Alloy as post & core materials:A Comparative Evaluation	Venkataraman KJ, Thanapathi S, Balasubramanian S, Gandhi SA, Sarojinikutty AC	Journal of pharmacy and bioallied sciences	2020
14.	33149524	Original article	Comparative Evaluation Phytic	Gandhi SA, Chandrasekar	Journal of pharmacy	2020

Dean
Velammal Medical College Hospital
and Research Institute
'Velammal Village'
Madurai-Tuticorin Ring Road
Anuppanadi, Madurai (TN)-625 009

			Acid as final rinse solution with other Chelating agents for Elimination of intra radicular smear : A SEM study	P, Nachimuthu J, Abraham CS, Venkataraman KJ	and bioallied sciences	
15.	32681681	Original article	Left bundle branch pacing: A comprehensive review.	Ponnusamy SS, Arora V, Namboodiri N, Kumar V, Kapoor A, Vijayaraman P.	Journal of cardiovascular Electrophysiology.	2020
16.	32089898	Case report	Acute Coronary Syndrome after 17 Years of Bare Metal Stent Implantation: "Very" Very Late Stent Thrombosis	Raghavendra Rao K, S. Reddy, J. R. Kashyap, K. Vikas, Hithesh Reddy, and Vadivelu Ramalingam	Case reports in Cardiology	2020
17.	32817832	Case report	Aborted ST-elevation myocardial infarction – an unusual complication of left bundle branch pacing	Ponnusamy SS, Vijayaraman P	HeartRhythm case reports	2020
18.	32726774	Original article	Comparison of Intravascular Ultrasound Virtual Histology Parameters in Diabetes versus Non-Diabetes with Acute Coronary Syndrome	Reddy S, Kadiyala V, Kashyap JR, Rao R, Reddy H, Kaur J, Kaur N, Ramalingam V	Cardiology	2020
19.	32819522	Original article	Electroanatomical mapping guided low fluoroscopy left	Ponnusamy SS, Bopanna D, Kumar S	JACC. Clinical electrophysiology	2020

Dean
Velammal Medical College Hospital
and Research Institute
'Velammal Village'
Madurai-Tuticorin Ring Road
Anuppanadi, Madurai (TN)-625 009

			bundle branch pacing			
20.	32700416	Original article	Changing atrial activation patterns during narrow complex tachycardia	Vadivelu R, Lokhandwala Y, Bansal R	Journal of cardiovascular electrophysiology	2020
21.	33204621	Original article	Left bundle branch pacing guided by premature ventricular complexes during implant	Ponnusamy SS, Vijayaraman P	HeartRhythm Case Rep	2020
22.	33043274	Original article	Status of Acute Myocardial Infarction in Southern India During COVID-19 Lockdown: A Multicentric Study	Meenakshisundaram R, Senthilkumaran S, Thirumalaikolundusubramanian P, Joy M, Jena NN, Vadivelu R, Ayyasamy S, Chandrasekaran VP	Mayo Clinic proceedings. Innovations, quality & outcomes	2020
23.	32553637	Original article	Acute hemodynamics of cardiac sympathetic denervation	Sinkar K, Bagchi A, Mahajan A, Vadivelu R, Venkatraman M, Motwani R, Vichare S, Joshi S, Parikh D, Vaz J, Lokhandwala Y	Indian pacing and electrophysiology journal	2020
24.	32573790	Case reports	Narrow QRS tachycardia with atrial and ventricular cycle length wobbling: What is the mechanism?	Ponnusamy SS, Ganesan V.	Pacing and clinical electrophysiology	2020
25.	32983593	Case reports	Catheter ablation of Pediatric Atrioventricular	Ponnusamy SS, Muthu G, Anand V.	The Journal of innovations in cardiac	2020

Dean
Velammal Medical College Hospital
and Research Institute
'Velammal Village'
Madurai-Tuticorin Ring Road

			nodal re-entrant tachycardia		rhythm management	
26.	32533686	Original article	Arrhythmia in Children and Adolescents and Outcome of Radiofrequency Ablation for Tachyarrhythmias - A Single Center Experience Over 16 Years	Bera D, Ramalingam V, Rathi C, Sharma R, Bachani N, Lokhandwala Y	Indian pediatrics	2020
27.	33296051	Original article	Association of culprit lesion plaque characteristics with flow restoration post-fibrinolysis in ST-segment elevation myocardial infarction: an intravascular ultrasound-virtual histology study	Rao K R, Reddy S, Kashyap JR, Ramalingam V, Dash D, Kadiyala V, Kumar S, Reddy H, Kaur J, Kumar A, Kaur N, Gupta A	The Egyptian heart journal	2020
28.	31866553	Case reports	Selective left bundle branch pacing for pediatric complete heart block	Ponnusamy SS, Muthu G, Bopanna D	Indian pacing and electrophysiology journal	2020

Dean
Velammal Medical College Hospital
and Research Institute
'Velammal Village'
Madurai-Tuticorin Ring Road
Aruppanadi, Madurai (TN)-625 009

Effect of Withaferin-A on aging induced behavioral and non-enzymatic antioxidant impairment in Wistar albino rat.

- **Source:** Drug Invention Today . Jan2020, Vol. 13 Issue 1, p84-89. 6p.

- **Author(s):** Banu, Mohammad Raziya; Ibrahim, Muhammed; Prabu, K.; Rajasankar, Srinivasagam

- **Abstract:** Aim: The objective of this study is to evaluate the effect of Withaferin-A (WA) on aging mediated changes on behavior, non-enzymatic antioxidant levels, and oxidative stress (OS). Materials and Methods: Animals were divided into Group I - young (3 months), Group II - aged (24 months), Group III - aged rat supplemented with WA (50 mg/kg b.w once in a day for 30 days), and Group IV - young rat supplemented with WA (50 mg/kg b.w). At the end of the 30th day, animals were subjected to behavioral analyses, and the striatum (ST) and substantia nigra (SN) were dissected out and subjected to various analyses. Results: The aged rat demonstrated increased catalepsy and akinesia, reduced motor activity (P < 0.001), markedly increased reactive oxygen species, and reduced non-enzymatic antioxidant levels (P < 0.001), which were significantly reversed after the supplementation of WA. Conclusion: The present data clearly signify the neuroprotective role of WA on ST and SN from aging induced behavioral impairment through repressing the OS.

Cells Tissues Organs

Tissue Engineering – Regenerative Medicine / Research Article

Withaferin-A Protects the Nigral Dopamine Neuron and Recovers Motor Activity in Aged Rats

Raziya Banu M.[a,b] · Ibrahim M.[c] · Prabhu K.[a] · Rajasankar S.[d]

Author affiliations

Keywords: Ageing Dopamine Withaferin-A Striatum Substantia nigra

Cells Tissues Organs 2019;208:59–65

https://doi.org/10.1159/000505183

ABSTRACT GET ARTICLE LOGIN / REGISTER

Abstract

Withaferin-A (WA) was evaluated for its neuroprotective efficacy on the dopamine (DA) neurons of the substantia nigra (SN) and striatum (ST) in aged rats. Wistar albino rats were divided into group I, young (3 months old); group II, aged (24 months old); group III,

aged rats supplemented with WA (50 mg/kg bodyweight once per day for 30 days), and group IV, young rats supplemented with WA (50 mg/kg bodyweight). At the end of the experiment period, the animals were subjected to various motor behavior analyses, and were sacrificed by transcardial perfusion. The brains were dissected out and subjected to various analyses, including histological, histomorphometrical, and immunolocalization of the tyrosine hydroxylase (TH) enzyme. The data of rotarod analysis ($p < 0.001$) showed a significant motor impairment in aged rats (number of falls 10.2 ± 0.86) and reduction in retention time (31.23 ± 2.56 s) compared to young controls (2.41 ± 0.35 and 84.05 ± 5.15 s). The stride length was significantly reduced ($p < 0.001$) in aged rats (4.21 ± 0.57 and 4.38 ± 0.61 cm) when compared to young control rats (6.98 ± 0.25 and 7.13 ± 0.70 cm). The histomorphometric data of the aged animals showed a significant reduction in the neuronal diameter ($p < 0.001$), density ($p < 0.001$), and volume ($p < 0.001$) in the SN of aged rats when compared to young rats. Immunohistology demonstrated a marked reduction in the levels of TH enzyme in both the SN and ST of aged animals when compared to young rats. Both structural and functional impairments were reversed in the aged animals after the supplementation of WA ($p < 0.001$). The present study clearly indicates that WA attenuates the ageing-mediated motor degenerative changes in the SN and ST of aged rats and ascertains its neuroprotective potential.

References

1. Abu Bakar MH, Azmi MN, Shariff KA, Tan JS. Withaferin A protects against high-fat diet-induced obesity via attenuation of oxidative stress, inflammation, and insulin resistance. Appl Biochem Biotechnol. 2019 May;188(1):241–59.
   External Resources
   - Crossref (DOI)
   - Pubmed/Medline (NLM)

2. Amende I, Kale A, Mccue S, Glazier S, Morgan JP, Hampton TG. Gait dynamics in mouse models of Parkinson's disease and Huntington's disease. J Neuroeng Rehabil. 2005;2:20.

3. Bayle N, Patel AS, Crisan D, Guo J, Hutin E. Contribution of step length to increase walking and turning speed as a marker of Parkinson's disease progression. PLoS One. 2016;11(4):e0152469.

4. Canadian Council on Animal Care. Guide to the care and use of experimental animals, vol 1, 2nd ed. Ottawa, CCAC, 1993.

5. Collier TJ, Kanaan NM, Kordower JH. Ageing as a primary risk factor for Parkinson's

ORIGINAL ARTICLE

INTERNATIONAL JOURNAL OF RESEARCH IN PHARMACEUTICAL SCIENCES

Published by JK Welfare & Pharmascope Foundation Journal Home Page: www.pharmascope.org/ijrps

Aromatic spice Nutmeg attenuates memory deficits in Rotenone model of Parkinson's disease

Muthuvel vijayan K[1,2], Prabhu K[3], Rajasankar S[*4]

[1]Department of Anatomy, Government Theni Medical college, Theni, Tamil Nadu, India
[2]Research Scholar, Department of Anatomy, Bharath University, Selaiyur, Chennai, Tamil Nadu, India
[3]Department of Anatomy, Bharath University, Selaiyur , Chennai, Tamil Nadu, India
[4]Department of Anatomy, Velammal Medical College, Madurai, Tamil Nadu, India

Article History:

Received on: 01 Jul 2020
Revised on: 05 Aug 2020
Accepted on: 07 Aug 2020

Keywords:

Anti- cholinesterase,
Memory,
Myristica fragrans seeds extract (MFSE),
Neuroprotection,
Nutmeg,
Parkinson's disease (PD),
Rotenone,
Dopamine (DA)

ABSTRACT

PD is a multifactorial neurodegenerative disorder with features such as tremor, rigidity, bradykinesia, postural instability, and dementia. Neuropathologically, selective loss or death of dopaminergic neurons is the hallmark of PD. In PD, elevated oxidative stress, mitochondrial dysfunction and neuroinflammation were reported. Rotenone (an isoflavone obtained from Fabaceae associated vegetation such as the jicama vine plant) induces oxidative stress, mitochondrial dysfunction, inflammation and apoptosis in cell line and animal models. It was useful in the evaluation of neuroprotective properties on cell line and animal models of PD. Drugs with anti-oxidant potential helped to control the cellular stress, free radical formation, neurotransmitter level in PD animal models. Nutmeg, an aromatic spice exhibited memory enhancing, anti-oxidant, anticonvulsant properties. It is an excellent body detoxifier and stimulator of the brain due to the presence of pharmacologically active compounds such as eugenol, isoelemicin, isoeugenol, methoxyeugenol, myristic acid, myristicin, saponins and lignin. Macelignan (a compound present in nutmeg) having the low molecular weight and hydrophobic nature could pass beyond the blood-brain barrier. In this study, we explored the cognitive profile of rotenone-induced model of PD treated with MFSE extract (MFSE) by behavioural tests (Morris water maze test, T-maze test and Elevated plus maze Test). Rotenone was injected to male Wistar albino rats by intraperitoneal route (2.5mg/kg daily) for 30days. MFSE treated rats showed significant improvement in cognition in rotenone-induced PD model. It might be due to its neuroprotective and anti-cholinesterase properties.

[*]Corresponding Author

Name: Rajasankar S
Phone: +91 04546 263668
Email: srsanatomy@gmail.com

ISSN: 0975-7538

DOI: https://doi.org/10.26452/ijrps.v11i4.3173

Production and Hosted by

Pharmascope.org

INTRODUCTION

PD is a persistent neurodegenerative ailment mainly affecting the locomotory behaviour of the aged population. Symptoms of PD are resting tremor, rigidity, inability to initiate movements, bradykinesia, poor balance in posture and dementia. Neuropathologically, PD is considered with discriminating loss of dopaminergic neurons in the nigrostriatal pathway (SN) and accumulation of insoluble proteins called α-synuclein inside the neurons, developing intra-cytoplasmic structures called as Lewy bodies (Parashar and Udayabanu, 2017). Accumulating proof suggests that elevated oxidative stress,

mitochondrial dysfunction and neuro-inflammation interrelate among, and eventually produce the neuronal death (Schapira and Jenner, 2011). Although the aetiology of PD is not known, it can be either inherited (~10 %) or sporadic (~ 90%) which occurred due to interaction of individual genetic susceptibility with environmental exposure (Sherer *et al.*, 2003). Mitochondrial complex I inhibitor pesticides like rotenone induce discerning destruction of DA neurons and extensively used for experimental PD model (Cicchetti *et al.*, 2009; McDowell and Chesselet, 2012). Rotenone (an isoflavone obtained from Fabaceae associated vegetation such as the Jicama vine plant) (Bové *et al.*, 2005) induces oxidative stress, mitochondrial dysfunction, inflammation and apoptosis in cell line and animal models (Gobi *et al.*, 2018; Dhanalakshmi *et al.*, 2016).

From ancient days, aromatic spices have been included in the food to improve the flavour and taste. They are considered as a valuable, safe and naturally available source of medicine for treating various diseases because of the numerous pharmacologically active constituents. The seeds of the Nutmeg (*Myristica fragrans*) Houtt belonging to Myristicaceae Family are extensively utilised spice due to their typical aroma and taste (Mishra *et al.*, 2018). It is used to flavour the food substances such as baked items, puddings, sweets, sausages, meats, saucers, vegetables and beverages (Panayotopoulos and Chisholm, 1970). It was used in Ayurveda, Unani, Chinese and folklore medicine (Neeraja and Margaret, 2016) to treat gastrointestinal dysfunction, rheumatism, obesity, diarrhoea and sleeping disorders (Vangoori *et al.*, 2018). It exhibited antifungal, spasmolytic, carminative, hepatoprotective, antiviral, anti-carcinogenic and anti-oxidant properties. It is an excellent body detoxifier and stimulator of the brain due to the presence of pharmacologically active compounds such as eugenol, isoelemicin, isoeugenol, methoxyeugenol, myristic acid, myristicin, saponins and lignin (Vangoori *et al.*, 2018).

Jissa *et al.* (2014) indicated that the oral administration of nutmeg attenuated memory deficits and decreased the acetylcholinesterase activity in rats. Nutmeg exhibited anticonvulsant activity against maximum electroshock, pentylenetetrazol and lithium sulphate-pilocarpine nitrate treatment in rats (Sonavane *et al.*, 2002). Recent research revealed that chronic dietary intake of Nutmeg seed enhanced beneficial, productive effect in the rat puppy's brain mitochondria, which is related with an increasing DA receptor (Veronica *et al.*, 2018). Myristica fragrans kernel and seed extract have anti-oxidant, anti-inflammatory, and anti-apoptotic properties against paracetamol and high-fat diet-induced experimental models of hepatotoxicity (Dkhil *et al.*, 2019; Sethi and Dahiya, 2018). In this study, therefore, we studied the cognitive behaviour of rotenone administered PD model with Myristica fragrans seed extract (MFSE).

MATERIALS AND METHODS

Chemicals

Rotenone was procured from Sigma Chemical Company, Bangalore, India.

Animals

Male Albino Wistar rats (225–250 g) were obtained, lodged in Polypropylene cages Central Animal House, Government Theni Medical College, Theni under normal conditions 12 hrs light / dark cycle and 60% humidity, without any restrictions to a standard pellet diet and water ad libitum. Animals were adapted for a week before initiating the experimental protocol. The experimental procedures were permitted by the Animal Ethics Committee of the Institute (Approval no: IAEC/02/2017).

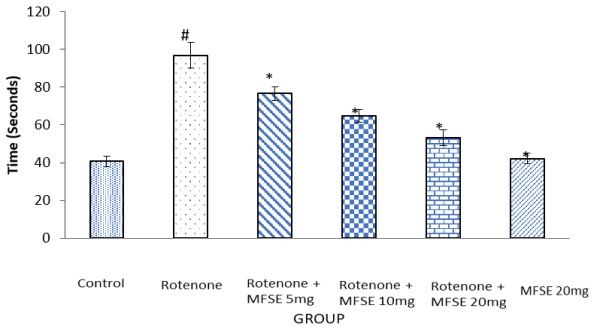

Figure 1: Effect of MFSE on T- maze test of experimental animals

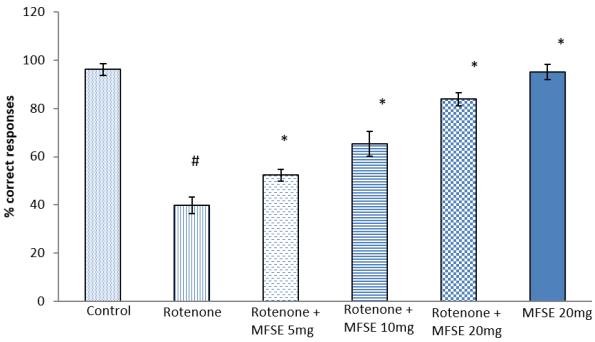

Figure 2: Evaluation of memory by Morris water maze test

Experimental design

In the study, 36 rats were randomly grouped (n = 6): control rats (0.5 ml of sunflower oil i.p. for 30 days),

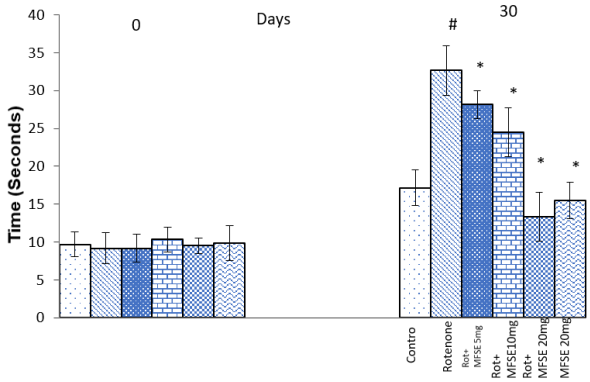

Figure 3: MFSE treated groups displayed gradual decline in TL in EPM test

rotenone only (2.5 mg/kg/day i.p in sunflower oil for 30 days), received rotenone (as group II) (Morais *et al.*, 2012) and a low dose of MFSE(5 mg/kg in saline was treated p.o. after one hour of rotenone treatment and continued up to 30 days) treated, rotenone and intermediate dosage of MFSE (10 mg/kg in saline p.o. for 30 days) treated, rotenone and a high dose of MFSE (20 mg/kg in saline p.o. for 30 days) treated and MFSE (20 mg/kg/day p.o. for 30 days) alone treated. T-maze test, Morris water maze test and Elevated plus Maze Test were performed.

Group I: Control (0.5 ml of sunflower oil i.p. for 30 days)

Group II: Received Rotenone **(**2.5 mg/kg/day i.p in sunflower oil for 30 days)

Group III: As group II + (After 1-hour ROT) MFSE (5mg/kg) p.o. for 30 days

Group IV: Received.as group II + (After 1 hour ROT) MFSE (10mg/kg) p.o. for 30 days

Group V: Received as.group II + (After 1 hour ROT) MFSE (20mg/kg) p.o. for 30 days

Group VI: MFSE (20mg/kg) p.o for 30 days

Preparation of nutmeg extract

MFSE extract was prepared, as mentioned by Ghorbaniana *et al.* (2019).

T-maze test

This test was performed as mentioned (Yang *et al.*, 2017). Shortly, the animals training were conducted in for two consecutive days (23 and 24). T-maze, rewards (food-choco chips Kelloggs) were kept at the end of one arm. Detection of food associates working memory. Each practising session comprised of 9 rounds, each round consists of two parts – forced run, optional run. In the forced run, one of the arms was shut with a sliding door; another arm was kept open with food at its end. After 30 sec, the choice run was allowed; both arms were free, reward (foods) were placed at the ends of two arms. The appropriate response was choosing the newly opened arm, which was shut at the forced run. On day 28, tests were taken, and its observations were noted. The analysis comprised of 3 run trials; animals were subjected to 2 optional runs following 1 forced run. After the trial sessions on 23 and 24^{th} day, animals were given access to food only for 1 hour, i.e., partial restriction to diet. On the experimental (25^{th} day) day, access to food was restricted before the test. After the animals completed their behavioural tests, there is no restriction to food ad libitum.

Morris water maze test

This test was carried out for evaluating the environmental knowledge and memory evaluation. In the test room, within a circular tub (71 inches diam $\times$ 24 inches), rats were permitted to swim to a stage. The tub was employed with tap water ($82\pm20\,^{\circ}$F) to a depth of 16inches. A round stage 4inches in diameter was positioned inferior to 2cm of water level, and water was made opaque by adding white talcum powder. On the 27^{th} day, animals were trained in session having four trials. Beginning positions were set dissimilar in all four trials. The time taken to locate the stage was noted up to a max 2 min. During the experiment, the stage was stationary and kept in position. The duration to board the stage was carefully documented. After 24 h (i.e., 28th day), rats were randomly placed separately over the brim of the pool and tested. Duration for getting into the hidden stage on 28^{th} day was taken into account as retention latency (Su *et al.*, 2010).

Elevated Plus-Maze (EPM) Test

The cognitive skill of the animal was analysed by this EPM method. Concisely, the equipment contained dual closed and double-exposed arms with a dimension of 50x 10x 40cm with an open roof; it was kept high above the ground level (50cm). The duration taken to travel from exposed arm to closed arm was noted as transfer latency (TL). Initially, rats were gently introduced into the open arm, and TL was taken into account. In case, the experimental animal was unable to enter into the closed part within 90 sec, we gently forced the animal to enter into it, and 1.5 min was noted for TL. As soon as the rats enter the closed arm, rats were permitted to discover the maze for 20sec; animals returned to their cages. On day 0 and 30, the TL was documented (Itoh *et al.*, 1991).

RESULTS

Figure 1 shows that treatment with MFSE remarkably ameliorated rotenone intoxicated cognitive dysfunctioning in T-maze.test. Each bar represents results as mean ± SD; n=6/group #P<0.001 compared with normal group and *P<0.001 compared with rotenone group using one-way analysis of variance. In our study, diminished functional memory was characterised in rotenone administered group by drastic declined precise responses, whereas MFSE enhanced the scores of right answers. MFSE improved the working memory by detecting the food within short period of time.

Effect of MFSE on memory evaluation in the Morris water maze test

On comparing with the control group, spatial memory dysfunction was found to be notable in rotenone alone group. From dosage of MFSE 5- 20mg, gradual improvement of spatial memory of rats was exhibited in the MFSE + Rot group (Figure 2). Each bar indicates mean±SD n=6 #P<0.001 compared withnormal group and *P<0.001 compared with rotenone group by one-way analysis of variance. MFSE 20mg group showed a similar behavioural profile of control groups.

MFSE attenuates the cognitive skill in the EPM test

With respect to the control group, TL was remarkably increased in the rotenone intoxicated group. On relating with rotenone intoxicated group, rot + MFSE group exhibited a sharp decline in TL. Each bar shows mean±SD, n=6, #P<0.001 compared with normal group and *P<0.001 compared with rotenone group using one-way analysis of variance (Figure 3).

DISCUSSION

Environmental exposure to pesticide such as rotenone might lead to neurodegenerative disorders like Alzheimer's disease, PD, Huntington's disease, Leber optic neuropathy. Precautions and safety measures must be followed to reduce the risk (Zhang *et al.*, 2006). Chronic administration of rotenone had been proved to produce cognitive and learning deficits (Kaur *et al.*, 2011). Deterioration of cognitive skills was witnessed in PD. It was reported that the cholinergic neurons were associated with CNS activities, including sleep and cognition (Shinomol and Muralidhara, 2011). Cholinesterase inhibitors were recommended for PD patients as they are having significant cholinergic deficits (van Laar *et al.*, 2011).

Intra-peritoneal rotenone injection resulted in cognitive impairment and reduced memory index. The striatum comprises of a population of cholinergic interneurons, and there are indications that cholinergic neurotransmission plays a role in striatal function (Müller and Bohnen, 2013). This could have contributed to the cognitive decline so observed. Drugs with anti-oxidant potential helped to control the cellular stress, free radical formation, neurotransmitter level in PD animal models. Hence, they are extensively preferred as promising anti-neurodegenerative agents. Cholinesterase inhibitors were stated to have a beneficial and therapeutic effect on cognitive disabilities (Kamal *et al.*, 2015).

Several plants derived compounds such as brown rice (Chompoopong *et al.*, 2016), cinnamaldehyde (Mehraein *et al.*, 2018), pepper (Ogunruku *et al.*, 2019) and drugs such as Ceftriaxone (Ruzza *et al.*, 2014; Ho *et al.*, 2014), piracetam (Verma *et al.*, 2015) were proved to be effective in treating dementia in experimental PD. Marine-derived natural products such as omega-3- fatty acid, inosine, etc., were currently under clinical trials against PD (Huang *et al.*, 2019). Moreover, Ho *et al.* (2011) revealed that D- cycloserine was advantageous in the management of biochemical, biological detrimental changes in experimental PD, including cognitive disorders, motor dysfunction.

MFSE were illustrated to enhance the cognitive and intellectual abilities in rats (Jissa *et al.*, 2014). MF extract was capable of reducing acetylcholinesterase activity which is more beneficial in the treatment of Alzheimer's disease (Singh *et al.*, 2020). Nutmeg oil was evidenced to be effective in the management of epilepsy (Ayaz *et al.*, 2017). Macelignan (a compound present in nutmeg) having a low molecular weight and hydrophobic nature could pass beyond the blood-brain barrier (Wu *et al.*, 2016). Allylguaiacol a compound present in numerous spices like cloves, cinnamon, basil, and nutmeg offers neuroprotective effect due to its anti-oxidant property, anti-apoptotic property and control of Transcription factor p65. Allylguaiacol could be fruitful in controlling the memory deficits in Alzheimer's, PD also other ailments (Lim *et al.*, 2018).

In a recent study, it was proved that MFSE was effective in controlling memory deficits in Alzheimer's disease (Singh *et al.*, 2020). This research study indicated that MFSE treated groups exhibited significant improvement in suitable reactions during T- maze test, a substantial reduction in duration to board the hidden stage in the MWM test and TL in the EPM test.

CONCLUSION

This study demonstrates that MFSE was effective against memory deficits in rotenone-induced PD model. It could be as a result of its promising cholinesterase inhibition, anti-oxidant, anti-carcinogenic, anti-epileptic properties. Still, further detailed research is in need to explore the underlying mechanism and compound responsible for it.

ACKNOWLEDGEMENT

Sincere thanks to Dr. Thirunavukarasu (Dean) Government Theni Medical College, Theni for providing infrastructure facilities and Dr. S. Ezhilarasan (Vice-principal) Government Theni College, Theni for his moral support.

Conflict of Interest

The authors declare that they have no conflict of interest for this study.

Ethical clearance

The Experimental Protocols were approved by the Institutional Animal Ethical Committee (Reg. No. 1112/2007/CPCSEA, Proposal No. 02/2017-GTMC).

Source of funding

No funding or grants were received for conducting this research.

REFERENCES

Ayaz, M., Sadiq, A., Junaid, M., Ullah, F., Subhan, F., Ahmed, J. 2017. Neuroprotective and Anti-Aging Potentials of Essential Oils from Aromatic and Medicinal Plants. *Frontiers in Aging Neuroscience*, 9:1–16.

Bové, J., Prou, D., Perier, C., Przedborski, S. 2005. Toxin-induced models of Parkinson's disease. *NeuroRX*, 2(3):484–494.

Chompoopong, S., Jarungjitaree, S., Punbanlaem, T., Rungruang, T., Chongthammakun, S., Kettawan, A., Taechowisan, T. 2016. Neuroprotective Effects of Germinated Brown Rice in Rotenone-Induced Parkinson's-Like Disease Rats. *NeuroMolecular Medicine*, 18(3):334–346.

Cicchetti, F., Drouin-Ouellet, J., Gross, R. E. 2009. Environmental toxins and Parkinson's disease: what have we learned from pesticide-induced animal models? *Trends in Pharmacological Sciences*, 30(9):475–483.

Dhanalakshmi, C., Janakiraman, U., Manivasagam, T., Thenmozhi, A. J., Essa, M. M., Kalandar, A., Khan, M. A. S., Guillemin, G. J. 2016. Vanillin Attenuated Behavioural Impairments, Neurochemical Deficts, Oxidative Stress and Apoptosis Against Rotenone Induced Rat Model of Parkinson's Disease. *Neurochemical Research*, 41(8):1899–1910.

Dkhil, M., Moneim, A. A., Hafez, T., Mubaraki, M., Mohamed, W., Thagfan, F., Al-Quraishy, S. 2019. Myristica fragrans Kernels Prevent Paracetamol-Induced Hepatotoxicity by Inducing Anti-Apoptotic Genes and Nrf2/HO-1 Pathway. *International Journal of Molecular Sciences*, 20(4):1–15.

Ghorbaniana, D., Ghasemi-Kasman, M., Hashemi-ana, M., Gorjia, E., Gola, M., Feizib, F., Kazemib, S. 2019. Myristica Fragrans Houtt Extract Attenuates Neuronal Loss and Glial Activation in Pentylenetetrazol-Induced Kindling Model. *Iranian Journal of Pharmaceutical Research*, 18(2):812–825.

Gobi, V. V., Rajasankar, S., Ramkumar, M., Dhanalakshmi, C., Manivasagam, T., Thenmozhi, A. J., Essa, M. M., Chidambaram, R. 2018. Agaricus blazei extract attenuates rotenone-induced apoptosis through its mitochondrial protective and antioxidant properties in SH-SY5Y neuroblastoma cells. *Nutritional Neuroscience*, 21(2):97–107.

Ho, S.-C., Hsu, C.-C., Pawlak, C. R., Tikhonova, M. A., Lai, T.-J., Amstislavskaya, T. G., Ho, Y.-J. 2014. Effects of ceftriaxone on the behavioral and neuronal changes in an MPTP-induced Parkinson's disease rat model. *Behavioural Brain Research*, 268:177–184.

Ho, Y. J., Ho, S. C., Pawlak, C. R., Yeh, K. Y. 2011. Effects of d-cycloserine on MPTP-induced behavioral and neurological changes: Potential for treatment of Parkinson's disease dementia. *Behavioural Brain Research*, 219(2):280–290.

Huang, C., Zhang, Z., Cui, W. 2019. Marine-Derived Natural Compounds for the Treatment of Parkinson's Disease. *Marine Drugs*, 17(4):1–20.

Itoh, J., Nabeshima, T., Kameyama, T. 1991. Utility of an elevated plus-maze for dissociation of amnesic and behavioral effects of drugs in mice. *European Journal of Pharmacology*, 194(1):71–76.

Jissa, G., Sai-Sailesh, K., Mukkadan, J. 2014. Oral administration of nutmeg on memory boosting and regaining in wistar albino rats. *Bali Medical Journal*, 3(1):3–10.

Kamal, Z., Ullah, F., Ayaz, M., Sadiq, A., Ahmad, S., Zeb, A., Hussain, A., Imran, M. 2015. Anticholinesterse and antioxidant investigations of crude extracts, subsequent fractions, saponins and flavonoids of atriplex laciniata L.: potential effectiveness in Alzheimer's and other neurological disorders. *Bio-*

logical Research, 48(1):1–11.

Kaur, H., Chauhan, S., Sandhir, R. 2011. Protective Effect of Lycopene on Oxidative Stress and Cognitive Decline in Rotenone Induced Model of Parkinson's Disease. *Neurochemical Research*, 36(8):1435–1443.

Lim, H. S., Kim, K. B. Y., Jeong, Y. J., J, S. 2018. Phytochemical allylguaiacol exerts a neuroprotective effect on hippocampal cells and ameliorates scopolamine-induced memory impairment in mice. *Behavioural Brain Research*, 339:261–268.

McDowell, K., Chesselet, M.-F. 2012. Animal models of the non-motor features of Parkinson's disease. *Neurobiology of Disease*, 46(3):597–606.

Mehraein, F., Zamani, M., Negahdar, F., Shojaee, A. 2018. Cinnamaldehyde attenuates dopaminergic neuronal loss in substantia nigra and induces midbrain catalase activity in a mouse model of Parkinson's disease. *Journal of Basic and Clinical pathophysiology*, 6(1):9–16.

Mishra, A., Rahman, S. Z., Khan, R. A., Bangladesh 2018. CNS Activity of Myristica fragrans Houtt. - An Experimental Study. *Bangladesh Journal of Medical Science*, 17:98–106.

Morais, L. H., Lima, M. M., Martynhak, B. J., Santiago, R., Takahashi, T. T., Ariza, D., Barbiero, J. K., Andreatini, R., Vital, M. A. 2012. Characterization of motor, depressive-like and neurochemical alterations induced by a short-term rotenone administration. *Pharmacological Reports*, 64(5):1081–1090.

Müller, M. L. T. M., Bohnen, N. I. 2013. Cholinergic Dysfunction in Parkinson's Disease. *Current Neurology and Neuroscience Reports*, 13(9):1–9.

Neeraja, P. V., Margaret, E. 2016. Therapeutic properties of Jatipal - Myristica Fragrance. *Houtt. International journal of pharmaceutical, chemical and biological sciences ijpcbs*, 6(4):385–394.

Ogunruku, O., Ogunyemi, B. O., Pepper 2019. Annuum linn) extract ameliorates alterations to neuronal cholinergic and purinergic enzyme activities in rotenone-intoxicated rat model of parkinson's disease. *Ife Journal of Science*, 21(1):249–259.

Panayotopoulos, D. J., Chisholm, D. D. 1970. Hallucenogenic effect of Nutmeg. Brithish medical. *J*, 1(5698):754–760.

Parashar, A., Udayabanu, M. 2017. Gut microbiota: Implications in Parkinson's disease. *Parkinsonism & Related Disorders*, 38:1–7.

Ruzza, P., Siligardi, G., Hussain, R., Marchiani, A., Islami, M., Bubacco, L., Delogu, G., *et al.* 2014. Ceftriaxone blocks the polymerization of α-synuclein and exerts neuroprotective effects in vitro. *ACS Chem. Neurosci.*, 5(1):30–38.

Schapira, A. H., Jenner, P. 2011. Etiology and pathogenesis of Parkinson's disease. *Movement Disorders*, 26(6):1049–1055.

Sethi, J., Dahiya, K. 2018. Myristica Fragrans (MF): Potential Role as an Antioxidant and AntiInflammatory Agent. *J Nat Ayurvedic Med*, 2(2):1–5.

Sherer, T. B., Betarbet, R., Testa, C. M., Seo, B. B., Richardson, J. R., Kim, J. H., Miller, G. W., Yagi, T., Matsuno-Yagi, A., Greenamyre, J. T. 2003. Mechanism of Toxicity in Rotenone Models of Parkinson's Disease. *The Journal of Neuroscience*, 23(34):10756–10764.

Shinomol, G. K., Muralidhara 2011. Bacopa monnieri modulates endogenous cytoplasmic and mitochondrial oxidative markers in prepubertal mice brain. *Phytomedicine*, 18(4):317–326.

Singh, A., Agarwal, S., Singh, S. 2020. Age related neurodegenerative Alzheimer's disease: Usage of traditional herbs in therapeutics. *Neuroscience Letters*, 717. Article Number - 134679.

Sonavane, G. S., C, P. R., Kasture, K. V. S., B, S. 2002. Anticonvulsant And Behavioural Actions Of Myristica Fragrans Seeds. *Indian Journal of Pharmacology*, 34(5):332–338.

Su, J., Sripanidkulchai, K., Wyss, J. M., Sripanidkulchai, B. 2010. Curcuma comosa improves learning and memory function on ovariectomized rats in a long-term Morris water maze test. *Journal of Ethnopharmacology*, 130(1):70–75.

van Laar, T., Deyn, P. P. D., Aarsland, D., Barone, P., Galvin, J. E. 2011. Effects of Cholinesterase Inhibitors in Parkinson's Disease Dementia: A Review of Clinical Data. *CNS Neuroscience & Therapeutics*, 17(5):428–441.

Vangoori, Y., Dakshinamoorthi, A., Rao, R. P., David, D. C., Babu, K. A. 2018. Effect of Myristica fragrans Extract on Food Intake and Body Weight in Experimental Models. *JOURNAL OF CLINICAL AND DIAGNOSTIC RESEARCH*, 12(2):1–5.

Verma, D., Joshi, N., Raju, K. S., Wahajuddin, M., Singhrm, S. 2015. Metabolic enhancer piracetam attenuates rotenone induced oxidative stress: a study in different rat brain regions. *Acta Neurobiol Exp*, 75(4):399–411.

Veronica, F., Lubis, L., S, A., Fitri, L. L., Rizal, A., P, A., Gunawan, H., Lesmana, R., Dandan, K. L., Supratman, U. 2018. A preliminary study of the effect of PPAR- γ agonist from Myristica fragrans houtt seed extract on the biogenesis of rat infant's brain mitochondria and D1 dopamine receptor. *Bali*

Medical Journal, 7(3):574–577.

Wu, N., Xu, W., Cao, G. Y., Yang, Y. F., Yang, X. B., Yang, X. W. 2016. The Blood-Brain Barrier Permeability of Lignans and Malabar icones from the Seeds of Myristica fragrans in the MDCK-pHaMDR Cell Monolayer Model. *Molecules*, 21(2):1–10.

Yang, J. S., Wu, X., Hg, Y., Teng, L. 2017. Tangeretin inhibits neurodegeneration and attenuates inflammatory responses and behavioural deficits in 1-methyl-4-phenyl-1,2,3,6-tetrahydropyridine (MPTP)-induced Parkinson's disease dementia in rats. *Inflammopharmacol*, 25(4):471–484.

Zhang, X., Jones, D., Gonzalez-Lima, F. 2006. Neurodegeneration Produced by Rotenone in the Mouse Retina: A Potential Model to Investigate Environmental Pesticide Contributions to Neurodegenerative Diseases. *Journal of Toxicology and Environmental Health, Part A*, 69(18):1681–1697.

Five Years Citation in Google scholar (2016 - 2020) is. 1451 * *IJPR IS INDEXED IN ELSEVIER EMBASE & EBSCO* *

INTERNATIONAL JOURNAL OF PHARMACEUTICAL RESEARCH

A Step Towards Excellence

Published by : Advanced Scientific Research

ISSN 0975-2366

Article Detail

Myristica Fragrans seeds alleviate motor behavioural changes in rotenone model of parkinsons disease

Author: MUTHUVEL KANAGASABAPATHY, PRABHU KALIYAPERUMAL, RAJASANKAR SRINIVASAGAM

Abstract: Parkinson's disease (PD) the second most common and progressive neurodegenerative disorder affecting the old aged people. PD caused due to the depletion of population of dopaminergic (DA) neurons in niagro striatal system of brain. Natural and synthetic substances such as 6-hydroxydopamine, Rotenone , 1-methyl-4-phenyl-1,2,3,6-tetrahydropyridine, Paraquat , LPS and cycad were ascertained to be neurotoxic, crossed the blood brain barrier and caused deleterious effects over Dopaminergic neurons. Rotenone (plant derived pesticide) inhibitor of complex I in mitochondrial electron transport chain causes dopaminergic neuron cell death. In the current study, we investigated the effect of MFSE against rotenone induced PD model in rats by behavioural parameters (open field test, narrow beam walking test, hanging test). Rats were administered rotenone by intra-peritoneal route (2.5mg/kg daily) 30days. MFSE treated rats alleviated rotenone induced motor behavioural impairments significantly. It might be due to its positive interaction between dopaminergic neurons mediated through its anti- inflammatory, anti-oxidant, anti- epileptic properties.

Keyword: Parkinsons Disease (PD), Nutmeg, Myristica fragrans , Rotenone (Rot)

DOI: https://doi.org/10.31838/ijpr/2020.12.03.176

Download: Request For Article

Five Years Citation in Google scholar (2016 - 2020) is. 1451 * *IJPR IS INDEXED IN ELSEVIER EMBASE & EBSCO* *

INTERNATIONAL JOURNAL OF PHARMACEUTICAL RESEARCH

A Step Towards Excellence

Published by : Advanced Scientific Research

ISSN 0975-2366

Article Detail

Myristica Fragrans seeds extract mitigate non-motor behavioural deficits and oxidative stress in Rotenone model of Parkinson's disease

Author: MUTHUVEL VIJAYAN KANAGASABAPATHY, SUMANA RADHAKRISHNAN, PRABHU K, RAJASANKAR SRINIVASAGAM

Abstract: Parkinson's disease (PD) is a multi-layered neurodegenerative ailment with cumulative loss of dopaminergic neurons over the limbic areas and nigro-striatal pathways. PD mainly affects the motor behavior of old aged population. Oxidative stress, mitochondrial dysfunction, accumulation of a- synuclein and neuro inflammation was the probable mechanism behind PD pathogenesis. In spite of various understandings, till now effective treatment is unfilled. In PD, both motor signs (tremor, rigidity, akinesia & postural imbalance) and non-motor (NM) symptoms (depression, anhedonia, autonomic dysfunction) were observed . NM deficits mainly affect the quality of life of PD patients. Rotenone and MPTP are the most widely used lipophilic neurotoxins (cross the blood brain barrier) for evaluating the neuro-protective potential of various compounds and drugs against PD. Nutmeg, an aromatic spice possess various pharmacological properties such as anti-diabetic, anti-epileptic, memory enhancer , aphrosidiac, anti-cancer. Rotenone was injected to male Wistar albino rats by intra-peritoneal route (2.5mg/kg daily) for 30days. In our previous study, we indicated that MFSE extract ameliorated motor, memory deficits in rotenone induced PD model. Current study focuses on Myristica fragrans seed (MFSE) extract against rotenone induced non-motor behavioural deficits and biochemical parameters. In PD NM models, forced swim test (FST) and sucrose intake test (SIT) were conducted to access the depressive behaviour, anhedonia. Oxidative stress were studied by biochemical parameters (lipid peroxidase TBARS, catalase, superoxide dismutase and glutathione peroxidase). MFSE extract (oral) treated groups displayed steady increase in climbing behaviour, low immobility time in FST and elevated percentage of sucrose intake in SIT. It might be due to its neuro-protective, anti-depressant properties.

Keyword: Nutmeg, Myristica fragrans , Rotenone, Parkinson's disease, Neuroprotection, Anti-depressant

DOI: https://doi.org/10.31838/ijpr/2021.13.01.152

Download: Request For Article

MUSCULOSKELETAL SURGERY
https://doi.org/10.1007/s12306-019-00606-1

ORIGINAL ARTICLE

Comprehensive treatment algorithm for management of thoracic and lumbar tubercular spondylodiscitis by single-stage posterior transforaminal approach

M. Subbiah[1] · **S. Shiromi**[1] · **K. Yegumuthu**[2]

Received: 25 February 2019 / Accepted: 30 April 2019

Abstract

Background Surgery in tubercular spondylodiscitis involves radical debridement and fusion by combined anterior and posterior or all posterior approaches with a posterolateral window with its associated morbidities. This study evaluates the outcome of a comprehensive treatment algorithm for thoracic and lumbar tubercular spondylodiscitis by a single-stage posterior transforaminal approach.

Methods One hundred and twenty-six patients with tubercular spondylodiscitis between T1 and S1 who underwent posterior surgery with/without fusion by transforaminal approach with a minimum follow-up of 2 years were analyzed. Radiological outcome was assessed by documenting healing with magnetic resonance imaging/computed tomography and radiographical fusion, while clinical outcome was assessed by visual analog score (VAS) for pain and Frankel grading for neurological recovery.

Results Of the 114 patients available for follow-up with a mean age of 53 years, complete radiological healing was observed in all patients (100%) with radiographical fusion in 97.4% and neurology recovered to Frankel E in all 37 patients with deficit. The preoperative VAS score of 9.2 improved significantly to 1.7 postoperatively, and all patients returned to their preoperative occupational activities at the final follow-up.

Conclusion This comprehensive treatment algorithm of single-stage posterior surgery by transforaminal approach in thoracic and lumbar tubercular spondylodiscitis provided good clinical and radiological outcomes. It aids in achieving the same surgical goals, obviating the need for extensive posterior or combined surgical approaches.

Keywords Spondylodiscitis · Tuberculosis · Single-stage posterior approach · Transforaminal approach

Introduction

Surgery is indicated in selected cases of spinal tuberculosis (TB) with deformity, instability and neurological deficit. Although complete extirpation of lesion by radical debridement is the gold standard, it creates a large anterior defect necessitating technically demanding reconstructive procedures that increase the morbidity including neurological deficit. In contrast, less aggressive debridement creates smaller defects that can be reconstructed by familiar transforaminal interbody fusion techniques while chemotherapy heals the remaining disease as osseous maturation of caseous material is a well-known entity in TB [1, 2].

We propose a comprehensive treatment algorithm (Fig. 1) of single-stage posterior surgery in the management of tubercular spondylodiscitis between T1 and S1 by transforaminal approach and evaluate its clinical and radiological outcome.

✉ M. Subbiah
subbuorth@yahoo.co.in

[1] Department of Orthopaedics and Spine Surgery, Velammal Medical College Hospital and Research Institute, Velammal Village, Airport-Mattuthavani Ring Road, Chinna Anuppanadi, Madurai, Tamil Nadu 625009, India

[2] Department of Pathology, Velammal Medical College Hospital and Research Institute, Velammal Village, Airport-Mattuthavani Ring Road, Chinna Anuppanadi, Madurai, Tamil Nadu 625009, India

Published online: 07 May 2019

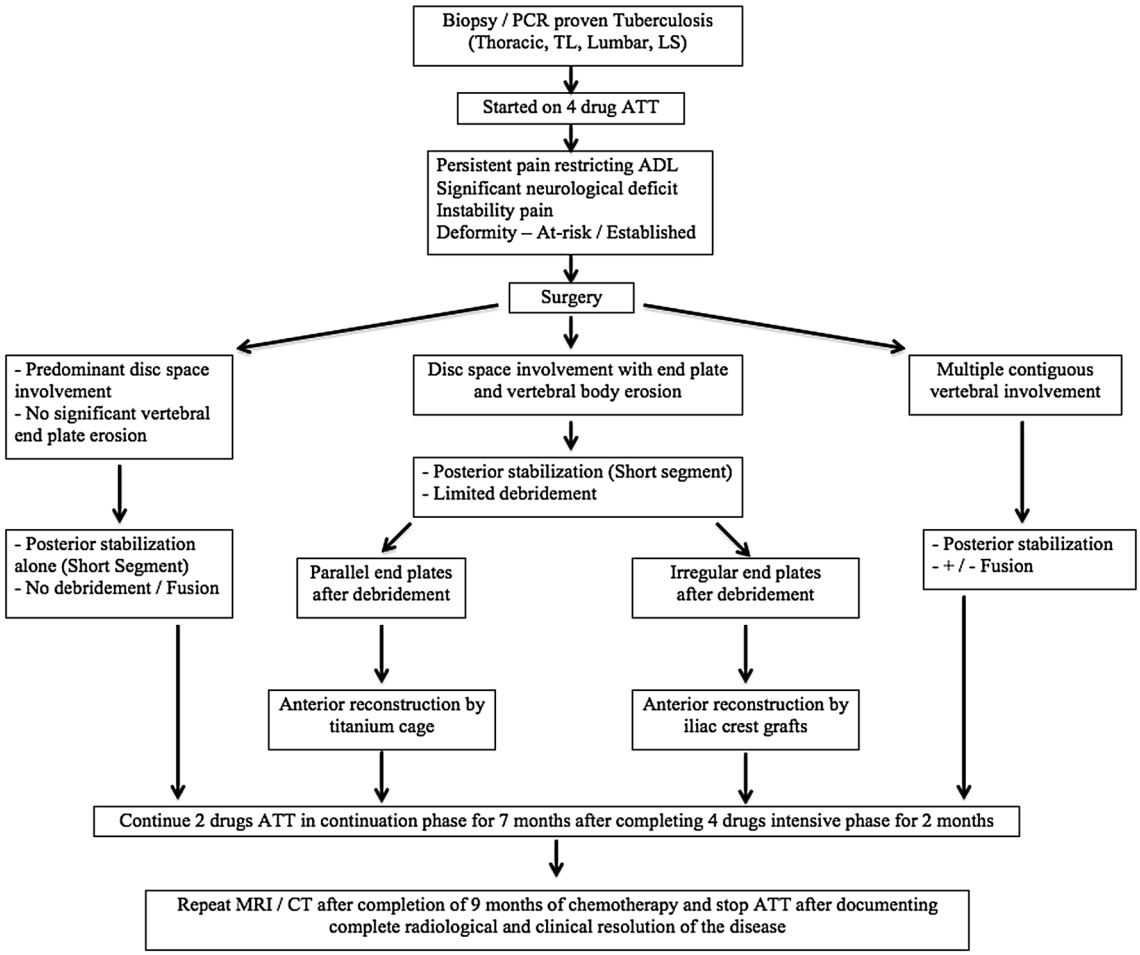

Fig. 1 Our surgical algorithm of management of thoracic, thoracolumbar, lumbar and lumbosacral tuberculosis. PCR, polymerase chain reaction; TL, thoracolumbar; LS, lumbosacral; ATT, antitubercular treatment; ADL, activities of daily living; MRI, magnetic resonance imaging; CT, computed tomography

Materials and methods

One hundred and twenty-six patients with biopsy proven TB between T1 and S1 who underwent surgery between June 2012 and January 2017 were included in the study. Ninety-four of them were males, and the remaining 32 were females. The mean age was 53 years (range 14–76 years). A detailed history with clinical examination was performed in all patients, and neurological deficit was classified according to Frankel grading system. Digital radiographs and magnetic resonance imaging (MRI) including whole spine were obtained to identify skip lesions. Computed tomography (CT)-guided biopsy was performed in all patients, and the sample was sent for histopathological examination (Fig. 2); TB polymerase chain reaction (PCR) was also analyzed for multidrug resistance. Cases with histopathological evidence of chronic granulomatous inflammation with Langhans giant cells and/or TB detected by PCR without multidrug resistance (MDR) were included in the study, and those with negative PCR and HPE were excluded. All patients were started on four-drug antitubercular treatment (ATT) in the intensive phase for 2 months. Patients with severe pain restricting their daily activities in spite of ATT for 3 weeks irrespective of the extent of bony involvement in radiographs, significant neurological deficit, pain due to clinical or mechanical instability and spinal deformity at presentation or those who will progress to deformity if left to heal conservatively underwent surgery.

Patients with predominant involvement of disk without significant radiographic bony endplate erosion of adjacent vertebrae underwent posterior stabilization alone (Fig. 3). Neither fusion nor debridement was attempted in these cases, as the aim was only to alleviate pain due to microinstability. One normal vertebra above and below the lesion was instrumented in thoracic spine while it was restricted only to involved segments in lumbar spine, provided the

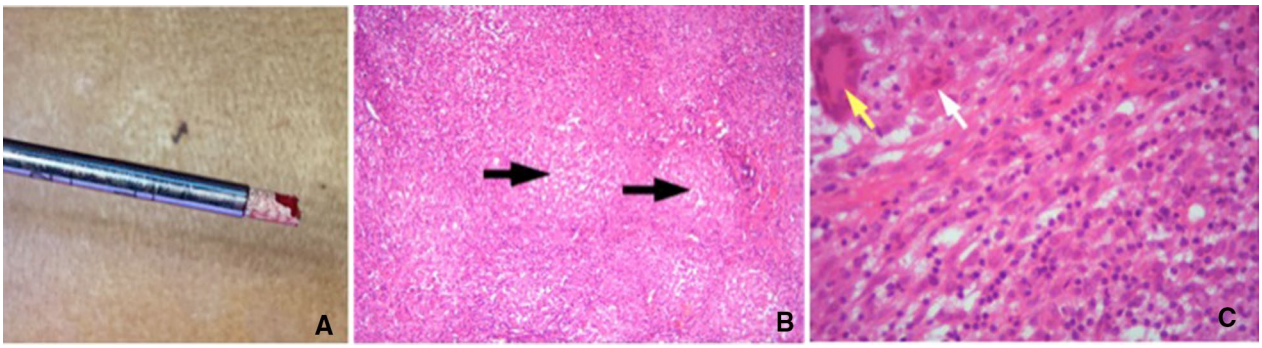

Fig. 2 Biopsy specimen obtained under CT guidance with Jamshidi needle (**a**) showing multiple well-formed granulomas (**b**—black arrows) under low-power field *H* and *E*×40*x*. White arrow (**c**) shows epithelioid cells, and yellow arrow (**c**) demonstrates Langhans-type giant cells in high-power field, *H* and *E*×40*x*

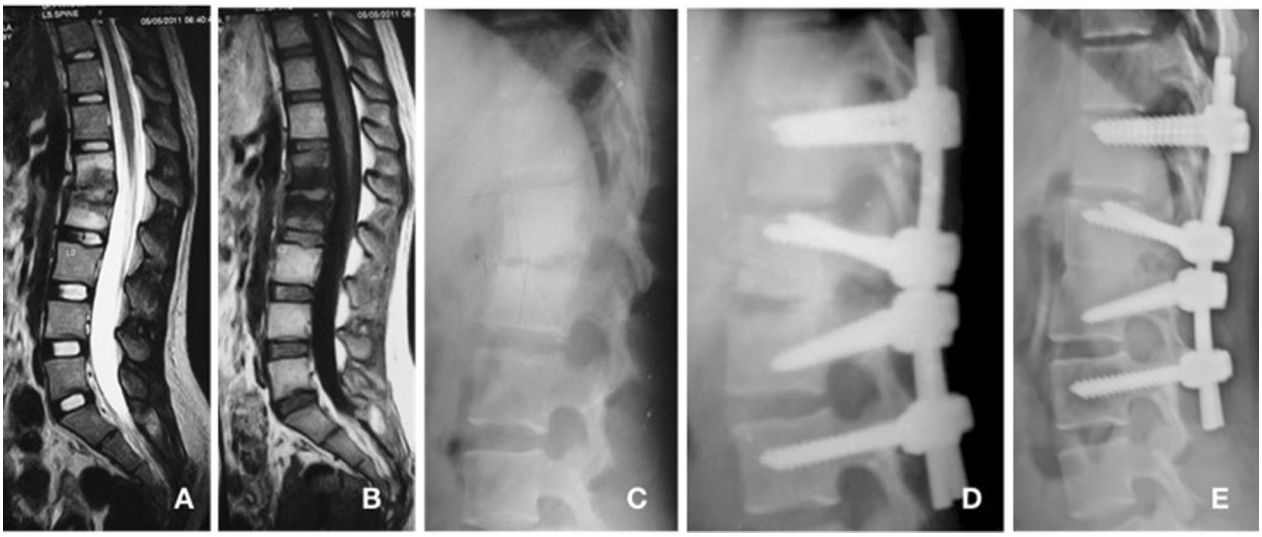

Fig. 3 T2-weighted MRI (**a**) showing spondylodiscitis of L1–L2 vertebra with involvement of intervening disk and T1-weighted MRI (**b**) showing bone marrow edema of the involved vertebral bodies. Plain lateral radiograph (**c**) shows collapse of L1–L2 disk space with minimal end plate erosions and minimal localized kyphosis. Postoperative lateral radiograph (**d**) showing posterior instrumentation with correction of local kyphosis without debridement or fusion and follow-up radiograph at 2 years (**e**) showing complete interbody fusion of L1–L2 without local kyphosis

bony purchase of screw was adequate. When the hold of pedicle screw was questionable, extension above/below was performed. Patients with radiological vertebral body erosions underwent limited debridement without aggressive curettage to minimize the anterior defect which was reconstructed and fused using a cage if the endplates were parallel (Fig. 4) or bone grafts if they were irregular after debridement (Fig. 5). Transforaminal lumbar interbody fusion (TLIF) was used for lumbar spondylodiscitis (Fig. 6), and the same transforaminal approach was also utilized for thoracic levels, obviating the need for rib resection and its associated pulmonary complications (Fig. 7). Patients with multiple contiguous involvement of adjacent vertebrae (Fig. 8) underwent posterior stabilization alone with/without debridement and fusion, depending on the extent of lesion. Instrumentation relieved pain in these cases in addition to preventing deformity.

All patients were made to sit from the first postoperative day (POD) and mobilized from second POD, if their neurology was normal. Periodic follow-up was done at 1, 2, 3, 6 and 9 months after surgery. Four-drug regimen in intensive phase was given for 2 months, and two drugs in continuation phase for 7 months, following which a repeat CT/MRI was done to assess healing. ATT was stopped after radiological and clinical documentation of healing. Further follow-up was done at 1, 1½ and 2 years after surgery. Radiological healing was confirmed by documenting fusion on radiographs, complete resolution of bony edema and abscess in

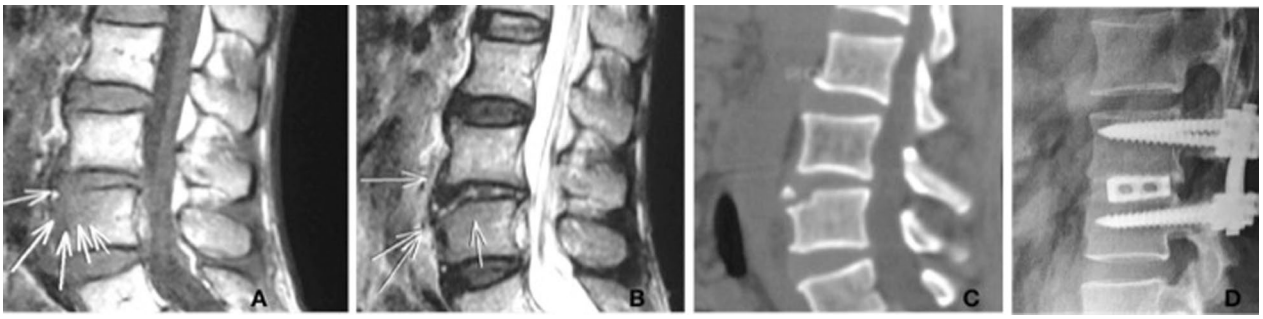

Fig. 4 T1W (**a**) and T2W (**b**) MRI images of L2–L3 tuberculosis demonstrating destruction of disk space, abscess formation with adjacent bone marrow edema and CT scan (**c**) showing destruction of inferior end plate. Final follow-up lateral radiograph (**d**) demonstrating complete interbody fusion following anterior reconstruction with interbody cage between the parallel end plates of L2 and L3 vertebrae

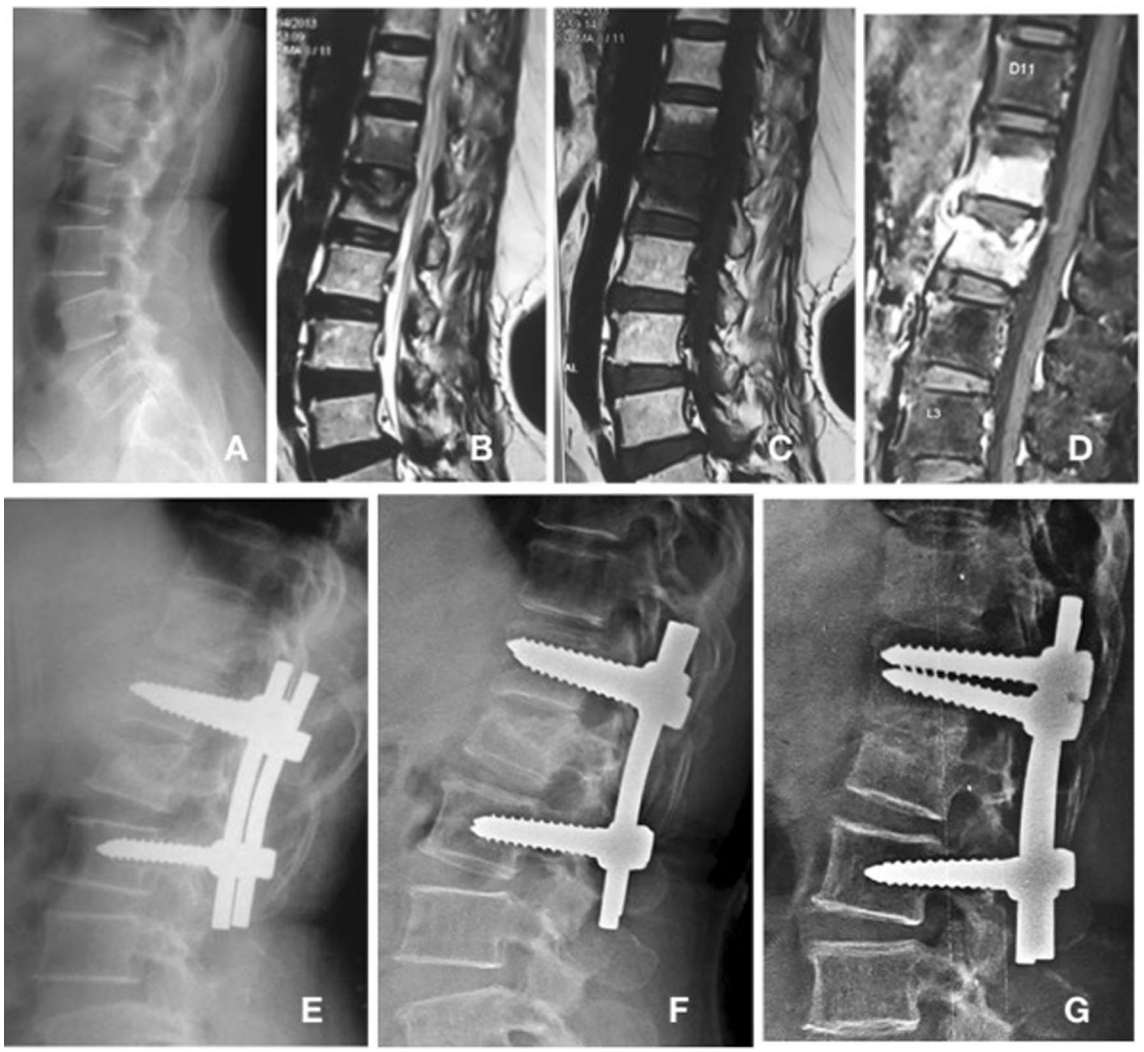

Fig. 5 Plain lateral radiograph (**a**) showing irregular destruction of upper end plate of L1 vertebra and T2W (**b**), T1W (**c**) and contrast MRI (**d**) demonstrating spondylodiscitis of T12–L1 with destruction of upper 1/3 of L1 vertebral body. Immediate postoperative lateral radiograph (**e**) showing short-segment posterior stabilization, debridement and fusion with iliac crest grafts between the irregular end plates. 6-month follow-up radiograph showing progression of fusion and final follow-up radiograph after 2 years showing complete T12–L1 fusion with minimal local kyphosis of 6°

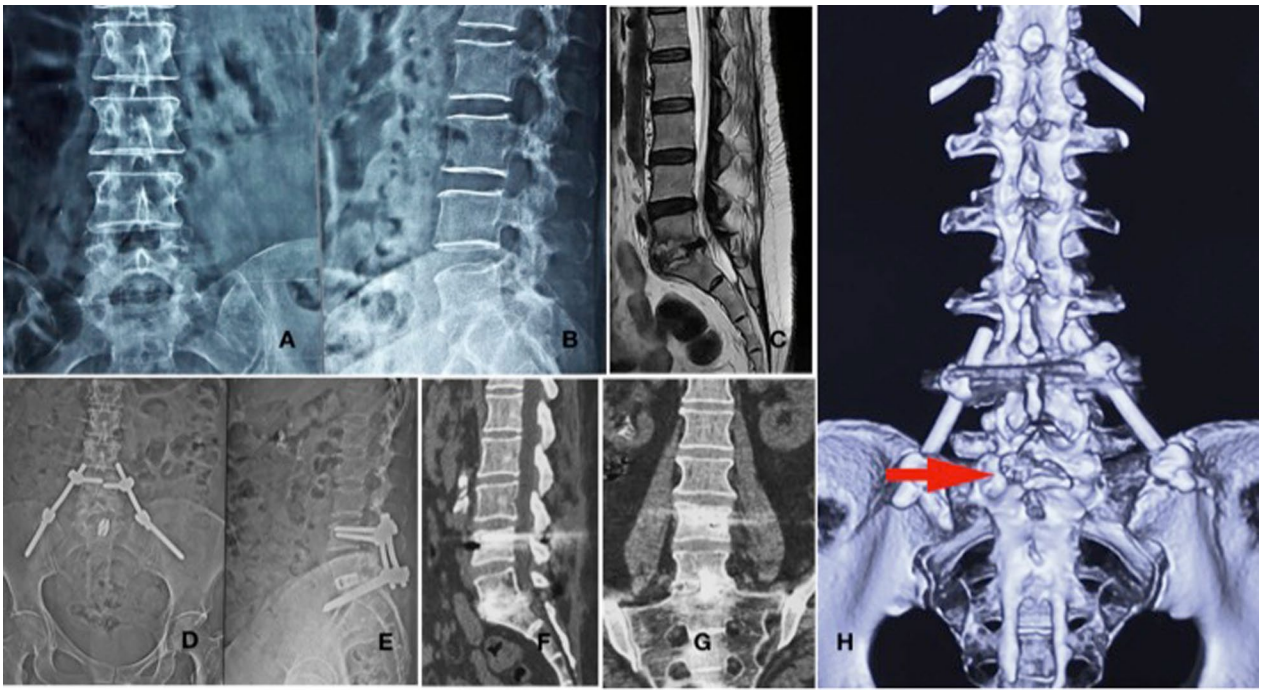

Fig. 6 Plain AP radiograph of lumbosacral spine (**a**) showing destruction of left S1 pedicle and lateral radiograph (**b**) showing collapsed L5–S1 disk space with bony end plate erosion. T2W MRI (**c**) showing L5–S1 spondylodiscitis and postoperative AP (**d**) and lateral radiograph (**e**) following short-segment stabilization with iliac screws and interbody fusion with titanium cage at L5–S1. 2 years follow-up coronal (**f**) and sagittal CT scan (**g**) showing complete interbody fusion between L5 and S1 and 3D reconstruction CT (**h**) image showing the unilateral limited transforaminal approach through which debridement and fusion was done

MRI/CT, while clinical resolution was assessed by VAS for pain and recovery of neurological deficit if any.

Results

Of 126 patients, 12 were lost for follow-up and the results were based on the analysis of remaining 114 patients. Eighty-seven patients were males, and the remaining 27 were females with a mean age of 53 years (range 14–76 years). Lumbar spine was involved in 26 cases, while thoracic spine was involved in 28, thoracolumbar spine in 41, lumbosacral spine in 12 and multiple vertebral involvement in seven patients. All patients had severe pain and were unable to perform their activities of daily living with a mean preoperative VAS score of 9.2. Neurological deficit was observed in 37 patients with six cases showing Frankel A, nine with Frankel B, 13 with Frankel C, nine with Frankel D and the remaining 77 were Frankel E with normal neurology.

Thirty-one patients underwent posterior stabilization alone, while debridement and fusion were performed in 83 patients, among which cage was used in 62 and grafts in 21 patients. All patients with neurological deficit improved significantly to Frankel E, while two of six patients with Frankel A neurology had minimal spasticity but were able to walk independently without aid. Complete interbody fusion was observed in 111 [97.4%] patients, while fusion was not visualized in three of seven cases with multiple vertebral involvements, in which only posterior stabilization was done. However, follow-up MRI in those cases revealed complete resolution of edema and abscess without any evidence of active disease. MRI/CT documented complete healing in all patients, following which ATT was discontinued. The mean operative duration was 80 min (range 45–105 min), and mean intraoperative blood loss was 200 ml (75–450 ml).

Superficial wound infection occurred in four patients, which responded well to conservative management with regular dressings and culture sensitive antibiotics. None of them had implant loosening/breakage, nor any had significant kyphotic deformity, necessitating further corrective procedures. The mean VAS score improved from a preoperative score of 9.2–1.7 postoperatively, and all patients were able to return to their routine preoperative occupational activities during their final follow-up of 2 years.

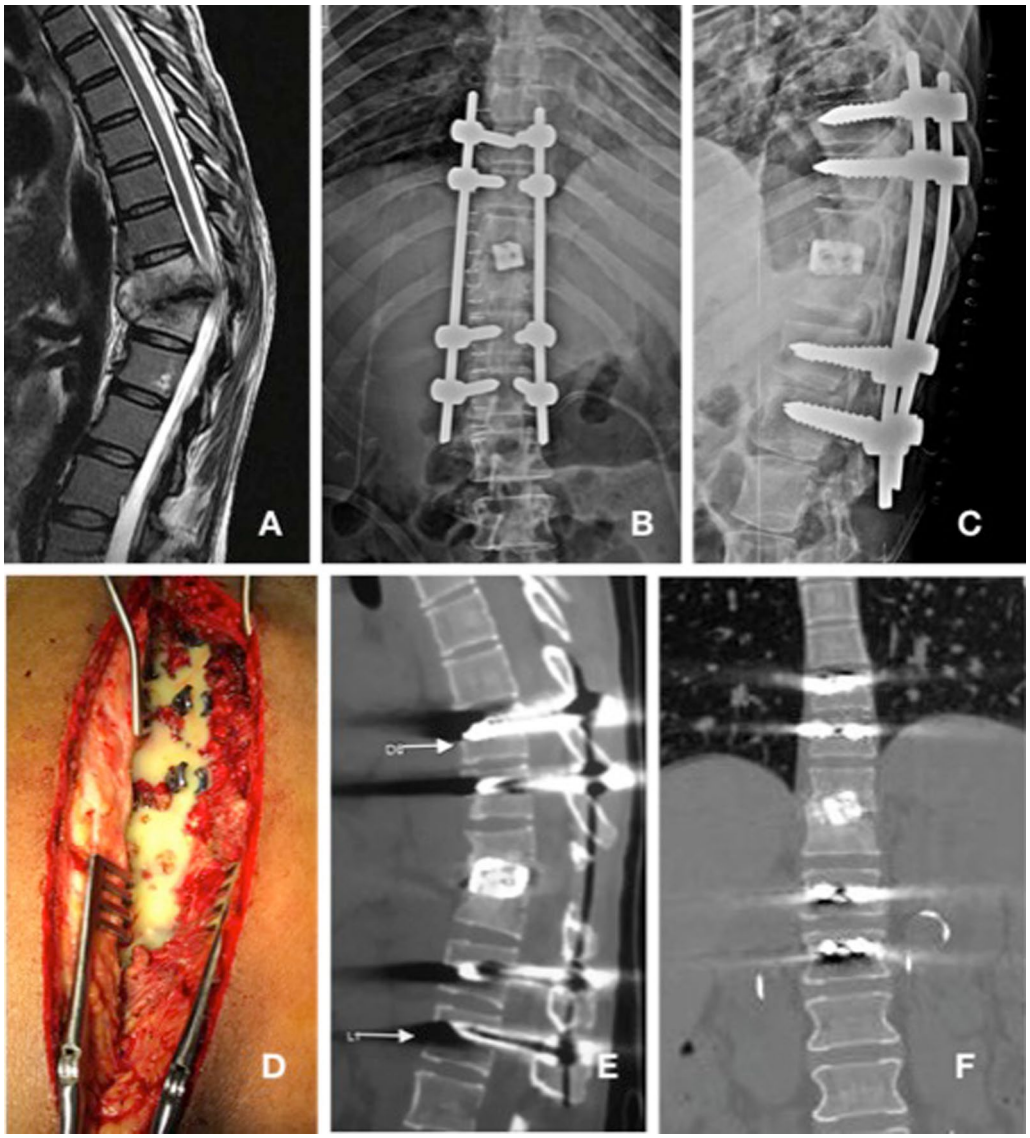

Fig. 7 Sagittal T2W MRI (**a**) showing destruction of T10–T11 vertebrae with intervening disk and kyphosis with paravertebral and epidural abscess compressing the spinal cord. Immediate postoperative AP (**b**) and lateral radiograph (**c**) after posterior stabilization and fusion with interbody cage following limited debridement between the retained portion of T10 and T11 vertebrae. **d** the intraoperative picture (**d**) depicting abscess draining through the same transforaminal route of debridement. Sagittal (**e**) and coronal CT (**f**) images at 2 years follow-up showing complete interbody fusion at the diseased level

Discussion

Spinal TB is predominantly a medical disease with antitubercular chemotherapy being the primary treatment modality [3, 4]. However, surgery is indicated for progressive deformity, mechanical instability and neurological deficit [5] with principles of radical debridement, decompression and deformity correction. The results of medical research council of UK comparing surgical and conservative management showed no significant difference in long-term outcome except for the fact that radical surgery was associated with lesser incidence of kyphotic deformity [6], while early surgical intervention prevents deformity and instability [7–10].

Surgery alone is insufficient without effective chemotherapy [3, 4], and it was even suggested that chemotherapy should be started at the earliest even when clinical and radiological features suggest TB [11]. The World Health Organization recommends 6 months chemotherapy for spinal TB but can be extended to 9 months if there is risk of disability, mortality and difficulty in assessing treatment response [11]. Spontaneous osseous maturation of caseated material following chemotherapy resulting in bony ankylosis is a notable entity even in conservatively

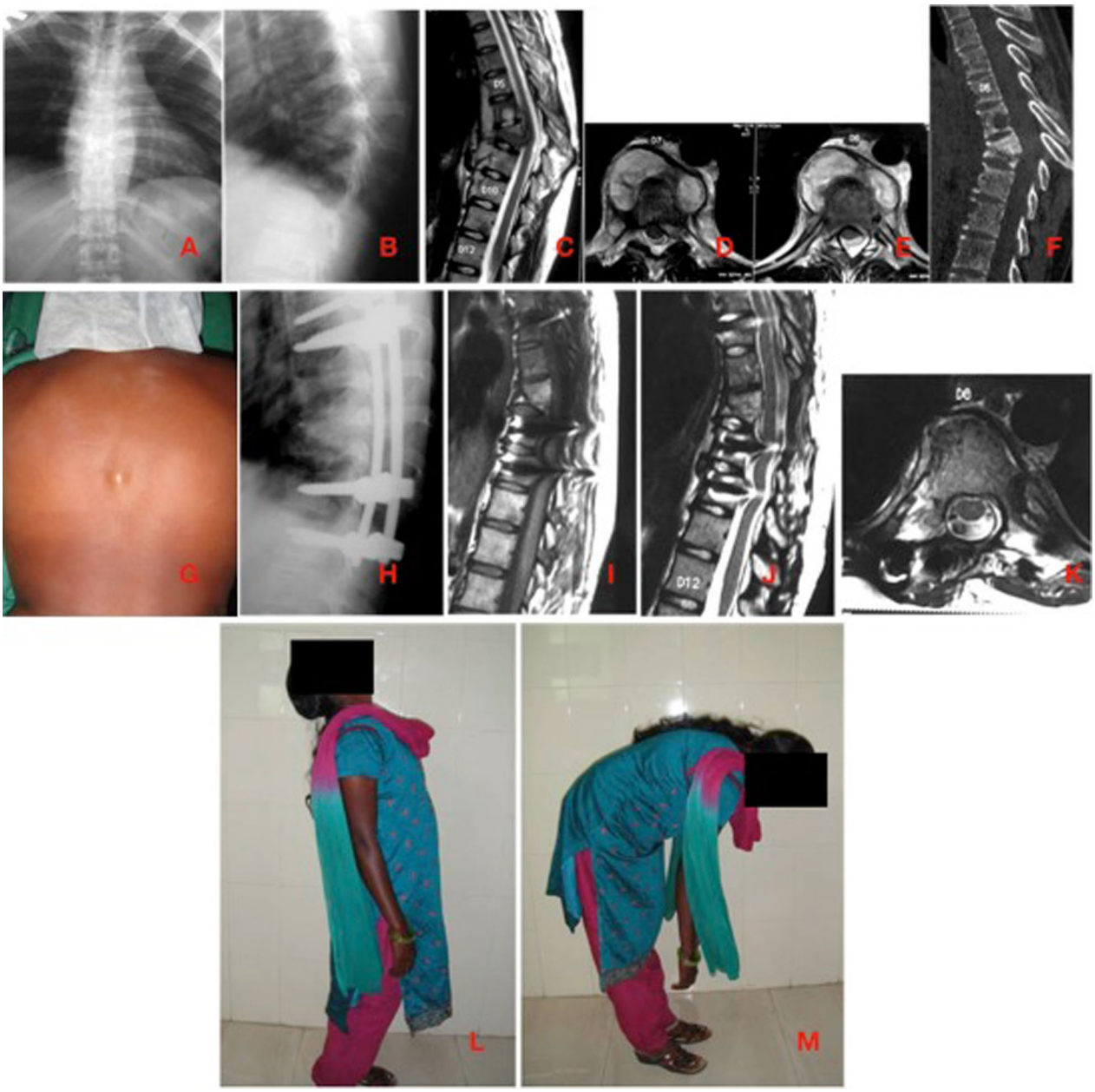

Fig. 8 Plain AP (**a**) and lateral radiograph (**b**) of thoracic spine showing destruction of T7–T8 vertebra with kyphotic deformity. Sagittal T2W (**c**) and axial T2W MRI images (**d**, **e**) showing multilevel tuberculosis with significant destruction of T7 and T8 with associated paravertebral abscess, kyphosis and cord compression. Sagittal CT scan (**f**) showing the extent of bony destruction at multiple levels and clinical photograph showing the gibbus (**g**). **h** postoperative lateral radiograph following posterior stabilization alone with correction of kyphotic deformity. **i**–**k** follow-up sagittal T1W, T2W and axial T2W MRI at 2 years showing complete healing of lesion with resolution of bony edema and abscess. **l**, **m** follow-up clinical picture with good range of extension and flexion

managed cases of spinal tuberculosis [1]. This allowed us to restrict the extent of anterior debridement that made reconstruction of anterior defect easier by transforaminal approach [12, 13] in contrast to combined and all posterior approaches with posterolateral window which are technically demanding and are associated with increased surgical duration, blood loss and prolonged hospitalization [14].

Debridement, decompression, stabilization and fusion are the main surgical principles irrespective of the choice of surgical approach which is individualized [15]. Combined approach achieves these principles better than standalone anterior or posterior surgeries [11]. The described surgical procedures include focal debridement alone, anterior radical surgery, combined posterior instrumentation

and anterior radical surgery and posterior radical surgery and posterior instrumentation [16]. Anterior approach is considered the gold standard as it gives direct access to disease site [14]. The Hong Kong procedure introduced by Ito and popularized by Hodgson & Stock involved radical anterior debridement with thorough excision of diseased foci till healthy, bleeding cancellous bone was exposed followed by strut grafting the defect [17]. Although it provided faster bony union, abscess resolution and lesser kyphotic deformities compared with debridement alone, it required prolonged immobilization and had graft-related complications including break or collapse of graft [18]. Modified Hong Kong procedure proposed addition of posterior instrumentation to support the graft till it forms a stable union with adjacent healthy vertebrae [19]. Posterior instrumentation provided good fixation and deformity correction with better functional outcome [20]. Combined approach of posterior instrumentation with anterior decompression and fusion achieved all principles but needed two separate incisions and prolonged duration [21].

Hence, we propose a comprehensive treatment algorithm of single-stage posterior transforaminal approach in the management of thoracic and lumbar tubercular spondylodiscitis from T1 to S1 which achieved 97.4% fusion with minimal blood loss, less surgical duration and less number of instrumented levels. The instrumentation in our algorithm was used merely as an adjunct to avoid complications and maintain spinal alignment till the drugs healed the disease. The transforaminal approach [12, 13] was used for debriding and fusing the tubercular focus in both lumbar and thoracic spine, obviating the need for rib resection as needed in other described posterior approaches. As the etiological diagnosis was made in every patient preoperatively with CT-guided biopsy and MDR was ruled out, we were able to limit the extent of debridement which made our anterior reconstructive procedures easier by the familiar transforaminal approach, leaving the residual disease to be healed by chemotherapy. Patients who underwent early surgery were able to ambulate from the second POD due to alleviation of pain due to stabilization of microinstability associated with the disease. In addition to alleviating pain by stabilizing the infective segment instrumentation also maintained spinal alignment and prevented kyphotic deformity while chemotherapy healed the disease.

The advantages of our comprehensive treatment algorithm include:

1. Single-stage posterior-only surgery.
2. Reconstruction of anterior defects by familiar transforaminal approach.
3. Restricting the number of levels instrumented.
4. Less surgical duration and blood loss.
5. Achieving good radiological and clinical outcomes by minimal debridement and technically easier reconstructive procedure.

The limitation of our study is a lack of control group for direct comparison of other combined/all posterior approaches and its inability to be used in severe kyphosis and complete destruction of more than one vertebral body which will require other described procedures in the literature.

Conclusion

This algorithm of single-stage posterior transforaminal approach for tubercular spondylodiscitis of thoracic and lumbar spine is effective in achieving good clinical and radiological outcomes with good fusion rates by familiar and technically simpler transforaminal approach, obviating the need for extensive posterior and combined surgical approaches.

Compliance with ethical standards

Conflict of interest All the authors declare that they do not have any conflict of interest.

Informed consent Informed consent was obtained from all individual participants included in the study.

References

1. Güzey FK, Emel E, Bas NS et al (2005) Thoracic and lumbar tuberculous spondylitis treated by posterior debridement, graft placement, and instrumentation: a retrospective analysis in 19 cases. J Neurosurg Spine 3(6):450–458
2. Tang MX, Zhang HQ, Wang YX, Guo CF, Liu JY (2016) Treatment of spinal tuberculosis by debridement, interbody fusion and internal fixation via posterior approach only. Orthop Surg 8(1):89–93
3. Nene A, Bhojraj S, Ortho D (2005) Results of nonsurgical treatment of thoracic spinal tuberculosis in adults. Spine J 5(1):79–84
4. Abbas A, Rizvi SRH, Mahesri M, Salahuddin HRA (2013) Conservative management of spinal tuberculosis: initial series from Pakistan. Asian Spine J 7(2):73–80
5. Kandwal P, Vijayaraghavan G, Jayaswal A (2016) Management of tuberculous infection of the spine. Asian Spine J 10(4):792–800
6. Jain AK (2010) Tuberculosis of the spine: a fresh look at an old disease. J Bone Joint Surg Br 92(7):905–913
7. Rasouli MR, Mirkoohi M, Vaccaro AR, Yarandi KK, Rahimi-Movaghar V (2012) Spinal tuberculosis: diagnosis and management. Asian Spine J 6(4):294–308
8. Rajasekaran S (2012) Kyphotic deformity in spinal tuberculosis and its management. Int Orthop 36(2):359–365

9. Jain A, Dhammi I, Jain S, Mishra P (2010) Kyphosis in spinal tuberculosis—prevention and correction. Indian J Orthop 44(2):127–136
10. Rajasekaran S (2002) The problem of deformity in spinal tuberculosis. Clin Orthop Relat Res 398:85–92
11. Garg RK, Somvanshi DS (2011) Spinal tuberculosis: a review. J Spinal Cord Med 34(5):440–454
12. Jain AK, Jain S (2012) Instrumented stabilization in spinal tuberculosis. Int Orthop 36(2):285–292
13. Jain A, Jain RK, Kiyawat V (2017) Evaluation of outcome of transpedicular decompression and instrumented fusion in thoracic and thoracolumbar tuberculosis. Asian Spine J 11(1):31–36
14. Alam MS et al (2015) Surgery for spinal tuberculosis: a multicenter experience of 582 cases. J Spine Surg 1(1):65–71
15. Bodapati PC, Vemula RCV, Mohammad AA, Mohan A (2017) Outcome and management of spinal tuberculosis according to severity at a tertiary referral center. Asian J Neurosurg 12(3):441–446
16. Moon MS (2014) Tuberculosis of spine: current views in diagnosis and management. Asian Spine J 8(1):97–111
17. Mak KC, Cheung KMC (2013) Surgical treatment of acute TB spondylitis: indications and outcomes. Eur Spine J 22(Suppl 4):603–611
18. Upadhyay SS, Sell P, Saji MJ, Sell B, Hsu LC (1994) Surgical management of spinal tuberculosis in adults. Hong Kong operation compared with debridement surgery for short and long term outcome of deformity. Clin Orthop Relat Res 302:173–182
19. Obaid-ur-Rahman SA, Hussain T (2009) Anterior surgical interventions in spinal tuberculosis. J Coll Phys Surg Pak 19(8):500–505
20. Garg B, Upendra B, Jayaswal A, Goswami A, Kandwal P (2012) Anterior versus posterior procedure for surgical treatment of thoracolumbar tuberculosis: a retrospective analysis. Indian J Orthop 46(2):165–170
21. Jain AK, Dhammi IK, Prashad B, Sinha S, Mishra P (2008) Simultaneous anterior decompression and posterior instrumentation of the tuberculous spine using an anterolateral extrapleural approach. J Bone Joint Surg Br 90(11):1477–1481

ORIGINAL ARTICLE

Impact of Care Bundle Implementation on Incidence of Catheter-associated Urinary Tract Infection: A Comparative Study in the Intensive Care Units of a Tertiary Care Teaching Hospital in South India

Geni VG Soundaram[1], Raja Sundaramurthy[2], Kathiresan Jeyashree[3], Vithiya Ganesan[4], Ramesh Arunagiri[5], Jhansi Charles[6]

Abstract

Introduction: Implementation of evidence-based infection control practices is the need of the hour for every institute to reduce the device-associated infections, which directly reflects the quality of care. As catheter-associated urinary tract infection (CAUTI) is the most common nosocomial infection, the study was planned to evaluate the impact of the catheter care bundle in reducing CAUTI incidence.

Material and methods: The prospective interventional study before and after the trial study was carried out in adult intensive care units over a period of 9 months (April–June 2017—pre-implementation phase; July–September 2017—training of healthcare worker and implementation of catheter care bundle; October–December 2017—post-implementation phase). Catheter-associated urinary tract infection rates pre- and post-implementation were expressed as incidence rates with Poisson confidence interval.

Results: Statistically significant reduction was found in the incidence of CAUTI (60%—from 10.7 to 4.5 per 1,000 catheter days). The key factors that contributed were significant reduction in device utilization ratio (from 0.71 to 0.56) and average catheter days per patient (from 4.8 to 3.7). This holistic approach has resulted in less incidence of CAUTI even among patients with risk factors and prolonged catheter days. Neuro ICU showed drastic improvement compared to other ICUs due to the poor baseline status of their care practices.

Conclusion: Adherence to all elements of care bundle brought a significant decrease in CAUTI. Implementing care bundle and auditing the adherence to each element should be included as a part of routine hospital infection control committee (HICC) practices.

Clinical significance: Hospital-acquired infection directly reflects on the quality care of the hospital. Bundle care is an "all or none" phenomenon. Adherence to each element will have some influence in reducing CAUTI in terms of reducing the device utilization ratio and average catheter days per patient. Auditing the care bundle adherence is having a positive influence on the outcome.

Keywords: Care bundle, Catheter-associated urinary tract infection, Intensive care unit.

Indian Journal of Critical Care Medicine (2020): 10.5005/jp-journals-10071-23473

Introduction

Hospital-acquired infections (HAIs) are the leading cause of morbidity and mortality in healthcare settings throughout the world, especially among the patients admitted in intensive care units (ICUs).[1,2] Apart from increasing the stress, discomfort, pain, and activity restrictions among the patients, HAI also increase the economic burden in the form of prolonged hospital stay, lost work days, and laboratory and drug costs.[3,4] Catheter-associated urinary tract infection (CAUTI) is the most common HAI accounting for 40% of all HAIs and the second most common cause of nosocomial septicemia.[5] According to the Centers for Disease Control and Prevention (CDC), CAUTI increases the morbidity and mortality by 2.8-fold and length of hospitalization by 1–3 days.[6] Approximately 25% of hospitalized patients undergo urinary catheterization, whereas among critically ill ICU patients, it reaches to more than 70%, resulting in >30 million urinary catheter insertions each year.[7] In majority of the cases, use of catheter without proper indication, prolonged catheter days, improper procedural technique, and improper catheter care contribute to the development of CAUTI.[8,9]

About 17–69% of CAUTIs can be prevented if CDC-recommended infection control measures are in place.[10] Educating and training the healthcare personnel and implementing practices for prevention of CAUTI contribute greatly to reduce the incidence of CAUTI.[9] Limited studies have assessed the impact of care practices on reduction of the infections once catheter is inserted.[11–13] But currently there is no defined infection control policy or guideline in India and the need of the hour is implementation of evidence-based infection control practices. So, this study was conducted to evaluate the impact of the catheter care bundle in reducing CAUTI incidence in our set-up.

[1,2,4–6]Department of Microbiology, Velammal Medical College Hospital and Research Institute, Madurai, Tamil Nadu, India

[3]Department of Epidemiology and Biostatistics, National Institute of Epidemiology, Chennai, Tamil Nadu, India

Corresponding Author: Raja Sundaramurthy, Department of Microbiology, Velammal Medical College Hospital and Research Institute, Madurai, Tamil Nadu, India, Phone: +91-0452-7113540, e-mail: rajacmc87@gmail.com

How to cite this article: Soundaram GVG, Sundaramurthy R, Jeyashree K, Ganesan V, Arunagiri R, Charles J. Impact of Care Bundle Implementation on Incidence of Catheter-associated Urinary Tract Infection: A Comparative Study in the Intensive Care Units of a Tertiary Care Teaching Hospital in South India. Indian J Crit Care Med 2020;24(7):544–550.

Source of support: Nil

Conflict of interest: None

Materials and Methods

This prospective interventional study was conducted in our tertiary care center. Medical intensive care unit (MICU), surgical intensive care unit (SICU), neurotrauma intensive care unit (neuro ICU), and cardiothoracic intensive care unit (CTICU) of our hospital were included in this study that spanned over a period of 9 months [April–June 2017—pre-implementation of catheter care bundle; July–September 2017—educating, training of healthcare worker (HCW), and implementation of catheter care bundle; October–December 2017—post-implementation of catheter care bundle]. The study was approved by our institutional ethics committee.

During the pre-implementation phase (April–June 2017), even though care bundle was not introduced, some elements of care bundle were in practice as a part of routine catheter care in our hospital. Full-time infection control nurses (ICNs) were trained by infection control officer to monitor the adherence of each element of bundle care. The bundle care audit reports collected by ICNs were analyzed by hospital infection control team on a monthly basis. ICU-wise adherence and nonadherence to each element of care bundle along with the details of individual staff (nurses and doctors) nonadherence to particular elements were noted cautiously. Surveillance of CAUTI was done as a part of routine activities of the hospital infection control committee (HICC). Following this, hospital healthcare personnel were educated regarding the importance each element of bundle care and training was given as per the need of each ICU. Training of implementation of catheter care bundle (both insertion and maintenance bundle) was conducted in batches for all HCWs including doctors for a period of 3 months (July–September 2017). Pre- and post-training evaluation and objective structured clinical evaluation (OSCE) were done to ensure that every HCW understood the concept. Meeting was held with all HCWs of ICU to address the need and possible difficulties in the implementation in their ICUs. Based on the discussion, availability of resources and staff rotation policies were regularized. Along with this, to motivate the HCWs, it was planned to felicitate the best adherence team with a shield of appreciation.

During the post-implementation phase (October–December 2017), urinary catheter insertion, maintenance, and removal was done based on standard guidelines of our HICC. Adherence to care bundle was ensured and monitored by ICNs using the audit form that was reviewed by infection control team at frequent intervals and surveillance for CAUTI was continued in the same manner as during the pre-implementation period. Surprise audits at various time intervals and by various teams were also carried out to rule out the possible confounding factor like monitoring influence (doing the work perfectly when someone is monitoring).

All catheterized adult patients (both gender) with indwelling urinary catheter (Foley's catheter) admitted in abovementioned ICUs during the study period (excluding training period) were included in the study. Catheterized ICU patients transferred to the general ward were followed up till 2 calendar days (1st day being the day of transfer). Patients only on condom catheter, suprapubic catheter, nephrostomy tube, and patients not consenting were excluded from the study.

CAUTI surveillance was done as per CDC recommendation. CAUTI (CDC definition) is defined as a UTI where an indwelling urinary catheter was in place for more than 2 calendar days on the date of event, with day of device placement being day 1, and an indwelling urinary catheter was in place on the date of event or the day before. If an indwelling urinary catheter was in place for more than 2 calendar days and then removed, the date of event for the CAUTI must be the day of discontinuation or the next day.[10] Study participants were observed for signs and symptoms of UTI, meticulously on a daily basis by ICNs. On clinical suspicion of UTI, the urine sample was collected under aseptic precautions by disinfecting a portion of the catheter tubing with alcohol and aspirating urine with a sterile syringe and needle. The collected sample was sent to the microbiology laboratory within 1 hour of the sample collection.

The urine was inoculated into CLED agar by the semiquantitative method using calibrated 1 µL loop with a diameter of 1.3 mm (Hi media Cat.no: LA023) and incubated at 35–37°C for 24 hours. Growth with colony count of $>10^5$ CFU/mL were included for surveillance. Pathogenic isolates grown were identified to the species level using Gram stain and conventional biochemical identification tests as per our laboratory protocol. Antimicrobial susceptibility testing was done by the Kirby Bauer disc diffusion method as per Clinical and Laboratory Standards Institute (CLSI) 2017 standards. Antibiotic discs were bought from Hi Media Laboratories Pvt. Ltd., Mumbai, India.

Statistical Analysis

Device utilization ratio, average catheter days per patient, and CAUTI rate were calculated using the following formulae:

- Device utilization ratio: No. of indwelling catheter days/no. of patient days
- Average catheter days per patient: No. of indwelling catheter days/no. of patients on catheter
- CAUTI incidence rate: No. of CAUTI/no. of indwelling catheter days × 1000

Catheter-associated urinary tract infection among various gender and age, pathogenic isolates, and the antibiotic sensitivity pattern were expressed as percentage. The CAUTI rates pre- and post-implementation were expressed as incidence rates with Poisson confidence interval and compared for statistically significant differences.

Results

A total of 1,233 patients were included in the study (631 patients—pre-implementation phase and 602 patients—post-implementation phase). The profile of the study participants is given in Table 1 and there was no statistically significant difference in the age, gender, and risk factor profile of the participants included during the pre- and post-implementation period. Most common age group was <50 years, males were more in number than females, and diabetes was the most common risk factor during both the study periods. The clinical diagnosis for which the participants were admitted did not vary significantly except for increased number of cases with gastrointestinal disease during the post-implementation period.

During the pre-implementation phase, overall and ICU-wise data regarding nonadherence to each element of bundle care are represented in Table 2. Documentation of assessment of readiness to remove the catheter (48.4%) and proper indication for catheterization (32.8%) were found to be the most commonly missed out elements.

A total of 32 out of 631 patients and 10 out of 602 patients developed CAUTI during the pre- and post-implementation phases, respectively. Various parameters of CAUTI surveillance during both the study periods are shown in Table 3. There was a statistically

Table 1: Profile of patients admitted in adult ICUs of a tertiary care institute in Southern India pre- (April–June 2017) and post-implementation (October–December 2017) of urinary catheter care bundle ($n = 1233$)

Variables	*Pre-implementation of urinary catheter care bundle (April–June 2017) (n = 631) n (%)*	*Post-implementation of urinary catheter care bundle (October–December 2017) (n = 602) n (%)*	*p value*
Age			0.258
≤50 years	341 (54)	324 (53.8)	
51–64 years	220 (34.9)	228 (37.9)	
65–79 years	65 (10.3)	44 (7.3)	
≥80 years	5 (0.8)	6 (1)	
Gender			0.286
Male	430 (68.1)	393 (65.3)	
Female	201 (31.9)	209 (34.7)	
Diagnostic condition			0.534
Neurological disease and procedure	269 (42.6)	257 (42.7)	
Pulmonary disease	14 (2.2)	5 (0.8)	
Cardiac disease and procedure	190 (30.1)	177 (29.4)	
GIT disease and procedure	30 (4.8)	4 (0.7)	0.001
Kidney disease and procedure	45 (7.2)	52 (8.6)	
Musculoskeletal disease	41 (6.6)	56 (9.3)	
Metabolic disease	12 (1.9)	6 (1)	
Other surgical procedure	24 (3.9)	40 (6.7)	
Poisoning	4 (0.7)	5 (0.8)	
Risk factors			
Diabetic	166 (26.3)	151 (25.1)	0.623
Calculi	14 (2.2)	7 (1.2)	0.225
Stricture	8 (1.3)	2 (0.3)	0.130
Neurogenic bladder	7 (1.1)	2 (0.3)	0.205
Prostatic enlargement	7 (1.1)	1(0.1)	0.088

ICU, intensive care unit

Table 2: Analysis of nonadherence to each bundle care elements among adult ICUs of a tertiary care institute in Southern India, during pre-implementation (April–June 2017) of urinary catheter care bundle ($n = 3003$)—overall and ICU-wise

	ICU (no. of patients on catheter/catheter days)				
	Overall 631/3003	*IMCU—91/484*	*SICU—202/849*	*Neuro ICU—170/1096*	*CTICU—168/574*
Bundle elements	*Not followed n (%)*	*Not followed n (%)*	*Not followed n (%)*	*Not followed n (%)*	*Not followed n (%)*
Proper indication documented	207/631 (32.8)	34/91 (37.4)	69/202 (34.2)	81/170 (47.6)	23/168 (13.7)
Closed drainage system	366 (12.2)	59 (12.2)	87 (10.2)	184 (16.7)	36 (6.3)
Urinary catheter secured/not obstructed	395 (13.2)	72 (14.9)	109 (12.8)	162 (14.8)	52 (9)
Drainage bag above floor and below bladder level	183 (6.1)	42 (8.7)	45 (5.3)	63 (5.7)	33 (5.7)
Hand hygiene	790 (26.3)	158 (32.6)	110 (13)	423 (38.6)	99 (17.2)
Vaginal/meatal care	197 (6.6)	38 (7.8)	37 (4.4)	73 (6.7)	49 (8.5)
Perineal care	889 (29.6)	172 (35.5)	224 (26.4)	396 (36.1)	97 (16.9)
Single-use glove while handling/ emptying	663 (22.1)	102 (21.1)	125 (14.7)	367 (33.5)	69 (12)
No contact b/t jug and bag	270 (9)	63 (13)	61 (7.2)	97 (8.9)	49 (8.5)
Separate jug for collecting	463 (15.4)	88 (18.2)	83 (9.8)	247 (22.5)	45 (7.8)
Assessment of readiness to remove—documented?	1452 (48.4)	226 (46.6)	354 (41.2)	723 (65.9)	149 (26)

significant decrease in the incidence of CAUTI [from the incidence rate of 0.010 with Poisson confidence interval (CI) of 0.007–0.015 during the pre-implementation phase to the incidence rate of 0.004 with Poisson CI of 0.002–0.008 during the post-implementation phase with the incidence ratio of 0.421 with Poisson CI of 0.211–0.839]. Similar to this statistically significant decrease also noted

Table 3: Impact analysis of catheter care bundle among patients admitted in adult ICUs in a tertiary care institute in Southern India, during pre- (April–June 2017) and post-implementation (October–December 2017) of urinary catheter care bundle (n = 1,233)–overall and ICU wise

	Overall		*IMCU*		*SICU*		*Neuro ICU*		*CTICU*	
	Pre	*Post*	*Pre*	*Post*	*Pre*	*Post*	*Pre*	*Post*	*Pre*	*Post*
Total no. of patients on urinary catheter	631	602	91	94	202	147	170	190	168	171
Total no. of catheter days[1]	3,003	2,225	484	388	849	564	1,096	868	574	405
Total no. of patient days[2]	4,234	3,996	1,314	1,115	988	914	676	753	1,256	1,213
Device utilization ratio (Poisson confidence interval)*	0.71 (0.684–0.735)	0.56 (0.533–0.580)	0.37	0.34	0.86	0.61	1.62	1.15	0.46	0.33
Average catheter days per patient** (p value =0.001)	4.8	3.7	5.3	4.1	4.2	3.8	6.5	4.5	3.4	2.4
No. of CAUTI	32	10	5	2	8	2	16	5	3	1
CAUTI incidence rate (Poisson confidence interval)***	10.7 (0.007–0.15)	4.5 (0.002–0.008)	10.3	5.1	10.6	3.5	14.6	5.7	5.2	2.4

*Device utilization ratio: no. of indwelling catheter days/no. of patient days
**Average catheter days per patient: No. of indwelling catheter days/no. of patients on catheter, $p = 0.001$
***CAUTI incidence rate: no. of CAUTI/no. of indwelling catheter days × 1000
[1]Catheter days—number of patients with indwelling urinary catheter collected daily at the same time and summed up for month for that specific location
[2]Patient days—number of patients in the patient care collected daily at the same time and summed up for month for that specific location

in the device utilization ratio [from the incidence rate of 0.709 with Poisson confidence interval (CI) of 0.684–0.735 during the pre- implementation phase to the incidence rate of 0.556 with Poisson CI of 0.533–0.580 during post-implementation phase with the incidence ratio of 0.785 with Poisson CI of 0.743–0.829]. Also there was a statistically significant reduction found in the average catheter days per patient (from 4.8 to 3.7 with the p value −0.001) after care bundle implementation. On analyzing the catheterized patients with risk factors, there was a statistically significant decrease in the incidence of CAUTI during the post-implementation phase even with associated risk factors as shown in Table 4.

Regarding catheter days, there was statistically significant increase in early removal of catheter during the post-implementation period. The percentage of patients in whom the catheter was in place for <5 calendar days has increased from 56.9 to 73.3%. Even among patients in whom catheter was in place for 5–10 or >10 days, there was a statistically significant decrease in incidence of CAUTI (p value = 0.001) during post-implementation as shown in Table 5.

Among patients who developed CAUTI, the most common age group was 65–79 years (43.7% and 70%); gender was male (59.3% and 70%); clinical diagnosis during admission was neurological disease (46.9% and 20%); and associated risk factor was diabetes (78.1% and 100%) during both pre- and post-implementation periods, respectively. *Escherichia coli* was the common organism isolated followed by *Pseudomonas aeruginosa* and all the Gram-negative organisms isolated were sensitive to colistin (Supplementary Tables S1 and S2).

Discussion

Catheter-associated urinary tract infection has become a major global health problem, leading to increased morbidity and mortality in healthcare settings especially in ICUs. As multiple factors like aseptic technique, hand hygiene, catheter care, and duration of catheterization can affect the incidence of CAUTI, a holistic approach becomes mandatory to reduce the incidence of CAUTI.[13]

Since the proportion of catheterized patients will always be comparatively higher in ICUs than wards, adult ICUs were included in the study. Analysis of adherence and nonadherence to each element of care bundle is essential before implementing care bundle in any set-up. Though documentation of assessment of readiness to remove the catheter and proper indication for catheterization (48.4 and 32.8%, respectively) were found to be the most commonly missed out elements, none of the care bundle element was fully adhered.

Our findings are in concordance with the study results of Lai et al., who also reported that among the care bundle elements compliance was lowest for daily review of need of catheter.[14] Since adherence was not to an agreeable level, as a HICC unit we analyzed the root causes for nonadherence. Lack of sufficient knowledge among HCWs, occasional unavailability of handrub/wash, disposable glove, and separate jug were identified and this lacunae was corrected by educating, training, and ensuring availability of all essential things for care bundle implementation.

Before analyzing the impact of care bundle in the post-implementation period, the probable confounding variables including patient number, age, gender, associated risk factors, and diagnostic condition for patients admitted were compared and found to be statistically insignificant except increased number of cases with gastrointestinal disease during the

Table 4: Analysis of risk factor with CAUTI among patients admitted in adult ICUs in a tertiary care institute in Southern India, during pre- (April–June 2017) and post-implementation (October–December 2017) of urinary catheter care bundle (n = 1233)

	Pre-implementation (n = 631)		*Post-implementation (n = 602)*		
Risk factor	*Total number*	*Number of CAUTI (%)*	*Total number*	*Number of CAUTI (%)*	*p value*
Diabetes	166	25 (15.1)	151	10 (6.62%)	0.01
Calculi	14	4 (28.6)	7	–	
Stricture	8	–	2	–	
Neurogenic bladder	7	1 (14.3)	2	–	
Prostatic enlargement	7	79 (100)	1	–	

Table 5: Analysis of catheter days with CAUTI incidence among patients admitted in adult ICUs in a tertiary care institute in Southern India pre- (April–June 2017) and post-implementation (October–December 2017) of urinary catheter care bundle (*n* = 1,233)

	No. of patients on catheter		*Number of CAUTI*		
Catheter days	*Pre-implementation (%)*	*Post-implementation (%)*	*Pre-implementation (%)*	*Post-implementation (%)*	*p value*
<5	359 (56.9)	441 (73.3)	Nil	Nil	0.001
5–10	258 (40.9)	158 (26.2)	20 (7.8)	8 (5.1)	
>10	14 (2.2)	3 (0.5)	12 (85.7)	2 (66.6)	

post-implementation period, which is not known to interfere with inference of the study.

On analyzing the impact of catheter care bundle, the incidence of CAUTI has dropped down by almost 60%, from 10.7 to 4.5 per 1,000 catheter days after implementation of bundle care. These results were found to be statistically significant. Our study findings are concordance with Prakash et al. and Blanck et al., who reported decrease in the CAUTI rate after implementing care bundle by 51.4% (from 4.86 to 2.36 per 1,000 catheter days) and 50% (from 8.4 to 4.3 per 1,000 catheter days), respectively.[12,15] Lesser reduction of 22.7% (3.86–2.98 per 1,000 catheter days) was reported by Lai et al.[14] This may be due to the factor that incidence of CAUTI was already very low even before implementing the catheter care bundle.

Our analysis revealed that the key factor that contributed to this 60% reduction in CAUTI was the decrease in the inappropriate use of catheter, which reflected as statistically significant reduction in the device utilization ratio and average catheter days per patient. The device utilization ratio came down from 0.71 to 0.56. Average catheter days per patient was dropped down from 4.8 to 3.7 with the *p* value of 0.001.

For each day the indwelling urinary catheter remains, the patient has 3–10% increased risk of acquiring CAUTI and risk of bacteriuria reaches nearly 100% if the catheter is in place for 4 weeks.[8] Statistically significant reduction was found on catheter days ($p = 0.006$); in nearly 75% of patients, catheter was removed in less than 5 days as compared to 56.9% in the pre-implementation period. Our study results also highlight that even while the catheter remains for 5–10 or >10 days, CAUTI incidence can be reduced from 7.8 to 5.1% and 85.7 to 66.6%, respectively, if catheter care bundle was properly implemented.

Our study results also depict that ideal catheter care can reduce CAUTI in spite of underlying risk factors as none of the patients with calculi, stricture, neurogenic bladder, or prostatic enlargement developed CAUTI in the post-implementation phase.

Statistically significant reduction of CAUTI found in our study may be due to the intensive education and training given to the HCWs about each element of care bundle and active continuous monitoring carried out by trained ICN on adherence to all steps of bundle care regularly during the post-implementation period. Surveillance and auditing might have had a positive influence on compliance to bundle care in our set-up. The two elements that were found to most commonly missed, i.e., documentation of assessment of readiness to remove the catheter (48.4%) and of proper indication for catheterization (32.8%) in the pre-implementation phase, were corrected in the post-implementation phase. And the holistic approach has resulted in less incidence of CAUTI even among patients with associated risk factors and prolonged catheter days.

Among the ICUs, neuro ICU showed a drastic improvement compared to other ICUs. This might be due to the poor baseline status. Nonpractice of catheter care elements, i.e., documentation of assessment of readiness to remove the catheter (65.9%), proper indication for catheterization (47.6%), hand hygiene (38.6%), perineal care (36.1%), and using disposable glove while emptying or handling urobag (33.5%), was higher compared to other ICUs during the pre-implementation phase and had the highest device utilization ratio (1.62), average catheter days per patient (6.5), and incidence of CAUTI (14.6 per 1,000 catheter days). Hence, proper implementation brought a marked change in neuro ICU.

On further analysis, it was found that no significant difference was found in the pre- and post-implementation phase of CAUTI presentation as CAUTI was most common among the age group of 65–79 years (43.7% and 70%), male gender (59.3% and 70%), and patient admitted for neurological disease (46.9% and 20%) in both pre- and post-implementation phases. Diabetic was the most common risk factor associated with CAUTI (78.1% and 100%) in both phases. In both phases, *E. coli* was the common organism isolated followed by *P. aeruginosa.* All the isolates showed better sensitivity to nitrofurantoin, amikacin, cotrimoxazole, imipenem, and 100% sensitivity to colistin during both phases.

Limitations

The study does not have a true control group. For ethical reasons, standard catheter care could not be withheld for patients, thus eliminating the possibility. This might have led to an underestimation of the impact of the catheter care bundle on CAUTI, since some of the measures in the bundle were practiced during the pre-implementation period as well. Care bundle ideally includes two components—procedural and maintenance bundle. Implementation of the procedural bundle was a challenge in our

set-up as the insertion of the device takes place in varied locations (casualty, operation theater, sometimes in ICUs) of our hospital. The change in the ICU staff structure was minimal during the study period. Since this is unavoidable and was not significant enough to affect the results of the study, the details are not mentioned. Pre- and post-implementation phases of the study were conducted during different seasons of the same year. A holistic approach including insertion bundle along with maintenance bundle will further reduce device-associated infections.

Clinical Significance

Hospital-acquired infections directly reflect on the quality care of the hospital and intervention. Bundle care is an "all or none" phenomenon. Our study results emphasize that even though few elements of care bundle were already in practice, adherence to all elements as a bundle brought a significant decrease in CAUTI. Adherence to each element will have some influence in reducing CAUTI in terms of reducing the device utilization ratio and average catheter days per patient. Auditing the care bundle adherence is having a positive influence in the outcome. Implementing care bundle and auditing the adherence to each element should be included as a part of routine HICC practices.

Research Quality and Ethics Statement

We declare that this scientific work complies with reporting quality, formatting, and reproducibility guidelines set forth by the EQUATOR Network. We also attest that this clinical investigation was determined to evaluate the impact of catheter care bundle in reducing CAUTI incidence in our set-up as there is no defined infection control policy and the need of the hour is implementation of evidence-based infection control practices, require the institutional ethics committee review, and the corresponding protocol was approved by our institute ethical committee (IEC Ref No.: VMCIEC/49/2017). We also certify that we have not plagiarized the contents in this submission and have done a plagiarism check.

Author's Contribution

Raja Sundaramurthy, Geni VG Soundaram have given the concepts and intellectual content. Raja Sundaramurthy, Geni VG Soundaram, Jeyashree Kathiresan designed the study. Raja Sundaramurthy, Geni VG Soundaram, Vithiya Ganesan, Ramesh Arunagiri carried out the literature search. Raja Sundaramurthy, Geni VG Soundaram, Jeyashree Kathiresan, Vithiya Ganesan have collected and analyzed the data. Raja Sundaramurthy, Geni VG Soundaram, Jeyashree Kathiresan, Jhansi Charles carried out the statistical analysis. Raja Sundaramurthy, Geni VG Soundaram done the manuscript preparation. Vithiya Ganesan, Ramesh Arunagiri have done the manuscript editing. Jhansi Charles, Jeyashree Kathiresan carried out the manuscript review.

The manuscript has been read and approved by all the authors, that the requirements for authorship as stated earlier in this document have been met, and that each author believes that the manuscript represents honest work and we would also like to state that the manuscript has not been submitted or accepted for publication anywhere.

Ethical Committee Approval

Ethical clearance obtained from Institute Ethical Committee, VMCH&RI, Madurai, Tamil Nadu, India. IEC Ref No.: VMCIEC/49/2017.

Acknowledgments

We would like to acknowledge our ICNs (Mrs. Maragathavalli, Mrs. Gokila, and Mrs. Devi) for their immense help during data collection. We would like to thank Dr Vijayanand, ICU in-charge ,for his valuable support for auditing the bundle care. We also like to give our gratitude to Dr Rajendran Tiruvannamalai, associate professor, for the constant support during the analysis.

References

1. Rosenthal VD, Maki DG, Salomao R, Moreno CA, Mehta Y, Higuera F, et al. Device-associated nosocomial infections in 55 intensive care units of 8 developing countries. Ann Intern Med 2006;145(8):582–591. DOI: 10.7326/0003-4819-145-8-200610170-00007.
2. Parida S, Mishra SK. Urinary tract infections in the critical care unit: A brief review. Indian J Crit Care Med 2013;17(6):370–374. DOI: 10.4103/0972-5229.123451.
3. Clec'h C, Schwebel C, Français A, Toledano D, Fosse J-P, Garrouste-Orgeas M, et al. Does catheter-associated urinary tract infection increase mortality in critically ill patients? Infect Control Hosp Epidemiol 2007;28(12):1367–1373. DOI: 10.1086/523279.
4. Tambyah PA, Knasinski V, Maki DG. The direct costs of nosocomial catheter-associated urinary tract infection in the era of managed care. Infect Control Hosp Epidemiol 2002;23(1):27–31. DOI: 10.1086/501964.
5. Nicolle LE. Catheter associated urinary tract infections. Antimicrob Resist Infect Control 2014;3(1):23. DOI: 10.1186/2047-2994-3-23.
6. Saint S. Clinical and economic consequences of nosocomial catheter-related bacteriuria. Am J Infect Control 2000;28(1):68–75. DOI: 10.1016/s0196-6553(00)90015-4.
7. Bagshaw SM, Laupland KB. Epidemiology of intensive care unit-acquired urinary tract infections. Curr Opin Infect Dis 2006;19(1):67–71. DOI: 10.1097/01.qco.0000200292.37909.e0.
8. Lo E, Nicolle LE, Coffin SE, Gould C, Maragakis LL, Meddings J, et al. Strategies to prevent catheter-associated urinary tract infections in acute care hospitals: 2014 update. Infect Control Hosp Epidemiol 2014;35(5):464–479. DOI: 10.1086/675718.
9. Gould CV, Umscheid CA, Agarwal RK, Kuntz G, Pegues DA. Healthcare infection control practices advisory committee. Guideline for prevention of catheter-associated urinary tract infections 2009. Infect Control Hosp Epidemiol 2010;31(4):319–326. DOI: 10.1086/651091.
10. Safety P, National Healthcare Safety Network (NHSN) Overview. [cited 2017 Jul 31]; Available from: https://www.cdc.gov/nhsn/pdfs/validation/2016/pcsmanual_2016.pdf.
11. Mathur P. Prevention of healthcare-associated infections in low- and middle-income countries: the "bundle approach. Indian J Med Microbiol 2018;36(2):155. DOI: 10.4103/ijmm.IJMM_18_152.
12. Prakash SS, Rajshekar D, Cherian A, Sastry AS. Care bundle approach to reduce device-associated infections in a tertiary care teaching hospital, South India. J Lab Physicians 2017;9(4):273–278. DOI: 10.4103/JLP.JLP_162_16.
13. Cooke FJ, Holmes AH. The missing care bundle: antibiotic prescribing in hospitals. Int J Antimicrob Agents 2007;30(1):25–29. DOI: 10.1016/j.ijantimicag.2007.03.003.
14. Lai C-C, Lee C-M, Chiang H-T, Hung C-T, Chen Y-C, Su L-H, et al. Implementation of a national bundle care program to reduce catheter-associated urinary tract infection in high-risk units of hospitals in Taiwan. J Microbiol Immunol Infect 2017;50(4):464–470. DOI: 10.1016/j.jmii.2017.01.006.
15. Blanck AM, Donahue M, Brentlinger L, Stinger KD, Polito C. A quasi-experimental study to test a prevention bundle for catheter-associated urinary tract infections. J Hosp Adm 2014;3(4):101. DOI: 10.5430/jha.v3n4p101.

Supplementary Table 1: Profile of patients with CAUTI admitted in adult ICUs of a tertiary care institute in Southern India before (April–June 2017) and after (October–December 2017) implementation of urinary catheter care bundle ($n = 42$)

Variables	*Before implementation of urinary catheter care bundle (April–June 2017) (n = 32) n (%)*	*After implementation of urinary catheter care bundle (September–November 2017) (n = 10) n (%)*
Age		
≤50 years	7 (21.9)	–
51–64 years	9 (28.1)	3 (30)
65–79 years	14 (43.7)	7 (70)
>80 years	2 (6.3)	–
Gender		
Male	19 (59.3)	7 (70)
Female	13 (40.7)	3 (30)
Diagnostic condition		
Neurological disease and procedure	15 (46.9)	2 (20)
Pulmonary disease	–	2 (20)
Cardiac disease and procedure	2 (6.3)	1 (10)
GIT disease and procedure	–	1(10)
Kidney disease and procedure	8 (25)	3 (30)
Musculoskeletal disease	5 (15.6)	–
Metabolic disease	1 (3.1)	1 (10)
Other surgical procedure	1 (3.1)	–
Risk factors		
Diabetic	25 (78.1)	10 (100)
Calculi	4 (12.5)	–
Neurogenic bladder	1 (3.1)	–
Prostatic enlargement	7 (21.9)	–
Organism isolated		
Escherichia coli	15 (46.9)	4 (40)
Pseudomonas aeruginosa	6 (18.7)	4 (40)
Klebsiella pneumoniae	6 (18.7)	1 (10)
Enterobacter species	3 (9.5)	–
Candida species	2 (6.2)	1 (10)

Supplementary Table 2: Antibiotic sensitivity pattern analysis of CAUTI isolates among patients admitted in adult ICUs in a tertiary care institute in Southern India pre- (April–June 2017) and post-implementation (October–December 2017) of urinary catheter care bundle ($n = 42$)

Antibiotic sensitivity pattern (%)—pre-implementation												
Uropathogen (no. of isolate)	CAZ	CTR	CPM	AK	GEN	COT	CIP	OF	NIT	PIT	IMP	CL
Escherichia coli (15)	6.6	6.6	6.6	46.6	20	46.6	0	0	86.6	46.6	60	100
Pseudomonas aeruginosa (6)	0	–	0	0	0	–	0	0	–	16.6	33.3	100
Klebsiella pneumoniae (6)	0	0	0	66.6	33.3	33.3	0	0	50	16.6	33.3	100
Enterobacter spp. (3)	33.3	33.3	33.3	66.6	66.6	33.3	33.3	33.3	66.6	33.3	66.6	100
Antibiotic sensitivity pattern (%)—post-implementation												
Uropathogen (no. of isolate)	CAZ	CTR	CPM	AK	GEN	COT	CIP	OF	NIT	PIT	IMP	CL
Escherichia coli (4)	25	25	25	75	50	50	0	0	75	25	50	100
Pseudomonas aeruginosa (4)	0	–	0	25	25	–	0	0	–	25	75	100
Klebsiella pneumoniae (1)	0	0	0	100	0	100	0	0	100	100	100	100

CAZ, ceftazidime; CTR, ceftriaxone; CPM, cefepime; AK, amikacin; GEN, gentamicin; COT, cotrimoxazole; CIP, ciprofloxacin; OF, ofloxacin; NIT, nitrofurantoin; PIT, Piperacillin-Tazobactum; IMP, imipenem; CL, colistin

INT J TUBERC LUNG DIS 24(2):180–188

http://dx.doi.org/10.5588/ijtld.19.0021

Financial support to the poor for the detection of smear-negative pulmonary and extra-pulmonary TB in Bangladesh

I. M. S. Munim,[1] H. D. Shewade,[2,3,4] K. Jeyashree,[5] S. Islam,[1] I. A. Rifat,[1] F. K. Patwary,[1] I. Begum,[1] M. K. Sarkar,[1] R. Mahmud,[1] M. S. Islam,[6] M. A. Islam[1]

[1]Communicable Disease Programme (TB), BRAC, Dhaka, Bangladesh; [2]International Union Against Tuberculosis and Lung Disease (The Union), Paris, France; [3]The Union South-East Asia, New Delhi, [4]Karuna Trust, Bengaluru, [5]Velammal Medical College Hospital and Research Institute, Madurai, India; [6]National Tuberculosis Control Programme, Ministry of Health and Family Welfare, Dhaka, Bangladesh

SUMMARY

BACKGROUND: The study was conducted in BRAC-administered areas of the Bangladesh National Tuberculosis (TB) Programme (42 of 64 districts). According to the 2013–2017 financial support scheme, direct costs due to TB diagnosis were reimbursed among economically disadvantaged people with presumptive smear-negative pulmonary (PTB) and extrapulmonary TB (EPTB).

OBJECTIVE: To describe the implementation of the scheme and associated changes in case notification.

DESIGN: This was a descriptive study involving programme data.

RESULTS: Between 2013 and 2017, persons reimbursed reduced from 125 680 to 88 763, and the case detection ratio increased from 18% to 24%. The number of patients with presumptive EPTB who were reimbursed decreased from 5024 to 3484. More than 95% were reimbursed for chest radiograph, fine-needle aspiration cytology and biopsy. However, large numbers of ancillary investigations were also reimbursed. During 2013–2017, the observed national quarterly new smear-negative PTB case notification rates (CNRs) were significantly higher than the forecasted CNRs (based on CNR trends during 2008–2012). New EPTB and all form TB CNRs increased but not significantly.

CONCLUSION: Implementation of the financial support scheme was accompanied by a significant improvement in new, smear-negative PTB notification. The absence of a comparison arm was a key limitation, but comparison was not possible as the scheme was implemented in all districts.

KEY WORDS: tuberculosis diagnosis; reimbursement; incentives; operational research; SORT IT

TUBERCULOSIS (TB) IS THE leading cause of death by a single infectious agent worldwide. In 2017, there were an estimated 10 million people with TB and 1.6 million TB deaths. With a population of 165 million and TB incidence of 221 per 100 000 population, Bangladesh is one of the high TB burden countries.[1]

In Bangladesh, of the estimated TB patients in 2011–2012, 51–55% were 'missing'.[2,3] One of the reasons for the low case notification rates (CNR 99–111/100 000 in 2011–2012 in selected areas) was the low detection of new, smear-negative pulmonary TB (PTB) and extra-pulmonary TB (EPTB) cases.[2,3] This could have been due to the fact that the diagnostic and treatment services were either unavailable or unaffordable.

TB diagnosis- and treatment-related costs comprise direct medical costs, direct non-medical costs (transport cost to a place of care, temporary accommodation cost including food) and indirect costs (income loss due to seeking and receiving treatment).[4] In Bangladesh, other than sputum microscopy, TB diagnosis tests are not provided free of cost.[5,6] This increases the patient costs for diagnosis of smear negative PTB and EPTB. TB-related costs are catastrophic for those from poor socio-economic status, impoverishing them further.[4]

Since 1994, BRAC, a development organisation, has been implementing TB Control Programme in Bangladesh in collaboration with the National TB Programme (NTP). Currently, BRAC is directly implementing TB care in 42 of 64 districts of Bangladesh (BRAC-administered areas) through funding from the Global Fund. The remaining districts are covered by sub-recipients (non-Governmental partner organisations) of BRAC under the stewardship of the NTP.[7]

Since 2013, BRAC, in collaboration with the NTP, has implemented a financial support scheme in all districts of Bangladesh for economically disadvan-

MSI and MAI contributed equally as senior authors/last authors.

Correspondence to: Sardar Munim Ibna Mohsin, Communicable Disease Programme (TB), BRAC Centre, 75 Mohakhali, Dhaka 1212, Bangladesh. email: sardar.munim@outlook.com, munim.s@brac.net

Article submitted 11 January 2019. Final version accepted 25 July 2019.

taged people with presumptive smear-negative PTB (up to 19 United States dollar, US$) and presumptive EPTB (up to US$38). Direct costs due to TB diagnostics were reimbursed, regardless of whether TB was diagnosed or not.

Globally, there is dearth of evidence on the benefits of reimbursement schemes for TB case detection. Available studies are limited to insurance schemes or services providers who provide directly observed therapy.[8–10] Furthermore, BRAC has patientwise information on the type of investigations reimbursed and time interval from investigations to reimbursement. The present study describes 1) the implementation of the financial protection scheme (2013–2017); 2) trends in the absolute number and CNRs among new smear-negative PTB, new EPTB and all forms of TB before (2008–2012) and during implementation (2013–2017) of the scheme; and 3) services received under the scheme and time intervals between various steps in the care pathway among people who were reimbursed in BRAC-administered areas of Bangladesh.

METHODS

Study design

This was a descriptive study involving record review.

Setting

General setting

Bangladesh, officially known as the People's Republic of Bangladesh (population: 162 million) shares land borders with India and Myanmar and is divided into eight administrative divisions.[11] Divisions are divided into districts (*zilas*, $n = 64$), which are further divided into sub-districts (*upazilas*, $n = 488$).

Bangladesh National TB Programme

Under the NTP, 42 district-level units, 297 treatment units (TUs), which provide TB services through 445 microscopy laboratories in BRAC-administered areas.

Financial support scheme

The flow from presumption to receipt of support and eventual diagnosis/treatment initiation has been shown in Figure 1. Public and private physicians refer people with presumptive smear-negative PTB and EPTB who are not able to pay for investigations to the nearest BRAC office within the catchment area of the TU for financial support. This is managed by BRAC's programme organiser. After investigation at a public or private facility, the person with presumptive TB is reimbursed on production of receipts for the costs incurred (diagnostic fees, transportation and food costs). Details of recipients of the scheme are entered in the financial support register at the BRAC office (linked to the TB TU) after the referred person returns with the bills.

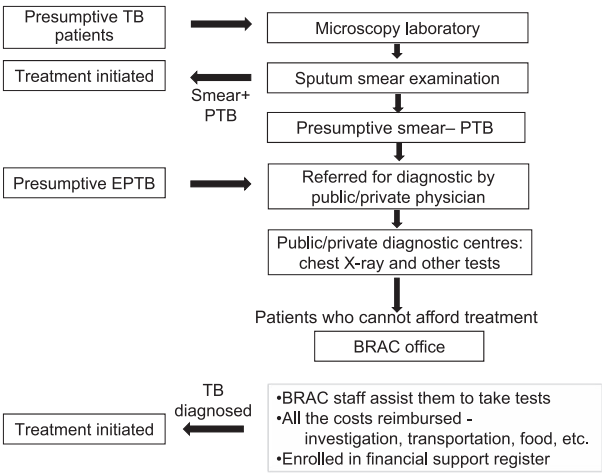

Figure 1 Financial support scheme for people with presumptive smear-negative TB and presumptive EPTB, Bangladesh. TB = tuberculosis; + = positive; PTB = pulmonary TB; – = negative; EPTB = extra-pulmonary TB.

Data from all the monthly reports are entered into the BRAC TB electronic management information system (MIS), which is routinely checked for quality.

Study population and data collection

For the first two study objectives, we extracted quarterly aggregate disease and financial data of 42 districts from BRAC MIS. For the third objective, we used data on recipients of financial support in BRAC-administered areas of Bangladesh. For the purpose of operational feasibility, we selected 25 TUs using stratified random sampling (21/297 BRAC TUs and 4/63 BRAC urban reporting units in cities) and included all the persons with presumptive, smear-negative PTB and EPTB who were reimbursed under the scheme during July–September 2017. Trained programme organisers collected the data under the supervision of the principal investigator. We randomly checked 10% of data collection forms (see Supplementary Data) for each sampled TU/reporting unit by referring to the original data sources.

Analysis and statistics

For the first two objectives, we used line and bar diagrams to depict the annual trends in various indicators using Excel (Microsoft, Redmond, WA, USA). For each year, we converted Bangladeshi taka (BDT) to US$ using the December conversion rates and adjusted for inflation (at 3% per year up to 2017).

We used the *forecast.ets* function in Excel 2016 (Microsoft) to generate the forecasted values for 2013–2017, based on the historical values for 2008–2012. Forecasted values were plotted beside the observed values in line diagrams. The forecasted national quarterly CNRs (along with 95% confidence intervals [CIs]) for the period 2013–2017 were compared with the observed CNRs. If the observed

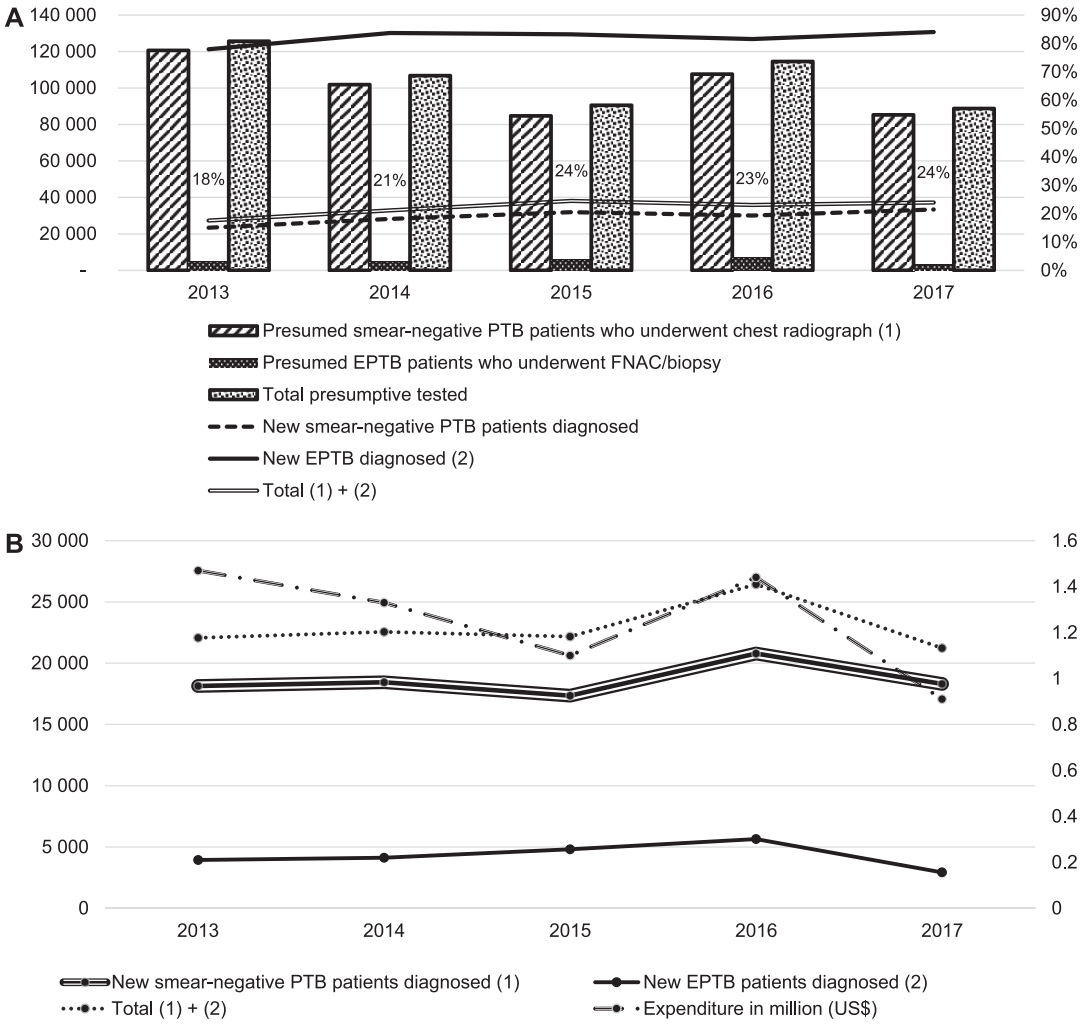

Figure 2 Annual trends in patient detection among individuals with presumptive TB who received financial support and budget expenditure in BRAC*-administered areas, Bangladesh, 2013–2017. **A)** Number of beneficiaries and the frequency of detection among them **B)** Frequency of detection among beneficiaries and budget expenditure: financial support vs. diagnosis of smear-negative pulmonary, extra-pulmonary and All TB cases. *A development organisation that has been implementing TB control programmes in Bangladesh in collaboration with the National TB Control Programme. Under BRAC-administered areas, there are 42 district level units, 297 TB treatment units and 445 peripheral microscopy laboratories (including urban areas). TB = tuberculosis; PTB = pulmonary TB; US$ = US dollars.

CNRs were beyond the 95% CIs, we assumed that the change in CNR during implementation was significant.

For the third objective, we double-entered, validated and analysed data using EpiData (v3.1 for entry and v2.2.2.183 for analysis; EpiData Association, Odense, Denmark). Results were summarised using number, frequency, proportion, median and interquartile ranges (IQRs).

Ethics

The study received ethics approval from BRAC, Ethical Review Committee, Dhaka, Bangladesh (BRAC ERC:09, dated 25 July 2018) and the Ethics Advisory Group of the International Union Against TB and Lung Disease, Paris, France (EAG No: 17/18, dated 12 April 2018). As this study involved the review of secondary patientwise and aggregate data, the ethics committees waived the requirement for informed consent.

RESULTS

People reimbursed and detection ratio under the scheme: annual trends (2013–2017)

In 2013, the number of persons reimbursed was very high but decreased from 125 680 in 2013 to 88 763 in 2017. The proportion of persons detected with TB increased from 18% to 24% in the same period. Overall TB detection ratio increased and was very high among patients with presumptive EPTB, gradually reaching 84% in 2017 (Figure 2).

Overall, budget expenditure amount fell from US$1.47 million in 2013 to 0.91 million in 2017. The annual detection under the scheme rose and fell in tandem with the amount of budget spent (Figure 2).

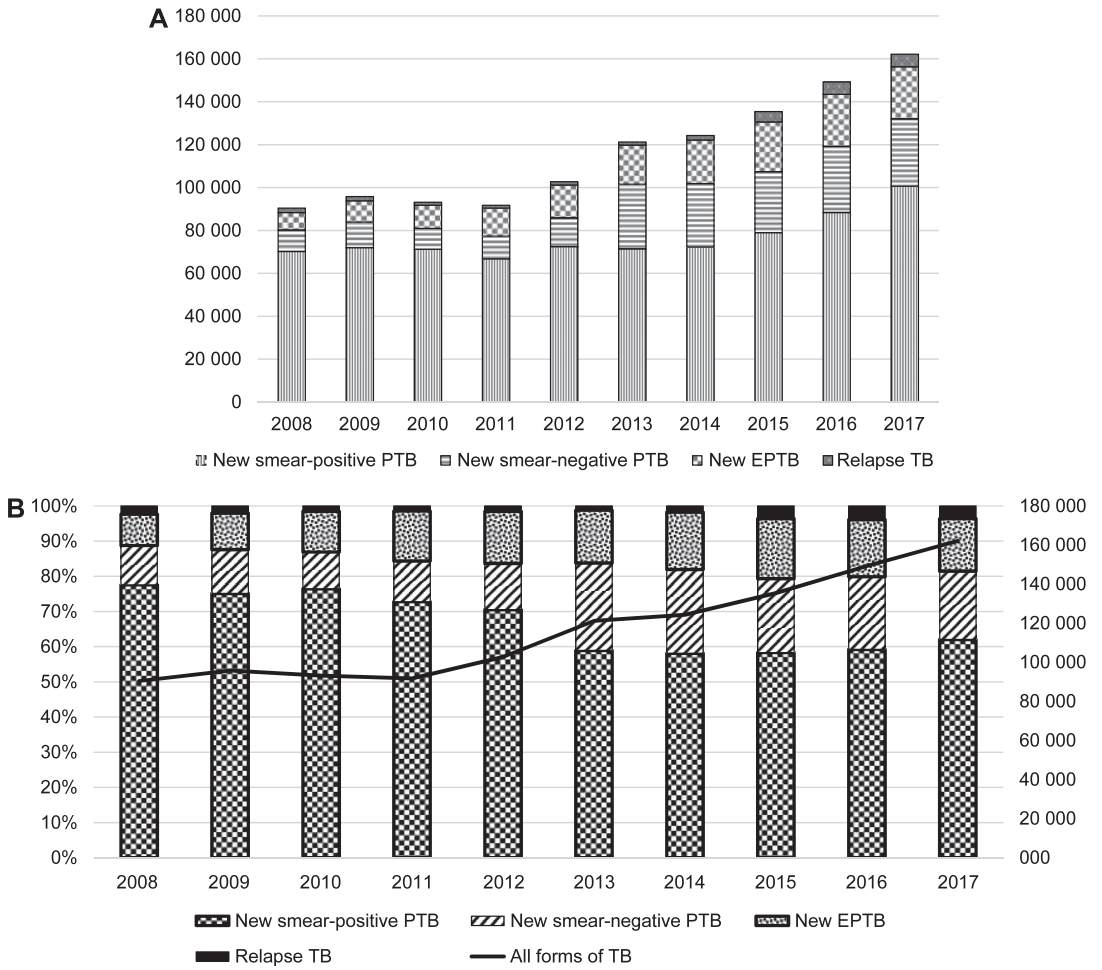

Figure 3 Annual trend in TB case notification before (2008–2012) and during (2013–2017) the implementation of financial support scheme in BRAC*-administered areas, Bangladesh, 2008–2017. *A development organisation, has been implementing TB control programme in Bangladesh in collaboration with the National TB Control Programme. Under BRAC-administered areas, there are 42 district level units, 297 TB treatment units and 445 peripheral microscopy laboratories (including urban areas). **A)** Absolute numbers of notifications of all TB patients, Bangladesh, 2008–2017; **B)** Hundred percent compound bar diagram. TB = tuberculosis; PTB = pulmonary TB; EPTB = extrapulmonary TB.

Annual trend in TB case notifications, 2008–2017

In 2008, there were 90 419 people with TB notified, of which 70 137 had new smear-positive PTB. However, in 2013, notification increased sharply up to 121 239, and the increasing trend was sustained up to 2017. The number of new smear-negative PTB increased from 10 110 in 2008 to 30 141 in 2013 and 31 453 in 2017. During the same period, the number of people detected with new EPTB increased from 8059 in 2008 to 18 181 in 2013 and 24 220 in 2017 (Figure 3).

Quarterly case notification rates: observed vs. forecasted (2013–2017)

There was a sharp rise in corresponding new smear-negative PTB CNR, which was sustained through 2017. Forecasting showed that the observed quarterly new smear-negative PTB CNR during 2013–2017 was significantly higher than the forecasted CNR. The new EPTB and all forms TB CNR was not significantly higher than the forecasted CNRs (Figure 4).

Profile of beneficiaries, test costs reimbursed and time intervals

Of the 1423 persons reimbursed (in a sample of 25 reporting units), 1376 were presumed to have smear-negative PTB and 47 had presumptive EPTB. Over 70% belonged to the 15–44-years age group; 49.2% were males. Government facilities had been the source of referral in 40.5% of cases, and the remaining were referred from private facilities (Table 1).

While chest radiographs (CXRs; 1320/1376, 95.9%) and fine-needle aspiration cytology or biopsy (44/47, 93.7%) were the most commonly reimbursed tests, complete blood count (1278/1376, 92.9%), Mantoux testing (415/1376, 30.2%) and renal function tests (216/1376, 15.7%) were also commonly reimbursed (Table 2). Among those receiving the Mantoux test, 91% (379/415) were adults (age ≥15 years).

The median total reimbursement received was US$11.8 (IQR 9.2–14.5); respectively US$9.7 (IQR

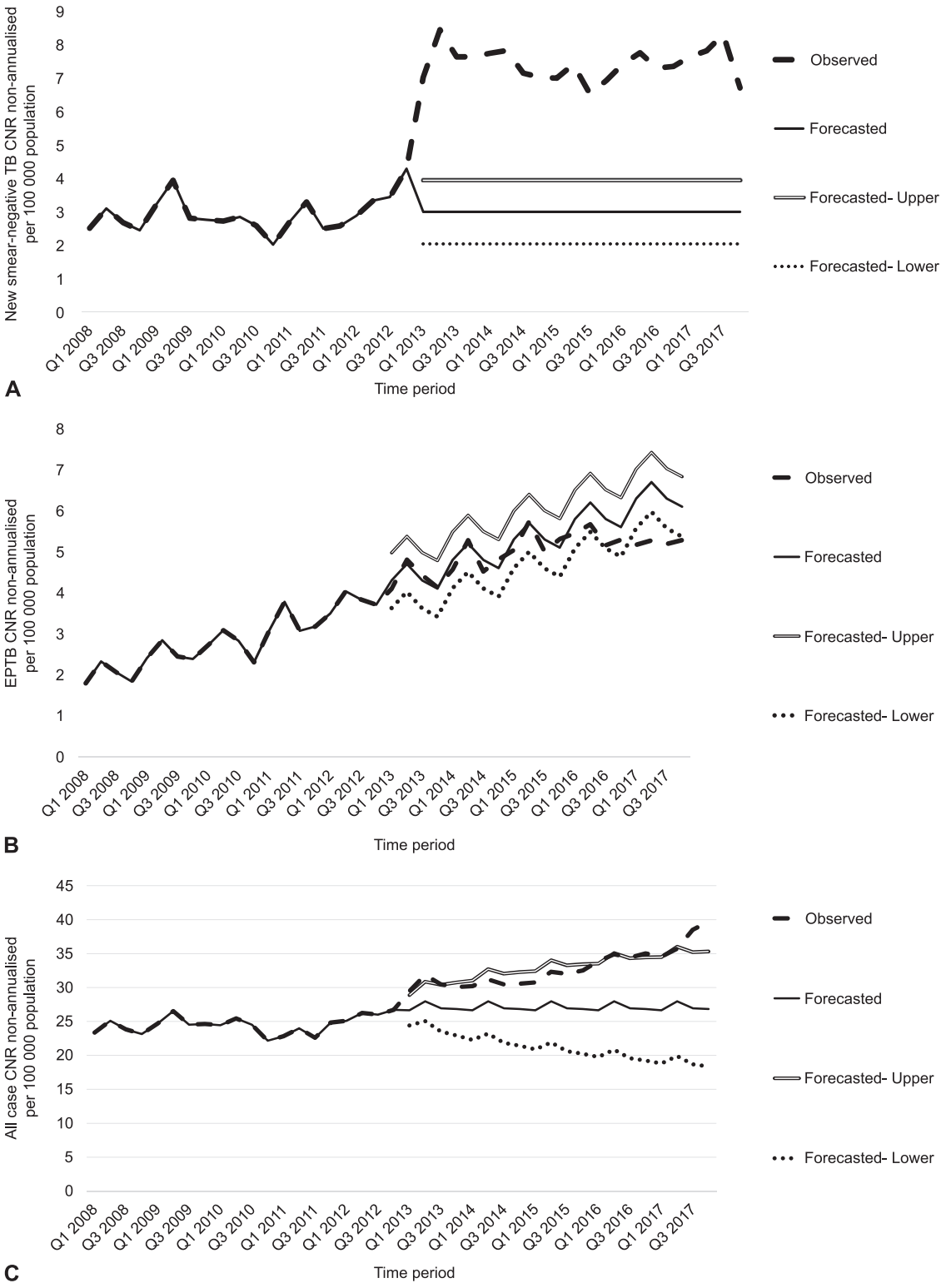

Figure 4 Comparison of observed versus forecasted* quarterly TB case notification rates during the implementation of the 2013–2017 financial support scheme in BRAC†-administered areas, Bangladesh. *Forecasting based on observed quarterly TB case detection rates before the implementation of the 2008–2012 financial support scheme. †A development organisation that has been implementing TB control programmes in Bangladesh in collaboration with the National TB Control Programme. Under BRAC-administered areas, there are 42 district level units, 297 TB treatment units and 445 peripheral microscopy laboratories (including urban areas). **A)** New smear-negative PTB; **B)** new EPTB; **C)** all form TB. TB = tuberculosis; PTB = pulmonary TB; EPTB = extrapulmonary TB; CNR = case notification rate.

Table 1 Sociodemographic, clinical and referral characteristics among people* with presumptive smear-negative pulmonary TB and presumptive extra-pulmonary TB who received financial support in BRAC†-administered areas, Bangladesh, July–September 2017

	Presumptive smear-negative pulmonary TB		Presumptive extra-pulmonary TB		Total	
Variable	*n*	(%)	*n*	(%)	*n*	(%)
Total	1376	(100)	47	(100)	1423	(100)
Age group, years						
<15	91	(6.6)	7	(14.9)	98	(6.9)
15–24	165	(12.0)	12	(25.5)	177	(12.4)
25–34	258	(18.8)	14	(29.8)	272	(19.1)
35–44	212	(15.4)	6	(12.8)	218	(15.3)
45–54	267	(19.4)	3	(6.4)	270	(19.0)
55–64	207	(15.0)	3	(6.4)	210	(14.8)
≥65	154	(11.2)	2	(4.3)	156	(11.0)
Missing	22	(1.6)	0	(0.0)	22	(1.5)
Sex						
Male	677	(49.2)	20	(42.6)	697	(49.0)
Female	699	(50.8)	27	(57.4)	726	(51.0)
Occupation						
Student	132	(9.6)	9	(19.1)	141	(9.9)
Household work	577	(41.9)	21	(44.7)	598	(42.0)
Unemployed	29	(2.1)	0	(0.0)	29	(2.0)
Daily wage labourer	170	(12.4)	2	(4.3)	172	(12.1)
Agriculture or animal rearing	283	(20.6)	10	(21.3)	293	(20.6)
Service	30	(2.2)	3	(6.4)	33	(2.3)
Shopkeeper or business	53	(3.9)	0	(0.0)	53	(3.7)
Professional	4	(0.3)	0	(0.0)	4	(0.3)
Other	58	(4.2)	1	(2.1)	59	(4.1)
Missing	40	(2.9)	1	(2.1)	41	(2.9)
Referred from						
Government facility	559	(40.6)	18	(38.3)	577	(40.5)
Private facility	805	(58.5)	29	(61.7)	834	(58.6)
Missing	12	(.9)	0	(0)	12	(.8)
Number diagnosed	219	(15.9)	42	(89.4)	261	(18.3)

* 21/297 BRAC TB treatment units and 4/63 BRAC urban reporting units were randomly selected, includes all the beneficiaries of social support scheme during the period of July–September 2017.
† A development organisation, which has been implementing the TB control programme in Bangladesh in collaboration with the Bangladesh National TB Control Programme. There are 42 district level units, 297 TB treatment units and 445 peripheral microscopy laboratories (including urban areas) under BRAC-administered areas.
TB = tuberculosis.

7.3–12.6) were received for investigations and US$1.3 (0.7–2.2) for transport. The median reimbursement for food and accommodation were US$2.4 (IQR 0.6–3.6) (Table 2). The median reimbursement by type of test was as follows: US$3.6 (IQR 3.0–4.8) for CXR, US$3.6 (IQR 3.6–4.8) for complete blood count, US$3.6 (IQR 2.4–3.6) for renal function test, US$3 (IQR 2.4–3.6) for Mantoux test and US$13.3 (IQR 11.8–18.2) for fine-needle aspiration cytology (Table 2). The median duration between investigations and reimbursement was 7 days (IQR 4–12) and between initial smear-negative results and treatment initiation was 9 days (IQR 6–15) (Table 3).

DISCUSSION

There is limited published literature worldwide on financial support to reimburse direct costs among people with presumptive smear-negative PTB and presumptive EPTB. We were therefore not able to find data from peer-reviewed studies for comparison.

A large number of people in BRAC-administered areas of Bangladesh were reimbursed under the scheme, with satisfactory (24%) detection ratio. Improvement in detection ratios despite reduction in the total number of people with presumptive TB screened (and reimbursed) over the years meant that BRAC improved its efficiency of fund and programme management. However, this also resulted in less people being detected under the scheme in 2017, which coincided with a sharp decline in the number of people with presumptive TB who were screened and budgets. During the implementation of the scheme, nationally, there was an increase in the absolute numbers of new smear-negative PTB, new PTB and all forms of TB notified.

There were significant improvements in new, smear-negative PTB CNRs during implementation; however, this did not translate into a consistent increase in all form TB CNRs, but for the initial and last few quarters of implementation. This was possibly due to a limited increase in new EPTB CNR attributable to the scheme. When compared to tests for presumptive smear-negative PTB, tests for

Table 2 Investigations and reimbursements (in US$)* among people† with presumptive smear-negative PTB and presumptive EPTB who received financial support in BRAC‡-administered areas, Bangladesh, July–September 2017

	Presumptive smear-negative PTB				Presumptive EPTB				All presumptive			
Variable	*n*	(%)	Median	[IQR]	*n*	(%)	Median	[IQR]	*n*	(%)	Median	[IQR]
Total reimbursement	1376	(100)	11.5	[9.1–14.1]	47	(100)	17.1	[12.4–21.8]	1423	(100)	11.8	[9.2–14.5]
Investigations	1376	(100)	9.7	[7.9–12.5]	47	(100)	13.3	[12.1–18.2]	1423	(100)	9.7	[7.3–12.6]
Transport allowance	1376	(100)	1.3	[0.7–2.2]	47	(100)	3	[1.8–4.7]	1423	(100)	1.3	[0.7–2.2]
Other	1376	(100)	2.4	[0.6–3.6]	47	(100)	0.8	[0.7–0.8]	1423	(100)	2.4	[0.6–3.6]
Tests performed												
Chest radiograph	1320	(95.9)	3.6	[3.0–4.8]	1	(2.1)	4.8	[4.8–4.8]	1321	(92.8)	3.6	[3.0–4.8]
Pleural tap	0		0	0	1	(2.1)	12.7	[12.7–12.7]	1	(0.1)	12.7	[12.7–12.7]
Complete blood count	1278	(92.9)	3.6	[3.6–4.8]	2	(4.3)	5.5	[5.2–5.8]	1280	(90)	3.6	[3.6–4.8]
Renal function test	216	(15.7)	3.6	[2.4–3.6]	0		0	0	216	(15.2)	3.6	[2.4–3.6]
Fine-needle aspiration cytology	0		0	0	42	(89.4)	13.3	[11.8–18.2]	42	(3)	13.3	[11.8–18.2]
Biopsy	0		0	0	2	(4.3)	26.7	[21.8–31.5]	2	(0.1)	26.7	[21.8–31.5]
Mantoux test	415	(30.2)	3	[2.4–3.6]	0		0	0	415	(29.2)	3	[2.4–3.6]
Ultrasonography	10	(0.7)	6.1	[5.2–6.1]	1	(2.1)	7.9	[7.9–7.9]	11	(0.8)	6.1	[5.5–6.1]
Transport for X-pert test	8	(0.6)	6.1	[6.1–6.1]	0		0	0	8	(0.6)	6.1	[6.1–6.1]
Other (transport cost)	787	(57.2)	1.5	[1.2–1.8]	1	(2.1)	2.4	[2.4–2.4]	788	(55.4)	1.5	[1.2–1.8]

* US$1 = BDT82.5.
† 21/297 BRAC TB treatment units and 4/63 BRAC urban reporting units were randomly selected, includes all the beneficiaries of social support scheme during the period of July–September 2017.
‡ A development organisation, which has been implementing the TB control programme in Bangladesh in collaboration with the Bangladesh National TB Control Programme. There are 42 district level units, 297 TB treatment units and 445 peripheral microscopy laboratories (including urban areas) under BRAC-administered areas.
PTB = pulmonary TB; EPTB = extra pulmonary TB; IQR = interquartile range; TB = tuberculosis; BDT = Bangladesh taka.

presumptive EPTB are costlier. Anecdotally, it is possible that the programme staff preferred to cover a greater number of people with presumptive smear-negative PTB than using the same amount of money to cover a fewer number of people with presumptive EPTB.

Individual-level analysis indicated that under the financial support scheme, time intervals from initial smear-negative results to investigations followed by reimbursement and treatment initiation were satisfactory. Long health system delays among TB patients have been reported from Bangladesh, especially if patients first visit informal health practitioners.[12]

Most people who were reimbursed for CXR were also reimbursed for complete blood count. One in six were reimbursed for renal function testing. Mantoux tests were performed in every third person, predominantly among adults. Among adults in high TB transmission settings, the test does not aid in the diagnosis of active TB.[13] The costs of one complete blood count or renal function test or Mantoux test were similar to one CXR. Therefore, although the average amount reimbursed per person was within the desirable limits, there is some scope to efficiently target the scheme to TB-specific tests and avoid reimbursing tests that are of minimal use for TB diagnosis (the scheme was implemented to detect more TB).

Study strengths and limitations

The study included aggregated, nationally representative data that covered two thirds of the country (BRAC-administered area). Individual-level beneficiary data were also taken from a nationally representative sample of reporting units under BRAC. Individual-level beneficiary data was quality-assured

Table 3 Time between referral and receipt of financial support among people* with presumptive smear-negative pulmonary TB and presumptive extra-pulmonary TB who received financial support in BRAC†-administered areas, Bangladesh, July–September 2017

	Presumptive smear-negative pulmonary TB			Presumptive extra-pulmonary TB			Total		
Turnaround time	*n*	Median	[IQR]	*n*	Median	[IQR]	*n*	Median	[IQR]^
Smear examination to treatment initiation	206	9	[6–15]	—	—	—	206	9	[6–15]
Smear examination to referral	1335	1	[0–4]	—	—	—	1335	1	[0–4]
Referral to investigations	1329	0	[0–1]	38	2	[0–7]	1367	0	[0–1]
Investigations to reimbursement	1345	7	[4–11]	47	15	[28–11]	1392	7	[4–12]
Reimbursement to treatment initiation	105	2	[0–6]	1	1	[1–1]	106	2	[0–6]

* 21/297 BRAC TB treatment units and 4/63 BRAC urban reporting units were randomly selected, includes all the beneficiaries of social support scheme during the period of July–September 2017.
† A development organisation, which has been implementing the TB control programme in Bangladesh in collaboration with the Bangladesh National TB Control Programme. There are 42 district level units, 297 TB treatment units and 445 peripheral microscopy laboratories (including urban areas) under BRAC-administered areas.
TB = tuberculosis; IQR = interquartile range.

with minimal data entry errors, as data were double-entered and validated.

However, the study had some limitations. First, as this intervention was implemented all over the country, in BRAC and in non-BRAC areas, we were unable to compare different arms; the study was thus restricted to a before-after analysis of the effect of the intervention on CNRs. Second, data on eligibility for the scheme (socio-economic status) was not routinely recorded by the programme. We were therefore not able to objectively assess whether or not the scheme had correctly targeted the poor. Patient-wise or reporting unit-wise aggregate data were not available on the number of presumptive smear negative PTB among those who were initially smear-negative at diagnosis and the number among these who were poor and therefore eligible for the scheme.. Hence, we were not able to assess the coverage of the scheme. Third, we did not take other interventions into consideration which might have had an effect on the increase in TB CNR during the intervention period.

Implications of the study

There are some policy and practice implications for BRAC. For greater efficiency of implementation, we recommend that the programme set an upper limit to the proportion of beneficiaries in a district or reporting unit who are reimbursed for more than a cut-off amount (say US$10). This could reduce the number of ancillary tests per person that do not help in TB diagnosis. To enable an objective assessment of targeting of the scheme, we recommend the addition of variables in laboratory microscopy registers to identify presumptive smear-negative PTB, presumptive EPTB and eligible beneficiaries (e.g., annual household income).

Future research

Cohort-wise assessment to determine the gaps in the care cascade from eligibility for investigations at public and private clinics and hospitals to referral for support and availing benefit may be carried out. This scheme has the potential to reduce catastrophic costs due to TB diagnosis, and patient cost surveys in Bangladesh should evaluate this factor as well. In future, patient and provider perspectives to identify areas for improvement, especially for presumptive EPTB may be explored through a qualitative systematic enquiry.

CONCLUSION

BRAC intends to support the Bangladesh NTP through the financial protection scheme in linking the poorest to diagnosis and improve the detection of new smear-negative PTB and new EPTB. Limitations notwithstanding, this study provides necessary evidence to suggest that there has been an increase in new smear-negative PTB CNR. However, there is need to increase the detection of new EPTB. We recommend addition of indicators in routine records to facilitate objective assessment of the scheme. The scheme could also focus reimbursing TB-specific diagnostics to improve its efficiency.

Acknowledgements

This research was conducted through the Structured Operational Research and Training Initiative (SORT IT), a global partnership led by the Special Programme for Research and Training in Tropical Diseases at the World Health Organization (WHO/TDR). The model is based on a course developed jointly by the International Union Against Tuberculosis and Lung Disease (The Union) and Medécins Sans Frontières (MSF/Doctors Without Borders). The specific SORT IT programme which resulted in this publication was jointly developed and implemented by The Union South-East Asia Office, New Delhi, India; the Centre for Operational Research, The Union, Paris, France; The Union, Mandalay, Myanmar; The Union, Harare, Zimbabwe; MSF Luxembourg Operational Research (LuxOR), Luxembourg; MSF Operational Centre Brussels (MSF OCB); Jawaharlal Institute of Postgraduate Medical Education and Research (JIPMER), Puducherry, India; Velammal Medical College Hospital and Research Institute, Madurai, India; National Centre for Tuberculosis Control and Prevention, China Centers for Disease Control and Prevention, Beijing, China; and Khesar Gyalpo University Medical of Sciences of Bhutan, Thimphu, Bhutan.

The author(s) received no specific funding for this work. The training programme was provided by the Department for International Development (DFID), London, UK. The funders had no role in study design, data collection and analysis, decision to publish, or preparation of the manuscript.

The data set and codebook used in this study are available on request from the corresponding author (sardar.munim@outlook.com)

Conflicts of interest: none declared.

Disclaimer: The contents of this paper do not necessarily reflect the views of the Government of Bangladesh, BRAC, Velammal Medical College Hospital and Research Institute, Karuna Trust or The Union.

References

1 World Health Organization. Global tuberculosis report, 2018. WHO/CDS/TB/2018.20. Geneva, Switzerland: WHO, 2018.
2 World Health Organization. Global tuberculosis report, 2012. WHO/HTM/TB/2012.6. Geneva, Switzerland: WHO, 2012.
3 World Health Organization. Global tuberculosis report, 2013. WHO/HTM/TB/2013.11. Geneva, Switzerland: WHO, 2013.
4 World Health Organization. Tuberculosis patient cost survey: a handbook. Geneva, Switzerland: WHO, 2017.
5 Bangladesh National Tuberculosis Control Programme. Tuberculosis control in Bangladesh. Annual report 2017. Dhaka, Bangladesh: NTP, 2017.
6 Bangladesh National Tuberculosis Control Programme. National guidelines and operational manual for tuberculosis control. 5th ed. Dhaka, Bangladesh: NTP, 2013.
7 BRAC. BRAC Annual Report 2017. Dhaka, Bangladesh: BRAC, 2016.
8 Pan Y, Chen S, Chen M, et al. Disparity in reimbursement for tuberculosis care among different health insurance schemes: evidence from three counties in central China. Infect Dis Poverty 2016; 5: 7.
9 Wei X, Zou G, Yin J, et al. Effective reimbursement rates of the rural health insurance among uncomplicated tuberculosis patients in China. Trop Med Int Health 2015; 20: 304–311.
10 Klein S J, Laufer F N. A simple methodology to finance public health initiatives: reimbursement for tuberculosis directly observed therapy services in New York State. J Public Health Manag Pract 1995; 1: 7–13.

11 World Health Organization. WHO Country profile: Bangladesh. Geneva, Switzerland: WHO, 2019. https://www.who.int/countries/bgd/en/ Accessed December 2019.
12 Rifat M, Rusen I D, Islam M A, et al. Why are tuberculosis patients not treated earlier? A study of informal health practitioners in Bangladesh. Int J Tuberc Lung Dis 2011; 15: 647–651.
13 US Department of Health and Human Services, Centers for Disease Control and Prevention. Mantoux tuberculin skin testing facilitator guide. Atlanta, GA, USA: CDC, 2013.

RÉSUMÉ

CONTEXTE : Les régions administrées par l'organisation non-gouvernmentale BRAC du Programme National Tuberculose du Bangladesh (42 sur 64 districts). Un système de soutien financier (2013–2017) a remboursé les coûts directs dus au diagnostic de tuberculose (TB) aux patients en difficultés économiques avec une suspicion de tuberculose pulmonaire (PTB à frottis négatif) et de TB extrapulmonaire (EPTB).

OBJECTIF : Décrire la mise en œuvre de ce système et des modifications associées en matière de notification des cas.

SCHÉMA : Etude descriptive basée sur les données du programme

RÉSULTATS : Entre 2013 et 2017, le nombre de patients remboursés est passé de 125 680 à 88 763 et le taux de détection des cas a augmenté de 18% à 24%. Le nombre des patients suspects d'EPTB qui ont été remboursés a diminué de 5024 à 3484. Plus de 95% ont été remboursés pour la radiographie pulmonaire, la cytologie par aspiration à l'aiguille et la biopsie. Un grand nombre d'autres investigations ont cependant également été remboursées. Entre 2013 et 2017, le taux observé au niveau national par trimestre de notification de nouveaux cas (CNR) de PTB à frottis négatif a été significativement plus élevé que prévu (basé sur les tendances du CNR entre 2008 et 2012). Les CNR des nouveaux cas de EPTB et de toutes les formes de TB ont augmenté mais pas significativement.

CONCLUSION : La mise en œuvre du système de soutien financier a été accompagnée par une amélioration significative de la notification des nouveaux cas de PTB à frottis négatif. L'absence de bras de comparaison a été une limitation majeure mais la comparaison n'a pas été possible puisque le système a été mis en œuvre dans tous les districts.

RESUMEN

MARCO DE REFERENCIA: Las zonas del programa nacional contra la tuberculosis (TB) de Bangladesh administradas por la organización BRAC (42 de 64 distritos). El plan de apoyo económico (2013–2017) reembolsaba los costos directos derivados del diagnóstico de la TB a las personas económicamente desfavorecidas, con baciloscopia negativa y presunción clínica de TB pulmonar (PTB) y con presunción de TB extrapulmonar (EPTB).

OBJETIVO: Describir la ejecución del plan de apoyo y los cambios observados en la notificación de casos.

MÉTODO: Fue este un estudio descriptivo a partir de los datos del programa.

RESULTADOS: Del 2013 al 2017 el número de personas que recibieron reembolso disminuyó de 125 680 a 88 763 y la proporción de casos detectados aumentó de 18% a 24%. El número de personas con presunción diagnóstica de EPTB que recibieron reembolso disminuyó de 5024 a 3484. Los reembolsos de la radiografía de tórax y de la citología y biopsia aspirativa fueron superiores al 95%. Sin embargo, también se reembolsó un gran número de investigaciones complementarias. Del 2013 al 2017, se observaron a escala nacional tasas trimestrales de notificación de casos (CNR) nuevos de PTB con baciloscopia negativa significativamente superiores a las previstas (según las tendencias de notificación del 2008–2012). Las CNR nuevos de EPTB y de todas las formas de TB aumentaron, pero sin alcanzar significación estadística.

CONCLUSIÓN: La ejecución del plan de apoyo económico indujo una mejoría significativa en la CNR de PTB con baciloscopia negativa. Una limitación importante del estudio fue la ausencia de grupo de referencia, pero la comparación no fue posible debido a que el plan se ejecutó en todos los distritos del país (BRAC y no BRAC).

Short Communication

Kathiresan Jeyashree, Jane S. Sathiavadivu and AbdulkaderRizwan Suliankatchi*

App-based tracking of smartphone use and its association with perceived stress and sense of coherence among undergraduate medical students in Southern India

https://doi.org/10.1515/ijamh-2018-0296
Received December 29, 2018; accepted January 24, 2019

Abstract

Objectives: Smartphone use, now a ubiquitous habit among the youth and psychological stress are interestingly juxtaposed. Sense of coherence (SOC) is the ability to comprehend a stressful situation and tackle it positively. This study measured the pattern of smartphone use, perceived stress, SOC and the inter-relationship between them among undergraduate medical students.

Methods: Perceived Stress Scale (PSS-10) and SOC-13 scales were used to measure perceived stress and SOC, respectively in 163 medical college students. 'App Usage', a mobile application was used to objectively record smartphone usage.

Results: Nearly two-thirds (64.4%) were female students. The mean (SD) SOC score was 48.7 (11.1) and the mean (SD) PSS score was 20.7 (6.2). SOC was inversely correlated ($r=-0.662$, $p<0.001$) with PSS. The median (IQR) duration of smartphone use was 3.4(1.8, 4.8) hours per day which was not significantly correlated with perceived stress (rho=0.12, p=0.26). Linear regression showed that male students used smartphones for a longer duration than females (p=0.0008), after controlling for confounders.

Conclusions: Medical college students use smartphones for an average of 3 to 4 h a day. Students with a better sense of coherence perceive less stress. Initiatives to improve the sense of coherence will help increase their resilience and reduce susceptibility to problematic use of smartphones.

Keywords: college students; psychological stress; sense of coherence; smartphone use.

Background

Smartphone use is one of the latest additions to the ever-expanding list of behaviors that affect health of the millennials. Besides communication, smartphones are used for entertainment, education, business, and a multitude of other purposes. Although they have enormous practical applications, problematic use of smartphones has been associated with many physical and psychological health issues. The commonly reported psychological effects of smartphone overuse are lack of concentration, sleeplessness, anxiety and stress [1–3]. The measurement of smartphone use for epidemiological purposes has been fraught with difficulties, the most important among them being the lack of a universally agreed upon definition of smartphone addiction or abuse [4]. Most published studies have used questionnaires such as the Smartphone Addiction Scale [5], or the Problematic Use of Mobile Phone scale [6] whereas others have depended on respondents' self-reported overuse or addiction.

Problematic use of smartphones has a bidirectional relationship with psychological health and stress. Smartphones can serve as a recreational tool to vent out stress but the excessive use of the same can lead to mounting of stress. Stress is a phenomenon that is increasingly being recognized as an important health condition in modern

***Corresponding author: Dr. Rizwan Suliankatchi Abdulkader**, Department of Statistics, Manonmaniam Sundaranar University, Abishekapatti, Tirunelveli, Tamil Nadu, 627012, India; ICMR-National Institute of Epidemiology, Chennai, Tamil Nadu, India, Phone: +918447284098, E-mail: sarizwan1986@gmail.com
Kathiresan Jeyashree and Jane S. Sathiavadivu: Department of Community Medicine, Velammal Medical College Hospital and Research Institute, Madurai, Tamil Nadu, India, E-mail: jshreek@gmail.com (K. Jeyashree), jane1611@yahoo.com (J.S. Sathiavadivu). https://orcid.org/0000-0001-6459-3659 (K. Jeyashree)

times. One of the commonly accepted definition states that 'stress is the perception of threat, with resulting anxiety, discomfort, emotional tension, and difficulty in adjustment' [7]. While stress is common to all age groups, the determinants, symptoms and effects of stress are different across different age groups. Consequently, any factor that increases or reduces stress is looked upon as being a potential target for behavior change [8].

College going students, especially medical undergraduates are experience a considerable amount of stress [9, 10]. Their approaches to dealing with stress can have a major influence on their health. One can respond to a stressful situation with a positive attitude or with a negative one. The ability to comprehend the whole picture of a stressful situation and the capacity to use the available resources to tackle it is known as the sense of coherence (SOC) [11]. SOC is one of the concepts related to the Salutogenesis theory – the origin of health. A strong SOC reflects a higher individual capability to comprehend and manage stress and weak SOC was associated with risk behaviors and poor self-reported health among adolescents [12–14]. A person with a poor SOC continues to experience increasing levels of stress, which in turn can have serious and debilitating health consequences [15, 16].

Our hypothesis is that smartphone use, SOC and perceived stress are associated with each other. Understanding this association is crucial to be able to bring about behavioral change to reduce levels of perceived stress. This study aimed to assess the pattern of smartphone usage, perceived stress, sense of coherence and the inter-relationship between them among a sample of medical undergraduate students.

Methodology

This analytical cross sectional study collected data from students pursuing their undergraduate degree in Medicine in a private medical college in South India. In India, students complete 12 years of schooling at 16–17 years of age after which they appear for a competitive examination and directly enter the medical undergraduate course. The undergraduate degree in India is M.B.B.S (Bachelor of medicine and Bachelor of Surgery) which is a five and half years long (Four and a half years plus one year of compulsory residential rotatory internship) course. On successful completion of the same, the students may go on to become general practitioners or choose to specialize in medical or surgical specialties, entry to which is again regulated by competitive entrance examinations.

Sample sizes for this study were calculated based on the formula for estimating a single proportion with a pre-stated precision level. It was not based on the need to prove or disprove a premeditated null hypothesis for detecting a difference between two groups. The inputs for the sample size formula were based on estimates of abnormal smartphone usage and stress from previous studies conducted in a similar population [4, 9, 10]. The minimum required sample sizes calculated were 84 for acquiring smartphone usage data and 173 for acquiring data on stress levels.

All eligible students studying in the second and third year were invited to participate in this study on a voluntary basis. The recruitment was based on pre-defined selection criteria and was continued till the required sample size was satisfied. However, at the end of the study the total number achieved was 163.

Study instruments

Three main parameters were measured in this study– duration of perceived stress, sense of coherence and smartphone usage.

The perceived stress levels were measured using the ten-item version of the perceived stress scale (PSS-10) [17, 18] and the sense of coherence was measured using the SOC-13 scale [19]. The SOC-13 captures three domains of sense of coherence – comprehensibility, manageability, and meaningfulness [11]. English version questionnaires of both PSS-10 and SOC-13 were self-administered. In addition to these, socio-demographic characteristics such as gender, year of study and economic class (according to *Kuppuswamy* scale 2017) were also collected [20].

Data on smartphone usage was measured with the help of a mobile application called *App Usage* [6], which measures the amount of time spent by the user in each application on the smartphone. Students were briefed about the mobile application and how to install the same in their respective mobile phones. The typical working days for the study populations are between Monday to Friday and the two day weekend comprising Saturday and Sunday. The app recorded the mobile phone usage of the students for three days (inclusive of one day on the weekend). Mobile usage data was collected during the same week (Sunday to Saturday) when SOC and perceived stress were measured, to avoid the influence of any major stressor that might occur in the interval between measurements. The data from the app was then exported to Excel and emailed by the student to the investigator.

Since *App Usage* could only be used only on android platforms, students who owned smartphones based on iOS or Microsoft OS could not provide mobile usage data. A total of 163 consenting and sequentially sampled students filled up the PSS and the SOC, of whom 85 agreed to share the smartphone usage data.

The study was approved by the Institute Ethics Committee of Velammal Medical College Hospital and Research Institute, Madurai. Informed written consent was obtained from the students. Confidentiality of information was maintained by restricting access to data to principal investigator only.

Statistical analysis

Data was entered using EpiData entry v.3.1, Odense, Denmark and analyzed using the software package, STATA v.11.0. Correlation between duration of smartphone use and the PSS and the SOC scores was calculated using Pearson product moment correlation or Spearman's rank correlation coefficients. Subgroup analysis by gender was presented wherever deemed necessary. Hierarchical multiple linear regression models were built to determine factors significantly associated with the duration of smartphone use and perceived stress. A p value of <0.05 was considered to be statistically significant. Model performance was assessed by means of R square and other related statistics.

Results

A total of 163 students participated in the study, of whom 105 (64.4%) were females. Most (92%) belonged to upper or upper middle class. The mean (SD) SOC score was 48.7 (11.1) and the mean (SD) PSS score was 20.7 (6.2). The SOC (p=0.3) and the PSS (p=0.68) were not significantly different across genders (Table 1).

Table 1: Perceived stress scale and sense of coherence scores among college going students (n=163).

Score	Male		Female		All	
	Mean	SD	Mean	SD	Mean	SD
Perceived stress (40)	21.0	6.7	20.6	5.9	20.7	6.2
Sense of coherence (91)	47.6	11.7	49.3	10.8	48.7	11.1
Meaningfulness (28)	15.9	4.1	17.1	3.9	16.6	4.0
Manageability (28)	14.6	5.0	14.9	4.8	14.8	4.8
Comprehensibility (35)	17.0	5.7	17.3	5.1	17.1	5.3

*Numbers within brackets are the maximum possible scores on the given scale.

The median (IQR) duration of smartphone use was found to be 3.43 (95% confidence intervals: 1.83, 4.77) hours. Females (2.52, 95% CI: 1.57, 3.73 h) used their smartphones for significantly (p=0.003) lesser time than males (4.02, 95% CI: 3.12, 5.09 h). Seventy percent of the students used the smartphone for 1–5 h in a day and 18% used smartphones for more than 5 h in a day. Based on the duration of use, the most commonly used apps were *YouTube* (18%), phone dialer (14%) and *WhatsApp* (13%). The mean (SD) age at which the participants had started using a mobile phone was 15.2 (2.6) years and the mean (SD) age at which they first owned a mobile phone was 17.3 (1.5) years.

The perceived stress score was inversely correlated with the SOC (r=−0.662, p<0.001); with increase in the sense of coherence, the perceived stress level decreased. Duration of smartphone use showed no significant correlation with perceived stress (rho=0.122, p=0.268) (Figure 1) or one's sense of coherence (rho=0.064, p=0.558). The younger a student was when s/he had owned the first mobile phone, the longer was their average per day duration of smartphone usage (rho=−0.245, p=0.024)

Female students used smartphones for a lesser duration as compared to their male counterparts (p=0.008). This association persisted even after controlling for factors such as age at owning first mobile phone, perceived stress, sense of coherence and socioeconomic status (Table 2).

Discussion

Our study among college going students aged 18–22 years in southern India showed that the daily average smartphone use duration was around 3.4 h. The mean perceived stress score among the students was 20.7, which was negatively correlated with their sense of coherence.

Smartphone use

Mobile phone addiction or abuse in itself is a rather vague term and its reported prevalence ranges from 0 to 38% worldwide, across all age groups [21]. Smartphone overuse has been documented to affect 39–44% of young adults in India [4]. A similar proportion has been documented among younger, school going adolescents too [22]. Problematic use of mobile phones leading to *ringxiety* or phantom ringing and *nomophobia* or fear of being out of

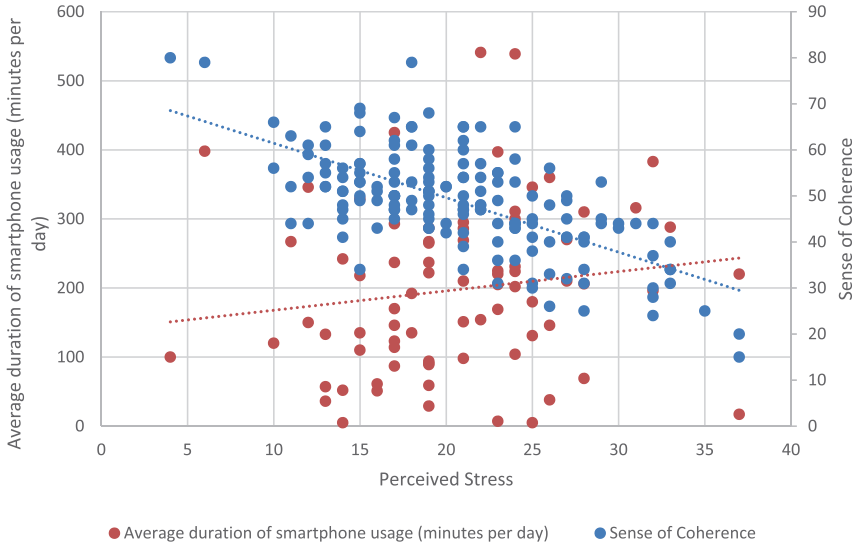

Figure 1: Correlation of perceived stress scale scores with sense of coherence and average duration of smartphone use among college going students.

Table 2. Factors associated with duration of smartphone use among college going students (n=85).

Factors	Coefficient	Standard error	p-Value	95% CI	
Perceived stress	4.93	2.87	0.09	−0.78	10.64
Sense of Coherence	2.59	1.44	0.07	−0.28	5.45
Gender (Female)	−72.01	26.34	0.008	−124.49	−19.54
Socioeconomic class					
Upper middle class	−32.71	26.42	0.22	−85.33	19.91
Lower middle class	−74.22	55.13	0.18	−184.01	35.56
Upper lower class	79.68	71.38	0.26	−62.46	221.82
Age at owning first mobile	−15.49	11.08	0.16	−37.55	6.57

mobile phone contact have been reported to affect 18–34% of medical college students in India [23, 24]. Neha et al., who performed a questionnaire, based assessment of the mobile phone use among medical college student's reported estimates comparable to ours [25].

On a typical working day, students are prohibited from using mobile phones within teaching premises in the college and the hospital, as is the rule in most medical colleges in India. This is expected to reflect in their usage of mobile phones during a typical working day. We had tried to circumvent this issue by calculating the duration of mobile phone use over three days including one day of the weekend. Further, it is not uncommon for students to use mobile phones in restricted areas such as classrooms and the usage is more during the night [26]. Hence, the current study is likely to provide a reasonably good estimate of the average duration of smartphone use in a day by a college going student.

We found that smartphone initiation at a younger age was associated with a longer daily use. Age is positively associated with the ability to self-regulate one's usage of smartphones and addictive smartphone behavior is lesser is the older compared to their younger counterparts [27]. This finding may provide a rationale to the recommendation that young children should not be exposed to screens given by some international societies. We found that males used the phone for a longer duration than the females. There is no consensus in this regard in existing literature where some studies found gender differentials similar to ours[28], some concluded the opposite [27, 29] and others found a comparable prevalence of smartphone addiction among males and females [30]. The motives to use smartphones and the psychological effects have been described to be different across both genders [30, 31]. Categorizing the exact purpose for which the smartphone was used, could have helped us interpret this difference.

Smartphone use and stress

Smartphone use has been reported to be associated with psychological conditions including low emotional stability, depression, anxiety, sleep disturbances and stress [1, 3, 32]. Stress has been hypothesized to be associated with problematic smartphone use as is the case with other addictions [2, 33–35]. On the other hand, paradoxically, mobile phones have also been used to track and help treat some psychological conditions [36, 37]. A statistically insignificant correlation was observed between average mobile phone usage duration and perceived stress in our study. A detailed understanding of the pattern of mobile use such as the type of apps used, most frequently used times, day and night usage and the people most frequently contacted for calls or messaging would have helped us understand the association better but due to the limited scope of the study we were unable to do such exploration. Our study was also limited by the small sample size for mobile phone usage duration making it difficult to draw emphatic conclusions about this association.

Stress and SOC

An individual's response to stress is modeled on different parameters that were effectively put together by Antonovsky to mean sense of coherence. Sense of coherence has been previously found to be negatively associated with stress and related symptoms [15]. Our study also confirmed a statistically significant negative correlation between SOC and stress. It may be worthwhile to invest in strategies that tap into the generalized resistance resources of the students and build their SOC to help them tackle stress. Stress, beyond allowable levels, is not only a deterrent to academic performance and also manifests as organic disorders of the body and mind.

The smartphone use, SOC and stress triad

While the relationship between stress and SOC is quite linear [15, 16, 38], the same is not true for smartphone use and SOC. Prior to the current study, there have been no attempts to examine the association between the two. Our study found a very weak correlation between the two. An individual's ability to draw from internal and external resources to combat a stressful situation determines his response. Mobile phones are an excellent medium of communication that have increased access to various resources and as such have the potential to contribute positively to one's SOC.

On the other hand, the problematic use of mobile phone, beyond a threshold, may be a reflection of poor SOC and thus contribute to high stress levels. Most addictions are used to distract oneself from a situation perceived as unmanageable. High mobile usage is expected to correlate with poor manageability scores on the SOC scale. A threshold-based stratification of the study population, as addicted or not addicted to mobile phones, would have helped us to study its correlation with SOC better. It is possible that none of the recruited students fall into the addicted category, thus leading to a lack of detectable correlation between SOC and mobile phone usage duration.

Strengths and limitations

Assessment of smartphone use can be done either based on calculation of time spent with it or based on behavioral patterns associated with smartphone usage. Both these measures can be self-reported or objectively assessed or measured. Self-reporting of mobile phone usage is known to suffer from disadvantages and its correlation with objectively assessed log data has been found to be less than satisfactory [39]. There are no studies from India that give an estimate of the average time, a student uses his or her mobile phone, using log-based data. To the best of our knowledge, this was the first study to use a smartphone application to collect data on phone usage duration. Since this is the first such attempt, we have refrained from establishing a cut-off to define overuse or addiction, which requires a study with a larger and more representative sample and measurement of many other confounders.

However, the convenient sample of medical college students limits the generalizability of the findings to all adolescents and young adults. Since the study was carried out only among medical students, it is generalizability to other types of students may be limited. The limited sample size of the study restricts the degree of precision as well as the generalizability of the findings to the larger general population of young adults. Although we recorded total duration of smart phone use, we did not collect data on the purpose of usage because we assumed that such data would be subjected to social desirability bias due to its self-reported nature. Information on other confounding factors that influence the relationship between stress and the duration of smartphone usage such as home, school, environment and mental health related factors were not recorded and this limited our ability to

develop a better explanatory model. Of the 163 participants only 85 agreed to provide smart phone usage data and we could not assess the effect of non-responders on the results. In light of this limitation, the results had been cautiously interpreted.

Conclusion

College students use smartphones for an average of 3 to 4 h in a day. Male and female students are equally stressed but students with better a sense of coherence report being less stressed.

Implications of the study

Mental health issues among adolescents and youth are a rising concern worldwide. Manifestations of stress in student population could vary and one such ill effect is addiction, which then initiates the vicious cycle of addiction-stress-addiction. Yet, through all these years of research, there have been no concrete or universal efforts to provide guidance to students in need nor have any preventive measures been implemented in a majority of the colleges. Initiatives to improve the sense of coherence among students will help them tackle stress positively.

Acknowledgments: None.
Funding: No funding was availed.
Author contributions: JK– conception of the idea, design of the study, data collection, data analysis, interpretation of results, writing the first draft, critically reviewing drafts and approval of final draft for publication, SJ– conception of the idea, design of the study, data collection, interpretation of results, critically reviewing drafts and approval of final draft for publication, and RSA– data analysis, interpretation of results, writing the first draft, critically reviewing drafts and approval of final draft for publication.
Competing interests: None.
Consent to participate: Written informed consent was obtained from all participants.
Consent for publication: All the authors have read the final draft of the manuscript and consent for publication.
Ethics approval: The Institute Ethics Committee of Velammal Medical College Hospital and Research Institute, Madurai approved the study.
Availability of data and material: The data is available on request with the corresponding author of the article.

References

1. Thomée S, Härenstam A, Hagberg M. Mobile phone use and stress, sleep disturbances, and symptoms of depression among young adults – a prospective cohort study. BMC Publ Health 2011; 11:66.
2. Samaha M, Hawi NS. Relationships among smartphone addiction, stress, academic performance, and satisfaction with life. Comput Human Behav 2016;57:321–5.
3. Sahin S, Ozdemir K, Unsal A, Temiz N. Evaluation of mobile phone addiction level and sleep quality in university students. Pakistan J Med Sci 2013;29:913–8.
4. Davey S, Davey A. Assessment of smartphone addiction in Indian adolescents: A mixed method study by systematic-review and meta-analysis approach. Int J Prev Med 2017;5:1500–11.
5. Kwon M, Lee JY, Won WY, Park JW, Min JA, Hahn C, et al. Development and validation of a smartphone addiction scale (SAS). PLoS One 2013;8:e56936.
6. Merlo LJ, Stone AM, Bibbey A. Measuring problematic mobile phone use: development and preliminary psychometric properties of the PUMP scale. J Addict 2013;2013:912807.
7. Fink G. Stress science: neuroendocrinology. San Diego: Academic Press, Elsevier Ltd; 2009.
8. Würtz ET, Fonager K, Mortensen JT. Association between sense of coherence in adolescence and social benefits later in life: a 12-year follow-up study. BMJ Open 2015;5:e006489.
9. Supe AN. A study of stress in medical students at Seth G.S. medical college. J Postgrad Med 1998;44:1–6. 10703558.
10. Dahlin M, Joneborg N, Runeson B. Stress and depression among medical students: a cross-sectional study. Med Educ 2005;39: 594–604.
11. Antonovsky A. The structure and properties of the sense of coherence scale. Soc Sci Med 1993;36:725–33.
12. Moksnes UK, Haugan G. Stressor experience negatively affects life satisfaction in adolescents: the positive role of sense of coherence. Qual Life Res 2015;24:2473–81.
13. Moksnes UK, Espnes GA. Stress, sense of coherence and subjective health in adolescents aged 13–18 years. Scand J Public Health 2017;45:397–403.
14. Elfassi Y, Braun-Lewensohn O, Krumer-Nevo M, Sagy S. Community sense of coherence among adolescents as related to their involvement in risk behaviors. J Community Psychol 2016; 44:22–37.
15. Flannery RB, Flannery GJ. Sense of coherence, life stress, and psychological distress: A prospective methodological inquiry. J Clin Psychol 1990;46:415–20.
16. McSherry WC, Holm JE. Sense of coherence: its effects on psychological and physiological processes prior to, during, and after a stressful situation. J Clin Psychol 1994;50:476–87.
17. Cohen S, Kamarck T, Mermelstein R. A global measure of perceived stress. J Health Soc Behav 1983;24:385.
18. Roberti JW, Harrington LN, Storch EA. Further psychometric support for the 10-item version of the perceived stress scale. J Coll Couns 2006;9:135–47.
19. Eriksson M, Lindström B. Validity of antonovsky's sense of coherence scale: a systematic review. J Epidemiol Community Health 2005;59:460–6.
20. Singh T, Sharma S, Nagesh S. Socio-economic status scales updated for 2017. Int J Res Med Sci 2017;5:3264–7.

21. Pedrero Pérez EJ, Rodríguez Monje MT, Ruiz Sánchez De León JM. Mobile phone abuse or addiction. A review of the literature. Adicciones 2012;24:139–52. 22648317.
22. Naik TD, Kadam YR, Patil SA, Gore AD. Mobile phone use and excess use among junior college students : a cross-sectional study. Int J Heal Allied Sci 2017;6:113–7.
23. Subba SH, Mandelia C, Pathak V, Reddy D. Ringxiety and the mobile phone usage pattern among the students of a medical college in South India. J Clin Diagn Res 2013;7:205–9.
24. Dixit S, Shukla H, Bhagwat AK, Bindal A, Goyal A, Zaidi AK, et al. A study to evaluate mobile phone dependence among students of a medical college and associated hospital of central India. Indian J Community Med 2017;35:339–41.
25. Nehra R, Kate N, Grover S, Khehra N, Basu D. Does the excessive use of mobile phones in young adults reflect an emerging behavioral addiction?. J Postgrad Med Educ Res 2012;46:177–82.
26. Tindell DR, Bohlander RW. The use and abuse of cell phones and text messaging in the classroom: a survey of college students. Coll Teach 2012;60:1–9.
27. van Deursen AJAM, Bolle CL, Hegner SM, Kommers PAM. Modeling habitual and addictive smartphone behavior: the role of smartphone usage types, emotional intelligence, social stress, self-regulation, age, and gender. Comput Human Behav 2015;45:411–20.
28. Aljomaa SS, AlQudah MF, Albursan IS, Bakhiet SF, Abduljabbar AS. Smartphone addiction among university students in the light of some variables. Comput Human Behav 2016;61:155–64.
29. Demirci K, Akgönül M, Akpinar A. Relationship of smartphone use severity with sleep quality, depression, and anxiety in university students. J Behav Addict 2015;4:85–92.
30. Chen B, Liu F, Ding S, Ying X, Wang L, Wen Y. Gender differences in factors associated with smartphone addiction: a cross-sectional study among medical college students. BMC Psychiatry 2017;17:341.
31. Chen C, Zhang KZK, Gong X, Zhao SJ, Lee MKO, Liang L. Examining the effects of motives and gender differences on smartphone addiction. Comput Human Behav 2017;75:891–902.
32. Augner C, Hacker GW. Associations between problematic mobile phone use and psychological parameters in young adults. Int J Public Health 2012;57:437–41.
33. Lam LT, Peng Z, Mai J, Jing J. Factors associated with internet addiction among adolescents. Cyber Psychology Behav 2009;12:551–5.
34. Lee H, Kim MS, Son HK, Ahn S, Kim JS, Kim YH. Discriminating power of socio-demographic and psychological variables on addictive use of cellular phones among middle school students. J Korean Acad Nurs 2007;37:957.
35. Chiu SI. The relationship between life stress and smartphone addiction on taiwanese university student: a mediation model of learning self-efficacy and social self-efficacy. Comput Human Behav 2014;34:49–57.
36. Proudfoot J, Clarke J, Birch M-R, Whitton AE, Parker G, Manicavasagar V, et al. Impact of a mobile phone and web program on symptom and functional outcomes for people with mild-to-moderate depression, anxiety and stress: a randomised controlled trial. BMC Psychiatry 2013;13:312.
37. Watts S, Mackenzie A, Thomas C, Griskaitis A, Mewton L, Williams A, et al. CBT for depression: a pilot RCT comparing mobile phone vs. computer. BMC Psychiatry 2013;13:49.
38. Larsson G, Kallenberg KO. Sense of coherence, socioeconomic conditions and health. Interrelationships in a nation-wide Swedish sample. Eur J Public Health 1996;6:175–80.
39. Boase J, Ling R. Measuring mobile phone use: self-report versus log data. J Comput Commun 2013;18:508–19.

BMJ Open

Household food insecurity among patients with pulmonary tuberculosis and its associated factors in South India: a cross-sectional analysis

Reshma Ayiraveetil ,[1] Sonali Sarkar,[1] Palanivel Chinnakali,[1] Kathiresan Jeyashree,[2] Mathavaswami Vijayageetha,[1] Pruthu Thekkur,[3,4] Subitha Lakshminarayanan,[1] Selby Knudsen,[5] Natasha S Hochberg,[5,6] C Robert Horsburgh,[5,6,7] Jerrold Ellner,[8] Gautam Roy[1]

To cite: Ayiraveetil R, Sarkar S, Chinnakali P, *et al*. Household food insecurity among patients with pulmonary tuberculosis and its associated factors in South India: a cross-sectional analysis. *BMJ Open* 2020;**10**:e033798. doi:10.1136/bmjopen-2019-033798

► Prepublication history and additional material for this paper are available online. To view these files, please visit the journal online (http://dx.doi.org/10.1136/bmjopen-2019-033798).

Received 12 September 2019
Revised 01 February 2020
Accepted 04 February 2020

For numbered affiliations see end of article.

Correspondence to
Dr Sonali Sarkar;
sarkarsonaligh@gmail.com

ABSTRACT

Objectives Food insecurity is 'the limited or uncertain availability of nutritionally adequate, safe foods or inability to acquire foods in socially acceptable ways'. Majority of tuberculosis (TB) cases of resource-poor settings experience food insecurity, which impacts treatment adherence and outcomes. We aimed to determine level of household food insecurity (HFI) and its associated factors in patients with pulmonary TB.

Design This is a cross-sectional analysis of data from an ongoing cohort study.

Setting National Tuberculosis Programme (NTP) in three districts of South India.

Participants All newly diagnosed pulmonary TB cases of the cohort enrolled in the NTP at the Designated Microscopy Centres (DMCs) and Primary Health Centres (PHCs) from October 2015 to October 2018.

Primary outcome measures The proportion of baseline HFI assessed using a validated HFI Access Scale was summarised as percentage with 95% CI. Possible association of sociodemographic, morbidity and behavioural characteristics with HFI was assessed using χ^2 test, and unadjusted prevalence ratios with 95% CI were calculated. The characteristics with values of p<0.2 in the univariate model were included in the multivariable generalised linear model (binomial function, log link) to derive adjusted prevalence ratios (aPRs) with 95% CI.

Result Of a total of 765 patients, 261 had HFI and the proportion was 34.1% (95% CI 30.8% to 37.6%). Mild, moderate and severe food insecurity was found in 17 (2.2%), 67 (8.8%) and 177 (23.1%) TB cases, respectively. Patients with TB who had monthly family income less than rupees 3000 (aPR 2.0; 95% CI 1.3 to 3.0), Karnofsky Score of 60 or less (aPR 1.5; 95% CI 1.1 to 1.9) and those who were employed (aPR 1.4; 95% CI 1.0 to 2.0) were independently associated with HFI.

Conclusions A high level of food insecurity was seen in households with TB cases. Additional food or cash assistance for this subgroup might improve food insecurity and thereby nutritional status.

Strengths and limitations of this study

- Use of a validated tool for assessing household food insecurity (HFI) which allows cross-country comparisons.
- We used data from a prospective cohort study which implemented quality assurance checks for data collection, entry and completeness that would have reduced missing data and data errors.
- We did not study the subgroup of previously treated patients with TB in whom levels of food insecurity could be higher due to financial loss caused by repeated episodes of TB.
- The study participants were from three selected districts in South India, so generalisability of the findings is limited.
- The model developed for assessing the factors associated with HFI was deficient due to the small sample size and unavailability of a few important confounding variables.

INTRODUCTION

Tuberculosis (TB) is the leading cause of death from a single infectious agent, ranking above HIV/AIDS, and is overall the ninth leading cause of death worldwide. In 2017, there were an estimated 1.3 million TB deaths among HIV-negative people. India contributes roughly 25% of global incident TB cases and there were an estimated 421 000 deaths annually due to TB in the year 2017.[1 2] In 2014, WHO endorsed the 'End TB strategy' in line with the Sustainable Development Goals developed by the United Nations (Goals 1, 2 and 3 deal with action on poverty, hunger and ensuring healthy lives and well-being of people) with a common aim to end the global TB epidemic.[1 3]

Food security is a state in which 'all people at all times have both physical and economic

access to sufficient food to meet their dietary needs for a productive and healthy life'.[4] Catastrophic health expenditure is a common consequence of TB diagnosis, treatment and care which can lead to impoverishment and in turn food insecurity for patients with TB. Food insecurity and undernutrition share a bidirectional relationship with TB; both cause TB and could be consequences of TB. Undernutrition in patients with active TB can lead to worsening of disease, drug toxicity, drug malabsorption, and death or relapse of disease.[5–7]

A recent national survey (2016) in Vietnam reported that 22% of households experienced food insecurity during TB treatment, this proportion being as high as 40% among the poorest wealth quintiles.[8] Food insecurity at the household level is common in India and is a strong risk factor for progression of latent infection to active TB in household contacts.[9] TB in India affects poor families and communities disproportionately, with a fourfold higher prevalence in those with a low standard of living index compared with those with a high standard of living index.[5] Food insecurity is also of greatest significance in households where levels of food insecurity and undernutrition are high at the time of diagnosis. Since food insecurity and undernutrition can coexist, patients with TB are unable to regain normal weight, despite effective treatment.

WHO (2013) in its guidelines 'Nutritional care and support for patients with tuberculosis' recommends assessment of food insecurity among TB cases and addressing the same with suitable packages including food assistance.[3] Recently, the Government of India has launched a cash assistance scheme for all TB cases to mitigate costs and improve nutritional status.[10] However, there may be households with more food insecurity that need more food assistance rather than equal assistance to all. In India, studies assessing household food insecurity (HFI) among TB cases are limited. Therefore, we aimed to determine the level of food insecurity and its associated factors using secondary data from a cohort of patients with pulmonary TB in South India.

METHODS

Study design

This is a cross-sectional analysis of data from a cohort study under Regional Prospective Observational Research for Tuberculosis (RePORT) India Consortium. Details of the study design have been previously reported.[11–14]

National Tuberculosis Programme

The study covers Puducherry district of the Union Territory of Puducherry (population ~1.3 million) and two adjoining districts of Tamil Nadu, that is, Villupuram (population ~3.5 million) and Cuddalore (population ~2.6 million). Under the National Tuberculosis Programme (NTP), TB diagnostic and treatment services are delivered through the designated microscopy centres (DMCs) and peripheral health institutions (PHIs) under tuberculosis units as nodal points for TB control activities at subdistrict level. Sputum smear microscopy remains the central component of TB diagnosis. Under NTP, both diagnosis and treatment are provided free of cost to the patients with TB. On diagnosis of TB, the patients are referred to the nearest PHI for initiation of treatment. Morbidity details (diabetes, HIV) and medication adherence, follow-up details and TB treatment outcomes of these patients are documented in individual TB treatment cards.

RePORT International

RePORT International represents a consortium of regional cohorts (RePORT India, RePORT Brazil, RePORT South Africa, RePORT China, RePORT Philippines and RePORT Indonesia) that are linked through the implementation of a common protocol for data and specimen collection. The objectives and composition of RePORT International are described elsewhere.[15]

One of the five teams under RePORT India, the Jawaharlal Institute of Postgraduate Medical Education and Research (JIPMER), Boston Medical Centre and Rutgers University, has established a pulmonary TB cohort of adults and children ≥6 years and their household contacts to identify biomarkers for risk of TB treatment failure and risk of development of TB in household contacts. TB cases diagnosed under NTP in the three districts (Puducherry, Cuddalore and Villupuram) were enrolled in the cohort at the DMCs and public health centres since 2014. Only newly diagnosed smear-positive and culture-positive pulmonary TB cases were included. Details on data collection and procedures were previously reported.[11–14]

Study population

For this analysis, we included all TB cases in the cohort enrolled from October 2015 to October 2018. Written informed consent was obtained from all participants before enrolment. Multidrug resistant and extremely drug resistant TB cases at diagnosis were excluded.

Study tool

The Household Food Insecurity Access Scale (HFIAS)[4] was used to assess food insecurity in the households in the past 30 days. The scale consists of nine items grouped under three domains: (1) Anxiety or uncertainty about the household food supply. (2) Insufficient quality. (3) Insufficient food intake and it's physical consequences.[4] The respondent is first asked an occurrence question, whether the condition in the question happened at all in the past 4 weeks (yes or no). If the respondent answers 'yes' to an occurrence question, a frequency-of-occurrence question is asked to determine whether the condition happened rarely (1–2 times), sometimes (3–10 times) or often (more than 10 times) in the past 4 weeks. Each item is scored on a range of 0 to 3; 0 for 'no occurrence' and 3 for 'often'. The minimum and maximum scores for a household are 0 and 27, respectively. The

scores were categorised into four levels of HFI: food secure and mild, moderately and severely food insecure[4] online supplementary file 1.

The Alcohol Use Disorders Identification Test (AUDIT)-C Questionnaire (a modified version of AUDIT)[16] was used to assess alcohol use among participants.

Data extraction, analysis and statistics

Of a total of 1229 TB cases enrolled in the cohort, we extracted data for 765 cases excluding two childhood TB cases; the initial 462 cases enrolled were not assessed for HFI because of not having the HFIAS in the study proforma during the initial phase of the project. The HFIAS was introduced in the revised study proforma after the 462 patients were already enrolled in the project. However, there was no difference in the baseline sociodemographic and clinical characteristics of the 462 patients excluded, compared with those included in the study.

Data were extracted from the RePORT India project database for the JIPMER site in a deidentified manner and analysed using Stata V.12.0 software. The proportion of HFI was summarised as percentage with 95% CI. Possible association of sociodemographic, morbidity-related and behavioural characteristics with HFI was assessed using χ^2 test, and unadjusted prevalence ratios with 95% CI were calculated. The characteristics with a value of p<0.2 in the univariate model were included in the multivariable generalised linear model (binomial function and log link) to derive adjusted prevalence ratios (aPRs) with 95% CI. The variables such as marital status, education, residence, number of earners in the household, HIV status, tobacco use, and alcohol use were not included for multivariate analysis.

Patient and public involvement

There was no patient or public involvement.

RESULTS

The mean (SD) age of the 765 individuals included in analysis was 44[14] years; 611 (80%) were male. Sociodemographic characteristics of the TB cases are described in table 1. Of the total participants, 131 (17%) did not have any formal education, about 77% were employed and 11% had monthly family income less than rupees 3000 (~US$43). Behavioural and disease-related characteristics are described in table 2. More than half (58%) were alcohol users (in the previous year) and 30% were current tobacco users. Of the total, 470 (61%) were underweight (body mass index (BMI) <18.5 kg/m2) and 5 patients (0.6%) were HIV-infected. The Karnofsky Score was 60 or less (require assistance for routine activities) in 29% of patients.

Overall, 261 patients had HFI and the proportion was 34.1% (95% CI 30.8% to 37.6%). Mild, moderate and severe food insecurity was found in 17 (2.2%), 67 (8.8%) and 177 (23.1%) TB cases, respectively. Components of food insecurity are described in table 3. Worry or anxiety about not having enough food was reported in 15% of TB households. In 21% of TB households, eating fewer meals in a day due to lack of enough food was reported.

Table 1 Sociodemographic characteristics of individuals with pulmonary tuberculosis (TB) in three districts of South India, 2015–2018 (n=765)

Characteristics	Frequency (%)
Age (in years)	
15–29	130 (17.0)
30–44	229 (29.9)
45–59	292 (38.2)
60 and above	114 (14.9)
Gender	
Male	611 (79.9)
Female	154 (20.1)
Marital status	
Never married	132 (17.3)
Married/living together	567 (74.1)
Separated/divorced/ widowed	66 (8.6)
Education (years of schooling)	
No formal education	131 (17.1)
1–5	160 (20.9)
6–10	317 (41.4)
>10	157 (20.5)
Employment	
Employed	588 (76.9)
Unemployed	177 (23.1)
Household Income per month (in rupees)	
<3000	80 (10.5)
3000–5000	296 (38.7)
5001–10000	279 (36.5)
>10000	94 (12.3)
Didn't answer	16 (2.0)
Number of individuals in house	
≤3	604 (78.9)
>3	161 (21.1)
Residence*	
Urban	338 (44.2)
Rural	409 (53.4)
Not recorded	18 (2.4)
Number of earners in the household	
None	15 (1.9)
One	509 (66.5)
Two or more	241 (31.6)
Religion	
Hindu	677 (88.5)
Christianity	54 (7.1)
Muslim	32 (4.2)
Others	2 (0.3)

Table 2 Morbidity and behavioural characteristics of individuals with pulmonary tuberculosis (TB) in three districts of South India, 2015-2018 (n=765)

Characteristic	Frequency (%)
Sputum smear grading at diagnosis	
1+	241 (31.5)
2+	255 (33.3)
3+	269 (35.2)
Karnofsky Score at diagnosis	
50–60	218 (28.5)
>60	547 (71.5)
HIV status	
Seropositive	5 (0.6)
Seronegative	760 (99.4)
RBS	
<200 mg/dL	531 (69.4)
≥200 mg/dL	234 (30.6)
Any other comorbidity*	
Yes	154 (20.2)
No	611 (79.8)
BMI	
<18.5	470 (61.4)
18.5–22.9	221 (28.9)
23–24.9	42 (5.5)
25 and above	29 (3.8)
Not recorded	3 (0.4)
Alcohol use†	
Ever	446 (58.3)
Never	319 (41.7)
Tobacco use‡	
Former	140 (18.3)
Current	231 (30.2)
Never	394 (51.5)

*Other comorbidities such as asthma, hepatitis, renal disease, cancer and breathing difficulty were reported by the participants.
†Alcohol use was measured for the past 1 year.
‡Current or prior habitual use of both smoking and smokeless forms of tobacco.
BMI, body mass index; RBS, random blood sugar.

Level of food insecurity in different subgroups is presented in table 4. In adjusted analysis, TB cases who had monthly family income less than rupees 3000 (aPR 2.0; 95% CI 1.3 to 3.0), Karnofsky Score of 60 or less (aPR 1.5; 95% CI 1.1 to 1.9) and those who were employed (aPR 1.4; 95% CI 1.0 to 2.0) had higher proportion of HFI.

DISCUSSION

Our study of newly diagnosed patients with pulmonary TB in the public sector in South India revealed that about a third of patients with TB experienced HFI and about one out of four patients experienced severe food insecurity at the time of diagnosis. Level of food insecurity was high in the low-income groups, those employed and those who had severe illness.

Prevalence of food insecurity in the general population of India is also high ranging from 45.5% to 77.2%.[17 18] Hence, HFI among patients with TB is common as it can be both a cause and consequence of TB. The national level survey from Vietnam (2016) reported 22% of patients with TB experienced HFI; lower levels of 6% were reported among patients with TB in Sri Lanka.[8 19]

Food insecurity was twice as high in low-income TB households (< rupees 3000) compared with their higher income counterparts. Catastrophic health expenditure, a consequence of TB diagnosis and treatment, can lead to worsening of food insecurity in low-income groups during the course of the disease.[5] These subgroups need to be provided additional assistance instead of 'equal for all' food or cash assistance benefits. Since income is usually under-reported, identifying such target groups may not be an easy task.

Food insecurity at the household level is a strong risk factor for progression of latent infection to active TB in household contacts.[9 20] Since food insecurity measures are applicable to all households, a wider approach of reducing food insecurity targeting all household contacts is needed.

In our study, about 60% of the patients with TB were underweight. Undernutrition is both an important risk factor for, and a common consequence of, TB. In food insecure households, undernutrition could be an intermediary step in the nutritional pathway of food insecurity leading to morbidity like TB. In India, undernutrition is highly prevalent in patients with TB and the dietary intake of calories is significantly lower (500–700 calories) than recommended.[21] As recommended by WHO, addressing undernutrition through nutritional counselling and support should be considered as part of the standard of care for people with TB. The recently launched 'Nikshay Poshan Yojana', a direct benefit transfer scheme by the government of India is a welcome step towards addressing undernutrition.[22] Our study did not include severely ill patients (Karnofsky Score <40) and previously treated patients with TB in whom undernutrition rates are expected to be high. This may partly explain why our study did not find an association between food insecurity and undernutrition, though previous studies have reported otherwise.[23–26] Also, we have assessed food insecurity at the household level, and BMI assessed is that of the individual patients. May be the patient's nutrition is maintained at the expense of other family members, so he or she may have had normal BMI. However, the temporality of the BMI, HFI and weight loss could not be established due to the cross-sectional nature of this study and we also failed to account for the sequence of these events during analysis. Thus, we fail to strongly comment on the causal pathways of association between HFI, BMI and weight loss. Also, we couldn't explore details on

Table 3 Components of household food insecurity among households of patients with pulmonary tuberculosis (TB) in three districts of South India, 2015–2018 (n=765)

	Occurrence*			
Occurrence questions	**No**	**Rarely**	**Sometimes**	**Often**
I.Worry or anxiety about food				
1.Worry that the household would not have enough food	648 (84.7)	52 (6.8)	62 (8.1)	3 (0.4)
II. Insufficient Quality of Food				
2.Any household member not able to eat the kinds of foods preferred because of lack of resources	636 (83.1)	67 (8.8)	60 (7.8)	2 (0.3)
3.Eating a limited variety of foods due to a lack of resources	680 (88.9)	40 (5.2)	45 (5.9)	0 (0.0)
4.Any household member having to eat some foods that they really did not want to eat because of lack of resources to obtain other types of food	611 (79.9)	53 (6.9)	91 (11.9)	10 (1.3)
III. Insufficient Quantity of Food				
5.Any household member having to eat a smaller meal than needed because there was not enough food	593 (77.5)	73 (9.5)	97 (12.7)	2 (0.3)
6.Eating fewer meals in a day because there was not enough food	601 (78.6)	89 (11.6)	73 (9.5)	2 (0.3)
7.There is no food of any kind to eat in your household because of a lack of resources to get food	625 (81.7)	73 (9.5)	60 (7.8)	7 (0.9)
8.Any household member going to sleep hungry at night because there was not enough food	643 (84.1)	70 (9.2)	51 (6.7)	1 (0.1)
9.Any household member going a whole day and night without eating anything because there was not enough food	631 (82.5)	73 (9.5)	57 (7.5)	4 (0.5)

*0=No, 1=Rarely (1–2 times in the past 4 weeks), 2=Sometimes (3–10 times in the past 4 weeks), 3=Often (more than 10 times in the past 4 weeks).

Table 4 Association of sociodemographic, morbidity and behavioural characteristics with household food insecurity among individuals with pulmonary TB in Puducherry, n=765

Characteristics	Total	Food insecurity*	Unadjusted PR† (95% CI)‡	Adjusted PR†, § (95% CI)‡
Total	765	261 (34.1)	–	–
Age (in years)				
15–29	130	48 (36.9)	1.4 (0.9–2.0)	1.2 (0.7–2.2)
30–44	229	86 (37.6)	1.4 (1.0–1.9)	1.4 (0.9–2.2)
45–59	292	96 (39.9)	1.2 (0.9–1.7)	1.2 (0.8–1.8)
60 and above	114	31 (27.2)	1.0	Ref
Gender				
Male	611	203 (33.2)	1.0	Ref
Female	154	58 (37.7)	1.1 (0.91.4)	1.2 (0.8–1.8)
Marital status				
Never married	132	42 (31.8)	0.9 (0.7–1.2)	–
Married/living together	567	196 (34.6)	1.0	–
Separated/divorced/widowed	66	23 (34.9)	1.008 (0.7–1.4)	–
Education (years of schooling)				
No formal education	131	40 (30.5)	1.0	–
1–5	160	54 (33.7)	1.10 (0.8–1.5)	–
6–10	317	114 (34.0)	1.2 (0.9–1.6)	–
>10	157	53 (33.8)	1.1 (0.8–1.6)	–
Employment				
Employed	588	206 (35.0)	1.1 (0.9–1.4)	1.4 (1.0–2.0)
Unemployed	177	55 (31.7)	1.0	Ref
Household income per month (in rupees)				
<3000	80	41 (51.3)	1.9 (1.3–2.4)	2.0 (1.3–3.0)
3000–5000	296	107 (36.2)	1.3 (1.0–1.6)	1.3 (0.9–1.7)
5001–10000	279	80 (28.7)	1.0	Ref
>10 000	94	24 (25.5)	0.9 (0.6–1.3)	0.9 (0.6–1.6)
Didn't answer	16	9 (56.3)	2.0 (1.2–3.1)	2.2 (1.1–4.5)
Number of individuals in the house				
≤3	604	198 (32.8)	1.0	Ref
>3	161	63 (39.1)	1.2 (0.9–1.5)	1.3 (0.9–1.8)
Residence¶				
Urban	338	114 (33.7)	1.0	–
Rural	409	143 (34.0)	1.03 (0.8–1.3)	–
Number of earners in the household				
None	15	5 (33.3)	1.0	–
One	509	177 (34.8)	1.04 (0.5–2.2)	–
Two or more	241	79 (32.8)	0.9 (0.5–2.1)	–
Sputum smear grading at diagnosis				
1+	241	68 (28.2)	1.0	Ref
2+	255	93 (36.5)	1.3 (1.0–1.7)	1.3 (0.9–1.7)
3+	269	100 (37.2)	1.3 (1.0–1.7)	0.4 (0.1–1.3)
Karnofsky Score at diagnosis				
50–60	218	97 (44.5)	1.5 (1.2–1.8)	1.5 (1.1–1.9)

Continued

Table 4 Continued

Characteristics	Total	Food insecurity*	Unadjusted PR† (95% CI)‡	Adjusted PR†, § (95% CI)‡
>60	547	164 (30.0)	1.0	Ref
HIV status				
Seropositive	5	3 (60.0)	1.0	–
Seronegative	760	258 (34.0)	0.6 (0.3–1.2)	–
RBS				
<200 mg/dL	531	197 (37.1)	1.4 (1.1–1.7)	1.1 (0.8–1.6)
≥200 mg/dL	234	64 (27.4)	1.0	Ref
Any other comorbidity				
Yes	154	53 (34.4)	1.01 (0.8–1.3)	–
No	611	208 (34.0)	1.0	–
BMI¶				
<18.5	470	177 (37.7)	1.2 (1.0–1.5)	1.06 (0.8–1.4)
18.5–22.9	221	68 (30.8)	1.0	Ref
23–24.9	42	12 (28.6)	0.9 (0.6–1.6))	0.9 (0.5–1.9)
25 and above	29	3 (10.3)	0.3 (0.1–1.0)	0.4 (0.1–1.3)
Alcohol use				
Ever	446	160 (35.9)	1.1 (0.9–1.4)	–
Never	319	101 (31.7)	1.0	–
Tobacco use				
Former	140	51 (36.4)	1.2 (0.9–1.5)	–
Current	231	86 (37.2)	1.2 (0.9–1.5)	–
Never	394	124 (31.5)	1.0	–

*Level of pood insecurity was assessed using the Household Food Insecurity Assessment Scale (HFIAS) for Measurement of Food Access-FANTAIII.
†PR, prevalence ratio.
‡CI.
§Adjusted for characteristics with a value of p<0.2 in the univariate model.
¶Residence—data are missing for 18 participants; Body Mass Index—data are missing for 3 participants.
BMI, body mass index; RBS, random blood sugar; TB, tuberculosis.

employment such as type of employment, which could be a risk factor for development of TB and could have influenced the income and thus the ability to purchase food items also.

Several studies support the notion that food insecurity negatively affects treatment adherence. Conditions of food insecurity (lack of adequate food, concern about daily food production) contribute to non-adherence to TB treatment as reported by qualitative studies.[27–29] Hence, identifying food insecurity at the time of diagnosis and linking the patients to food assistance or social security programmes is needed. We plan to report the effect of food insecurity on adherence and TB treatment outcomes in a separate paper.

Strengths of the study include use of a validated tool[4] for assessing HFI which allows cross-country comparisons. We used the data from a prospective cohort study which implemented quality assurance checks for data collection and entry that would have reduced missing data and data errors. There were a few limitations in the study. Our study included patients identified in the public sector alone and food insecurity levels may be different in patients accessing TB care in the private sector. Since, repeated episodes of TB may be a cause for financial loss leading to food insecurity, the levels could be higher in previously treated patients with TB and we did not study this subgroup. The study participants were from three selected districts in South India, so generalisability of the findings is limited. Being a cross-sectional analysis, causal relationships of factors with food insecurity cannot be inferred. The model we constructed for exploring factors associated with HFI was deficient as a few important confounding variables were included and also, the small sample size (power) was less for performing rational statistical analyses. Thus, the factors associated with HFI need to be interpreted with caution considering this major limitation in the multivariate analysis.

CONCLUSION

To conclude, HFI was experienced by one in three patients with TB and this was twice more in low-income groups. Additional food or cash assistance to food insecure patients with TB and household contacts will improve food insecurity and undernutrition.

Author affiliations
[1]Department of Preventive and Social Medicine, Jawaharlal Institute of Postgraduate Medical Education and Research (JIPMER), Puducherry, India
[2]Department of Community Medicine, Velammal Medical College, Madurai, Tamilnadu, India
[3]Centre for Operational Research, International Union Against Tuberculosis and Lung Disease, Paris, France
[4]The Union South-East Asia Office, New Delhi, India
[5]Section of Infectious Diseases, Department of Medicine, Boston University School of Medicine, Massachusetts, United States
[6]Department of Epidemiology, Boston University School of Public Health, Massachusetts, United States
[7]Department of Global Health, Boston University School of Public Health, Massachusetts, United States
[8]Department of Medicine, Rutgers University, New Jersey, United States

Acknowledgements This cross-sectional analysis was conducted through the Structured Operational Research and Training Initiative (SORT IT), a global partnership led by the Special Programme for Research and Training in Tropical Diseases at the World Health Organisation (WHO/TDR). The model is based on a course developed jointly by the International Union Against Tuberculosis and Lung Disease (The Union) and Medécins sans Frontières (MSF/Doctors Without Borders). The specific SORT IT programme which resulted in this publication was jointly developed and implemented by: The Union South-East Asia Office, New Delhi, India; the Centre for Operational Research, The Union, Paris, France; Department of Preventive and Social Medicine, Jawaharlal Institute of Postgraduate Medical Education and Research, Puducherry, India; Department of Community Medicine and School of Public Health, Postgraduate Institute of Medical Education and Research, Chandigarh, India; Department of Community Medicine, All India Institute of Medical Sciences, Nagpur, India; Dr. Rajendra Prasad Centre for Ophthalmic Sciences, All India Institute of Medical Sciences, New Delhi, India; Department of Community Medicine, Pondicherry Institute of Medical Science, Puducherry, India; Department of Community Medicine, Kalpana Chawla Medical College, Karnal, India; National Centre of Excellence and Advance Research on Anaemia Control, All India Institute of Medical Sciences, New Delhi, India; Department of Community Medicine, Sri Manakula Vinayagar Medical College and Hospital, Puducherry, India; Department of Community Medicine, Velammal Medical College Hospital and Research Institute, Madurai, India; Department of Community Medicine, Yenepoya Medical College, Mangalore, India; Karuna Trust, Bangalore, India and National Institute for Research in Tuberculosis, Chennai, India. Authors would like to thank the funders, the index cases, their families, and the staff that worked on the RePORT India project. We also acknowledge the contribution of the Data Coordinating Centre at Boston Medical Centre, US.

Contributors RA:Principal Investigator (PI), conception/ design of the protocol, data capture, development of data capture tool, data analysis/interpretation, drafting/critically reviewing the paper, giving approval for the final version to be published. SS: Acquisition of data, conception/ design of the protocol, revision of manuscript, critically reviewing the paper, giving approval for the final version to be published. PC: Conception/design of the protocol, development of data capture tool, data analysis/interpretation, drafting/critically reviewing the paper, giving approval for the final version to be published. KJ: Conception/design of the protocol, development of data capture tool, data analysis/interpretation, drafting/critically reviewing the paper, giving approval for the final version to be published. MV: Data analysis and interpretation, critically reviewing the paper, giving approval for the final version to be published. PT: Conception, data analysis, revision of manuscript, critically reviewing the paper, giving approval for the final version to be published. SL: Conception, project management, critically reviewing the manuscript, giving approval for the final version to be published. SK: Data curation and management, reviewing the manuscript, giving approval for the final version to be published. NSH: Project administration and supervision, critically reviewing and editing the manuscript, giving approval for the final version to be published. CRH: Critically reviewing and editing the manuscript, giving approval for the final version to be published. JE: Acquisition of data, critically reviewing the manuscript, giving approval for the final version to be published. GR: Acquisition of data, critically reviewing the manuscript, giving approval for the final version to be published.

Funding The training programme, within which this paper was developed, and the open access publication costs were funded by the Department for International Development (DFID), UK and La Fondation Veuve Emile Metz-Tesch (Luxembourg). The RePORT India project has been funded in whole or in part with Federal funds from the Government of India's (GOI) Department of Biotechnology (DBT), the Indian Council of Medical Research (ICMR), the US National Institutes of Health (NIH), National Institute of Allergy and Infectious Diseases (NIAID), Office of AIDS Research (OAR), and distributed in part by Civilian Research and Development Foundation (CRDF) Global.

Disclaimer The contents of this publication are solely the responsibility of the authors and do not represent the official views of the DBT, the ICMR, the NIH, or CRDF Global. The funders had no role in study design, data collection and analysis, decision to publish, or preparation of the manuscript.

Competing interests None declared.

Patient consent for publication Not required.

Ethics approval Ethics approval was obtained from the Institutional Ethics Committee of JIPMER (Ref.No: JIP/IEC/2013/4/194) and Institute Review Board of Boston Medical Center (IRB No: H-32657/7-05-2017) for the cohort study. The study protocol for this secondary analysis was reviewed and approved by the Ethics Advisory Group of the International Union Against Tuberculosis and Lung Disease (99/18), Paris, France.

Provenance and peer review Not commissioned; externally peer reviewed.

Data availability statement Data are available upon reasonable request. The technical appendix, statistical code and data set will be available upon request from the Corresponding author.

ORCID iD
Reshma Ayiraveetil http://orcid.org/0000-0002-2417-6639

REFERENCES

1 World Health Organization. *End TB global tuberculosis report 2017*. Geneva, 2017: 147.
2 Central TB Division. TB India-Annual Report 2017. India TB Rep [Internet]. 2017;1–173. Available: https://tbcindia.gov.in/WriteReadData/TB India 2017.pdf
3 World Health Organization. WHO Guideline : Nutritional care and support for patient with tuberculosis. In: *WHO Guidel Nutr care support patient with Tuberc*. World Heal Organ, 2013.
4 Coates J, Swindale A, Bilinsky P, *et al*. *Household food insecurity access scale (HFIAS) for measurement of food access: indicator guide*. Washington, DC: Food Nutr Tech, 2007.
5 Central TB Division. Guidance document: nutritional care and support for patients with tuberculosis in India, 2017. Available: http://www.tbcindia.nic.in/WriteReadData/Guidance Document - Nutritional Care %26 Support for TB patients in India.pdf
6 Bhargava A, Benedetti A, Oxlade O, *et al*. Undernutrition and the incidence of tuberculosis in India: national and subnational estimates of the population-attributable fraction related to undernutrition. *Natl Med J India* 2014;27:128–33.
7 Sinha P, Davis J, Saag L, *et al*. Undernutrition and tuberculosis: public health implications. *J Infect Dis* 2019;219:1356–63.
8 Nhung NV, Hoa NB, Anh NT, *et al*. Measuring catastrophic costs due to tuberculosis in Viet Nam. *Int J Tuberc Lung Dis* 2018;22:983–90.
9 Jubulis J, Kinikar A, Ithape M, *et al*. Modifiable risk factors associated with tuberculosis disease in children in Pune, India. *Int J Tuberc Lung Dis* 2014;18:198–204.
10 Central TB Division. National strategic plan for tuberculosis elimination 2017-2025. *Dir Gen Heal Serv Minist Heal Fam Welf* 2017:110–108.

11 Van Ness SE, Chandra A, Sarkar S, *et al*. Predictors of delayed care seeking for tuberculosis in southern India: an observational study. *BMC Infect Dis* 2017;17:1–9.
12 Hochberg NS, Sarkar S, Horsburgh CR, *et al*. Comorbidities in pulmonary tuberculosis cases in Puducherry and Tamil Nadu, India: opportunities for intervention. *PLoS One* 2017;12:e0183195.
13 Hoyt KJ, Sarkar S, White L, *et al*. Effect of malnutrition on radiographic findings and mycobacterial burden in pulmonary tuberculosis. *PLoS One* 2019;14:e0214011–11.
14 Leong S, Zhao Y, Joseph NM, *et al*. Existing blood transcriptional classifiers accurately discriminate active tuberculosis from latent infection in individuals from South India. *Tuberculosis* 2017;2018:41–51.
15 Hamilton CD, Swaminathan S, Christopher DJ, *et al*. Report international: advancing tuberculosis biomarker research through global collaboration. *Clin Infect Dis* 2015;61:S155–9.
16 Babor TF, Saunders JCH-BJB, Monteiro MG. The alcohol use disorder identification test. guidelines for use in primary care. *World Heal Organ Geneva* 2015;2:1–41.
17 Chinnakali P, Upadhyay RP, Shokeen D, *et al*. Prevalence of household-level food insecurity and its determinants in an urban resettlement colony in North India. *J Heal Popul Nutr* 2014;32:227–36.
18 Joshi A, Arora A, Amadi-Mgbenka C, *et al*. Burden of household food insecurity in urban slum settings. *PLoS One* 2019;14:e0214461–24.
19 Jayasuriya NA, Nayanathara L, Iddamalgoda N, *et al*. *Food security and nutrition among the tuberculosis infected patients. A case study among the patients screened at chest clinic of medical research Institute of Colombo, Sri Lanka*. World Food Programme: Food security analysis(VAM), 2014.
20 Bloem MW, Saadeh R. Foreword: the role of nutrition and food insecurity in HIV and tuberculosis infections and the implications for interventions in resource-limited settings. *Food Nutr Bull* 2010;31:S289–91.
21 Swaminathan S, Padmapriyadarsini C, Sukumar B, *et al*. Nutritional status of persons with HIV infection, persons with HIV infection and tuberculosis, and HIV-negative individuals from southern India. *Clin Infect Dis* 2008;46:946–9.
22 Yadav S, Atif M, Rawal G. Nikshay Poshan Yojana- another step to eliminate TB from India. *IP Indian J Immunol Respir Med* 2018;3:28–9.
23 Gupta K, Gupta R, Atreja A, *et al*. Tuberculosis and nutrition. *Lung India* 2009;26:9–16.
24 Park HO, Kim SH, Moon SH, *et al*. Association between body mass index and sputum culture conversion among South Korean patients with multidrug resistant tuberculosis in a tuberculosis referral hospital. *Infect Chemother* 2016;48:317–23.
25 Lönnroth K, Williams BG, Stadlin S, *et al*. Alcohol use as a risk factor for tuberculosis - a systematic review. *BMC Public Health* 2008;8:289.
26 Podewils LJ, Holtz T, Riekstina V, *et al*. Impact of malnutrition on clinical presentation, clinical course, and mortality in MDR-TB patients. *Epidemiol Infect* 2011;139:113–20.
27 Mekonnen HS, Azagew AW. Non-adherence to anti-tuberculosis treatment, reasons and associated factors among TB patients attending at Gondar town health centers, Northwest Ethiopia 11 medical and health sciences 1103 clinical sciences 11 medical and health sciences 1117 public Hea. *BMC Res Notes* 2018;11:1–8.
28 Munro SA, Lewin SA, Smith HJ, *et al*. Patient adherence to tuberculosis treatment: a systematic review of qualitative research. *PLoS Med* 2007;4:e238–45.
29 Diefenbach-Elstob T, Plummer D, Dowi R, *et al*. The social determinants of tuberculosis treatment adherence in a remote region of Papua New Guinea. *BMC Public Health* 2017;17:1–12.

Advances in Spondyloarthritis: Update 2020

Subramanian Nallasivan

Vinod Ravindran

Spondyloarthritis (SpA, earlier term ankylosing spondylitis) is though predominantly a disease affecting the axial and peripheral skeleton, its systemic involvement can be debilitating. There are several areas about this entity where still uncertainties exist. Although it's mainly a disease of adolescent men, women also do develop SpA. Cutaneous (psoriasis), gut (colitis), eyes (uveitis), and spine (sacroiliitis) are common extra-articular manifestations.

Current evidence points to a long delay in adequate assessment and appropriate diagnosis of individuals suffering from inflammatory back pain or other symptoms. This delay unfortunately is universal.

On the management front of SpAs, rapid advances have been made. With increasing usage of biological agents such as anti-tumor necrosis factor (TNF) and interleukin (IL)-16 inhibitors, the lifestyle of these patients has changed.

This annual supplement of *Indian Journal of Rheumatology* focuses on the newer insights to this disease. Expert authors have discussed recent advances in several areas, including pathogenesis, HLA B27, newer imaging tools for early diagnosis, and current treatment strategies, including biologics and biosimilars.

Malaviya in his chapter on the history of SpA brings to our notice several interesting facts. Jain and Moorthy have focused on pathogenesis of SpA and cytokine-mediated disease. Ahmed and Misra have delved on HLA B27, the genetic link in the evolution of SpA. Sham and Ravindran have discussed the classification criteria used in SpA research and its possible implications to clinical practice.

Magnetic resonance imaging (MRI) has transformed the way SpA is diagnosed by allowing early diagnosis of sacroiliitis. Chen and colleagues in their chapter have discussed MRI and other imaging modalities in SpA.

Pathak and Gaffney have discussed spectrum of diseases under SpAs including colitis, Crohn's disease, uveitis, and psoriasis. Chauhan has discussed how the eyes are the gateway to systemic manifestations. Hackett and Coates have highlighted the shared immunopathological link between psoriasis and SpAs. Hafis and Agarwal have discussed inflammatory bowel diseases-related SpAs and elucidated how it can be screened in patients with inflammatory back pain.

Recent insights into the immune mediators of the inflammatory cascade have resulted in targeted treatment strategies in patients with SpAs. Sulfasalazine has been used for several decades in this disease, and Shankar and Hegde have discussed recent evidence on such DMARD treatments. Castillo-Gallego *et al.* have thrown more light on the "new kids on the block" – TNF blockers, IL-17 blockers, and IL-22 monoclonal antibodies in achieving effective disease control and remission in patients with SpAs.

We thank all the authors (please see page Siii and Siv) and reviewers (please see page S71) for their extremely valuable contributions to this supplement. We express our sincere gratitude to Prof. Vikas Agarwal, Editor-in-Chief, for inviting us to guest edit this supplement on SpAs.

We hope this supplement would benefit the readers by providing up-to-date developments in the field of SpA.

Happy reading!

Financial support and sponsorship

Nil.

Conflicts of interest

There are no conflicts of interest.

Subramanian Nallasivan, Vinod Ravindran[1]

Rosemary Mission Hospital, Tirunelveli, Tamil Nadu,
[1]Centre for Rheumatology, Calicut, Kerala, India

Address for correspondence:
Dr. Subramanian Nallasivan,
Consultant Rheumatologist, Rosemary Mission Hospital,
Vannarpettai, Tirunelveli, Tamil Nadu, India.
E-mail: drsubramanian14@gmail.com

Received: February, 2020
Accepted: March, 2020
Published: May, 2020

Access this article online	
Website: www.indianjrheumatol.com	Quick Response Code
DOI: 10.4103/0973-3698.238193	

How to cite this article: Nallasivan S, Ravindran V. Advances in spondyloarthritis: Update 2020. Indian J Rheumatol 2020;15:S1.

Original Article

Risk factors for alcohol use relapse after abstinence in patients with alcoholic liver disease

Arun AC[1], Nityashree Ilangovan[1], Jenish Rajma[2]

Departments of [1]Medical Gastroenterology, and [2]Paediatrics, Velammal Medical College Hospital and Research Institute, Madurai, Tamil Nadu, India

Abstract

Introduction: In patients with alcoholic liver disease, abstinence from alcohol is an important aspect of treatment. Once abstinence is achieved, the challenge is to avoid relapse of alcohol use. This study aims to analyse the significant risk factors for alcohol relapse thereby identifying the patients with high risk for recidivism to have an early social and medical intervention. **Methodology:** This was an observational and a retrospective type of study. Patients with chronic liver disease and had alcohol use relapse after abstinence were classified into Group A. Patients who did not have relapse after abstinence were classified into Group B. The two groups were compared for various social and personal and disease related factors. Student "t" test was used for raw data and Chi square test was used for consolidated data to find significant difference between variables. **Results:** Overall nine factors were analysed. The factors which were found to be significant for predicting relapse are quantity of alcohol consumption per week, duration of abstinence, associated smoking, marital status, severity of liver disease (Child-Pugh scoring system). The other factors like age of starting alcohol consumption, duration of alcohol consumption, family history of alcohol intake and MELD score were not statistically significant. **Conclusion:** This study identifies the risk factors associated with alcohol relapse in patients with alcoholic liver disease. The data from this study can be used to identify individuals who are high risk for relapse and treat them with pharmacological and psychosocial methods to prevent relapse.

Keywords: Alcohol abstinence, alcohol relapse factors, alcohol use relapse, chronic liver disease

Introduction

Alcoholic liver disease is one of the most common causes of advanced liver cirrhosis, portal hypertension and Hepatocellular Carcinoma. It is the second most common indication for liver transplantation after cirrhosis caused by viral hepatitis.[1] Fat accumulation in liver cells (Fatty Liver) is the earliest response to alcohol consumption. It can be found in about 90% of heavy drinkers. Fatty liver due to alcohol is reversible once the person stops consuming alcohol. However once cirrhosis develops, it becomes irreversible. Cirrhosis can develop in about 10% of patients who consume alcohol heavily within five years.[2]

During treatment of alcoholic liver disease, the most important aspect to be addressed by the physician is abstinence to alcohol. The primary care physicians who treat these patients should adequately counsel the patients and relatives regarding the need of complete abstinence for proper recovery from liver disease. Various tools have been used to detect alcohol relapse in patients who have achieved abstinence. Among them Carbohydrate-deficient transferrin has been proved to be a useful supplementary tool for detecting alcohol relapse.[3] Once abstinence is achieved, the biggest challenge during treatment is avoiding recidivism. The morbidity and mortality due to alcoholic liver disease is much higher in those with the relapse of alcohol

Address for correspondence:
Dr. Arun AC,
B3, Rajsesh Mahal Apartment, 34, Bharathi Ula Road, Madurai, Tamil Nadu - 625020, India.
E-mail: acarun@outlook.com

Received: 09-07-2020 **Revised:** 17-09-2020
Accepted: 23-10-2020 **Published:** 31-12-2020

Access this article online

Quick Response Code:

Website: www.jfmpc.com

DOI: 10.4103/jfmpc.jfmpc_1401_20

How to cite this article: Arun AC, Ilangovan N, Rajma J. Risk factors for alcohol use relapse after abstinence in patients with alcoholic liver disease. J Family Med Prim Care 2020;9:5995-9.

use compared to those who are abstinent.[4,5] So there is a need to identify the risk factors for relapse of alcohol use in patients of alcoholic liver disease. This study aims to analyse the significant risk factors for alcohol relapse thereby identifying the patients with high risk for recidivism to have an early social and medical intervention.

Materials and Methods

This was an observational and a retrospective type of study. For the purpose of the study, patients with alcoholic liver disease who relapsed after abstinence and who stayed without relapse after abstinence were operationally defined. Alcohol use disorder (AUD) was defined based on the fifth edition of Diagnostic and Statistical Manual of Mental Disorders (DSM-5) published by the American Psychiatric Association.[6]

Abstinence was defined as "adults between the age of 18 and 65 years who had met the DSM-5 criteria for AUD and is now abstinent for a minimum period of 3 months". Relapse was defined as "adults who had met the DSM-5 criteria for AUD and were abstinent for at least 1 month, after which they relapsed and are now fulfilling the DSM-5 criteria for at least 1 month".

Approval for the study was obtained from the Institutional Ethics Committee (04-08-2017). Patients who gave written informed consent were included in the study. All consecutive patients who attended the Gastroenterology outpatient department during the period of research (January 2019 to December 2019) with the diagnosis and follow up of alcoholic liver disease with past history of alcohol dependence were included in the study.

The patients who were enrolled were categorised into two groups. The patients who developed alcohol use relapse after its abstinence were categorized into Group A. The patients who stay without relapse to alcohol use after its abstinence were categorized into Group B.

A detailed personal data was taken from the patient's record regarding the age of starting the alcohol consumption, the years of alcohol use and the time of alcohol abstinence and time period of its relapse. History regarding social factors for alcohol relapse including marital status, occupation, socio-economic status were also be obtained from the medical records and telephonic conversations. The various significant risk factors that contributed to the relapse were also elicited from the history.

The baseline laboratory and radiological investigations were obtained from the old records to assess the severity of liver disease and its correlation with abstinence and relapse. The severity of their disease was graded according to Child-Pugh scoring system[7] and the Model for End stage Liver Disease (MELD)[8] scoring systems.

The data were entered in Microsoft excel datasheet. The demographic data and the baseline investigations of chronic liver disease of both the group of patients were documented. Data analysis was performed by using SPSS 16.0 (IBM SPSS statistics, New York, USA). Student "t" test was used for raw data and Chi square test for consolidated data to test the significance of difference between variables. A 'p' value which is less than 0.05 is taken to show significant association.

Results

A total of 77 patients were enrolled in the study after obtaining informed consent. The patients who developed alcohol use relapse after its abstinence were categorized into Group A (n = 35). The patients who stayed without relapse of alcohol use after its abstinence were categorized into Group B (n = 42). Individual factors were analysed for significance between the two groups. Overall nine factors were analysed which included age of starting alcohol consumption, duration of alcohol consumption before abstinence, quantity of alcohol consumption per week, duration of abstinence, associated habits like smoking, marital status, family history of alcohol intake, severity of liver disease (Child-Pugh scoring system and MELD score).

The factors which predict the chance of alcohol relapse with statistical significance are enlisted in Table 1. The quantity of alcohol intake was found to be a significant factor in predicting alcohol relapse. Those who were consuming more than 500 gm alcohol per week were found to have more chance for relapse than those who were consuming less than 500 gm ($p = 0.04$). When the duration of abstinence was compared between the two groups, it was found that, higher the duration of abstinence, better is the chance of abstinence and the association was significant ($p < 0.001$).

When the marital status of the participants of the study was compared, it was found that those who were married had significantly less chance of alcohol relapse than those who are single ($p = 0.011$). Those who smoke had more chance for alcohol relapse than those who do not smoke ($p = 0.019$). When the participants were classified according to the severity of liver disease according to the Child-Pugh scoring system, those who had severe liver dysfunction had significantly higher alcohol relapse rate ($p = 0.004$).

The factors which did not have a statistical significance between alcohol relapse group and abstinence group are enlisted in Table 2. It was analysed whether the age of starting alcohol consumption had an effect on recidivism, however it was statistically significant ($p = 0.166$). There was no significant difference between the two groups in the duration of alcohol consumption before abstinence ($p = 0.053$). The family history of alcohol consumption was analysed between the two groups; however, it was not statistically significant ($p = 0.268$). When the severity of liver disease was classified according to the MELD

Table 1: Factors significant for predicting alcohol use relapse

Characteristics	Total	Group A (Relapse)	Group B (Abstinent)	*P*
Duration of abstinence (Months)				
≤6	31	21	10	<0.001
7-12	12	4	8	
13-24	14	9	5	
25-60	9	1	8	
>60	11	0	11	
Marital Status				
Married	65	25	40	0.011
Single	12	10	2	
History of smoking				
Yes	45	26	19	0.019
No	26	9	23	
Quantity of alcohol consumption (gm per week)				
<500	43	15	28	0.04
≥500	34	20	14	
Cirrhosis Stage				
Child A	13	3	10	0.004
Child B	46	18	28	
Child C	18	14	4	

Table 2: Factors not significant for predicting alcohol use relapse

Characteristics	Total	Group A (Relapse)	Group B (Abstinent)	*P*
Age of starting alcohol (years)				
≤20	10	6	4	0.166
21-30	38	19	19	
31-40	19	6	13	
>40	10	4	6	
Duration of alcohol use (years)				
≤10	33	11	21	0.053
11-20	28	13	15	
21-30	13	8	5	
≥31	4	3	1	
Family History of alcohol intake				
Yes	42	22	20	0.268
No	35	13	22	
MELD score				
0-10	12	1	11	0.051
>10 and <18	38	18	20	
>18 and <24	19	12	7	
>24	8	4	4	

score, there was no statistically significant difference between the two groups (p = 0.051).

Discussion

Our study analyses the different factors which may contribute to the relapse of alcohol use after abstinence in patients with alcohol related chronic liver disease. We analysed nine factors and found that five factors are significantly associated with alcohol relapse.

The quantity of alcohol consumption per week was more in the relapse group than in the abstinence group which means that more the addiction to alcohol, more is the chance for relapse. The presence of another addiction like smoking increased the risk of alcohol relapse. So, deaddiction for smoking should be considered along with deaddiction of alcohol. The duration of abstinence was another factor that significantly predicted relapse in our study. As the duration of abstinence increased, the chance of relapse decreased. So, it should be understood that the pharmacological therapy and psychosocial support are more important in the initial period of abstinence.

Another important factor that predicted relapse was the marital status. The possible explanation was that those who were married had better social support to prevent relapse. The relapse rate was significantly higher in those who were single. When the

chronic liver disease was graded according to the Child-Pugh scoring system, those who had advanced liver disease had higher chance of relapse. This may be due to the fact that those who had advanced liver disease had the previous tendency for non-compliance to drugs and so not compliant to alcohol abstinence also.

Only few studies are available in English literature regarding the risk factors leading to recidivism after alcohol abstinence.[9,10] Rongbin *et al.*[11] conducted a study on risk factors for alcohol use relapse among patients with psychiatric illnesses. They recruited 451 patients and analysed various factors responsible for alcohol use relapse. They found that duration of psychiatric symptoms, marital status, and deception about alcohol use correlated with alcohol use relapse. They concluded that those who are single had high risk for alcohol use relapse and the relapse was higher between first and fifth years of onset of psychiatric symptoms.

Satapathy *et al.*,[12] formulated a scoring system called HALT score to predict harmful alcohol relapse post liver transplantation (LT) based on four variables which included age at LT, non-alcohol related criminal history, pre-LT abstinence period and number of drinks per day. They found that the HALT score identified LT candidates at significant risk for alcohol relapse, potentially guiding transplant centres for pre- and post-LT interventions for improved patient outcomes. In a recent review by Hera Schlagintweit *et al.*,[13] the studies regarding the behavioural and psychosocial interventions to prevent alcohol relapse were analysed. They concluded that behavioural interventions are a fundamental component of alcohol use disorder treatment, however limited research was available in evaluating behavioural alcohol interventions among alcoholic liver disease patients. In a comprehensive review by Akhil Shenoy *et al.*,[14] it was concluded that multidisciplinary treatment that includes medications and psychotherapies along with support groups, family engagement would reduce the chance of alcohol relapse.

There is very little Indian data available in this context. Kailash Suresh Kumar *et al.*[15] studied the various demographic, clinical and psychosocial factors associated with relapse in 66 patients with alcohol dependence. They found that among the demographic factors, family history of substance dependence and past history of relapses were significantly associated with alcohol use relapse. Among the clinical variables, younger age of onset of dependence and shorter time to develop dependence were significantly associated with relapse. In a review of various studies on alcohol relapse, Narendra Choudhary *et al.*, concluded that main predictors of relapse are pretransplant abstinence, psychiatric comorbidities, and lack of social support. They concluded that studies which had active involvement by psychiatrist had lower relapse rate.[16]

The other social and clinical factors which were analysed in our study including the age of starting alcohol, duration of alcohol consumption, family history of alcohol consumption, MELD score did not have any statistically significant difference. Our study can be used to identify patients who come under the high risk criteria for relapse, who are to be comprehensively treated with both medical and psychosocial therapies in order to prevent their relapse after abstinence.

Our study has a few methodological limitations such as being a retrospective study, which might have a recall bias. The sample size is small due to a shorter duration of study. However, this research can be set as a stepping stone for further studies in future with more variables and longer study period. To summarize our study, the risk factors which were significantly associated with alcohol relapse were marital status, presence of another addiction, quantity of alcohol consumption, duration of abstinence and presence of advanced liver disease.

Conclusion

This study has been conducted to identify the risk factors associated with alcohol relapse in patients with alcoholic liver disease. Among the social and clinical variables analysed, marital status, duration of abstinence, quantity of alcohol consumption, smoking and cirrhosis staging according to the Child-Pugh scoring system were found to be the factors with significant difference. The data from this study can be used to identify the subset of patients who are at high risk for relapse and treat them with pharmacological and psychosocial methods to prevent relapse.

Declaration of patient consent

The authors certify that they have obtained all appropriate patient consent forms. In the form the patient (s) has/have given his/her/their consent for his/her/their images and other clinical information to be reported in the journal. The patients understand that their names and initials will not be published and due efforts will be made to conceal their identity, but anonymity cannot be guaranteed.

Financial support and sponsorship

Nil.

Conflicts of interest

There are no conflicts of interest.

References

1. Bosetti C, Levi F, Lucchini F, Zatonski WA, Negri E, La Vecchia C, *et al.* Worldwide mortality from cirrhosis: An update to 2002. J Hepatol 2007;46:827-39.
2. Pfitzmann R, Schwenzer J, Rayes N, Seehofer D, Neuhaus R, Nüssler NC. Long-term survival and predictors of relapse after orthotopic liver transplantation for alcoholic liver disease. Liver Transpl 2007;13:197-205.
3. Kollmann D, Rasoul-Rockenschaub S, Steiner I, Freundorfer E, Györi GP, Silberhumer G, *et al.* Good outcome after liver transplantation for ALD without a 6 months abstinence

rule prior to transplantation including post-transplant CDT monitoring for alcohol relapse assessment – A retrospective study. Transpl Int 2016;29:559-67.

4. Zhang W, Huang ZY, Sha JM, Du J. Related factors of repeating drinking in patients with alcohol dependence after withdrawal. Zhongguo Xian Dai Yi Sheng 2015;11:4-7.
5. Shiffman S. Relapse following smoking cessation: A situational analysis. J Consult Clin Psychol 1982;50:71-86.
6. American Psychiatric Association. Diagnostic and Statistical Manual of Mental Disorders. 5th ed.. Washington, DC, USA: American Psychiatric Association; 2013. p. 154-96.
7. Child CG, Turcotte JG. Surgery and portal hypertension. In: Child CG, editor. The Liver and Portal Hypertension. Philadelphia: Saunders; 1964. p. 50-8.
8. Malinchoc M, Kamath PS, Gordon FD, Peine CJ, Rank J, ter Borg PC. A model to predict poor survival in patients undergoing transjugular intrahepatic portosystemic shunts. Hepatology 2000;31:864-71.
9. Tapert SF, Ozyurt SS, Myers MG, Brown SA. Neurocognitive ability in adults coping with alcohol and drug relapse temptations. Am J Drug Alcohol Abuse 2004;30:445-60.
10. Jhanjee S. Evidence based psychosocial interventions in substance use. Indian J Psychol Med 2014;36:112-8.
11. Zeng R, Wang L, Xie Y. An analysis of factors influencing drinking relapse among patients with alcohol-induced psychiatric and behavioral disorders. Shanghai Arch Psychiatry 2016;28:147-53.
12. Satapathy SK, Thornburgh C, Heda R, Jiang Y, Kedia SK, Nair SP, *et al*. Predicting harmful alcohol relapse after liver transplant: The HALT score. Clin Transplant 2020;34:e14003.
13. Schlagintweit HE, Lynch MJ, Hendershot CS. A review of behavioral alcohol interventions for transplant candidates and recipients with alcohol-related liver disease. Am J Transplant 2019;19:2678-85.
14. Shenoy A, Salajegheh A, Shen NT. Multimodal multidisciplinary management of alcohol use disorder in liver transplant candidates and recipients. Transl Gastroenterol Hepatol 2020. doi: 10.21037/tgh. 2020.02.22.
15. Sureshkumar K, Kailash S, Dalal PK, Reddy MM, Sinha PK. Psychosocial factors associated with relapse in patients with alcohol dependence. Indian J Psychol Med 2017;39:312-5.
16. Choudhary NS, Saraf N, Mehrotra S, Saigal S, Soin AS. Recidivism in liver transplant recipients for alcohol-related liver disease. J Clin Exp Hepatol 2020. In press. doi: 10.1016/j.jceh. 2020.08.011.

Original Article

Fracture Resistance of Titanium, Chrome–Cobalt, and Gold Alloy as Post and Core Materials: A Comparative Evaluation

Karunakaran Jeyaraman Venkataraman[1], Sathya Thanapathi[1], Sathyanarayanan Balasubramanian[1], Shrimanikandan Ayappa Gandhi[2], Anagha Chandrasekharan Sarojinikutty[1]

[1]Department of Conservative Dentistry, JKK Nataraja Dental College & Hospital, Komarapalayam, Tamil Nadu, India, [2]Department of Craniofacial Surgery & Dentistry, Velammal Medical Hospital & Research Institute, Madurai, Tamil Nadu, India

Received : 02-03-2020.
Revised : 10-03-2020.
Accepted : 31-03-2020.
Published : 28-08-2020.

ABSTRACT

Aim: This study aimed to comparatively evaluate the fracture resistance of different metallic post and core materials. **Materials and Methods:** Twenty-four maxillary–central incisors were selected, standardized, and segregated into three groups (GP I–III) (n = 8) based on the type of alloy used for post and core preparation. GP I (gold alloy [Au]), GP II (chrome–cobalt alloy [Co–Cr]), and GP III (titanium alloy [Ti]) were comparatively evaluated for use as post and core materials. The teeth were endodontically treated and tooth preparation for post core was done. Metal post and cores were fabricated using indirect wax pattern and luted. Teeth were mounted on resin bases, fracture testing was done, and type of fractures were analyzed. **Results:** Mesiodistal type of fracture was the most common among experimental groups with a percentage incidence of 54.20%. The comminuted type of fracture was the next most common with a percentage incidence of 29.2%. The incidence of buccolingual, transverse, and other type of fracture was not common and had a percentage incidence of 29.2%, 4.2%, 8.3% and 4.2% respectively. Group II had the highest fracture resistance with a mean value of 742.89 N. Group III and Group I had mean values of 482.33 and 361.1123 N. Statistically significant difference between experimental groups (I and II) and (II and III) was observed in load values of root fracture ($P < 0.05$). **Conclusion:** On the basis of the protocols used and limitations of this study, among metallic post and core materials tested, GP II had the highest fracture resistance values. Further evaluation of these different post and core systems, new alloy formulations designed specifically for use as post and core materials, and assessment in a clinical setting is recommended.

Keywords: *Chrome-cobalt alloy, gold alloy, metallic post and core materials, post and core, post-endodontic restoration, titanium alloy*

Introduction

Excessive tooth structure removal and subsequent dehydration are responsible for affecting fracture resistance of restored tooth structure after endodontic therapy.[1] Resistance to fracture after endodontic therapy depends primarily on remaining dentin thickness, especially in a buccolingual direction.[2] Creation of excessive stress during obturation and use of higher concentration of irrigants with prolonged exposure times increase susceptibility of tooth to fracture, which reduces long-term survival rate, which is undesirable. Endodontic therapy should ideally

Access this article online

Quick Response Code:

Website: www.jpbsonline.org

DOI: 10.4103/jpbs.JPBS_205_20

Address for correspondence: Dr. Karunakaran Jeyaraman Venataraman, Department of Conservative Dentistry, JKK Nataraja Dental College & Hospital, Komarapalayam 638183, Tamil Nadu, India. E-mail: kkaran8@yahoo.com

How to cite this article: Venkataraman KJ, Thanapathi S, Balasubramanian S, Gandhi SA, Sarojinikutty AC. Fracture resistance of titanium, chrome–cobalt, and gold alloy as post and core materials: A comparative evaluation. J Pharm Bioall Sci 2020;12:S583-8.

reinforce the residual tooth structure. A considerable amount of radicular dentin in coronal and middle one-third is intentionally removed during biomechanical instrumentation, more so in case of curved canals, which weakens root structure.[3]

Rotary instruments exert considerable stresses in certain portions of canal wall and form microcracks, which become areas of increased stress concentration and predisposes to root fracture. These cracks spread or extend slowly over a period to the surface, eventually resulting in root fracture.[4] Stress concentration of radicular dentin in coronal one-third of root under lateral forces makes teeth susceptible to fracture at cementoenamel junction. The amount of remaining radicular and coronal dentin is directly proportional to fracture resistance.[5] Single file systems have been reported to reduce the amount of stresses on canal walls.[6] Fractures that occur post endodontic therapy can either be horizontal or vertical root fractures. Retreatment procedures also further removes dentin from within the canal rendering retreated teeth more susceptible to fracture. This study aims to comparatively analyze resistance to fracture of gold alloy (Au), chrome–cobalt (Co–Cr), and titanium alloy (Ti) post and core preparations in maxillary central incisors.

Materials and Methods

Extracted permanent maxillary central incisors were cleansed, and analyzed using radiovisiography. Twenty-four teeth with mature, intact root apices were selected. Mesiodistal and buccolingual diameters at the level of cementoenamel junction were tabulated with digital vernier calipers. Samples were weighed using precision weighing scale, tested for normality, and were evenly distributed across three experimental groups (n = 8) and stored (4°C, normal saline) [Figure 1].

Access was done and 15K-file (Dentsply Maillefer, Ballaigues, Switzerland) was inserted passively in canal until tip was visualized and adjusted to apical foramen. Working length was calculated by subtracting 0.5 mm from the recorded value, and canal preparation was done to master apical file size 40 using hand files (step-back preparation). A 3% sodium hypochlorite (8 mL) as initial and 17% ethylenediaminetetraacetic acid (EDTA) (5 mL/3 min) final were used for irrigation. A post-final rinse of 5 mL of distilled water was done.

Obturation was done by cold lateral condensation, and samples were stored at 37°C at 100% relative humidity for 72 h. Teeth were decoronated 3 mm from the deepest point of cementoenamel junction by comparing mesial and distal surfaces using a digital vernier caliper. Gutta-percha from canal was removed using Touch N Heat device (SybronEndo Orange, CA, USA), walls were cleared of sealer using Hedstrom files and size-1 Peeso reamer with care not to remove radicular dentin. A minimum apical seal of 5 mm was retained. Samples were assessed using radiovisiography for consistent finish and gutta-percha removal from canal.

Crown preparation was done using TF–12 flat-end tapered fissure bur (SS White burs) with a tip diameter of 1 mm, core ferrule was given using thin-tapered fissure burs. An anti-rotation notch was given for a depth of approximately 2 mm using flat-end tapered fissure bur on the thickest portion of root. Core height of all samples was standardized to 3 mm. Apical end of the post space preparation was assessed, gauged, and standardized to a specific width. The walls were cleansed, sealed with cotton plugs, and stored. Group I post and core wax pattern was fabricated using stainless steel sprue former (18 g) with medium inlay wax (dental inlay casting wax, GC, Newport Pagnell, UK). Subsequently after debubblizing and investing, pattern was cast (BEGO induction casting machine) with Au (20 carats) using a lost wax technique. In Group II, direct technique was used to fabricate post and core wax pattern using prepared sprue former (18 g) with a modeling wax (Geo Crowax; Renfert, Hilfingen, Germany). After debubblizing and investing, casting was done (BEGO induction casting machine, BEGO Bremer Goldschlägerei Wilh. Herbst GmbH & Co. KG, Bremen, Germany) with Co–Cr (Colado CC, Ivoclar Vivadent, AG, Principality of Liechtenstein) using lost wax technique. In Group III, root canal impressions obtained using direct wax patterns were scanned with digital scanner and a three-dimensional image was generated. Post and core was then fabricated using a laser sintering process for Ti (SISMA MYSINT 100, laser metal fusion).

Samples from each group were mounted on base (1.5” × 1.5” × 1.5”) vertically at an angle of 30° to long axis, clear epoxy resin was poured and allowed to set for 72 h and coded. They were kept covered by moist cotton till fracture testing. Samples were tested with the help of universal testing machine using a custom metal indenter (3 mm) with a crosshead speed of 1 mm/min, and the results were recorded.

Fracture types were observed, grouped, and recorded. The results were assessed by two different operators, compared, and tabulated. The samples were distributed across groups based on their weights and homogenicity. They were statistically assessed for normality of these variables. The results of fracture test were statistically analyzed using one-way analysis of variance (ANOVA)

test of variance with Tukey *post hoc* test for multiple comparisons.

Results

Group II had the highest fracture resistance with a mean value of 742.89 N. Groups III and I had mean values of 482.33 and 361.1123 N, respectively. Statistically significant difference between the experimental groups (I and II) and (II and III) in load values of root fracture ($P < 0.05$) [Figures 2–5] was observed.

Mesiodistal type of fracture was the most common among experimental groups with a percentage incidence of 54.20%. The incidence of comminuted, buccolingual, transverse, and other type of fractures were 29.2%, 4.2%, 8.3%, and 4.2%, respectively [Figures 6–8].

Discussion

Endodontic therapy should reinforce residual tooth structure in a way that it prevents untoward events long term.[7] To effectively access and prepare apical one-third, considerable amount of radicular dentin in coronal and middle one-third is removed. Factors

GROUPS (n= 8)	TYPE OF ALLOY
I	GOLD ALLOY
II	NICKEL CHROMIUM ALLOY
III	TITANIUM ALLOY

Figure 1: Post and core grouping

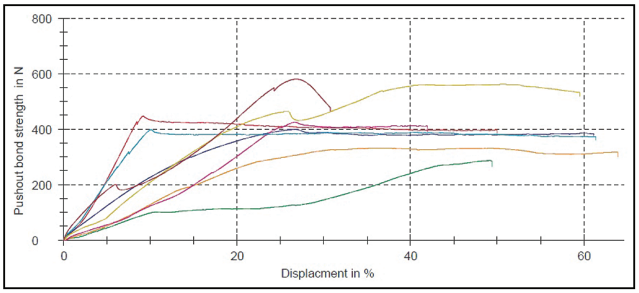

Figure 2: Fracture resistance Group I

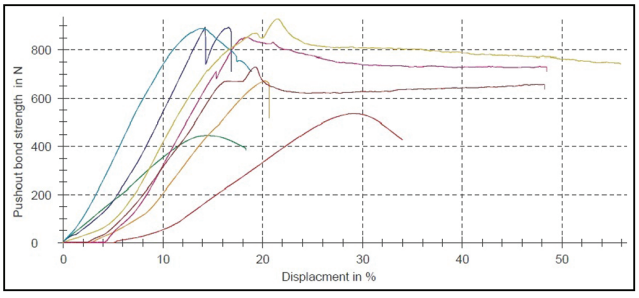

Figure 3: Fracture resistance Group II

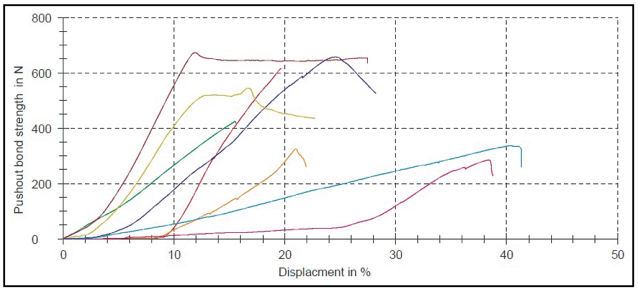

Figure 4: Fracture resistance Group III

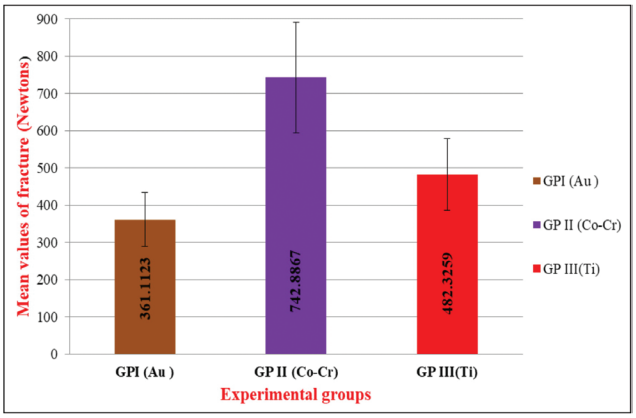

Figure 5: Fracture mean

Experimental Groups (n=8)	PERCENTAGE OF INCIDENCE				
	Buccolingual	Mesiodistal	Communited	Transverse	Others
I	0	50	25	12.5	12.5
II	0	62.5	37.5	0	0
III	12.5	50	25	12.5	0
OVERALL	4.2	54.2	29.2	8.3	4.2

Figure 6: Fracture types

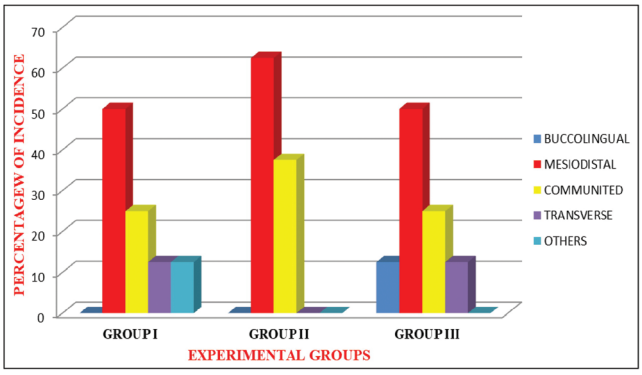

Figure 7: Fracture distribution

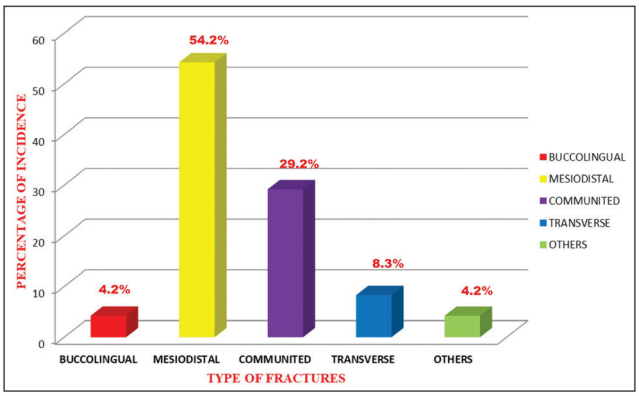

Figure 8: Incidence of fracture

affecting fracture susceptibility are tooth structure loss, trauma, age, tooth type, degree of calcification, excessive dentin removal, dehydration of dentin subsequent to endodontic therapy, obturation-induced stresses, and irrigant action on canal walls, which reduces long-term survival rate. Root thickness and ability to resist lateral dislodging forces have a directly proportional relationship. Fracture resistance improves with increase in the remaining root dentin thickness buccolingually.[8]

Vertical fractures can happen before, during, or after endodontic therapy. Roots are split along their long axis in vertical fracture and rarely occur as a result of acute trauma. Clinical studies revealed that 11%–13% of extracted teeth after endodontic treatment have been associated with vertical fractures[8] and most often have unfavorable prognosis.[9] Craze lines and cracks on canal walls become areas of high stress concentration and over a period extend to surface eventually, resulting in vertical root fracture. Cracks usually begin at the apex of root and propagate at the cervical.

Horizontal fractures are the most common, and they occur mainly in the anterior region due to frontal impact. They are common in middle one-third and rarely occur in apical and coronal one-third of root. Successful management of transverse root fracture depends on fracture line position, mobility of coronal segment, status of radicular, and coronal pulp tissues. Prognosis for teeth with transverse or horizontal root fractures is usually good.[10] Verified pulp necrosis has been reported with a percentage incidence of 43.7%, and the treatment depends on the position of tooth after it was fractured, the mobility of coronal segment, the status of the pulp, and the position of fracture line.[11] Repair and healing occurs either by hard tissue union, which is a desirable, bony ingrowth, fibrous healing, or granulation tissue formation. Fractures as a result of fatigue due to repetitive occlusal forces have been reported in teeth, which are vital. The position and relationship of fracture line to gingival crevice is the most important factor, affecting the long-term prognosis. Coronal and middle one-third fractures have less favorable prognosis compared to apical root fractures. In infrabony fractures with no communication to gingival sulcus, meticulous oral hygiene and appropriate treatment options result in successful outcomes.

Rotary files used for gutta-percha removal during retreatment have been shown to remove surface dentin. Further enlargement of apical third to achieve better cleansing contributes to reduced fracture resistance. There has been a positive correlation between the removal of dentin during retreatment procedures and the reduction of fracture resistance.[12]

Newer generation of materials improve bond between radicular dentin, sealer, and sealer–core interface, which improves fracture resistance. Modulus of elasticity of obturation material should ideally be approximate to that of radicular dentin for root reinforcement.[13] Priming radicular dentinal surface improves bond between sealer, dentin, and core. Also the modulus of elasticity of obturating material, post, and sealer has to match that of radicular dentin, leading to even distribution of induced stresses, and borne by components of monoblock.[14]

Failure rates were almost double where adequate post-endodontic restoration was not done.[15] Use of intra-orifice barriers effectively decreases coronal leakage and improves fracture resistance.[16,17] Cast post and core preparation removes radicular dentin, needs multiple clinical visits, leading to more turnover time, and has an elastic modulus, which is high (200 Gpa) compared to tooth structure, which can predispose to fractures.[18] Metallic post failures are most often due to root fracture, post-fracture, or post-retention loss. In endodontically treated teeth, the amount of remaining dentin and the provision of ferrule increase survival rate. Studies with longer follow-up have been recommended.[19]

Endodontic irrigation leads to an alteration of chemical composition, organic and inorganic phases of radicular dentin, which affects microhardness, permeability, and solubility leading to changes in the ability of teeth to resist fracture under varying loads. EDTA affects fracture resistance based on the exposure time and concentration.[20]

Sealers contributing to improving fracture strength of the roots have been evaluated.[21] Adhesion to canal walls increases mechanical interlocking and reduces risk of fracture.[22] Obturation material and technique

choices impact the resistance of root to fracture. Gutta-percha along with adhesive resin sealers have been reported to improve the fracture resistance.[23] Adhesive ionomer coating on gutta-percha for a thickness of 2 microns to which a adhesive ceramic sealer could be bonded to form a tertiary monoblock improves facture resistance.[24]

Gutta-percha used with a resin-based sealer has several advantages but its hydrophobic nature and its inability to sufficiently reinforce the root have fuelled the development of hydrophilic materials, which penetrate dentinal tubules and use moisture in dentinal walls, which allows the material to bond to root canal wall and core, which reinforces the root. Polymerization shrinkage of the resin-based sealers due to high C-factor associated with root canal results in sealer contraction post filling and weakening bond between sealer and canal wall, leading to reduced resistance to fracture. A novel sealer, which has the property of sealer expansion, due to its self-expanding and hydrophilic composition significantly increased the resistance to fracture.[25]

There has been a positive correlation between the microcrack formation and the incidence of root fractures. Root fracture is a gradual propagation of craze lines and microcracks in radicular dentin.[26] Microcracks are formed as a result of rotational forces that are being applied to canal walls. Increased incidence, reported with some rotary instrumentation techniques, is related to design features of rotary instruments such as tip size, cross-sectional geometry, pitch, and taper. Hand instruments produce a less dentinal defects compared to rotary instruments.[27] Investigators have found a proportional relationship between rotary instrument design and vertical fractures.[28] Migration from a rotary to reciprocating motion, involving different clockwise, counter-clockwise angles, results in minimal torsional, flexural stresses, and less radicular dentin binding. Reciprocating file systems produce significant amount of incomplete dentinal cracks in apical third when compared to rotary files.[29] Both hand and reciprocating instruments induced the formation of dentinal defects during the canal preparation.[30] Self-adjusting file drastically changes the way in which canal is prepared. Straightening of curved canals is reduced because of the absence of a rigid core and pliability of file.[6] The file removes a surface layer of dentin, which results in a canal of larger dimensions but a similar cross section.[31]

Cracks or craze lines that extend from external surface of root into dentin, which do not reach the root canal lumen and structural defects in root dentin, have been found to cause fractures due to amplification of induced stresses at these formed microcracks.[32] They were found in areas away from direct contact of rotary instruments. One possible reason is that stress generated during instrumentation of canals is transmitted to external surface of teeth where it overcomes bonds in dentin to form these craze lines, microcracks, and eventually resulting in fractures.[33,34]

This *in vitro* study evaluated the fracture strength on extracted maxillary central incisors, and due to large amount of variations in volume and weight of roots among the samples selected, sufficient protocols were followed for the standardization of controllable factors. Normality testing of these variables was assessed statistically, and distributions were found to be normal at 5% level of significance.

Conclusion

Radicular dentin should be preserved as much as possible during endodontic therapy. The choice of instrumentation protocols followed, obturating technique, and the choice of materials has to be customized to individual tooth based on preoperative analysis, which would lead to better long-term outcomes. Metallic post and core preparations seem an attractive option. Development of newer alloy systems and materials, which are biocompatible and match elastic modulus of dentin, are recommended.

Financial support and sponsorship

Nil.

Conflicts of interest

There are no conflicts of interest.

References

1. Robbins JW. Restoration of the endodontically treated tooth. Dent Clin North Am 2002;46:367-84.
2. Sedgley CM, Messer HH. Are endodontically treated teeth more brittle? J Endod 1992;18:332-5.
3. Sornkul E, Stannard JG. Strength of roots before and after endodontic treatment and restoration. J Endod 1992;18:440-3.
4. Yoldas O, Yilmas S, Atakan G, Knudsen C, Kasan Z. Dentinal microcrack formation during root canal preparations by different rotary NiTi instruments and the self-adjusting file. J Endod 2012;38:232-5.
5. Lertchirakarn V, Timyam A, Messer HH. Effects of root canal sealers on vertical root fracture resistance of endodontically treated teeth. J Endod 2002;28:217-9.
6. Metzger Z, Teperovich E, Zary R, Cohen R, Hof R. The self-adjusting file (SAF). Part 1: respecting the root canal anatomy—a new concept of endodontic files and its implementation. J Endod 2010;36:679-90.
7. Johnson ME, Stewart GP, Nielsen CJ, Hatton JF. Evaluation of root reinforcement of endodontically treated teeth. Oral Surg Oral Med Oral Pathol Oral Radiol Endod 2000;90:360-4.

8. Fuss Z, Lustig J, Tamse A. Prevalence of vertical root fractures in extracted endodontically treated teeth. Int Endod J 1999;32:283-6.
9. Meister F Jr, Lommel TJ, Gerstein H. Diagnosis and possible causes of vertical root fractures. Oral Surg Oral Med Oral Pathol 1980;49:243-53.
10. Lo Giudice R, Lizio A, Cervino G, Fabiana N, Francesco P, Ausiello P, *et al*. The horizontal root fractures. Diagnosis, clinical management and three-year follow-up. Open Dent J 2018;12:687-95.
11. Al-Nazhan S, Andreasen JO, Al-Bawardi S, Al-Rouq S. Evaluation of the effect of delayed management of traumatized permanent teeth. J Endod 1995;21:391-3.
12. Ganesh A, Venkatesh Babu N, John A, Deenadhayalan G, Kandaswamy DA. Comparative assessment of fracture resistance of endodontically treated and retreated teeth: an *in-vitro* study. J Cons Dent 2014;17:61-5.
13. Williams C, Loushine RJ, Weller RN, Pashley DH, Tay FR. A comparison of cohesive strength and stiffness of resilon and gutta-percha. J Endod 2006;32:553-5.
14. Tay FR, Pashley DH. Monoblocks in root canals: a hypothetical or a tangible goal. J Endod 2007;33:391-8.
15. Swartz DB, Skidmore AE, Griffin JA. Twenty years of endodontic success and failures. J Endod 1983;9:198-202.
16. Yavari HR, Samiei M, Shahi S, Aghazadeh M, Jafari F, Abdolrahimi M, *et al*. Microleakage comparison of four dental materials as intra-orifice barriers in endodontically treated teeth. Iran Endod J 2012;7:25-30.
17. Roghanizad N, Jones JJ. Evaluation of coronal microleakage after endodontic treatment. J Endod 1996;22:471-3.
18. Sarkis-Onofre R, Skupien JA, Cenci MS, Moraes RR, Pereira-Cenci T. The role of resin cement on bond strength of glass-fiber posts luted into root canals: a systematic review and meta-analysis of *in vitro* studies. Oper Dent 2014;39: E31-44.
19. Marchionatti AME, Wandscher VF, Rippe MP, Kaizer OB, Valandro LF. Clinical performance and failure modes of pulpless teeth restored with posts: a systematic review. Braz Oral Res 2017;31:e64.
20. Uzunoglu E, Aktemur S, Uyanik MO, Durmaz V, Nagas E. Effect of ethylenediaminetetraacetic acid on root fracture with respect to concentration at different time exposures. J Endod 2012;38:1110-3.
21. Bhat SS, Hegde SK, Rao A, Mohammed SAK. Evaluation of resistance of teeth subjected to fracture after endodontic treatment using different root canal sealers: an *in-vitro* study. J Indian Soc Pedod Preventive Dent 2012;4:305-9.
22. Jhamb S, Nikhil V, Singh V. Effect of sealers on fracture resistance of endodontically treated teeth with and without smear layer removal: an *in vitro* study. J Conserv Dent 2009;12:114-7.
23. Sandikci T, Kaptan RF. Comparative evaluation of the fracture resistances of endodontically treated teeth filled using five different root canal filling systems. Niger J Clin Pract 2014;17:667-72.
24. Celikten B, Uzuntas CF, Gulsahi K. Resistance to fracture of dental roots obturated with different materials. Biomed Res Int 2015;2015:591031.
25. Hegde V, Arora S. Fracture resistance of roots obturated with novel hydrophilic obturation systems. J Conserv Dent 2015;18:261-4.
26. Bolla M, Muller-Bolla M, Borg C, Lupi-Pegurier L, Laplanche O, Leforestier E. WITHDRAWN: root canal posts for the restoration of root filled teeth. Cochrane Database Syst Rev 2016;11:CD004623.
27. Shori DD, Shenoi PR, Baig AR, Kubde R, Makade C, Pandey S. Stereomicroscopic evaluation of dentinal defects induced by new rotary system: "protaper NEXT". J Conserv Dent 2015;18:210-3.
28. Kim HC, Lee MH, Yum J, Versluis A, Lee CJ, Kim BM. Potential relationship between design of nickel-titanium rotary instruments and vertical root fracture. J Endod 2010;36:1195-9.
29. Bürklein S, Tsotsis P, Schäfer E. Incidence of dentinal defects after root canal preparation: reciprocating versus rotary instrumentation. J Endod 2013;39:501-4.
30. Helvacioglu-Yigit D, Aydemir S, Yilmaz A. Evaluation of dentinal defect formation after root canal preparation with two reciprocating systems and hand instruments: an *in-vitro* study. Biotechnol Equip 2015;29:368-73.
31. Hof R, Perevalov V, Eltanani M, Zary R, Metzger Z. The self-adjusting file (SAF). Part 2: mechanical analysis. J Endod 2010;36:691-6.
32. Gudoutos EE. Fracture mechanics: an introduction. 2nd ed. Dordrecht, The Netherlands: Springer Publishers; 2005. pp. 79-94.
33. Shemesh H, van Soest G, Wu MK, Wesselink PR. Diagnosis of vertical root fractures with optical coherence tomography. J Endod 2008;34:739-42.
34. Shemesh H, Wesselink PR, Wu MK. Incidence of dentinal defects after root canal filling procedures. Int Endod J 2010;43:995-1000.

Original Article

A Comparative Evaluation of Phytic Acid as Final Rinse Solution with Other Chelating Agents for Elimination of Intraradicular Smear: A Scanning Electron Microscopy Study

Shrimanikandan Ayappa Gandhi, Preetha Chandrasekar[1], Jayaprakash Nachimuthu[1], Chris S. Abraham[1], Karunakaran Jeyaraman Venkataraman[1]

Department of Craniofacial Surgery & Dentistry, Velammal Medical Hospital & Research Institute, Madurai, Tamilnadu, India, [1]Department of Conservative Dentistry, JKK Nataraja Dental College & Hospital, Komarapalayam, Tamilnadu, India

Received : 17-02-2020.
Revised : 24-02-2020.
Accepted : 06-03-2020.
Published : 28-08-2020.

ABSTRACT

Aim: The aim of this study was to compare radicular smear layer removal ability of different solutions of phytic acid (PA) with other chelating agents when used in specific irrigant protocols. **Materials and Methods:** Seventy four maxillary central incisors were collected, standardized, and canals were prepared. A total of 5% sodium hypochlorite was used as the initial rinse solution (8mL). Samples were divided into control (Group I—normal saline and II—7% ethylenediaminetetraacetic acid) and experimental groups (Group III, IV, V, VI, VII, and VIII) based on the type of final rinse solution used, that is, 5% PA, 10% PA, 17% PA, 5% citric acid (CA), 10% CA, and 17% CA (5mL). Samples were coded, buccolingually divided into two halves, dehydrated, mounted, splutter coated, and examined under scanning electron microscope. **Results:** Group IV had the least smear and debris in coronal, middle, and apical thirds with mean scores of 1.06 and 1.3, respectively. When compared with Group II, no statistically significant difference was found ($P > 0.05$). Overall, the Group III had the lowest erosion scores at apical, middle, and coronal one-third with a mean of 1.68. Group VII had the highest amount of erosion with loss of peritubular and intertubular dentin at all levels. **Conclusion:** The role of PA as final rinse solution for the removal of radicular smear is promising and comparable to other chelating agents.

Keywords: *Chelating agents, final rinse solution, irrigant solution, phytic acid, root canal irrigants, smear*

Introduction

Biomechanical preparation procedure during endodontic therapy aims to prepare, cleanse the canal system, and eliminate microorganisms.[1] The smear formed during canal preparation contains both organic and inorganic constituents, and no single irrigant solution effectively removes both.[2] Biomechanical preparation can propel constituents of smear into radicular dentin for depths of up to 40 µm.[3-5] When surface active agents are used to enhance irrigant efficacy, capillary action, and adhesive forces further push smear for depths of up to 110 µm.[6,7] Different techniques have been suggested for effective smear elimination from canal ramifications.[8,9]

Access this article online

Quick Response Code:

Website: www.jpbsonline.org

DOI: 10.4103/jpbs.JPBS_186_20

Address for correspondence: Dr. Shrimanikandan A, Asst. Professor, Department of Craniofacial surgery & Dentistry, Velammal medical hospital & Research Institute, Madurai, Tamilnadu – 625 009. E-mail: kkaran8@yahoo.com

How to cite this article: Gandhi SA, Chandrasekar P, Nachimuthu J, Abraham CS, Venkataraman KJ. A comparative evaluation of phytic acid as final rinse solution with other chelating agents for elimination of intraradicular smear: A scanning electron microscope study. J Pharm Bioall Sci 2020;12:S576-82.

Nygaard-Østby, in 1957, used chelating agents to negotiate calcified and narrow canals. They have been used as irrigant solutions aiming for removing inorganic constituents of smear by chelation. Ethylenediaminetetraacetic acid (EDTA) is popularly being used for smear removal in a concentration of 17%.[10] It is also recommended for use as a lubricant during rotary instrumentation procedures. Chelating agents have found a definitive role in endodontic therapy as final rinse solutions as use of sodium hypochlorite alone has been inefficient in removing inorganic smear components. EDTA as a final rinse solution is very effective. Various irrigant solutions with properties of chelation have been experimented with. Citric acid (CA), etidronate (HEBP), and tetracycline have been found to be effective as chelating agents.[11,12] Various synthetic chemicals used as final rinse solutions during biomechanical preparation when extruded beyond the apex even in minute quantities induce undesirable side effects and can harm periapical tissues. The hazards encountered due to the use of sodium hypochlorite have propelled investigators to look for safer, biocompatible alternatives.[13] Natural substances when used for treatment have lesser side effects compared to synthetic drugs and less antibiotic resistance.

In 1855, inositol hexaphosphate (IP6) was identified, and it is found in nuts, legumes, whole grains, cereals, and seeds. It is an energy source for the germinating plants. IP6 has excellent properties of chelation and functions as an antioxidant by a process of chelating divalent cations, such as copper and iron. This prevents the generation of reactive oxygen species responsible for carcinogenesis and cellular damage.[14,15] Animal studies have shown that IP6 is safe when administered in high doses for long periods. It has found a role as an implant coating for magnesium alloy where it improves corrosion resistance and stimulates new bone formation. It is also known as phytic acid (PA) and myo-inositol hexaphosphate.[16,17]

Materials and Methods

Seventy-four extracted human permanent maxillary central incisors were collected, cleansed, and analyzed using radiovisiography. Teeth with mature, intact root apices were coded, standardized to 15 mm from apical tip, apical third covered with wax, and embedded in plastic cups filled with polyvinyl siloxane. This simulated *in vivo* closed apex conditions preventing irrigant extrusion beyond apex, and they were randomly divided into two control (n = 5) and six experimental groups (n = 8) [Table 1, Figure 1]. The canals were instrumented up to size F3 ProTaper rotary files (Dentsply Maillefer, Ballaigues, Switzerland) as per manufacturer instructions. A total of 8 mL was used as initial rinse. A total of 5 mL of the irrigant was used as final rinse as per the respective group for 3 min. The irrigant was delivered using a ProRinse 28-gauge side-vent needle (Dentsply, Tulsa Dental, Tulsa, Oklahoma) at working length.

During the first minute, needle was withdrawn 5 mm inserted back to working length followed by 180° rotation alternatively three times. A F2 size gutta-percha cone (Dentsply Maillefer) was inserted to working length and withdrawn six times (manual dynamic activation) during second minute to improve the irrigant replacement at apical third. After 3 min, a post final irrigation rinse of 10 mL of distilled water was carried out.

The teeth were divided into two halves in a buccolingual plane using diamond disc, and the half containing the most visible part of the apex was selected, coded, and stored. The split halves were placed in 10% neutral buffered formalin solution at 18°C for 24 h, post fixed in osmium tetroxide (1% wt/vol), and dehydrated in graded solutions of isopropyl alcohol (Nice Chemicals, Cochin, India). Separation markings of 5 mm were made for coronal, middle, and apical thirds, and samples were exposed to ultraviolet light in a sterilization chamber and stored in sterile pouches. They were mounted on aluminum stubs with carbon tape (Royal tapes, Chennai, India), sputter coated with a 20–30 nm thin layer of gold (Quorum, East Sussex, United Kingdom), examined using a scanning electron microscope with a high resolution (SIGMA 0336 Fesem, Zeiss, Munich, Germany). Images were obtained at ×2000 magnification using digital image analysis software and stored appropriately for subsequent analysis. Micrographs were recorded for each millimeter of specimen for coronal, middle, and apical thirds of root, and scoring was done by

Table 1: Initial and final rinse solutions

GROUPS (n= 5-8)	INITIAL RINSE	FINAL RINSE
I - Negative Control (n=5)	Normal Saline	Normal Saline
II – Positive Control (n=5)	5% NaOCl	17% EDTA
III	5% NaOCl	5% Phytic Acid
IV	5% NaOCl	10% Phytic Acid
V	5% NaOCl	17% Phytic Acid
VI	5% NaOCl	5% Citric Acid
VII	5% NaOCl	10% Citric Acid
VIII	5% NaOCl	17% Citric Acid

independent operators, compared, and tabulated. The smear, debris, and erosion were evaluated using criteria developed by Caron *et al.*,[18] Dadresanfar *et al.*,[19] and Torabinejad *et al.*,[20] respectively.

Results

Group II (17% EDTA) and Group IV (10% PA) had least smear scores at the coronal, middle and apical thirds respectively [Figure 2]. At coronal and middle thirds, Group V (17% PA) was very effective and was as efficient as Groups II and IV at coronal and middle thirds. At apical third, it was less effective than Group IV. There was no significant difference between Groups II and IV ($P > 0.05$). In this study, Group II (17% EDTA) and Group VII (10% CA) presented least amounts of debris among all groups at the apical middle and coronal thirds, respectively. Group IV (10% PA) and Group VI (5% CA) were very efficient in removing debris at coronal and middle thirds [Figure 3]. There was no significant difference between the Groups II and VII ($P > 0.05$). Among experimental groups, Group VII (10% CA) had most values for erosion at the coronal, middle, and apical one-third, respectively. Group II (17% EDTA), Group IV (10% PA), and Group VII (10% CA) had comparable levels of erosion at all three levels [Figure 4]. Apical third of the root had the highest smear, debris and least values for erosion [Figure 5]. On statistical comparison and analysis, no significant difference was observed between the Groups IV and VII ($P > 0.05$) [Figure 6].

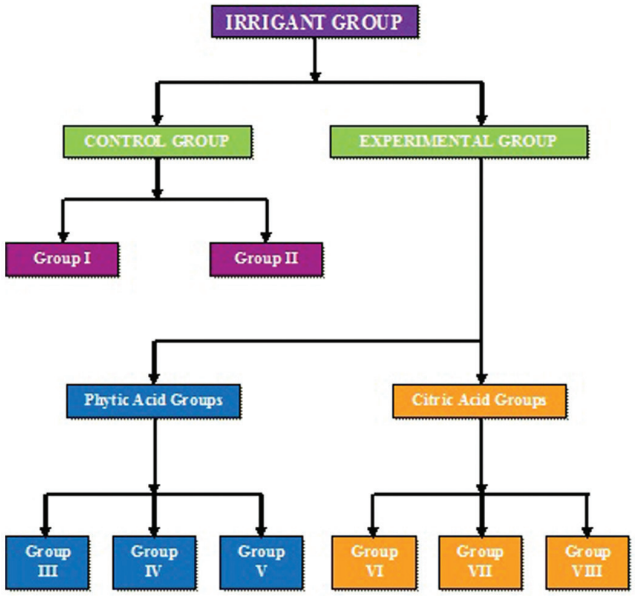

Figure 1: Irrigant group

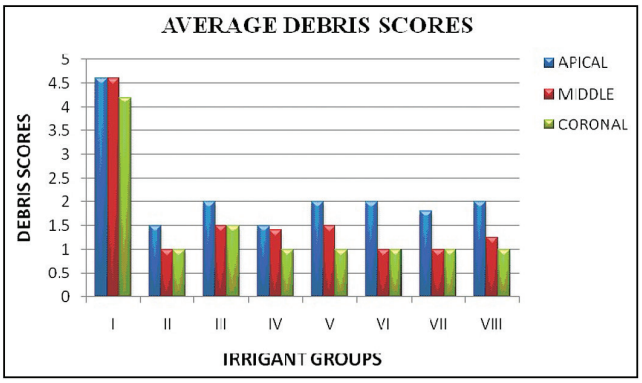

Figure 3: Average debris scores

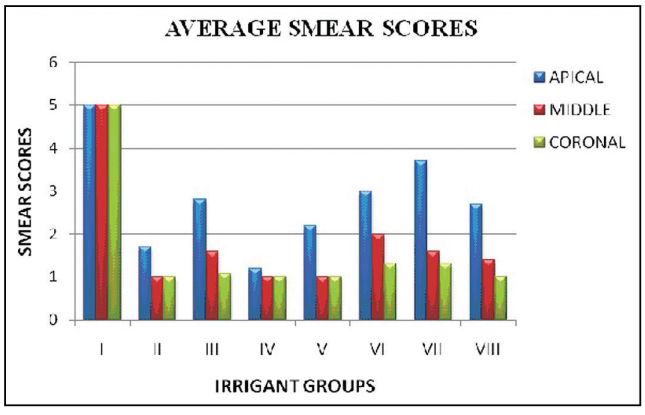

Figure 2: Average smear scores

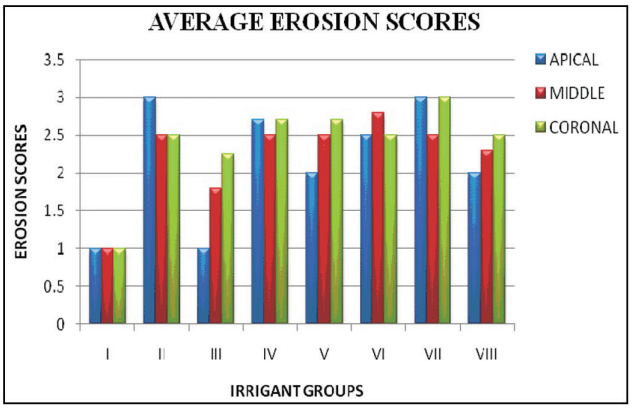

Figure 4: Average erosion scores

Discussion

Removal of vital pulp and necrotic remnants, microbes, their by-products, smear, and debris is essential for successful outcomes of therapy. The rotary instruments act primarily in central lumen leaving isthmi, cul-de-sac of the canal system untouched. These areas due to inadequate cleansing, serve as a reservoir for microbial proliferation and impairs achieving a hermetic seal.[21,22] Smear layer elimination significantly enhances apical and coronal seal after obturation. It is independent of site of leakage, type of sealer, obturation technique, duration, and type of dye used for testing. Failure

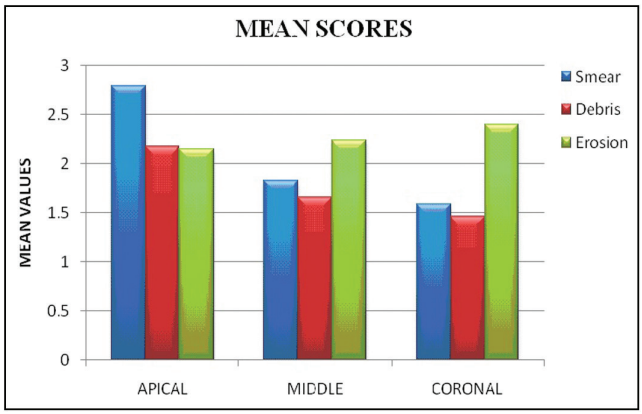

Figure 5: Mean scores – Apical, Middle and Coronal

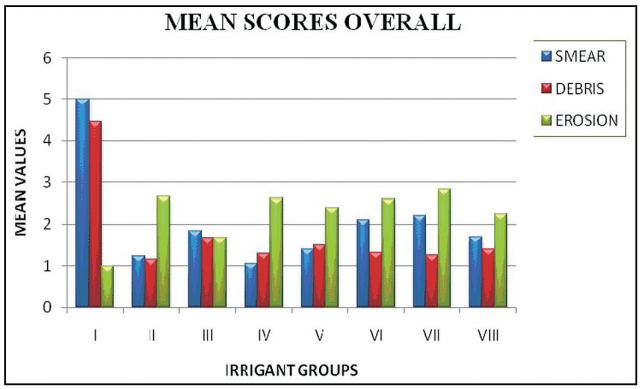

Figure 6: Overall mean scores

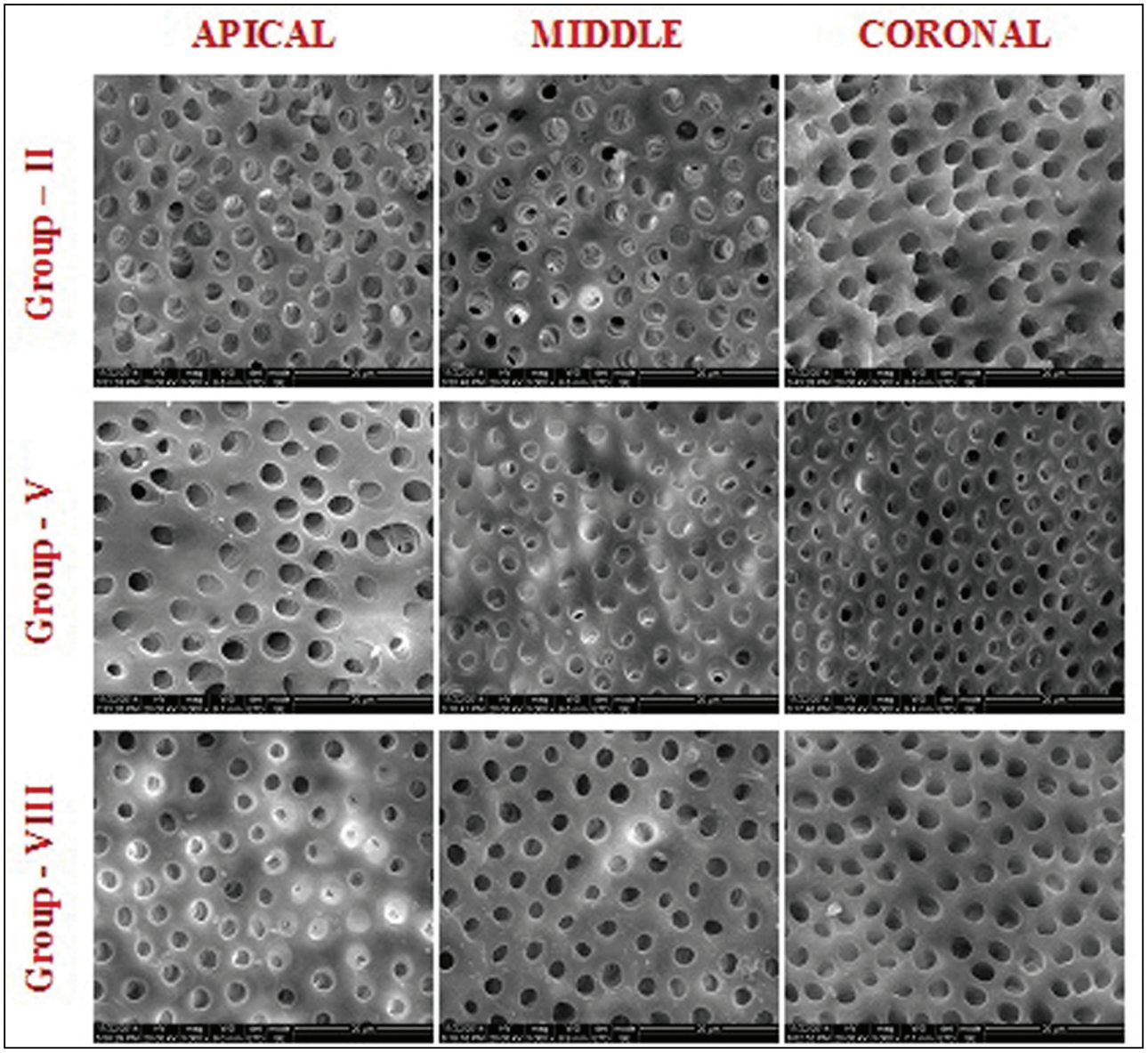

Figure 7: Scanning electron microscopic comparison – Gp- II,V, VIII

to obtain a hermetic seal affects the prognosis and outcome of endodontic therapy.[23]

Poor treatment outcomes are due to inadequate cleansing and persistent hidden infections within root canals. Sequential use of irrigant solutions during canal preparation has been advocated to eliminate microbes from within canals. These solutions have undesirable effects on periradicular tissues.[24] Irrigating solutions used during endodontic procedures need to be safe and biocompatible. A number of naturally derived substances have been tried as final rinses during endodontic therapy. This study evaluates a naturally derived chelating agent PA as a final rinse comparatively with other chelating agents. Microbial resistance is also a common issue encountered with the use of chemical irrigants repetitively. The natural derivatives have a vital role in these kinds of situations as being available as alternative safe, biocompatible, and nontoxic materials.

This study was conducted in maxillary central incisor teeth where canal preparation was standardized using a custom protocol. Custom prepared PA solutions of 5%, 10%, and 17% was compared with 17% EDTA, 5%, 10%, and 17% CA solutions for its efficacy as a final rinse solution.[10] Group II and IV presented least amounts of smear among all groups. The Group V was also effective in removing smear and was as efficient on comparison with Groups II and IV at coronal and middle one-third of root. At the apical one-third, it was less effective than group IV. No significant difference was observed between Groups II and IV ($P > 0.05$). The CA groups were fairly efficient in removing smear at coronal and middle one-third. It was not as effective at apical thirds of root [Figure 7-9].

The selection of irrigant is of utmost importance in cleansing the canal system. Addition of surfactants, increasing irrigant temperature, volume, and activation has been advocated to improve irrigant efficacy. Use of two different irrigants in a sequence is commonly done to overcome shortcomings associated with the use of a single irrigant. Investigators tried out new methodologies and realized that combinations of irrigants were the most effective at smear layer removal, as per the concept of a working and a final irrigant solution.[25,26] Sequential use of organic and inorganic solvents for smear elimination was tried as no single solution was effective in removing both organic and inorganic constituents. A total of 5% sodium hypochlorite solution and 17% EDTA were found to be most effective when used as initial and final rinses.[27] Irrigant solution must be in contact with entire canal wall for a sufficient period to be effective. This

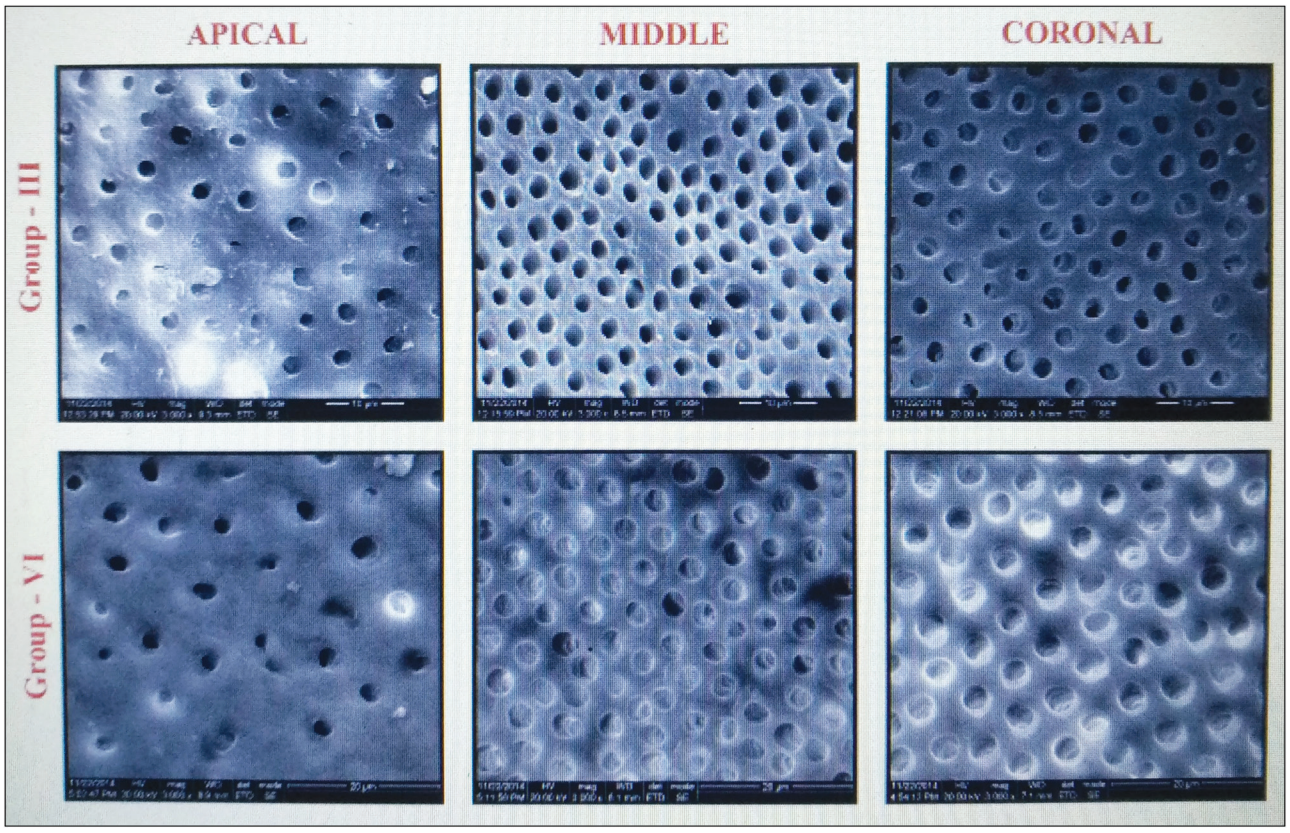

Figure 8: Scanning electron microscopic comparison Gp- VI,III

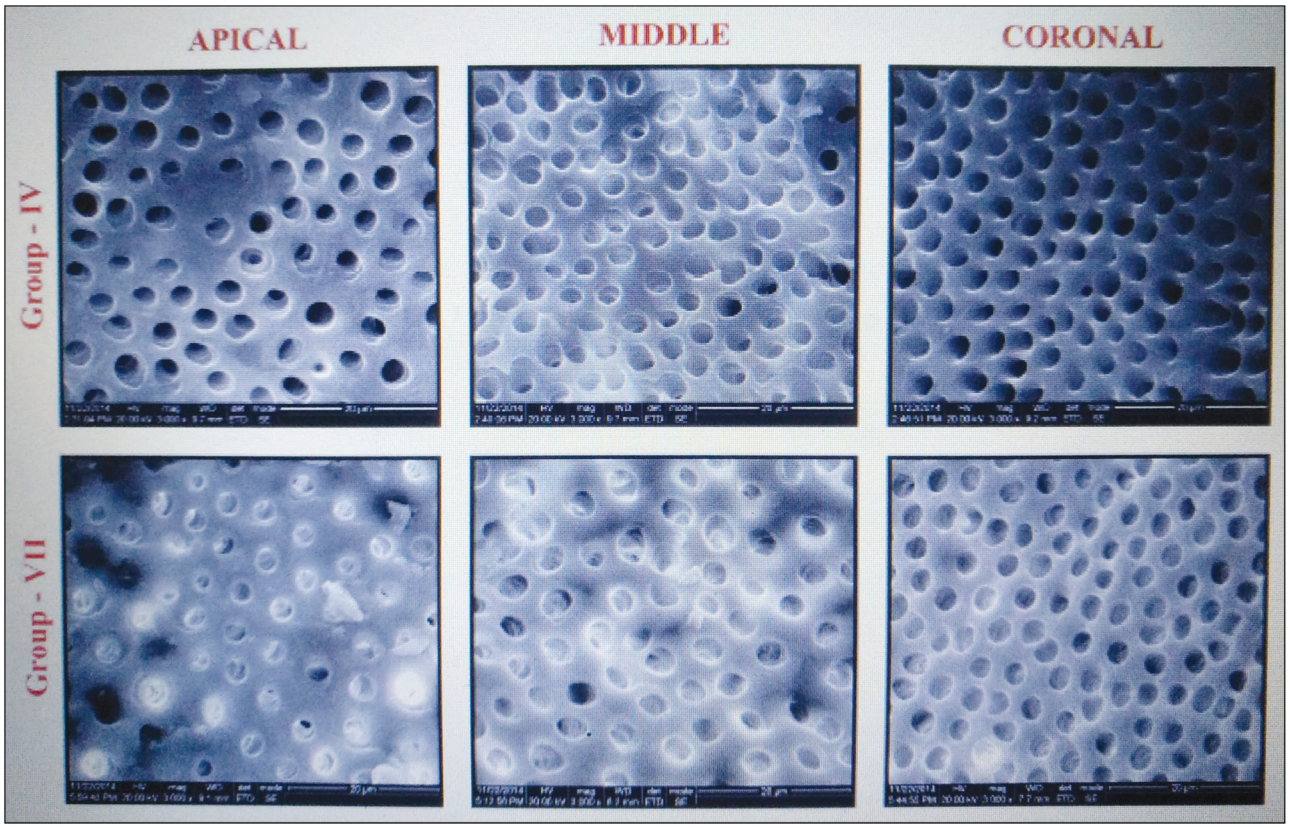

Figure 9: Scanning electron microscopic comparison – Gp – IV, VII

study used a side-vent needle for delivery of irrigant with vent placed at 1 mm from tip in a customized irrigant protocol. Computational dynamic fluid flow has shown the limitations of a side-vent needle on irrigant replacement, and suitable modifications were made to enhance irrigant replacement in a custom-designed conventional irrigation protocol. The volume of irrigant also plays a vital role, and in this study, 8 mL during the initial and 5 mL during the final rinse were used. The duration of the exposure of final rinse solution is also important as providing sufficient time enhances irrigant action and efficacy. Apical third presented with the most amounts of smear and debris when compared to coronal and middle one third. With suitable assessment of ideal concentration, duration of exposure, and volume, it was found that PA has the potential to be successfully used as a final rinse solution.[28-32]

Conclusion

The use of PA as a final rinse solution in biomechanical preparation procedures during endodontic therapy is promising as it was found to be fairly effective at all thirds of the root canal. The results are comparable to 17% EDTA, which has been used widely as a final rinse solution. Being natural and biocompatible, PA seems an ideal candidate for use as a final rinse solution, and further studies, which explore other aspects of its viability as a final rinse solution and evaluation in a clinical setting, are recommended. This study was conducted in straight canals, and more difficult and challenging conditions would be present in posterior teeth, which have smaller root canals with more ramifications and curvature.

Financial support and sponsorship

Nil.

Conflicts of interest

There are no conflicts of interest.

References

1. Haapasalo M, Endal U, Zandi H, Coil JM. Eradication of endodontic infection instrumentation and irrigation solutions. Endod Top 2005;10:77-102.
2. Zehnder M. Root canal irrigants. J Endod 2006;32:389-98.
3. Eick JD, Wilko RA, Anderson CH, Sorensen SE. Scanning electron microscopy of cut tooth surfaces and identification of debris by use of the electron microprobe. J Dent Res 1970;49:1359-68.
4. Brännström M, Johnson G. Effects of various conditioners and cleaning agents on prepared dentin surfaces: a scanning electron microscopic investigation. J Prosthet Dent 1974;31:322-30.
5. McComb D, Smith D. A preliminary scanning electron microscopic study of root canals after endodontic procedures. J Endod 1975;1:238-42.

6. Mader CL, Baumgartner JC, Peters DD. Scanning electron microscopic investigation of the smeared layer on root canal walls. J Endod 1984;10:477-83.
7. Aktener BO, Cengiz T, Pişkin B. The penetration of smear material into dentinal tubules during instrumentation with surface-active reagents: a scanning electron microscopic study. J Endod 1989;15:588-90.
8. Gu LS, Kim JR, Ling J, Choi KK, Pashley DH, Tay FR. Review of contemporary irrigant agitation techniques and devices. J Endod 2009;35:791-804.
9. Violich DR, Chandler NP. The smear layer in endodontics—a review. Int Endod J 2010;43:2-15.
10. Mohammadi Z, Shalavi S, Jafarzadeh H. Ethylenediaminetetraacetic acid in endodontics. Eur J Dent 2013;7: S135-42.
11. Khedmat S, Shokouhinejad N. Comparison of the efficacy of three chelating agents in smear layer removal. J Endod 2008;34:599-602.
12. Souza SM, Silva TL. Demineralization effect of EDTA, EGTA, CDTA and citric acid on root dentin: a comparative study. Braz Oral Res 2005;19:188-92.
13. Sipavičiūtė E, Manelienė R. Pain and flare-up after endodontic treatment procedures. Stomatologija 2014;16:25-30.
14. Richa W, Dharti G, Gaurav S, Bhupinder K. Traditional and newer root canal irrigants in endodontics: an overview. Int J Innov Drug Discov 2014;4:133-9.
15. Ali M, Shuja M, Zahoor M, Quadri I. Phytic acid: how far have we come? Afr J Biotechnol 2010;9:1551-4.
16. Chen Y, Zhao S, Liu B, Chen M, Mao J, He H, *et al*. Corrosion-controlling and osteo-compatible Mg ion-integrated phytic acid (Mg-PA) coating on magnesium substrate for biodegradable implants application. ACS Appl Mater Interfaces 2014;6:19531-43.
17. Nassar M, Hiraishi N, Tamura Y, Otsuki M, Ohya K, Tagami J. Phytic acid: an alternative root canal chelating agent. J Dent Res 2014;93:871.
18. Caron G, Nham K, Bronnec F, Machtou P. Effectiveness of different final irrigant activation protocols on smear layer removal in curved canals. J Endod 2010;36:1361-6.
19. Dadresanfar B, Khalilak Z, Delvarani A, Vatanpour M, Pourassodallah M. Effect Of ultrasonication with EDTA or MTAD on smear layer, debris and erosion scores. J Oral Sci 2011;53:31-6.
20. Torabinejad M, Cho Y, Khademi AA, Bakland LK, Shabahang S. The effect of various concentrations of sodium hypochlorite on the ability of MTAD to remove the smear layer. J Endod 2003;29:233-9.
21. Czonstkowsky M, Wilson EG, Holstein FA. The smear layer in endodontics. Dent Clin North Am 1990;34:13-25.
22. Bjorvatn K. Antibiotic compounds and enamel demineralization: an *in vitro* study. Acta Odontol Scand 1982;40:341-52.
23. Sharavan A, Hagudoost A, Adi A, Rahimi H, Shadifon F. Effect of smear layer on sealing ability of canal obturation: a systematic review and meta analysis. J Endod 2007; 33:96-105.
24. Georgi T, Lambrianidis T, Zarra T. Tissue damage after inadvertent citric acid extrusion during root canal treatment: report of a case. Balkan J Stomatol 2013;17:101-6.
25. Baumgartner JC, Brown CM, Mader CL, Peters DD, Shulman JD. A scanning electron microscopic evaluation of root canal debridement using saline, sodium hypochlorite, and citric acid. J Endod 1984;10:525-31.
26. Kaufman AY, Greenberg I. Comparative study of the configuration and the cleanliness level of root canals prepared with the aid of sodium hypochlorite and bis-dequalinium-acetate solutions. Oral Surg Oral Med Oral Pathol 1986;62:191-7.
27. Karunakaran JV, Kumar SS, Kumar M, Chandrasekhar S, Namitha D. The effects of various irrigating solutions on intra-radicular dentinal surface: an SEM analysis. J Pharm Bioallied Sci 2012;4:S125-30.
28. Paragolia R, Franco V, Fabiani C, Giardino L, Palazzi F, Cheiffi N, *et al*. Comparison of smear layer removal using four final rinse protocols. Int Dent 2007;7:50-6.
29. Shamsuddin AM, Vucenik I, Cole KE. IP6: a novel anti-cancer agent. Life Sci 1997;61:343-54.
30. Prosser HJ, Brant PJ, Scott RP, Wilson AD. The cement-forming properties of phytic acid. J Dent Res 1983;62: 598-600.
31. Nassar M, Hiraishi N, Islam MS, Aizawa M, Tamura Y, Otsuki M, *et al*. Effect of phytic acid used as etchant on bond strength, smear layer, and pulpal cells. Eur J Oral Sci 2013;121:482-7.
32. Nygaard-Østby B. Chelation in root canal therapy: ethylenediaminetetraacetic acid for cleansing and widening of root canals. Odontologisk Tidskrift 1957;65:3-11.

Shunmuga Sundaram ORCID iD: 0000-0002-7059-425X

Pugazhendhi Vijayaraman ORCID iD: 0000-0003-2230-100X

Left Bundle Branch Pacing: A Comprehensive Review

Author Details

1. Dr. Shunmuga Sundaram MD., DM., PDF (EP)., CEPS

   Assistant Professor, Department of Cardiology

   Velammal Medical college hospital and research institute

   Madurai, Tamilnadu, India

2. Dr. Vanita Arora MD., DNB., FRCP., FCSI., FISE
   Senior consultant Cardiac electrophysiologist and Interventional cardiologist
   Max Healthcare Super Speciality Hospital, New Delhi
3. Dr. Narayanan Namboodiri MD., DM., DNB., PDF (EP)
   Professor, Department of Cardiology
   Sree Chitra Tirunal Institute for Medical Sciences and Technology
   Trivandrum, Kerala
4. Dr. Vivek Kumar MD., DM.,
   Consultant, Max Healthcare Super Speciality Hospital, New Delhi
5. Dr. Aditya Kapoor MD., DM.,
   Professor, Department of Cardiology
   Sanjay Gandhi Postgraduate Institute of Medical Sciences
   Lucknow
6. Dr. Pugazhendhi Vijayaraman, MD., FHRS
   Professor of Medicine, Geisinger Commonwealth School of Medicinie
   Geisinger Heart Institute, MC 36-10

This article has been accepted for publication and undergone full peer review but has not been through the copyediting, typesetting, pagination and proofreading process, which may lead to differences between this version and the Version of Record. Please cite this article as doi: 10.1111/jce.14681.

1000 E Mountain Blvd, Wilkes-Barre, PA 18711

Corresponding Author:

Dr. Narayanan Namboodiri MD., DM., DNB., PDF (EP)

Professor, Department of Cardiology

Sree Chitra Tirunal Institute for Medical Sciences and Technology

Trivandrum, Kerala

Email Id: kknnamboodiri@gmail.com

Disclosures:

PV: Honoraria, consultant, research, fellowship support: Medtronic, consultant: Boston

Scientific, Abbott, Biotronik, Eaglepoint LLC

Key Words: Physiological pacing, left bundle pacing, heart failure, conduction system, dyssynchrony

Short Title: Left Bundle Branch Pacing

Fundging: None

Abstract

Cardiac pacing is the only effective therapy for patients with symptomatic brady-arrhythmia. Traditional right ventricular apical pacing causes electrical and mechanical dyssynchrony resulting in left ventricular dysfunction, recurrent heart failure and atrial arrhythmias. Physiological pacing activates the normal cardiac conduction thereby providing synchronized contraction of ventricles. Though His

bundle pacing (HBP) acts as an ideal physiological pacing modality, it is technically challenging and associated with troubleshooting issues during follow up. Left bundle branch pacing (LBBP) has been suggested as an effective alternative to overcome the limitations of HBP as it provides low and stable pacing threshold, lead stability and correction of distal conduction system disease. This paper will focus on the implantation technique, troubleshooting, clinical implications and a review of published literature of LBBP

Left Bundle Branch Pacing: A Comprehensive Review

1. Introduction

Chronic right ventricular (RV) pacing is known to cause deleterious effects in the form of atrial arrhythmias, left ventricular (LV) dysfunction and recurrent heart failure hospitalization[1]. The alternative sites such as septum and right ventricular outflow tract have not shown consistent results in improving the clinical outcomes[2,3]. His bundle pacing (HBP) has emerged as an ideal form of physiological pacing, as it activates the normal cardiac conduction system resulting in synchronized contraction of ventricle thereby avoiding RV pacing related complications[4]. Deshmukh et al first reported the feasibility of permanent HBP using conventional RV leads with manually shaped stylets[5]. With the availability of dedicated sheaths and the lead, HBP has been increasingly adopted. Though several studies have shown its feasibility and efficacy, concerns regarding lead stability, higher threshold, and early battery depletion has limited its widespread clinical application[6].

Huang et al[7], first demonstrated the direct capture of left bundle (LB) by placing the lead deep inside the septum resulting in synchronized activation of

ventricles. Since then, left bundle branch pacing (LBBP) has emerged as an alternate modality to deliver physiological pacing as it overcomes many of the limitations of the HBP. This review describes the criteria and techniques of LBBP, troubleshooting difficult cases and reviews the published literature.

2. Conduction system anatomy

In 1906 Tawara first described the AV node, existence of His bundle and its left and right branches[8]. The bundle of His is a cylindrical fascicle and has two segments – the penetrating portion (PHB) and the branching portion (BHB)[9]. The PHB is about 5 to 10mm in length overlying the atrial portion of the membranous septum. The BHB extends for about 5 to 10mm from the point where the posterior fibers of left bundle arise to the point where LB completely branches out and right bundle begins. Hence there is no true branching into left and right bundle, and is often referred to as pseudo bifurcation (fig 1). The proximal LB fans out beneath the LV sub endocardium to form a wider target for pacing as compared to the narrow His bundle. It divides into anterior and posterior fascicles each heading towards the corresponding papillary muscle head. The left posterior fascicle is composed of multiple bands of fibers as compared to thin tendon like anterior fascicle. Subsequently the fascicles give rise to Purkinje fibers which arborizes into the ventricular myocardium.

3. Left bundle branch pacing (LBBP)

LBBP is defined as the direct capture of left main bundle or one of its fascicles along with the LV septal myocardium at low output (<1 V at 0.5ms pulse width)[10]. Commonly, the 4.1F diameter 3830 SelectSecure^{tm} pacing lead (Medtronic Inc, Minneapolis, MN) is positioned deep inside the interventricular septum 1-1.5 cm

below the His bundle (fig 2). In addition to demonstrating a paced QRS of right bundle branch conduction delay pattern, at least one of the following criteria should be demonstrable to confirm direct capture of the left bundle or its branches:

a. Demonstration of left bundle (LB) potential with LB- local ventricular electrogram interval of 20-35ms.
b. Demonstration of transition in QRS morphology from non-selective to selective left bundle capture or nonselective to LV septal capture with decrementing output
c. Peak left ventricular activation time as measured in lead V5,6 <80ms
d. Programmed deep septal stimulation to demonstrate refractory period of LB

A. Paced QRS morphology

The unipolar paced QRS morphology should generally demonstrate right bundle branch conduction delay (qR or Qr) pattern in lead V1. QRS duration alone is a poor predictor of LB capture. Often, it is an incomplete right bundle branch block (RBBB) pattern rather than complete block and the paced QRS morphology could be influenced by the level of capture of the distal His bundle or proximal LB, distal conduction system disease and septal-Purkinje connections. LV septal pacing without capturing the LB can also produce RBB delay pattern but with prolonged LV free wall activation. A superior (anterior) location in the septum or near the distal His bundle may not always demonstrate a RBBB pattern during pacing. Alternately in patients with normal His conduction, pacing near the proximal left bundle may rapidly conduct to the right bundle and result in near-normal QRS morphology.[11]

B. Peak Left Ventricular activation time

The peak Left ventricular activation time (pLVAT) is measured from the onset of the pacing spike to the peak of the R wave in the lead V5-6. It indicates the rapidity of LV free wall activation. pLVAT measurements are used to decide the depth of the pacing lead and capture of the conduction system. If pLVAT is short at high output (10 V) and prolonged at low output (2V), it indicates the lead is away from the LB region and has to be carefully advanced slightly further to reach the LB (fig 6). If LB is captured, pLVAT remains short and constant (<80ms) irrespective of the pacing output. This may be prolonged in patients with intraventricular conduction defects and ischemic cardiomyopathy with significant scar. While early observations have suggested pLVAT<80 ms to indicate conduction system capture, this criterion has not been fully validated.

C. Demonstration of left bundle potential

Left bundle potential is a sharp high frequency signal preceding the local ventricular electrogram by 20-35ms. LB potential should be recorded in patients with baseline narrow QRS or RBBB. In patients with LBBB, antegrade activation of left bundle cannot occur during sinus rhythm as there is a complete block of conduction either in His bundle or in the proximal left bundle. Hence LB potential is not observed in these patients. However, HBP at high output by dual lead technique as suggested by Huang et al[10] with a second 3830 lead will correct LBBB and restore LB activation to produce LB potential. Retrograde LB potential can also be recorded at the end of the local electrogram in the LB lead while pacing RV apex.

D. Demonstration of non-selective and selective LB capture

Similar to HBP, LBBP can also be selective and non-selective. Transition from nonselective to selective LB capture or nonselective LB capture to LV septal myocardial only capture can be usually demonstrated during threshold testing (at near-threshold outputs). Selective capture of LB (S-LB) is characterized by distinct iso-electric interval before the local EGM at low pacing output and the duration of the segment corresponds to the interval between LB potential to onset of surface QRS. This can also be demonstrated by change in paced QRS morphology from qR to rSR in lead V1 with fixed pLVAT while doing unipolar threshold measurement (fig 3). In non-selective LB capture (NS-LB), there is no distinct isoelectric segment and QRS onset is immediately after the pacing artefact with pseudo-delta wave. In NS-LB to LV septal transition, paced QRS morphology remains the same in V1 (qR) but the QRS duration widens along with prolongation of pLVAT. Additionally, no clear change may demonstrable on the local electrogram.

E. Programmed deep septal stimulation protocol

Programmed stimulation from pacing lead can be done to demonstrate (a) change in QRS morphology and duration; (b) refractory periods of the LB and the septal myocardium. This will differentiate LB capture from LV septal capture by change in QRS morphology, rightward shift in axis, global increase in QRS duration and delayed R wave peak in lead V5 and V6 (fig 4). Jastrzebski et al[12], showed in 146 patients the average septal refractory period was shorter than LB refractory period (263.0±34.4ms vs. 318.0±37.4ms). This protocol will be useful in confirming LB capture in patients where QRS morphology change could not be demonstrated during threshold testing

4. Procedural Techniques

4.1 Implantation Tools

The implantation tools are similar to HBP. The Medtronic 3830 SelectSecure^{tm} lead (4.1 F) is used along with C315His fixed curve sheath. In some countries deflectable C304His sheath is available which can be used for patients with difficult anatomy.

Pre-procedural echocardiography may be performed to assess the thickness of basal interventricular septum in multiple views and to assess for the presence of septal scar due to prior myocardial infarction in patients with cardiomyopathy. Dilatation of cardiac chambers, ventricular hypertrophy and presence of valvular regurgitation are also to be assessed as it may affect the procedural success. Cardiac MRI is an option before LBBP to look specifically for basal septal scar in patients with ischemic or non-ischemic cardiomyopathy. Pre-procedural antibiotics are to be given as per institutional protocols.

4.2 Target Site:

Unlike HBP where the target is narrow, LBBP has a wider area to place the lead but on the left side of the septum. In HBP, His potentials are targeted and pace mapping done before screwing the lead. In LBBP, there are no specific potentials to be targeted initially as we are working on the right side of the septum. It is important to know the distal extent of His signals before placing the LBBP lead. This can be done either by (a) placing a quadripolar mapping catheter at the His bundle region which can act as fluoroscopic landmark or (b) placing additional 3830 SelectSecure^{tm} lead at His bundle region which can later be positioned at in the right atrium. The ideal site to

target is around 1-1.5cm below the His bundle along an imaginary line drawn from distal His signals to the RV apex in right anterior oblique (RAO) 30º view (fig 2). Pace mapping at this site will often show a "W" pattern in lead V1 with a notch at the nadir of the QS complex, tall R in lead II and RS in lead III. Lead aVR and aVL will show discordant QRS complexes similar to parahisian VPCs. In our experience, the "W" pattern in lead V1 may not be seen in 20% of patients and not mandatory to have before fixing the lead.

4.3 Lead fixation:

C315 His sheath to interventricular septum orientation is an important factor in the success of LBBP. The lead helix length of the 3830 lead is 1.8mm. The distance between the tip of the lead and the proximal and distal part of the ring electrode of the lead is 11mm and 15mm respectively. Prior knowledge of the thickness of interventricular septum and the length of radio-opaque segment of 3830 lead is important to determine the safe depth of the lead into the septum. Once the site is confirmed in RAO 30° fluoroscopy view, C315 sheath is rotated counterclockwise so that the hub of sheath should point towards right hand of the implanter (3 'O clock position on a clock face in LAO 45° fluoroscopy view). This will orient the sheath perpendicular to the interventricular septum. The counterclockwise torque on the sheath should be maintained while advancing the lead. It is preferable to rotate the lead with both hands while a second operator maintains the sheath position. The sheath should be close to the tip of the electrode of the lead before screwing the lead into the septum. Rapid rotations of the lead by one or two hands is suggested to achieve penetration of lead body behind the helix into the septum till it reaches the LV subendocardium. It is easy to appreciate the lead advancement in LAO 30-45º

fluoroscopy view during the rapid lead rotations (video 1). Continuous recording of intracardiac lead tip electrogram is difficult as the connector-pin has to be detached to provide rapid lead rotations. Lack of revolving connector-pin is a limitation with current implantation technique.

There are 3 important parameters to be monitored while advancing the lead deep inside the septum (fig 5): (a) paced QRS morphology – the notch on the nadir of 'W' in lead V1 will gradually ascend up to form an R wave; (b) unipolar pacing impedance increases gradually before it drops by 100-200 ohms as the lead reaches LV subendocardium; (c) unipolar lead electrogram will display significant injury current. Su et al[29],[13] demonstrated LB current of injury (COI) in 67% of the patients with LB potential. Though there was no significant difference in capture threshold in patients with and without COI (0.64± 0.24 vs 0.74 ± 0.26 V/0.5ms, selective capture of LB was more common in COI (+) group than COI (-) group (54.5% vs 0%; p <0.001). Lead perforation into the LV cavity must be recognized by a significant drop in impedance of more than 200 ohms, unipolar lead impedance of less than 400 ohms, increase in capture threshold, decrease in sensed R wave amplitude and/or loss of injury current in the unipolar electrogram. If lead perforation occurs, the lead should be repositioned at a different site rather than just simply withdrawing the lead.

4.4 When to stop further rotations?

The unipolar pacing lead impedance, pLVAT and presence of left bundle potential are the factors that determine the depth of the lead. Paced QRS duration alone is a poor predictor. Paced QRS and pLVAT duration are measured by performing differential pacing at 10V and 2V output. The pLVAT is measured in lead V5 or V6 from the onset of pacing artefact to the peak of R wave preferably at

100mm/second recording speed. If the paced QRS duration and LVAT are shorter at 10 V and prolonged at 2V the lead tip has to be advanced further by half to one turn. Once the LB is reached, paced QRS morphology will show qR or rSR in lead V1 and LVAT will be short and constant (<80ms) at high and low outputs (fig 6). LB potential should be noted in patients with narrow complex or RBBB at baseline. Unipolar pacing impedance should preferably be more than 500 ohms. Premature complexes of RBBB pattern may be noted during lead fixation. These PVCs may demonstrate LB potentials (helpful in patients with complete heart block or LBBB). Further rotations are to be avoided if LVAT is short and constant (<80ms) at 10V and 2V output, LB potential recorded or unipolar pacing impedance of around 500-550 ohms with low capture threshold (<1.0V at 0.5ms pulse width). 2-3 ml of contrast injection through the sheath in LAO 30º fluoroscopy view (fig 7, video 2) will be useful in measuring the depth of the lead. The leads often have an oblique course and are on average implanted at a depth of 1.4±0.23 cm[15]

4.5 Failure of LBBP

The reported success rate of LBBP is between 80.5% to 97%[14,15,20]. The reasons for failure are inadequate sheath support, improper sheath – septum orientation, failure to penetrate the lead deep into the septum, tissue lodged in the helix, septal scar or entanglement of septal tricuspid leaflet. Both the gloves and the lead must be dry to achieve rapid turns. In case of basal septal scar, posterior fascicular pacing can be attempted by targeting the mid and posterior septum. Posterior fascicular capture is characterized by demonstration of Purkinje potential on the lead electrogram, short LVAT (<80ms), left anterior hemiblock pattern on 12 lead ECG.

4.6 Sheath Removal

Once the lead is secured, the sheath is pulled back into the right atrium. The pacing parameters must be checked in both unipolar and bipolar configuration before slitting the sheath. Since part of the anodal ring will be intraseptal, anodal capture threshold has to be measured by decremental pacing in bipolar configuration. Lead V1 will show change in QRS morphology from QS pattern (as the anodal ring captures the right side of the septum) to qR or rSR pattern once it loses capture (fig 8). Additionally, a change in the local electrogram can also be observed.

Providing an adequate slack to the lead is important as excessive slack can cause lead perforation and inadequate slack can result in lead dislodgements. Formation of an alpha loop by the lead is very common after slitting the sheath and it can be undone in RAO view by retracting the lead slowly with a slight counterclockwise torque (fig 9, video 3). Deciding the extent of the slack for pediatric patient is difficult and it should be adequate to accommodate for the growth of the child[16]

If LBBB could be completely corrected by LBBP at a low threshold, dual chamber pulse generator can be used with RA lead connected to atrial port and 3830 SelectSecure^{tm} lead connected to the ventricular port. RBB delay due to LB capture can be corrected by adjusting AV delay and pacing output (fig 10). Radiation dose during LBBP can be minimized by using electroanatomic mapping to create the geometry of cardiac chambers and tag the distal His signals which facilitate the placement of lead[21]

5. Programming the pulse generator:

Since the lead is placed at the LB, it takes 20-30 seconds for the impulse to reach the ventricular myocardium. Hence the AV delay has to be programmed 20-30 seconds less than the nominal values. Other parameters including unipolar and bipolar capture thresholds, anodal capture, native AV node conduction and underlying indication for pacing have to be considered while programming the pulse generator.

There are two important ways to correct the RBB conduction delay pattern produced by LB capture: (a) programming the output above the anodal threshold, as anode captures right side of septum (fig 8); (b) by optimizing the AV delay to allow native fusion through RBB (fig 10). The RBB delay correction avoids the theoretical risk of LV-RV dyssynchrony.

6. Complications of LBBP

A. *Septal perforation* – Acute lead perforation into the LV cavity can be recognized by increase in capture threshold, fall in unipolar impedance below 500 ohms or reduction in sensed R wave amplitude. The lead has to be re-implanted at a different site. Late lead dislodgement into the LV cavity is reported[22], hence patients have to be carefully monitored for this during follow-up.

B. *RBB injury* – There is a chance of injuring the RBB by the C315 sheath or by the open helix of the pacing lead. Hence temporary pacing lead has to be placed in patients with LBBB to provide back-up pacing. As the right bundle courses anterior and superior to left bundle, the C315 sheath has to kept below the level of his bundle during mapping to minimize the injury to RBB.

C. *Lead dislodgement* – Vijayaraman et al[15], reported acute dislodgement in 3 out of 93 patients who underwent LBBP. Ensuring adequate slack, aiming for good pacing parameters and repositioning the lead at a different site in case perforation occurs will minimize the risk of dislodgement. The risk of late rise in threshold and need for lead repositioning is rare as compared to HBP.

D. *Septal artery injury* – There is a risk of injuring the septal branch of left anterior descending artery. Aborted ST elevation myocardial infarction during LBBP due to lead induced injury is reported[23]. This can be minimized by placing the lead at-least 1 cm below the His bundle region.

E. *Thrombo-embolism* – Though not reported, there is a theoretical risk of thrombo-embolism if part of the helix is exposed to the LV cavity. Post procedure echocardiography is warranted in all patients to assess the depth of the lead and to look for exposed helix in to the left ventricular cavity. If helix is seen exposed, along with low impedance, high thresholds and loss of myocardial injury in the unipolar tip electrogram, lead repositioning at a different site has to be considered as it may produce thrombo-embolic complications. It is likely that in many patients, a small portion of the tip of the helix is exposed to LV cavity. However, if the electrical parameters such as low capture threshold, pacing impedance >500 ohms and myocardial current of injury on unipolar tip electrogram are confirmed, then the lead position is acceptable.

7. HBP Vs LBBP

Conduction system capture can be achieved by both HBP and LBBP. HBP is anatomically challenging as we are aiming for a narrow target zone but it provides the most physiological form of pacing as there is a complete

recruitment of conduction system. Selective capture of His bundle ranges between 26-50%[24,25] as it is surrounded by electrically inert tissue. The implantation technique is challenging with a longer learning curve[26]. HBP has low sensed R-wave amplitude which may result in atrial oversensing and ventricular under sensing. High pacing thresholds either at the time of implantation or during follow-up may result in early battery depletion and pulse generator change in 5-10% of patients. The success rate for correction of distal conduction system disease is lower in patients with intraHisian block and/or LBBB[24,27]. On the contrary, LBBP aims for wide target area with fibers of LBB fanning on the left sub-endocardium. LBBP provides low and stable threshold with no significant sensing issues. LB potentials are observed at the time of implantation in 30 to 80% of the study population[17,20]. LBBP has the advantage of correcting the distal conduction system disease as the pacing lead effectively bypasses the diseased segment[34]. In patients undergoing AV junction ablation, LBBP provides adequate safety margin for ablation as the lead is away from AV node. As compared to the vast available clinical evidence with HBP, LBBP lacks long term data on safety. The criteria for LB capture has not been validated in large trials, hence there may be difficulty in distinguishing left septal capture from LB capture. The implication for lead extraction in patients with long-term LBBP is another major concern.

8. Clinical Implications of LBBP

LBBP has more chance for correcting distal conduction disease as compared to HBP since it bypasses the level of block in majority of the patients. Vijayaraman et al[24] reported 84% success rate for HBP in unselected patients with AV block (93% AV nodal and 76% infra nodal) at threshold of 1.3 ± 0.9V at

0.5ms with 5% lead revision rate. Li et al[17], showed 90% success rate for LBBP patients with AV conduction disease (30 out of 33 patients). In patients requiring pacing after TAVR where distal conduction system is predominantly affected Vijayaraman et al[34], showed HBP was successful in 63% (29/46 patients) and LBBP in 93% (26/28 patients). LBBP was associated with higher success rate and lower pacing thresholds compared with HBP.

LBBP is emerging as an excellent alternative to cardiac resynchronization therapy. As compared to HBP, LBBP can correct distal conduction disease and provide excellent lead stability and low capture threshold. Huang et al[18] reported 97% success rate in a prospective multicenter study involving 63 patients with non-ischemic cardiomyopathy (NICM) and LBBB along with normalization of LVEF (>50%) at 1 year. Zhang et al[19], demonstrated resynchronization of ventricular contraction with reverse remodeling and significant improvement in clinical symptoms after LBBP in patients with heart failure, low ejection fraction and LBBB.

A largest retrospective multicenter study by Vijayaraman et al[39], assessed the feasibility and outcomes of LBBP in CRT eligible patients. CRT could be successfully achieved by LBBP in 277 out of 325 attempted patients (85% success rate) which included 44% of ischemic cardiomyopathy patients. QRS morphology was LBBB in 39%, RBBB in 17% and intraventricular conduction defect in 15%. LBBP resulted in significant reduction in QRS duration from 152 ± 32ms to 137 ± 22ms (p value<0.01). LVEF improved from 33 ± 10 % to 44 ± 11% (p value<0.01). Improvement in LVEF was noted in both ischemic and non-ischemic patients and similarly in patients with LBBB and non-LBBB. There was

significant reduction in LV end-diastolic and LV end-systolic volumes. The lead threshold and R wave amplitude (0.6±0.3V@0.5ms and 10.6±6mV at implantation) remained stable during follow up of 6 ± 5 months. Clinical response (improvement in NYHA functional class by at least one class) was noted in 72% of patients. Echocardiographic response (defined as ≥5% increase in LVEF) observed in 73% of patients. 31% of patients were super-responders (defined as an absolute improvement in EF ≥ 20% of improvement of EF to >50% in patients with baseline EF ≤35%). The authors concluded that LBBP is a feasible, safe and provides an effective option for CRT. The available studies on left bundle pacing is summarized in the table below. Of the 1343 published cases, the overall procedural success rate was 90.87%. The average pacing threshold was 0.624 V/0.5ms and paced QRS duration 117.5ms. 14 patients required a re-do procedure for lead revision (1.04%). No major complications like lead sensing issues, threshold rise, intramural hematoma, or thrombo-embolic complications reported.

9. Future directions

LBBP is emerging as a safe and effective way of physiological pacing but there are several concerns which need to be addressed. SelectSecure^{tm} lead is primarily meant for site selective septal pacing. Significant portion of the lead behind the helix is buried inside the septum and the long-term effect of myocardial contractility on the lead insulation is not known. The possibilities of injury to coronary artery branches, late lead migration into LV cavity and potential thrombo-embolic complications are to be considered during follow up of patients. Lead extraction is another major concern that has to be carefully evaluated in future studies. Further advances in the delivery sheaths and improvements in lead design may

improve the procedural ease and success. Prospective randomized trials are required to confirm the long-term safety and effectiveness of LBBP.

References

1. Wilkoff BL, Cook JR, Epstein AE, et al: Dual chamber pacing or ventricular backup pacing in patients with an implantable defibrillator: Dual Chamber and VVI Implantable Defibrillator (DAVID) Trial. JAMA. 2002; 288:3115-123.
2. Domenichini G, Sunthorn H, Fleury E, et al. Pacing of the interventricular septum versus the right ventricular apex: A prospective, randomized study. Eur J Intern Med. 2012;23(7):621-7.
3. Kaye GC, Linker NJ, Marwick TH et al. Effect of right ventricular pacing lead site on left ventricular function in patients with high-grade atrioventricular block: results of the Protect-Pace study. Eur Heart J 2015;36(14):856-62
4. Vijayaraman P, Chung MK, Dandamudi G, et al. His bundle pacing. J Am Coll Cardiol 2018;72: 927–47.
5. Deshmukh P, Casavant DA, Romanyshyn M,et al. Permanent, direct His-bundle pacing: a novel approach to cardiac pacing in patients with normal His-Purkinje activation. Circulation 2000;101:869–77.
6. Subzposh FA, Vijayaraman P. Long-term results of His bundle pacing. Card Electrophysiol Clin 2018;10:537–42.
7. Huang W, Su L, Wu S, et al. A novel pacing strategy with low and stable output: Pacing the left bundle branch immediately beyond the conduction block. Can J Cardiol 2017;33:1736. e1–3.
8. Tawara S. Das Reizleitungssystem des Saügetierherzens. Jena: GustavFischer; 1906:135–8 [149].

9. Rosenbaum MB, Elizari MV, Lázzari JO. The Hemiblocks. NewConcepts of Intraventricular Conduction based on Human, anatomical and Clinical Studies. Tampa Tracings; 1970269 [Olsmar, Fla].
10. Huang W, Chen X, Su L, et al. A beginner's guide to permanent left bundle branch pacing. Heart Rhythm 2019;16;1791-6
11. Wu S, Su L, Zheng R, Xu L, Huang W. New onset intrinsic and paced QRS morphology or right bundle branch block pattern after atrioventricular nodal ablation: Longitudinal dissociation or anatomical bifurcation? J Cardiovasc Electrophysiol 2020 Apr 6. Doi:10.1111/jce.14469 [Epub ahead of print]
12. Jastrzebski M, Moskal P, Bednarek A, et al. Programmed deep septal stimulation – a novel manoeuvre for the diagnosis of left bundle branch capture during permanent pacing. J Cardiovasc Electrophysiol 2020;Jan 13.doi:10.1111/jce.14352
13. Su L, Xu T, Cai M et al. Electrophysiological characteristics and clinical values of left bundle branch current of injury in left bundle branch pacing. J Cardiovasc Electrophysiol. 2020;31(4):834-42
14. Chen K, Li Y, Dai Y, et al. Comparison of electrogram characteristics and pacing parameters between left bundle branch pacing and right ventricular pacing in patients receiving pacemaker therapy. Europace 2019;21:673-80
15. Vijayaraman P, Subzposh FA, Naperkowski A, et al. Prospective evaluation of feasibility, electrophysiologic and echocardiographic characteristics of left bundle branch area pacing. Heart Rhythm 2019;16:1774–1782.
16. Ponnusamy SS, Muthu G, Bopanna D. Selective left bundle branch pacing for pediatric complete heart block. Indian Pacing Electrophysiol J 2020;78-80.

17. Li X, Li H, Ma W, et al. Permanent Left bundle branch area pacing for atrioventricular block: Feasibility, safety, and acute effect. Heart Rhythm 2019;16:1766-73.
18. Huang W, Wu S, Vijayaraman P, et al. Cardiac resynchronization therapy in patients with non-ischemic cardiomyopathy utilizing left bundle branch pacing. J Am Coll Cardiol EP 2020;(article in press)
19. Zhang J, Wang Z, Cheng L, et al. Immediate clinical outcomes of left bundle branch area pacing vs conventional right ventricular pacing. Clin Cardiol 2019; 42:768–73.
20. Li Y, Chen K, Dai Y et al. Left bundle branch pacing for symptomatic bradycardia: Implant success rate, safety, and pacing characteristics. Heart Rhythm 2019;16:1758–65.
21. Ponnusamy SS, Bopanna D, Kumar S. Electro-anatomical mapping guided low fluoroscopy left bundle branch pacing. J Am Coll Cardiol EP 2020 (article in press)
22. Ravi V, Larsen T, Ooms S, et al. Late-onset Interventricular septal perforation from left bundle branch pacing. HeartRhythm Case Rep. 2020 (Article in press)
23. Ponnusamy SS, Vijayaraman P. Aborted ST-elevation myocardial infarction-An unusal complication of left bundle branch pacing. HeartRhythm Case Rep. 2020 (Article in press)
24. Vijayaraman P, Naperkowski A, Ellenbogen KA, et al. Electrophysiologic insights into site of atrioventricular block. JACC Clin Electrophysiol. 2015;1:571–581.

25. Sharma PS, Dandamudi G, Herweg B, et al. Permanent His-bundle pacing as an alternative to biventricular pacing for cardiac resynchronization therapy: a multicenter experience. Heart Rhythm. 2018;15:413–420.

26. Knee D, Arnold AD, Jaztrzebski M et al. His bundle pacing, learning curve, procedure characteristics, safety and feasibility: insights from a large international observational study. J Cardiovasc Electrophysiol. 2019;30:1984-93

27. Upadhyay GA, Cherian T, Shatz DY, et al. Intracardiac delineation of septal conduction in left bundle branch block patterns: Mechanistic evidence of left intrahisian block circumvented by His bundle pacing. Circulation. 2019;139:1876-88

28. Hou X, Qian Z, Wang Y, et al. Feasibility and cardiac synchrony of permanent left bundle branch pacing through the interventricular septum. Europace. 2019;21(11):1694-702

29. Zhang W, Huang J, Qi Y et al. Cardiac resynchronization therapy by left bundle branch area pacing in patients with heart failure and left bundle branch block. Heart Rhythm 2019;16:1783–90.

30. Vijayaraman P, Naperkowski A, Ellenbogen KA, Dandamudi G. Electrophysiologic insights into site of atrioventricular block: Lessons from permanent His bundle pacing. J Am Coll Cardiol Electrophysiol. 2015;6:571-81

31. Jiang Z, Chang Q, Wu Y, Ji L, Zhou X, Shan Q. Typical BBB morphology and implication depth of 3830 electrode predict QRS correction by left bundle branch area pacing. Pacing Clin Electrophysiol 2020;43:110-7

32. Wang J, Liang Y, Wang W, et al. Left bundle branch area pacing is superior to right ventricular septum pacing concerning depolarization-repolarization reserve. J Cardiovasc Electrophysiol 2020;32:313-22

33. Cai B, Huang X, Li L, et al. Evaluation of cardiac synchrony in left bundle branch pacing: insights from echocardiographic research. J Cardiovasc Electrophysiol 2020;32:560-9

34. Vijayaraman p, Cano O, Koruth JS, et al. His-Purikinje conduction system pacing following transcatheter aortic valve replacement – feasibility and safety. J Am Coll Cardiol EP 2020 (article in press)

35. Hasumi E, Fujju K, Nakanishi K, Komuro I. Impacts of left bundle/peri-left bundle pacing on left ventricular contraction. Circ J 2019;83:1965-7

36. Chen K, Li Y, Dai Y, et al. Comparison of electrocardiogram characteristics and pacing parameters between left bundle branch pacing and right ventricular pacing in patients receiving pacemaker therapy. Europace 2019;21:673-80

37. Wang S, Wu S, Xu L, et al. Feasibility and efficacy of His bundle pacing or left bundle pacing combined with AV node ablation in patients with persistent atrial fibrillation and implantable cardioverter-defibrillator therapy. J Am Heart Assoc. 2019;17;8(24).e014253. doi 10.1161/JAHA 119.014253

38. Wu S, Su L, Vijayaraman P, et al. Left bundle branch pacing for cardiac resynchronization therapy: Non-randomized on treatment comparison with His bundle pacing and biventricular pacing. Can J Cardiol 2020 (article in press)

39. Vijayaraman P, Sundaram S, Cano O, et al. Left bundle branch pacing for cardiac resynchronization therapy: Results from international LBBP collaborative study group. HRS 2020 – Late breaking clinical trial

40. Ponnusamy SS, Muthu G, Kumar M, et al. Mid-term feasibility, safety and outcomes of left bundle branch pacing – Single center experience. Journal of Interventional Cardiac Electrophysiology 2020. doi.org/10.1007/s10840-020-00807-w

Figures

Fig 1: Conduction system anatomy – Left posterior fibers branch out first from His bundle first followed by left anterior fibers. RBB is a direct continuation of His bundle. The encircled portion is hence labelled as pseudo-bifurcation site. Also note the fibers for left and right bundle are pre-destined in the His bundle region itself

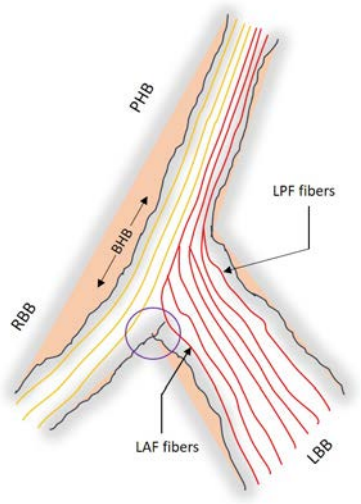

Fig 2: The ideal site to position the LBBP lead is around 1-1.5 cm below the His bundle along an imaginary line drawn from distal His signals to RV apex in RAO 25º fluoroscopy view. HB – His bundle, RBB – Right bundle branch, LBB- Left bundle branch, RVA – RV apex

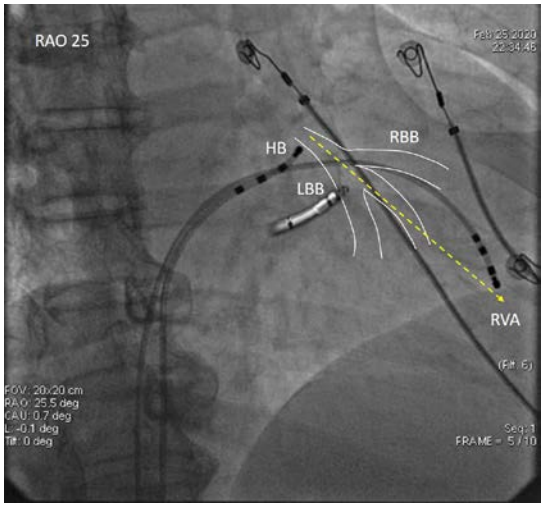

Fig 3: Demonstration of non-selective to selective capture of LB capture while checking unipolar threshold. Note the distinct local EGM on the pacing lead after the pacing spike with change in QRS morphology from qR to rSR pattern. His d and His p – His bundle electrogram distal and proximal, LBB- LB pacing lead, LB U – LB pacing lead unipolar electrogram, RVA – Right ventricle electrogram

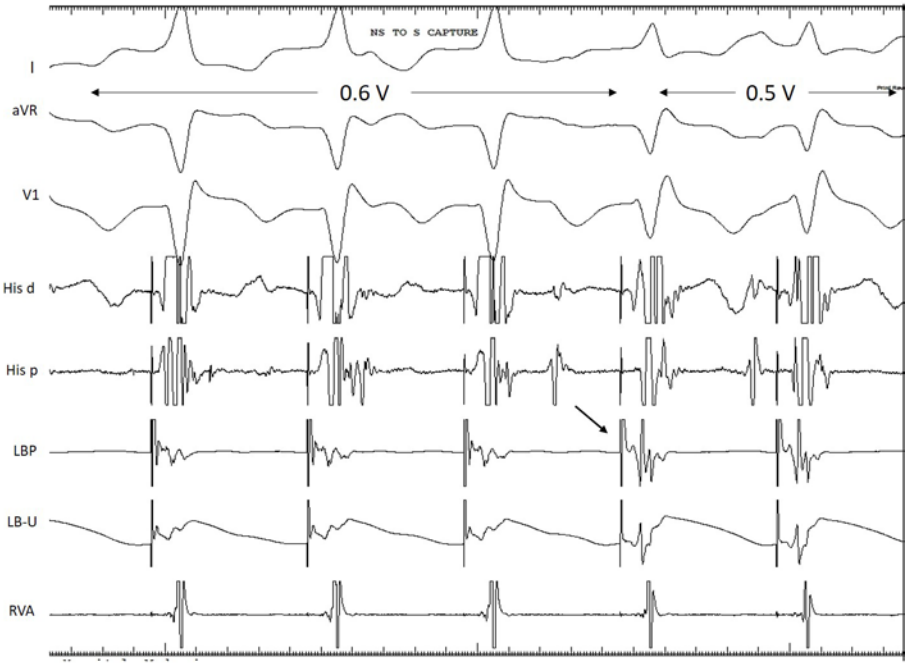

Fig 4: Demonstration of LB and septal myocardial refractory period in patient with baseline LBBB – Programmed deep septal stimulation from the pacing lead (LBP) showed LB refractory period of 320ms (LB + septal myocardial capture till 320ms) and septal myocardial refractory period of 300ms. Change in QRS morphology, axis and prolongation of duration noted after loss of LB capture at S1 600ms, S2 310ms

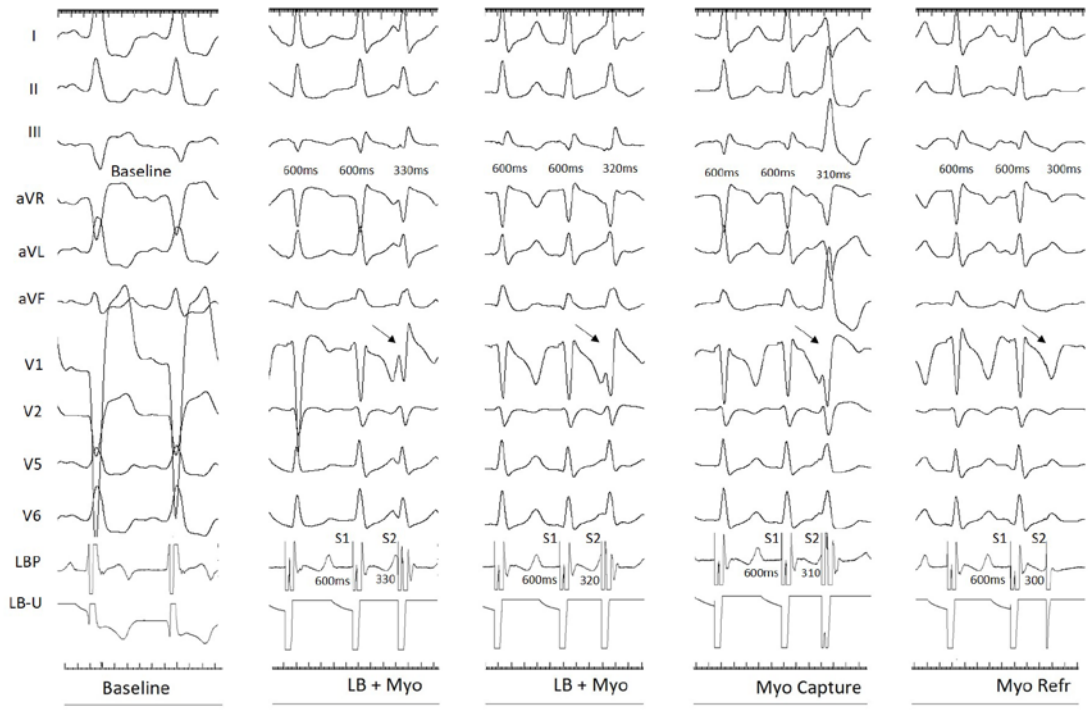

Figure 5: Progressive change in QRS morphology. Initial pacing from RV side of the septum showed 'W' pattern. The notch gradually ascended up to form R wave as the lead goes deep into the septum. LB potential (LB Po) can be seen in all patients with antegrade activation of left bundle. His -d and His p – His bundle distal and proximal electrograms, LBB – LB pacing lead electrogram, His Po – His bundle potential, LV-IVS – LV side of the interventricular septum

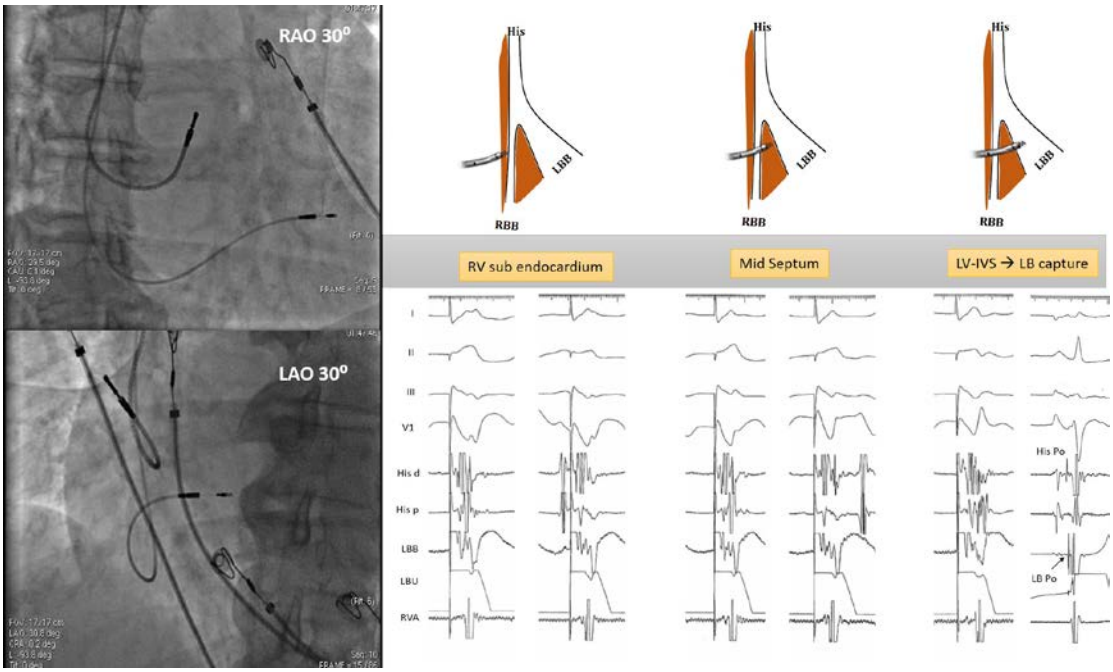

Figure 6: LVAT measurements are useful in deciding the depth of the lead. At site 1 pacing lead showed far field low frequency LB potential (A) with surface ECG showing LVAT of 85ms (b). Additional half a turn resulted in sharp LB potential (C) with LVAT of 65ms (D).

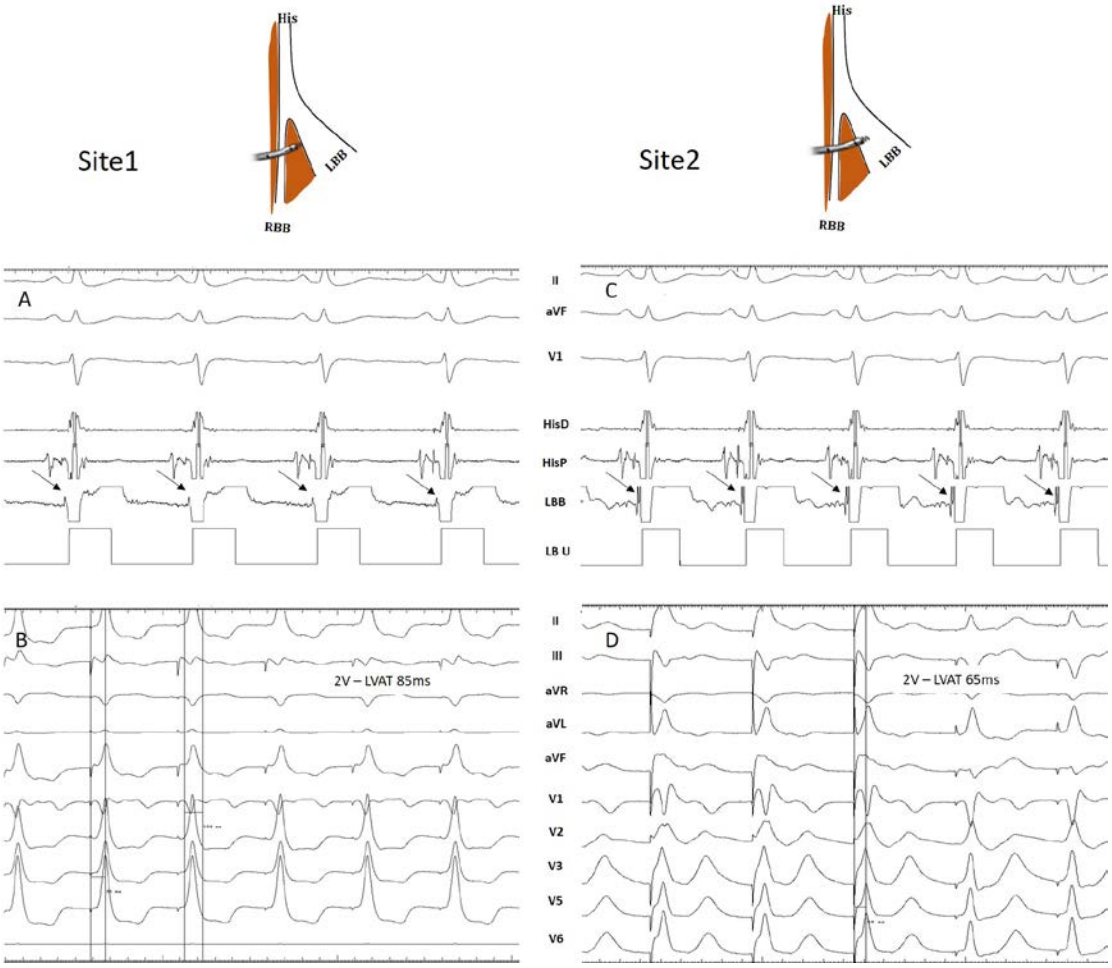

Fig 7: Sheath angiography in LAO 30º fluoroscopy view showing the depth of the lead inside the septum

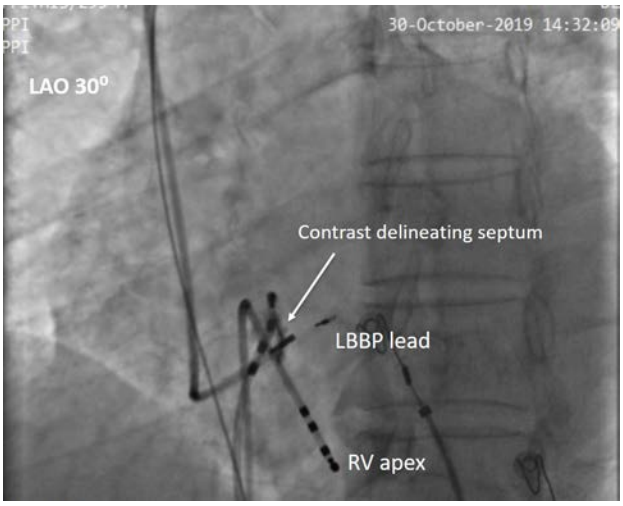

Figure 8: Demonstration of anodal capture threshold. Once anode loses capture the paced QRS morphology change from QS to QR pattern and the pacing lead EGM show distinct local electrogram after the pacing spike

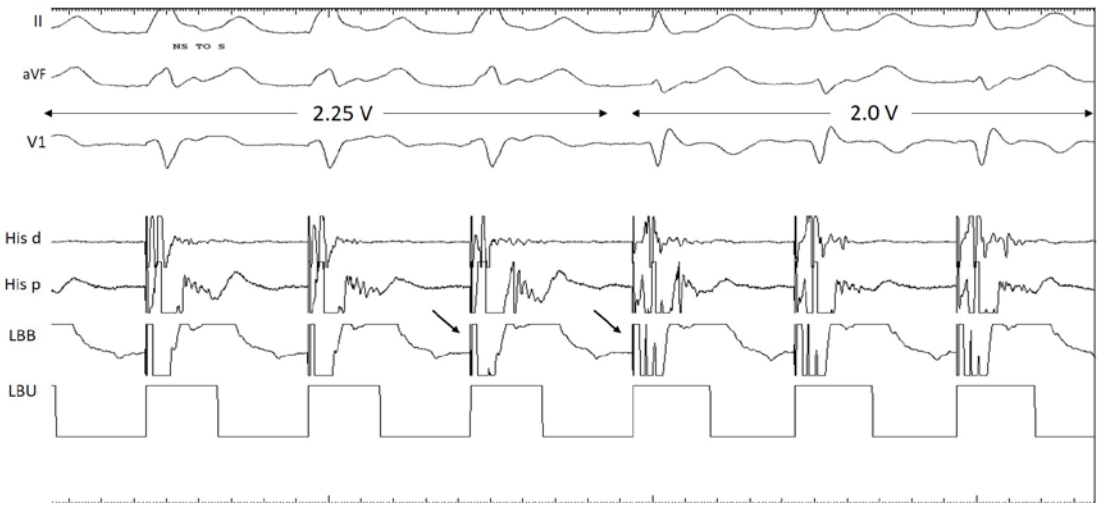

Figure 9: Alpha loop of the pacing lead after sheath removal

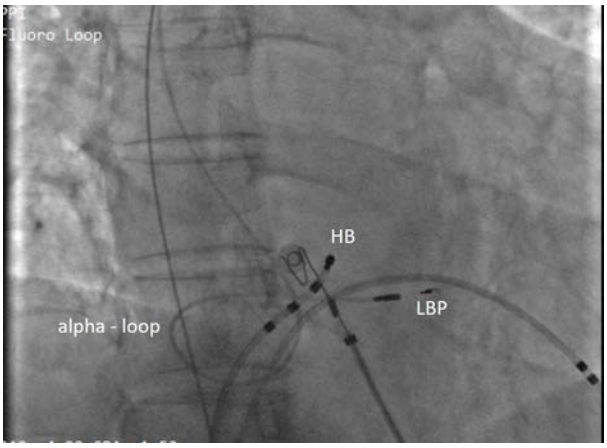

Figure 10: LBBB correction by LBBP for LV dysfunction with heart failure. RBB delay pattern in lead V1 could be masked by optimizing the AV delay and pacing output

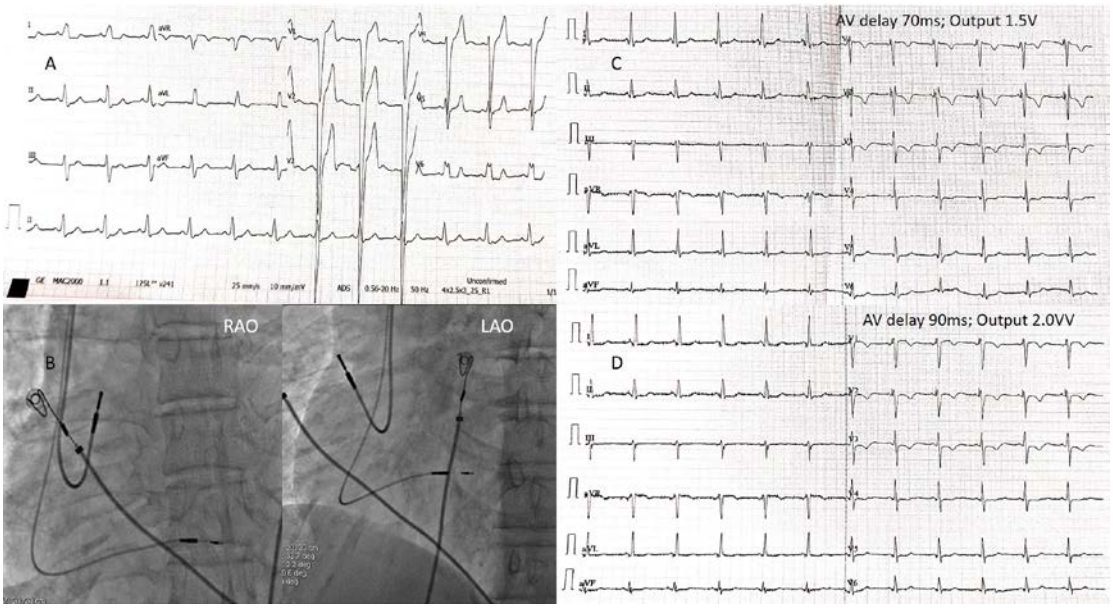

Table 1: Published studies on Left bundle branch pacing

Sl. No	Study	Number of patients[n]	Implant success rate[%]	Paced QRS[ms]	Threshold At implant V@0.5ms	R wave at implant[mV]	Lead revision rates	Objective of the study
1	Vijayaraman et al [15]	100	93%	136±17	0.6 ± 0.4	10 ± 6 mV	3 % (3)	Prospective study in patients requiring pacing for bradycardia or heart failure

								indications
2	Li et al[20]	87	80.5%	113.2 ± 9.9	0.76 ± 0.22	11.99±5.36	0	Prospective study in patients requiring pacing for bradycardia indications
4	Hou et al [28]	56	NR	117.8 ± 11.0	0.5±0.1	17±6.7	0	Prospective study assessing LV synchrony in HBP vs LBBP vs RVP
5	Li et al [17]	33	90.9%	112.8 ± 10.9	0.76 ±0.26	14.4	3.03 (1)	Prospective study of LBBP in AV block
6	Zhang et al[19]	23	95%	112.6 ± 12.14	0.68±0.2	9.28 ± 5.00	0	Prospective comparative study of LBBP over RVP in 44 consecutive patients
7	Hasumi et al [35]	21	81%	116 ± 8.3	0.77 ± 0.07	9.1 ± 1.4	0	Retrospective study assessed the feasibility of LBBP in failed HBP for AV block
8	Chen et al [36]	20	NR	111.8 ± 10.7	0.73 ± 0.2	NR	0	Prospective study to compare the feasibility and ECG patterns during LBBP vs RVP
9	Jastrzebski et al [12]	143	NR	111.9 ± 15.1	0.6 ± 0.3	9.0 ± 5.1	NR	Prospective study to analyze the programmed deep septal stimulation in regard to diagnosis of LBB capture
10	Su et al [13]	115	NR	111.4 ± 10.3	0.6 ± 0.2	11.3 ± 5.4	0	Retrospective study to assess LB current of injury in LBBP
11	Cai et al (33)	40	90%	101 ± 8.7	0.49 ± 0.22	11.7 ± 5.3	0	Prospective study to assess the cardiac synchrony in SSS patients undergoing LBBP Vs RVP
12	Wang et al [32]	66	94%	121.4 ± 9.8	0.94 ± 0.21	12.1 ± 3.6	4.5%(3)	Prospective randomized study to compare the depolarization and repolarization measures between LBBP Vs RVP
13	Vijayaraman et al [34]	28	93%	125 ±15	0.64 ± 0.3	14 ± 8	0	Retrospective study to assess the feasibility of HPCSP pacing after TAVR (LBBP and HBP)
14	Ponnsuamy SS et al [40]	99	94%	110.8 ±12.4	0.59± 0.22	14.1± 7.1	0	Prospective study to assess the efficacy and mid-term outcomes of LBBP in Indian population
1	Zhang et al[29]	11	NR	129.09 ± 15.9	0.83 ±0.16	9.1 ± 3.4	0	Study assessing clinical outcomes of LBBP in patients with HF, reduced LVEF and LBBB
2	Wang et al [37]	8	94.5%	NR	0.79 ± 0.18	NR	NR	Retrospective study assessed the efficacy of HPCSP + AVJ ablation in patients with AF and ICD
3	Huang et al [18]	63	97%	118 ± 12	0.5 ± 0.15	11.1 ± 4.9	0	Prospective study to assess the feasibility and efficacy of LBBP in LBBB with NICM
4	Wu et al [38]	32	100%	110.8 ± 11.1	0.49 ± 0.13	11.2 ± 5.1	0	Prospective study to compare CRT efficacy of LBBP, HBP and BiV pacing.

5	Jiang et al (31)	73 (63+10)	Atypical BBB – 30% (3) Typical BBB – 82.5% (52) Overall 75.3%	133 ± 14 118 ± 14	0.6 ± 0.2	13.6 ± 7.6	0	Retrospective study to assess whether typical use of strict criteria to define BBB predicts LBBP success
6	Vijayaraman et al [39]	325	85%	137 ±22	0.6 ±0.3	10.6 ± 6	2.5 % (7)	Retrospective study assessed the feasibility and outcomes of LBBP in CRT eligible patients
	Total	***1343***	***90.87%***	***117.5***	***0.624***	***11.7***	***1.04% (14)***	

Hindawi
Case Reports in Cardiology
Volume 2020, Article ID 9628719, 5 pages
https://doi.org/10.1155/2020/9628719

Case Report

Acute Coronary Syndrome after 17 Years of Bare Metal Stent Implantation: "Very" Very Late Stent Thrombosis

Raghavendra Rao K,[1] **S. Reddy**,[1] **J. R. Kashyap**,[1] **K. Vikas**,[1] **Hithesh Reddy**,[1] **and Vadivelu Ramalingam**[2]

[1]*Department of Cardiology, Government Medical College and Hospital, Sector 32, Chandigarh 160030, India*
[2]*Department of Cardiology, Velammal Medical College Hospital and Research Institute, Madurai 625009, India*

Correspondence should be addressed to Raghavendra Rao K; sarjubmc90@gmail.com

Received 30 September 2019; Accepted 24 December 2019; Published 6 February 2020

Academic Editor: Alfredo E. Rodriguez

Very late stent thrombosis (VLST) is a catastrophic and life-threatening complication after percutaneous coronary intervention which presents as an acute coronary syndrome with significantly high mortality and morbidity. VLST is a rare entity with drug-eluting stents and even rarer with bare metal stents. The exact pathophysiologic mechanism of VLST after BMS implantation is not known although various mechanisms have been proposed. Recently, in-stent neoatherosclerosis with intimal plaque rupture has been proposed as a potential mechanism of VLST after BMS. We report a rare case of VLST occurring 17 years after BMS implantation with angiographic and intravascular imaging evidence which provides insight into the mechanisms of VLST.

1. Introduction

Coronary stents are the mainstay of percutaneous coronary interventions and have significantly reduced the rates of restenosis and acute vessel closure [1]. Drug-eluting stents (DES) are preferred over bare metal stents (BMS) since DES significantly reduces in-stent restenosis (ISR) by inhibiting neointimal proliferation. However, stent thrombosis (ST) remains an uncommon but catastrophic complication which usually presents as acute coronary syndrome (ACS) with STEMI (ST elevation myocardial infarction) though it can also present as sudden death, arrhythmias, or acute heart failure [2]. Incidence of stent thrombosis has markedly reduced with the use of dual antiplatelet therapy (DAPT) and adequate optimization of stent implantation [1]. According to the Academic Research Consortium criteria and classification, ST is classified according to the time since stent implantation. Acute ST occurs during the stenting procedure or within the subsequent 24 hours, subacute ST occurs between 1 and 30 days after implantation, late ST occurs between 1 month and 1 year, and very late ST occurs more than 1 year after the procedure [3]. A new term "very (or extreme) very late stent thrombosis (VVLST)" was suggested when ST occurred after five years of stent implantation [2, 4]. Very late stent thrombosis (VLST) occurs more frequently with DES than with BMS, and majority of VLST occurs within 1–4 years of stent implantation. VLST occurring after five years of stent implantation is an exceedingly rare phenomenon, and it is still a rarer entity with BMS [2, 5]. We report a case of "very" very late stent thrombosis occurring 17 years after BMS implantation which presented as acute ST segment elevation myocardial infarction.

2. Case Report

A 76-year-old man first reported in the year 2000 with acute-onset retrosternal chest pain of 24-hour duration. Electrocardiogram showed ST segment elevation in the inferior leads with normal sinus rhythm. Apart from diabetes mellitus, other conventional risk factors like obesity, hypertension, smoking, and family history of ischemic heart disease were absent. Routine investigations were within normal limits. Echocardiogram revealed inferior wall hypokinesia with an ejection fraction of 40% with no mitral regurgitation. After

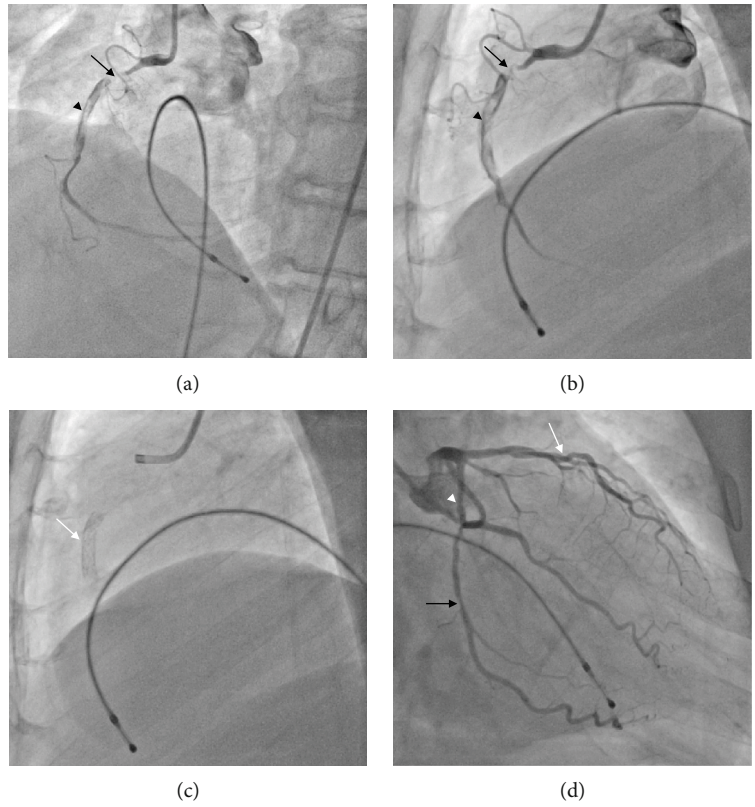

Figure 1: (a) Coronary angiography showing RCA in LAO cranial view with maximum stenosis just proximal to the native bare metal stent (black arrow) and thrombosis within the stent (black arrowhead). (b) RCA in lateral view with 95% stenosis (black arrow) and thrombus inside the stent (black arrowhead). (c) Native bare metal stent (white arrow). (d) RAO caudal view shows plaque in LAD (white arrow) with 30% stenosis in the proximal LCX (white arrowhead) and 50% stenosis in the obtuse marginal artery (black arrow).

receiving a loading dose of aspirin (325 mg), clopidogrel (600 mg), and atorvastatin (80 mg), the patient was taken up for coronary angiography. Coronary angiography revealed a normal left main artery (LM), left circumflex artery (LCX), and left anterior descending artery (LAD). The right coronary artery (RCA) had a significant stenosis in the midsegment, and the patient underwent PCI to RCA with implantation of a bare metal stent (BMS) in the mid-RCA. Drug-eluting stents (DES) were not available at that point of time anywhere in the country. His recovery was uneventful and was discharged on the 4th day on daily aspirin (150 mg), clopidogrel (75 mg), metoprolol (25 mg), atorvastatin (80 mg), and oral hypoglycemic agents. He was on a regular follow-up every 3–6 months since the time of his first coronary intervention. Clopidogrel was stopped after 12 months, and he was advised to continue other medications. The patient remained asymptomatic and was on a regular medical follow-up with no discontinuation of medical therapy at any point of time.

In January 2017, the patient presented to us with sudden-onset chest pain radiating to the left shoulder of one-hour duration and an episode of syncope. His pulse rate was 40/min regular, and his blood pressure is 90/60 mmHg. Electrocardiogram showed sinus bradycardia with ST elevations in leads II, III, and aVF. The cardiac enzyme troponin T was positive, and echocardiography showed hypokinesia of the inferior wall with no mitral regurgitation and a left-ventricular ejection fraction of 45%. Blood sugars were well controlled with normal renal function tests and a hemogram. The patient underwent temporary pacemaker insertion in view of the syncopal episode and bradycardia. Coronary angiography revealed proximal LAD plaque, proximal LCX 30% stenosis, and obtuse marginal 50% stenosis. In proximal RCA 95% stenosis, the mid-RCA stent was thrombus laden extending to the distal RCA. A posterior descending artery (PDA) and posterior left ventricle (PLV) branches were normal (Figures 1(a)–1(d)). He was given loading doses of aspirin (325 mg), clopidogrel (600 mg), and atorvastatin (80 mg) and was taken up for primary PCI to RCA via a right femoral approach. The right coronary artery was engaged with a Judkins right guiding catheter (6 French, 3.5), and the lesion was crossed using a $0.014''$ BMW guidewire (Balance Middleweight Universal wire, Abbott Vascular, CA, USA). An IVUS (Eagle Eye® Platinum digital IVUS catheter, Volcano Corporation, CA, USA) pullback was taken from distal RCA which showed thrombus extending from proximal to distal RCA. There was plaque rupture at the proximal stent edge and thrombus. Within the stent, there was neoatherosclerosis in the midregion with intimal plaque rupture, spotty calcification, and thrombosis (Figures 2(a)–2(e)). Significant plaque burden and thrombus were also noted in the distal RCA. Eptifibatide (GP IIbIIIa inhibitor) infusion was started, and manual thrombus aspiration was done using a 6 French

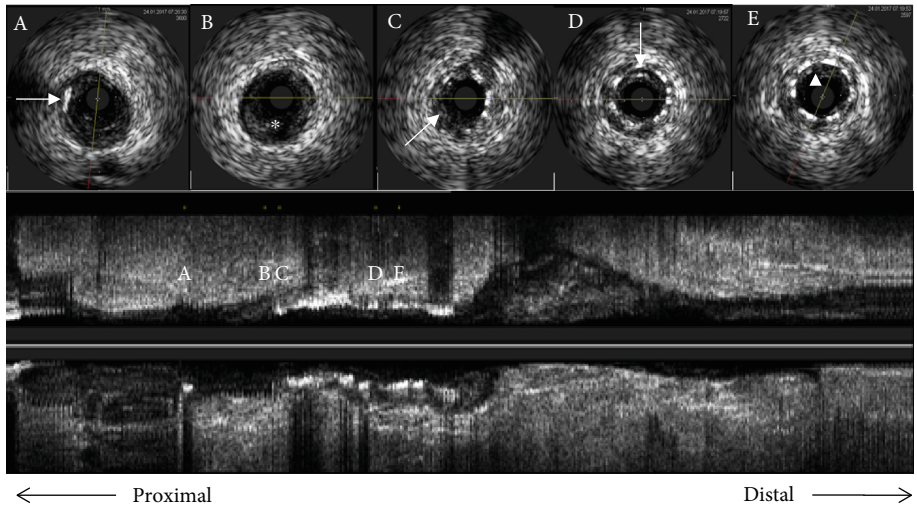

Figure 2: Cross-sectional and longitudinal views: baseline IVUS pullback images from distal to proximal RCA demonstrating (a) an arc of calcium in the proximal RCA (white arrow), (b) a site of plaque rupture at the proximal stent edge (white asterisk), (c) thrombus inside the stent (white arrow), (d) spotty calcification within the stent (white arrow), stent struts (black arrow), and (e) a site of plaque rupture within the stent (white arrowhead).

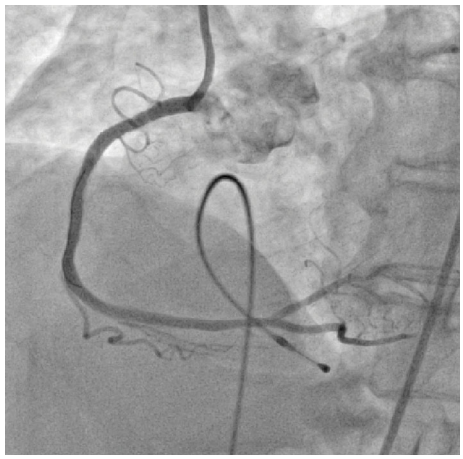

Figure 3: Final angiographic view post-PCI showing adequate stent expansion with good distal opacification.

Thrombuster II® (Kaneka Corporation, Osaka, Japan). The lesion was predilated with a SPRINTER® semicompliant 2.5 × 15 mm balloon (Medtronic, Minneapolis, USA) from distal to proximal RCA at 10-12 atm. The stent Xience Prime (2.75 × 38 mm) (2nd-generation everolimus-eluting stent, Abbott Vascular, CA, USA) was deployed in mid-RCA to distal RCA at 10 atm, the second stent Xience Prime (3 × 38 mm) was deployed in proximal RCA to mid-RCA at 12 atm overlapping with the previous stent, and the third stent Xience Prime (3.5 × 28 mm) was deployed from ostial to proximal RCA at 12 atm overlapping with the previous stent. Postdilatation of the distal to ostial RCA stents was done using SPRINTER® noncompliant balloons (Medtronic, Minneapolis, USA) (2.75 × 9 mm, 3 × 12 mm, and 3.5 × 12 mm) successively at 12-18 atm. Postprocedure angiography showed TIMI III flow (Figure 3), and an IVUS pullback was taken which showed good stent strut apposition (Figures 4(a)–4(e)). The patient was discharged in a stable condition on dual antiplatelets and statins.

3. Discussion

VLST is an exceedingly rare complication of PCI with recent studies showing an incidence of approximately 0.5% per year with BMS that reaches up to 2% per year with DES. Most cases present as an ST segment elevation myocardial infarction carrying high morbidity and mortality with an annual mortality rates of 10% to 20% [6, 7]. We present a case of "very" very late stent thrombosis occurring 17 years after implantation of a bare metal stent. Our case highlights the importance that the underlying pathophysiologic mechanisms are multifactorial. To the best of our knowledge, this is the first case to report with the longest duration after bare metal stent implantation to thrombosis with an intravascular imaging guidance. Earlier, Acibuca and colleagues reported a case of BMS thrombosis occurring after two decades; however, in their report, intravascular ultrasound (IVUS) was not done and the exact duration was not clear [8]. Our case is unique as IVUS was performed and we demonstrated that multiple factors are responsible for plaque rupture leading to VLST such as (a) persistent peristent strut chronic inflammation leading to plaque rupture at the proximal stent edge, (b) neoatherosclerosis inside the stent which led to plaque rupture, and (c) the presence of calcium suggesting longer duration of the atherosclerotic plaque and subsequent plaque rupture due to a calcified nodule.

Earlier, Sarkees et al. had reported VLST occurring 13 years after BMS implantation which occurred upon termination of antiplatelet therapy [9]. History of discontinuation of antiplatelet therapy was not there in our case. Randomized trials have shown that the incidence of stent thrombosis within the first year of implantation is identical in patients

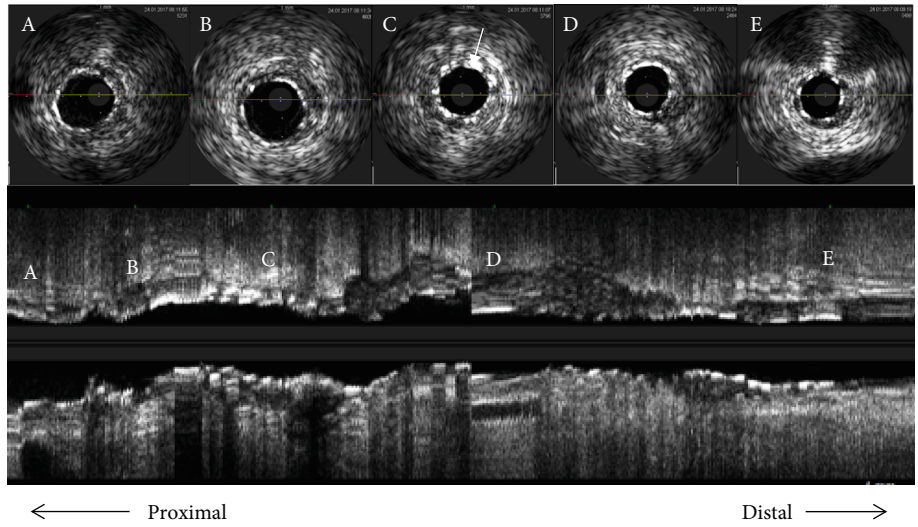

Figure 4: Poststenting IVUS pullback showing adequate stent expansion with an MLD/CSA (minimum lumen diameter/cross-sectional area) of (a) 3.13 mm/8.43 mm^2 at the proximal RCA, (b) 3.23 mm/8.92 mm^2 at the previous stent proximal edge, (c) 2.85 mm/6.46 mm^2 at the stent overlapping region (white arrow), (d) 2.54 mm/5.49 mm^2 at the distal RCA, and (e) 2.39 mm/4.78 mm^2 at the very distal RCA.

with DES and those with BMS. However, after 1 year, a modest increase is observed in VLST after DES implantation compared to that after BMS implantation [10]. The exact pathophysiologic mechanism for VLST after BMS implantation is not known, but various mechanisms have been proposed. BMS have a rapid endothelialization after implantation which is usually completed by 3 to 6 months unlike DES which takes a longer period; hence, the inflammatory response does not seem to be the triggering cause of VLST with BMS [5, 11, 12].

Of the various hypotheses proposed for VLST after BMS implantation, the most important and plausible mechanism being in-stent neoatherosclerosis and subsequent plaque rupture which presents as an ACS and the histological features are indistinguishable between patients with VLST and patients with ACS unrelated to stent thrombosis [6]. Yumoto et al. showed that VLST after BMS might be caused by a thrombus formation subsequent to a calcified atherosclerotic plaque rupture [11]. Stent strut malapposition and positive arterial remodeling and late acquired stent malapposition have also been suggested as probable etiologies for VLST after BMS [13]. Late stent malapposition occurs with both DES and BMS though it is more common after DES implantation and increases the risk of VLST [12]. In the present case, there was no clear IVUS evidence of stent malapposition. Metallic stent struts being a foreign body can induce persistent peristrut chronic inflammation which can accelerate atherosclerotic changes and subsequent plaque rupture [14]. Long-term follow-up studies using intravascular imaging guidance after BMS implantation have shown that the neointima transforms into lipid-laden tissue with narrowing of the lumen, expansion of the neovascularization into the intima, calcification, and advanced atherosclerotic changes like intimal disruption with thrombus formation leading to ACS [15]. Our case showed the presence of calcium in both the native vessel and the stented segment along with evidence of neointimal rupture, plaque rupture at the proximal stent edge possibly due to peristent strut inflammation, and superimposed thrombus formation.

4. Conclusion

Based on our case study and IVUS analysis, we conclude that multiple mechanisms contribute to VLST after BMS implantation predominantly due to neoatherosclerotic plaque rupture, peristent strut chronic inflammation leading to plaque rupture, and calcific atherosclerotic plaque rupture. All the above mechanisms either alone or in combination may lead to plaque rupture eventually causing acute coronary syndrome.

Conflicts of Interest

The authors declare that they have no conflicts of interest.

References

[1] R. Jaffe and B. H. Strauss, "Late and very late thrombosis of drug-eluting stents: evolving concepts and perspectives," *Journal of the American College of Cardiology*, vol. 50, no. 2, pp. 119–127, 2007.

[2] S. Gupta, "Very very late stent thrombosis: 9.5 years after DES implantation," *Indian Heart Journal*, vol. 68, Supplement 2, pp. S39–S43, 2016.

[3] D. E. Cutlip, S. Windecker, R. Mehran et al., "Clinical end points in coronary stent Trials," *Circulation*, vol. 115, no. 17, pp. 2344–2351, 2007.

[4] A. Kaliyadan, H. Siu, D. L. Fischman et al., ""Very" very late stent thrombosis: acute myocardial infarction from drug-eluting stent thrombosis more than 5 years after implantation," *The Journal of Invasive Cardiology*, vol. 26, no. 9, pp. 413–416, 2014.

[5] S. Windecker and B. Meier, "Late coronary stent thrombosis," *Circulation*, vol. 116, no. 17, pp. 1952–1965, 2007.

[6] M. S. Herrera, J. A. Restrepo, A. F. Buitrago, M. G. Mejía, and J. H. Díaz, "Very late bare metal stent thrombosis," *Case Reports in Critical Care*, vol. 2013, Article ID 856095, 2 pages, 2013.

[7] E. J. Armstrong, D. N. Feldman, T. Y. Wang et al., "Clinical presentation, management, and outcomes of angiographically documented early, late, and very late stent thrombosis," *JACC: Cardiovascular Interventions*, vol. 5, no. 2, pp. 131–140, 2012.

[8] A. Acibuca, D. M. Gerede, and V. K. Vurgun, "Bare-metal stent thrombosis two decades after stenting," *Cardiovascular Journal of Africa*, vol. 26, no. 4, pp. e19–e21, 2015.

[9] M. L. Sarkees, A. A. Bavry, J. M. Galla, and D. L. Bhatt, "Bare metal stent thrombosis 13 years after implantation," *Cardiovascular Revascularization Medicine*, vol. 10, no. 1, pp. 58-59, 2009.

[10] G. W. Stone, J. W. Moses, S. G. Ellis et al., "Safety and efficacy of sirolimus- and paclitaxel-eluting coronary stents," *The New England Journal of Medicine*, vol. 356, no. 10, pp. 998–1008, 2007.

[11] K. Yumoto, T. Anzai, H. Aoki et al., "Calcified plaque rupture and very late stent thrombosis after bare-metal stent implantation," *Cardiovascular Intervention and Therapeutics*, vol. 26, pp. 252–259, 2011.

[12] J. Kotani, M. Awata, S. Nanto et al., "Incomplete neointimal coverage of sirolimus-eluting stents: angioscopic findings," *Journal of the American College of Cardiology*, vol. 47, no. 10, pp. 2108–2111, 2006.

[13] A. Caixeta, V. C. Braga, and G. S. Mintz, "Very late stent thrombosis with bare-metal stent: identifying severe stent malapposition and underexpansion by intravascular ultrasound," *Einstein (São Paulo)*, vol. 11, no. 3, pp. 364–366, 2013.

[14] K. Inoue, K. Abe, K. Ando et al., "Pathological analyses of long-term intracoronary Palmaz–Schatz stenting: is its efficacy permanent?," *Cardiovascular Pathology*, vol. 13, no. 2, pp. 109–115, 2004.

[15] M. Takano, M. Yamamoto, S. Inami et al., "Appearance of lipid-laden intima and neovascularization after implantation of bare-metal stents: extended late-phase observation by intracoronary optical coherence tomography," *Journal of the American College of Cardiology*, vol. 55, no. 1, pp. 26–32, 2009.

Aborted ST-elevation myocardial infarction—An unusual complication of left bundle branch pacing

Shunmuga Sundaram Ponnusamy, MD, DM,* Pugazhendhi Vijayaraman, MD, FHRS†

*From the *Velammal Medical College, Madurai, India, and †Geisinger Heart Institute, Wilkes Barre, Pennsylvania.*

Introduction

Conduction system pacing ensures rapid activation of both ventricles, resulting in synchronized contraction. His bundle pacing (HBP) is the most physiological pacing modality but is limited by higher thresholds and lower success rates in patients with wide QRS. Left bundle branch pacing (LBBP) has been proposed by Huang and colleagues[1] as an alternative strategy to overcome the limitations of HBP. Since the pacing lead is positioned deep in the basal interventricular septum, the possibility of injuring coronary artery branches is a concern. In this report, we describe a case of aborted ST-elevation myocardial infarction during LBBP lead implantation.

KEY TEACHING POINTS

- Left bundle branch pacing (LBBP) overcomes many of the limitations of His bundle pacing, as it provides conduction system capture at low and stable threshold.
- Though LBBP has the potential to be an effective alternative to cardiac resynchronization therapy, the safety of LBBP needs continued evaluation.
- Injury to coronary artery branches (septal perforators) during LBBP lead implantation is a concern.
- We describe an interesting case of aborted ST-segment elevation myocardial infarction during LBBP likely due to arterial spasm induced by trauma during implantation.

Case report

A 65-year-old woman with nonischemic cardiomyopathy, left ventricular (LV) ejection fraction of 30%, left bundle branch block (LBBB), QRS duration of 160 ms (Figure 1A), and recurrent heart failure was referred for cardiac resynchronization therapy. Coronary angiography performed 2 years ago was normal. LBBP was attempted using a 3830 SelectSecure pacing lead and C315His sheath (Medtronic Inc, Minneapolis, MN) at a right ventricular septal site 1 cm apical and inferior to the distal His region. The lead was advanced deep into the septum with 4–5 rapid turns. The paced QRS demonstrated qR morphology in lead V_1 (Supplemental Figure S1). Unipolar pacing impedance increased gradually from 350 ohms on the right side of the septum to 700 ohms before it decreased to 400 ohms. The patient developed angina, diaphoresis, and hypotension. Electrocardiogram (ECG) showed significant ST elevation in leads I, aVL, and V_1–V_3 with reciprocal changes in II, III, and aVF (Figure 1B). The lead was immediately withdrawn and repositioned 1.5 cm posterior and apical to the initial location. Urgent coronary angiography showed a major septal branch at the initial lead placement site (deep septum) with TIMI 3 flow in the left anterior descending (LAD) artery (Figure 2, Videos 1 and 2). The ST-segment changes resolved within 10 minutes. During threshold testing at the second pacing site, nonselective-to-selective left bundle branch capture was demonstrated with paced QRS duration of 110 ms (Figure 3A). The pacing threshold was 0.3 V at 0.6 ms pulse width, unipolar lead impedance 650 ohms, and sensed R wave 10 mV. ECG showed symmetrical T-wave inversion in precordial leads suggestive of T-wave memory from prior LBBB (Figure 3B). Postprocedure echocardiogram did not show new wall motion abnormalities. Peak troponin I was 0.23 ng/mL (normal 0.01–0.08 ng/mL). Hospital course was uneventful, and the patient was discharged the next day. The patient's functional status improved from New York Heart Association class III at baseline to class II during follow-up. LV ejection fraction had improved to 45% at 1 month.

KEYWORDS Cardiac resynchronization therapy; Heart failure; Left bundle branch pacing; Left bundle branch block; ST elevation
(Heart Rhythm Case Reports 2020;6:520–522)

Shunmuga Sundaram Ponnusamy has no disclosures. Pugazhendhi Vijayaraman discloses the following: honoraria, consultant, research, fellowship support: Medtronic; consultant: Boston Scientific, Abbott, Biotronik, and Eaglepoint LLC. **Address reprint requests and correspondence:** Dr Pugazhendhi Vijayaraman, Professor of Medicine, Geisinger Commonwealth School of Medicine, Geisinger Heart Institute, MC 36-10, 1000 E Mountain Blvd, Wilkes-Barre, PA 18711. E-mail address: pvijayaraman1@geisinger.edu.

https://doi.org/10.1016/j.hrcr.2020.05.010

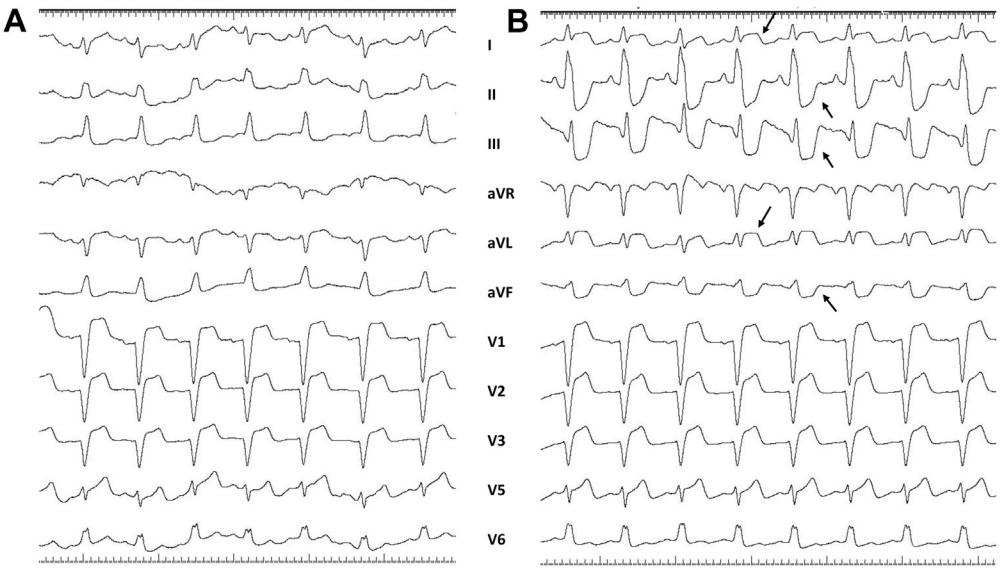

Figure 1 **A:** Baseline electrocardiogram (ECG) showing complete left bundle branch block with QRS duration of 160 ms. **B:** ECG during anginal pain showed ST-segment elevation in leads I, aVL, and V_1–V_3 with reciprocal ST depression in inferior leads.

Discussion

The differential diagnosis for the aborted nonatherosclerotic ST-elevation myocardial infarction in our patient is (1) coronary vasospasm resulting from trauma to the septal arterial branch or (2) micro-emboli into the coronary artery from the lead tip at the LV endocardium with subsequent spontaneous resolution.

There was a large septal branch at the implanted site (Figure 3) and it is likely that the trauma caused by the pacing lead might have produced vasospasm of the LAD artery. No arterial injury or bleeding into the myocardium could be demonstrated by coronary angiography. The ECG changes had resolved within 10 minutes, prior to the angiography. The other possibility is perforation of the LBBP lead into the LV cavity followed by embolization of thrombus from the lead tip into the LAD branches. Spontaneous resolution of micro-thrombus may have occurred, as both ST-segment elevation and anginal pain had resolved by the time angiography was done. Although there was a significant decrease in pacing impedance from 700 to 400 ohms, we did not observe high pacing threshold or loss of R waves at this site. In our experience, acute perforation of the lead tip into the LV cavity during LBBP lead implantation is seen in approximately 3%.[2] Perforation can be recognized by a decrease in unipolar pacing impedance to <400 ohms, significant reduction in R-wave amplitudes, and increase in capture thresholds to >3 V. The electrograms from the LBBP lead will also demonstrate loss of myocardial injury current. In our patient, none of these features other than a decrease in pacing impedance was observed. Air embolism into the diagonal artery is another possibility, but angiography failed to demonstrate air bubble or slow flow owing to increase in microcirculatory resistance

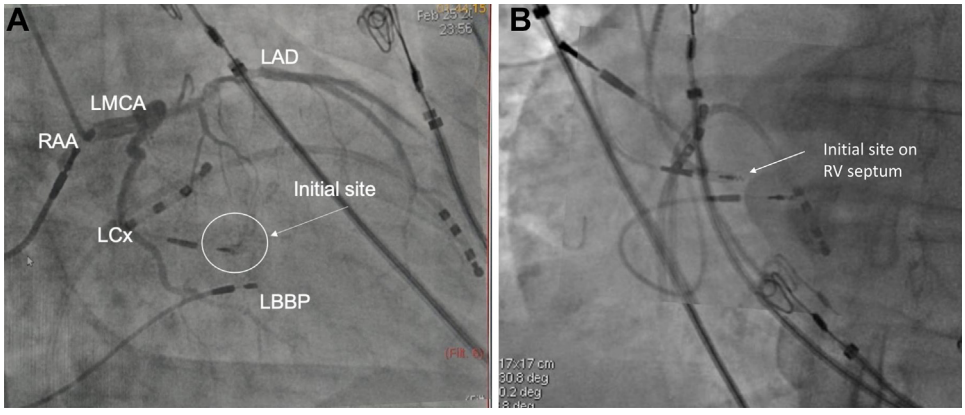

Figure 2 **A:** Right anterior oblique 30° fluoroscopy view showing the intial pacing site (right ventricular septal) superimposed on the final pacing site and its relation to the septal branch of the left anterior descending artery (LAD). LBBP = left bundle branch pacing lead; LCx = left circumflex artery; LMCA = left main coronary artery; RAA = right atrial appendage. **B:** Left anterior oblique 30° fluoroscopy view showing the initial and final pacing sites. RV = right ventricular.

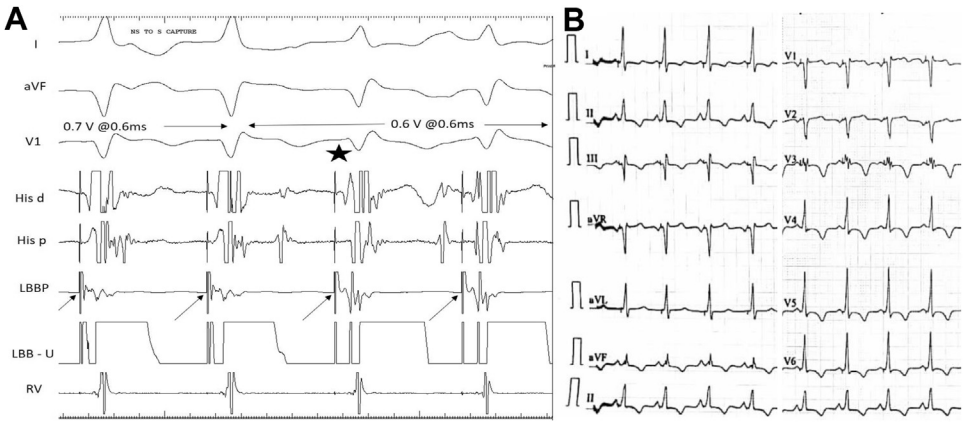

Figure 3 **A:** Demonstration of nonselective-to-selective left bundle capture during threshold testing; note the change in QRS morphology from qR to rSR pattern along with discrete local ventricular electrogram after the pacing spike during selective capture. **B:** Twelve-lead electrocardiogram after left bundle branch block correction by left bundle branch pacing (LBBP) showing qR pattern in V_1 with T-wave memory changes.

in response to air. Once recognized, acute septal perforation is managed by removal of the pacing lead and repositioning at a different site. Late perforation of the LBBP lead is a major concern, as this may cause thromboembolic complications. So far, thromboembolic complication has not been reported in literature.

Theoretically, coronary artery injury can occur when the lead is placed deep in the proximal septum. This is the first reported case of ST elevation during LBBP lead implantation. Based on the above findings, we believe that coronary artery spasm induced by the LBBP lead is the likely cause for the transient ST elevation observed in this patient.

LBBP is characterized by capture of left bundle or its fascicular branches along with septal myocardium at low output (<1 V at 0.5 ms pulse width). Huang and colleagues[1] first reported successful LBBP for a patient with heart failure and LBBB. Deep septal placement of the lead below the His bundle region resulted in LBBB correction at low pacing output (0.5 V at 0.5 ms). The LV ejection fraction had improved from 34% to 62% with regression of LV dimensions. LBBP overcomes many of the limitations of HBP, as it provides low and stable thresholds, lead stability, and ability to correct distal conduction system disease. LBBP has the potential to be an effective alternative for cardiac resynchronization therapy. Zhang and colleagues[3] demonstrated that LBBP can improve LV dyssynchrony in patients with systolic heart failure and LBBB. Huang and colleagues[4] reported 97% success rate in a multicenter prospective study involving 63 patients with nonischemic cardiomyopathy and LBBB. In our patient, LBBB could be successfully corrected by LBBP, with subsequent improvement in functional status and LV ejection fraction. The long-term effects of deep septal placement of the lead and the challenges of lead extraction from this site are currently unknown and need further evaluation in long-term clinical trials.

Appendix
Supplementary data

Supplementary data associated with this article can be found in the online version at https://doi.org/10.1016/j.hrcr.2020.05.010.

References

1. Huang W, Su L, Wu S, et al. A novel pacing strategy with low and stable output: pacing the left bundle branch immediately beyond the conduction block. Can J Cardiol 2017;33:1736.e1–1736.e3.
2. Huang W, Chen X, Su L, Xia X, Vijayaraman P. A beginner's guide to permanent left bundle branch pacing. Heart Rhythm 2019;16:1791–1796.
3. Zhang J, Wang Z, Cheng L, et al. Immediate clinical outcomes of left bundle branch area pacing vs conventional right ventricular pacing. Clin Cardiol 2019;42:768–773.
4. Huang W, Wu S, Vijayaraman P, et al. Cardiac resynchronization therapy in patients with non-ischemic cardiomyopathy utilizing left bundle branch pacing. JACC Clin Electrophysiol 2020. In press.

Cardiology

Cardiovascular Imaging: Research Article

Comparison of Intravascular Ultrasound Virtual Histology Parameters in Diabetes versus Non-Diabetes with Acute Coronary Syndrome

Reddy S.[a] · Kadiyala V.[a] · Kashyap J.R.[a] · Rao R.[a] · Reddy H.[a] · Kaur J.[a] · Kaur N.[a] · Ramalingam V.[b]

Author affiliations

Keywords: Diabetes mellitus (DM) Intravascular ultrasound (IVUS) Thin-cap fibroatheroma (TCFA) American diabetes Association (ADA)

Cardiology 2020;145:570–577

https://doi.org/10.1159/000508886

Abstract

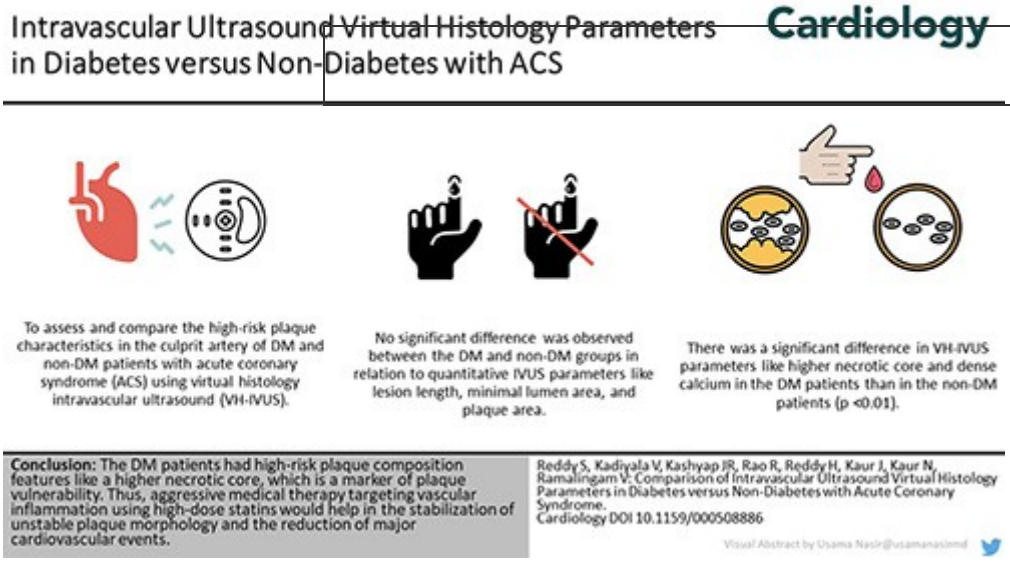

Introduction: The progression and pattern of coronary atherosclerosis in diabetes mellitus (DM) is different from non-DM, leading to a higher rate of vascular complications in DM. ***Objective:*** This study aims to assess and compare the high-risk plaque characteristics in the culprit artery of DM and non-DM patients with acute coronary syndrome (ACS) using virtual histology intravascular ultrasound (VH-IVUS). ***Methods:*** A total of 158 ACS patients were included, 63 of whom were known to have DM. IVUS analysis was done in the de novo target vessel and culprit lesion for which percutaneous coronary intervention was planned. Culprit lesions with a visual-estimate angiographic stenosis of <70% were excluded. ***Results:*** The mean age of patients was 52.4 ± 11.6 years. The study group comprised 82% men, 31% with hypertension, and 39.87% with DM. No significant difference was observed between the DM and non-DM groups in relation to quantitative IVUS parameters like lesion length, minimal lumen area, and plaque area. However, there was a significant difference in VH-IVUS parameters like higher necrotic core and dense calcium in the DM patients than in the non-DM patients ($p < 0.01$). The occurrence of VH-derived thin-cap fibroatheroma (VH-TCFA) in the culprit vessel was significantly higher in the DM group than in the non-DM group (25.3 vs. 5.2%; $p < 0.01$). Positive vessel-wall remodeling was noted in both groups without any significant difference ($p = 0.74$). ***Conclusion:*** The DM patients had high-risk plaque composition features like a higher necrotic core, which is a marker of plaque vulnerability. Thus, aggressive medical therapy targeting vascular inflammation using high-dose statins would help in the stabilization of unstable plaque morphology and the reduction of major cardiovascular events.

References

1. Grundy SM, Benjamin IJ, Burke GL, Chait A, Eckel RH, Howard BV, et al. Diabetes and cardiovascular disease: a statement for healthcare professionals from the American

JACC: CLINICAL ELECTROPHYSIOLOGY VOL. 6, NO. 8, 2020

PUBLISHED BY ELSEVIER

Electroanatomical Mapping-Guided Low Fluoroscopy Left Bundle Branch Pacing

Shunmuga Sundaram Ponnusamy, MD, DM, Dasarath Bopanna, MD, DM, Surya Kumar, MBBS

A 70-year-old man with complete heart block, recurrent syncope, and normal left ventricular function was referred for pacemaker implantation. An option to perform left bundle branch pacing (LBBP) (1) using electroanatomic mapping guidance was discussed with the patient and informed consent was obtained. Three-dimensional (3D) mapping was done using the ENSITE Velocity system (Abbott, Plymouth, Minnesota). Three-dimensional geometry of the right atrium (RA), right atrial appendage (RAA), and right ventricle (RV), along with distal extent of the His signal (**Figure 1A**) and potential LBBP sites in the RV was created using a decapolar catheter (Abbott) from the right femoral vein (**Figure 2A**). Once 3D geometry was created, LBBP was attempted using the 3830 SelectSecure lead and C315 His sheath (Medtronic Inc., Minneapolis, Minnesota). The pacing lead tip was visualized using the 3D system. The sheath, along with the lead, was placed perpendicular to the septum below the tagged His bundle signals with transient fluoroscopy guidance, and pace mapping was done (Video 1). Approximately 2 cm below the distal His bundle region (**Figure 2B**), pacing showed a "W" pattern in lead V_1 (**Figure 1B**) (2). Rapid turns were performed to advance the lead deep inside the septum (**Figure 2C**). Following lead fixation, the paced electrocardiogram showed qR in lead V_1 with a duration of 110 ms (**Figure 1D**) and peak left ventricular activation time of 58 ms (**Figure 1C**). The pacing threshold was 0.3 V at 0.6-ms pulse width with a unipolar pacing impedance of 660 ohms and a sensed R-wave of 11 mV. Transient fluoroscopy was used for sheath removal. The atrial lead could be easily placed in the RAA using 3D geometry (Video 2). LBBP lead and RA lead implantation required 58 and 30 s of fluoroscopy time, respectively (**Figures 3A and 3B**). The overall fluoroscopic time was 88 s. Significant reduction in fluoroscopy time and radiation dose was achieved by electroanatomic mapping guided LBBP (3,4).

ADDRESS FOR CORRESPONDENCE: Dr. Shunmuga Sundaram Ponnusamy, Department of Cardiology, Velammal Village, Velammal Medical College Hospital and Research Institute, Madurai 625009, Tamilnadu, India. E-mail: shunmuga.pgi@gmail.com.

From the Department of Cardiology, Velammal Medical College Hospital and Research Institute, Madurai, Tamilnadu, India. The authors have reported that they have no relationships relevant to the contents of this paper to disclose.

The authors attest they are in compliance with human studies committees and animal welfare regulations of the authors' institutions and Food and Drug Administration guidelines, including patient consent where appropriate. For more information, visit the *JACC: Clinical Electrophysiology* author instructions page.

Manuscript received April 13, 2020; revised manuscript received May 6, 2020, accepted May 8, 2020.

ISSN 2405-500X/$36.00 https://doi.org/10.1016/j.jacep.2020.05.020

FIGURE 1 Electrograms and Electrocardiograms

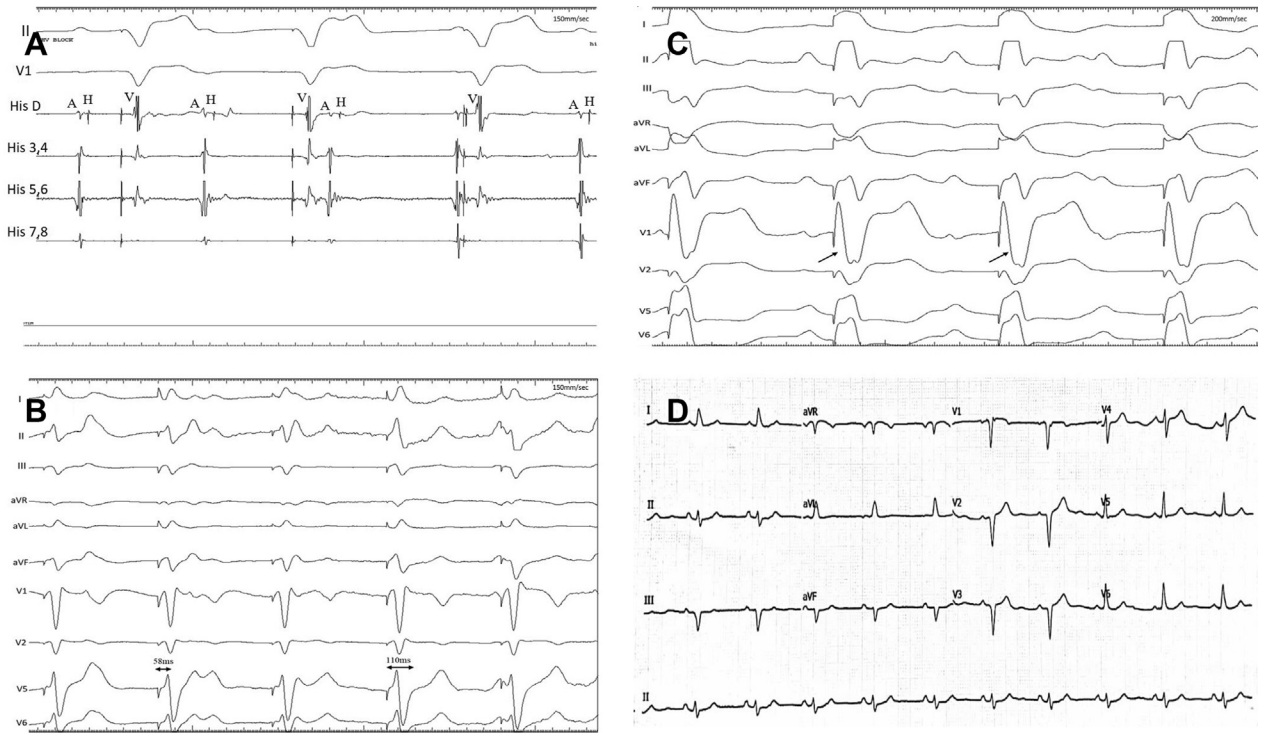

(A) Baseline intracardiac electrogram showing HV block. **(B)** Target site, 2 cm below the His bundle signals where pacing showed a "W" pattern in lead V_1 **(black arrow)**. **(C)** Left bundle branch paced QRS duration 110 ms and peak left ventricular activation time of 58 ms (Video 2). **(D)** Final 12-lead electrocardiogram after 3-dimensional (3D)-guided left bundle branch pacing.

FIGURE 2 Electroanatomical Mapping-Guided LBBP

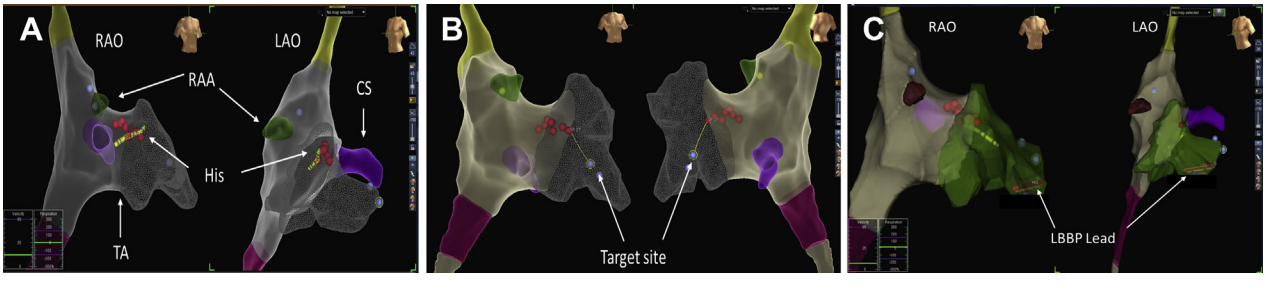

(A) 3D geometry created using decapolar catheter. **(B)** Target site was tagged **(blue dot)** where pacing showed a "W" pattern in lead V_1. **(C)** The pacing lead (left branch bundle pacing [LBBP]) could be visualized inside the interventricular septum after fixation. CS = coronary sinus; His = His potentials; LAO = left anterior oblique; LBBP = left bundle branch pacing; RAA = right atrial appendage; RAO = right anterior oblique; TA = tricuspid annulus.

FIGURE 3 **Final Lead Position After 3D-Guided LBBP**

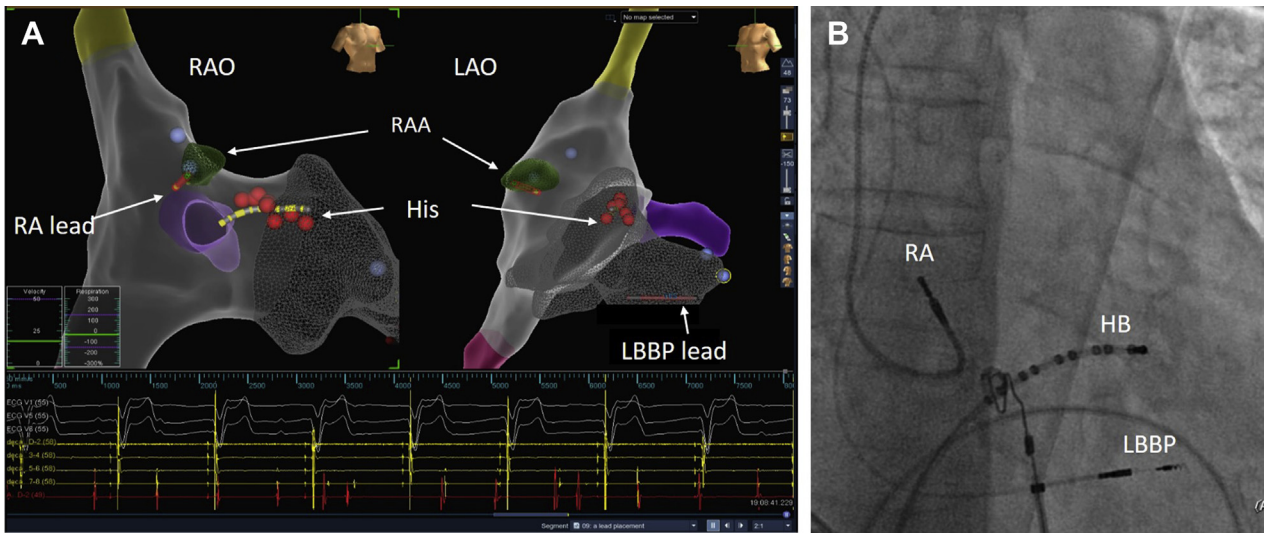

(A) ENSITE image (Abbott, Plymouth, Minnesota) and **(B)** RAO 25-degree fluoroscopic view. HB = His bundle; RA = right atrial; other abbreviations as in Figure 2.

REFERENCES

1. Vijayaraman P, Panikkath R, Mascarenhas V, Bauch TD. Left bundle branch pacing utilizing three-dimensional mapping. J Cardiovasc Electrophysiol 2019;30:3050–6.

2. Chen K, Li Y. How to implant left bundle branch pacing lead in route clinical practice. J Cardiovasc Electrophysiol 2019;30:2569–77.

3. Venneri L, Rossi F, Botto N, et al. Cancer risk from professional exposure in staff working in cardiac catheterization laboratory: insights from the National Research Council's biological effects of ionizing radiation VII report. Am Heart J 2009;157:118–24.

4. Sharma PS, Huang HD, Trohman RG, Naperkowski A, Ellenbogen KA, Vijayaraman P. Low fluoroscopy permanent His bundle pacing using electroanatomic mapping- a feasibility study. Circ Arrhythm Electrophysiol 2019;12:3006967.

KEY WORDS electroanatomical map, left bundle pacing, low fluoroscopy

APPENDIX For supplemental videos, please see the online version of this paper.

Ramalingam Vadivelu ORCID iD: 0000-0002-7195-3648

Raghav Bansal ORCID iD: 0000-0002-1649-8013

Title page

Type of manuscript: EP rounds

Title of the article:

Changing atrial activation patterns during narrow complex tachycardia

Authors: Ramalingam Vadivelu, MD, DM[1], Yash Lokhandwala, MD, DM[1], Raghav Bansal MD, DM[1]

Institution affiliation and address:

[1]Department of Cardiology, Bandra Holy Family Hospital and Research Centre, Mumbai, India-400050

Name and address of corresponding author:

Dr Ramalingam Vadivelu MD, DM

Consultant Cardiologist and Electrophysiologist,

Bandra Holy Family Hospital and Research Centre, Mumbai, India-400050

Phone number: +91-9821167542 Fax Number: 022-26518373

Email id: vvelu00@gmail.com

This article has been accepted for publication and undergone full peer review but has not been through the copyediting, typesetting, pagination and proofreading process, which may lead to differences between this version and the Version of Record. Please cite this article as doi: 10.1111/jce.14685.

No financial support or grant was received

Conflict of interest statement

There are no conflicts of interest regarding this work from authors

Number of words: 1095 **Number of figures**: 3

Short title: Changing atrial activation during SVT

Key words: Mitral isthmus block, prior RF ablation, accessory pathway

Changing atrial activation patterns during narrow complex tachycardia

A 53- year old woman presented with recurrent episodes of paroxysmal tachycardia with a structurally normal heart. She had undergone an electrophysiology study in an outside hospital which revealed orthodromic atrioventricular reentrant tachycardia (ORT) using a concealed left posterolateral accessory pathway (AP), for which radiofrequency ablation was performed. But tachycardia recurred three months later. In view of significant symptoms, she came to us for a repeat procedure. The AH and HV intervals were 77 ms and 45 ms respectively. Narrow complex tachycardia (tachycardia 1) with a cycle length (CL) of 300 ms was easily and repeatedly induced and terminated (Figure 1, left panel) by a premature ventricular complex (PVC). Shortly another tachycardia (tachycardia 2) with CL of 255 ms was induced and terminated (Figure 1, right panel) by a premature ventricular complex. Later, during tachycardia 2, a spontaneous change was seen (Figure 2). Are we dealing with a single tachycardia mechanism?

Discussion

Tachycardia 1 in Figure 1, left panel, shows an eccentric atrial activation pattern with the earliest 'A' in channels CS3,4 and CS1,2 located in the left posterolateral region. The ventriculoatrial (VA) time even at this site is quite long and there is no bracketing. A His-refractory PVC delivered from the left ventricle terminates the tachycardia without activation of the atrium, confirming ORT as the mechanism, using a left free wall accessory pathway. Tachycardia 2 (Figure 1, right panel) has a clearly different atrial activation pattern with the earliest atrial activation in CS78 and CS910, near the mouth of the coronary sinus, though with a relatively long VA interval. This is also an ORT, being terminated by a His-refractory PVC delivered from the left ventricle, without activation of the atrium. Hence the differential diagnoses include: i) Only 1 left free wall accessory pathway, with intermittent local periannular (mitral isthmus) conduction block resulting in coronary sinus disconnection, due to the previous ablation; ii) Two APs, left lateral and inferoparaseptal (posteroseptal) and iii) Two APs, left lateral and right sided. A single left ventricular His-refractory PVC terminating tachycardia made a right sided AP unlikely and this was ruled out by mapping the tricuspid annulus during the tachycardia.

Figure 2 shows tachycardia with two different atrial activation patterns. A later His-refractory PVC from the left ventricle results in following changes: i) Fusion QRS complex; ii) Prolongation of tachycardia CL from 255 ms to 300 ms and iii) Change in mitral annular atrial activation pattern from concentric to eccentric with a longer initial local VA time. So here differential diagnoses could be either 1) Two left sided APs, the ORT utilising the left posterior AP being terminated by the PVC and the

ORT utilising the left lateral AP being immediately initiated or ii) ORT using the same left lateral AP, with concentric mitral annular atrial activation in the initial two beats due to local mitral isthmus block; the PVC 'peels away' this conduction block.

The left Panel of Figure 3 explains the concentric activation pattern. Local conduction block due to previous ablation does not allow the coronary sinus to get activated from the atrial end of the AP during tachycardia. The activation then could have proceeded up the left atrium to the Bachman's bundle and thence, to the right atrium. However, in that case the atrium in the peri-AV nodal area would have been activated before the coronary sinus ostium region. In our case, the coronary sinus ostium is activated earlier, with the 'A' in the His bundle region later. So the previous ablation energies had also produced a conduction block higher up, preventing the Bachman's bundle from getting engaged. This is further confirmed by Figure 2, where we see that the 'A' maintains the same rsr'S'R" morphology in the HISD channel and the same delay after the 'A' in CS910 during both types of tachycardia.

Hence it was decided to map in the lateral mitral annular region during left ventricular pacing. At the left posterolateral region 1 cm above the mitral annulus, the earliest fragmented atrial activation was found. Upon starting radiofrequency energy the AP conduction was immediately abolished and retrograde AV nodal conduction was seen. After this successful ablation, complete VA block was seen with adenosine during left ventricular pacing. Despite isoprenaline, no AP conduction was seen and no tachycardia was inducible.

Left atrial- coronary sinus disconnection, also termed mitral isthmus conduction delay or block, is a peculiar phenomenon that can occur during ablation of a left free wall AP, when several energies are delivered inferiorly while the actual AP inserts higher

up.[1,2] This is one of the important reasons for failure of ablation, as the operator may erroneously think that the AP pathway conduction was abolished when retrograde conduction changes from an eccentric to a concentric pattern.

References

1. Singh B, Sapra R, Gupta RK, Ghose T, Trehan R, Kaul U. Left atrial-coronary sinus dissociation following an attempt at RF ablation for a left lateral accessory pathway. Indian Heart J 2003;55:376-378.
2. Bulava A, Hanis J, Sitek D. Mitral isthmus conduction block: intriguing result of radiofrequency catheter ablation for a left concealed accessory pathway. Europace 2010;12(4):579-581.

Figure legends

Figure1: The **left panel** shows a narrow complex tachycardia (tachycardia 1) with eccentric retrograde activation. The coronary sinus (CS) 9,10 dipoles are at the ostium, while the CS 1,2 dipoles are in the left lateral region; His bundle electrograms, distal and proximal (HISD, HISP), and left ventricular (LV) electrograms are also displayed. The tachycardia is terminated by a LV extrastimulus. The **right panel** shows a narrow complex tachycardia (tachycardia 2) with concentric atrial activation, terminated by a LV extrastimulus.

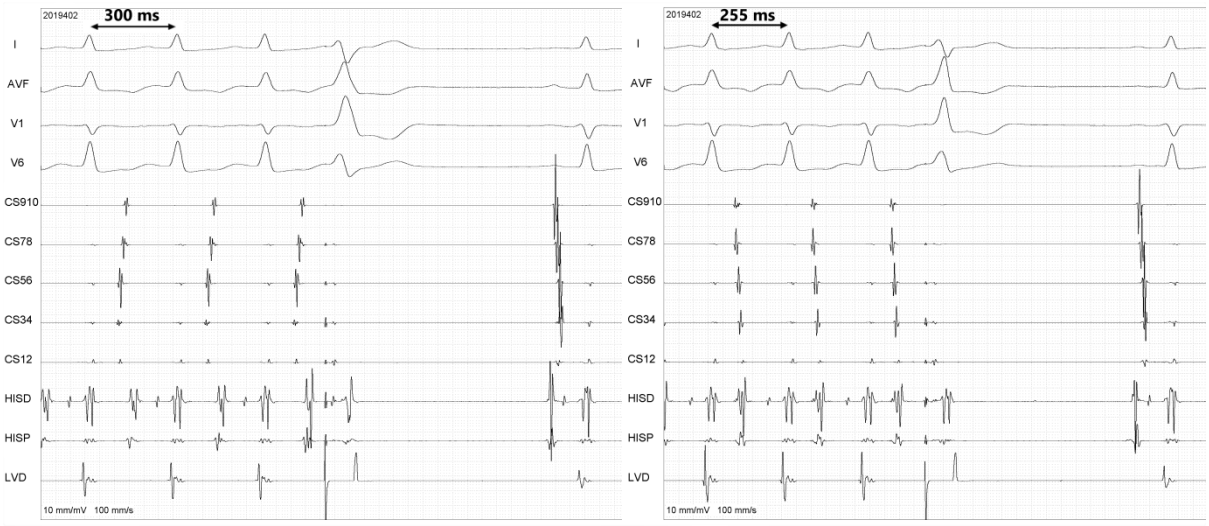

Figure 2: This trace shows narrow complex tachycardia with two different atrial activation patterns. The first two beats show concentric mitral annular activation pattern. The third beat depicts a LV extrastimulus with a fusion QRS complex, which changes the atrial activation to an eccentric pattern. The cycle length also prolongs from 255 ms to 300 ms. The unchanging delay between the atrial activation in the HISD and CS 9,10 channels is denoted by the double headed arrow.

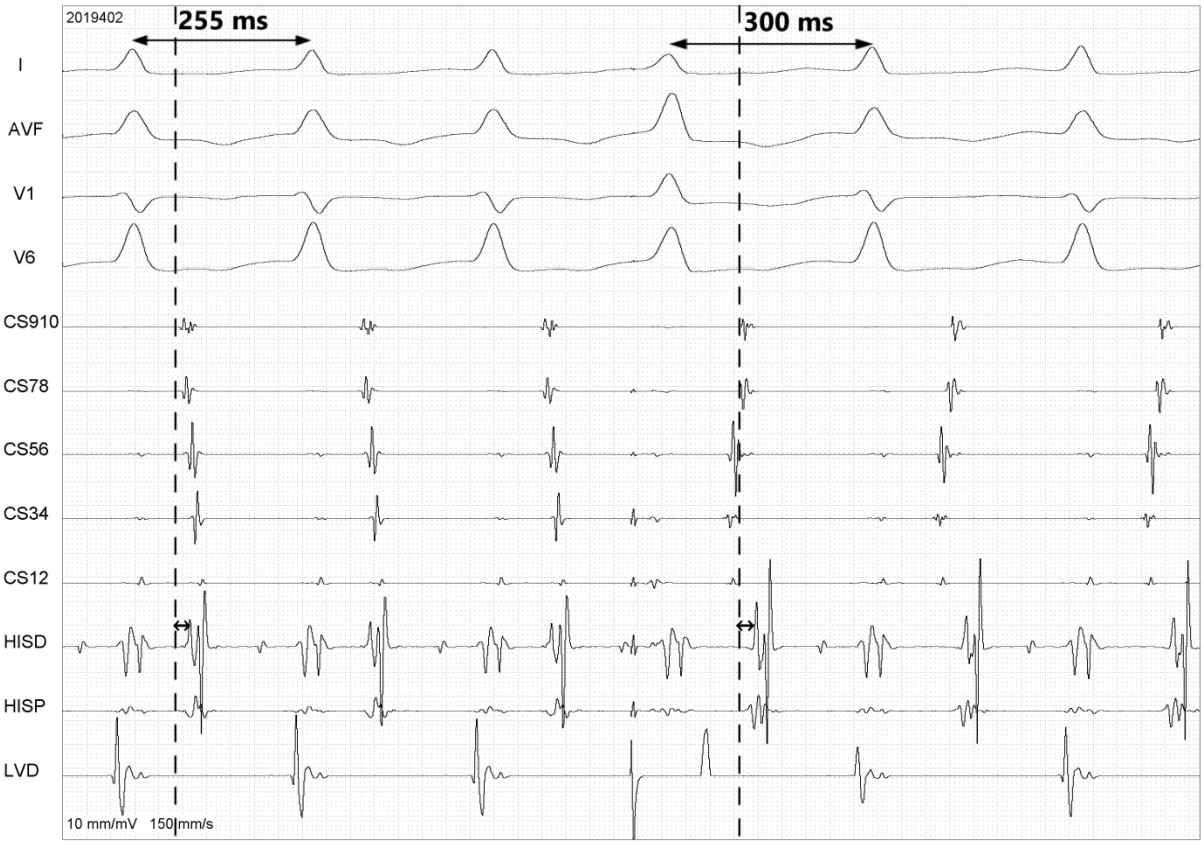

Figure 3: Cine images in left anterior oblique 40^0 views. The thick black arrow represents the accessory pathway, the black bars denote the areas of conduction block and the white arrows show the proposed routes of atrial activation during tachycardia. The **left panel** is the proposed route of atrial activation during local mitral isthmus conduction block, with concentric activation pattern. The **right panel** shows atrial activation with local delay, accounting for the long local VA time in CS1,2 followed by eccentric activation pattern.

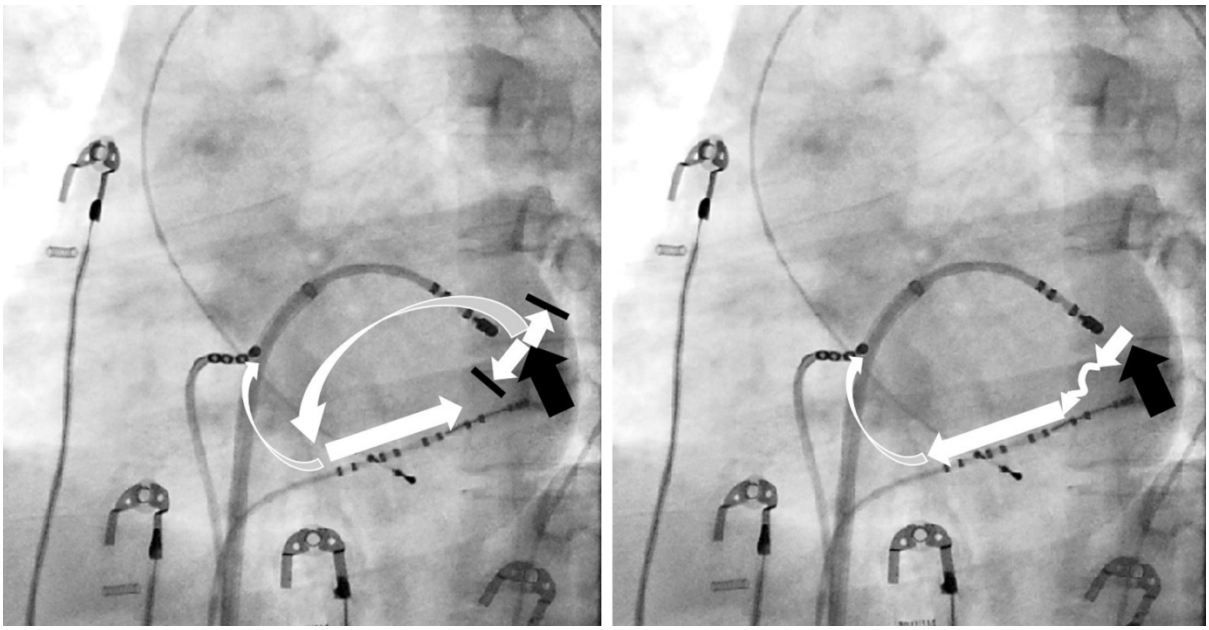

Left bundle branch pacing guided by premature ventricular complexes during implant

Shunumuga Sundaram Ponnusamy, MD, DM, Pugazhendhi Vijayaraman, MD, FHRS

From the Department of Cardiology, Velammal Medical College Hospital and Research Institute, Madurai, India, and Geisinger Commonwealth School of Medicine, Wilkes-Barre, Pennsylvania.

Introduction

Physiological pacing has witnessed a rapid growth in the last decade. His bundle pacing (HBP) provides electrical and mechanical synchrony but may be limited by high pacing thresholds and higher need for lead revisions.[1] Left bundle branch pacing (LBBP) has recently been shown to be a promising alternative to HBP. Several criteria for successful left bundle capture have been proposed[2] but need to be validated. LBBP involves advancing the lead deep into the septum by rapid rotations. The goal is to place the lead adjacent to the left bundle branch in the left ventricular (LV) subendocardial region without perforation into the LV cavity. We describe premature ventricular complex (PVC)-guided lead implantation as a novel approach to perform LBBP.

Case report

Case 1

A 65-year-old woman with nonischemic cardiomyopathy, left bundle branch block (LBBB), and LV dysfunction (ejection fraction 30%; interventricular septal [IVS] thickness 11 mm) was referred for cardiac resynchronization therapy. After informed consent was obtained, LBBP was performed using C315 His sheath and 3830 SelectSecure lead (Medtronic, Minneapolis, MN). The pacing lead was positioned deep inside the septum 1.5 cm apical to the distal His bundle region by 4–5 rapid turns. During positioning of the lead deep inside the septum, PVCs with changing morphology were noted. Rotation was stopped immediately on observing PVC (PVC1) with narrow QRS duration and qR (right bundle branch [RBB] delay) in lead V_1 [Figure 1A (i)]. No potentials were noted during baseline LBBB rhythm. The pacing threshold was 0.3 V at 0.5 ms and pacing impedance of 580 ohms. The final left bundle branch (LBB) paced QRS morphology mimicked PVC1 (Figure 1A [ii]) with duration of 124 ms (peak LV activation time [pLVAT] 78 ms). RBB delay was corrected by optimizing the AV interval and pacing output (Figure 1A [iii]). Contrast angiography showed the lead was deployed at a depth of 10 mm inside the septum

Case 2

A 35-year-old woman with nonischemic cardiomyopathy, LBBB, and LV dysfunction (ejection fraction 28%; IVS thickness 11 mm) was referred for cardiac resynchronization therapy. LBBP was performed using C315 His sheath and 3830 SelectSecure lead (Medtronic). PVCs with changing morphology were noted during lead advancement. Rotation was stopped immediately on observing a PVC (PVC2) with narrow QRS duration and rSR (RBB delay) pattern in lead V_1 (Figure 1B [i]). No potentials were noted during baseline LBBB rhythm. Nonselective to selective capture of LBB could be demonstrated by change in QRS

KEY TEACHING POINTS

- Left bundle branch pacing is an effective alternative for His bundle pacing as it overcomes its limitations.
- Premature ventricular complexes (PVCs) with changing morphology from QS pattern to right bundle branch (RBB) conduction delay pattern (qR or rSR) in lead V_1 along with QRS duration reduction are observed as the lead traverses the septum before reaching the left bundle branch area.
- Occurrence of PVCs with narrow QRS duration and RBB delay pattern confirms left bundle branch capture.
- PVC-guided lead placement would help in final positioning of the lead and avoid septal perforation into the left ventricular cavity.

KEYWORDS AV junction ablation; Cardiac resynchronization therapy; Heart failure; Left bundle pacing; Premature ventricular complex
(Heart Rhythm Case Reports 2020;6:850–853)

Funding: This research did not receive any specific grant from funding agencies in the public, commercial, or not-for-profit sectors. Disclosures: Shunumuga Sundaram Ponnusamy: None. Pugazhendhi Vijayaraman: Honoraria, consultant, research, fellowship support: Medtronic; consultant: Boston Scientific, Abbott, Biotronik, Eaglepoint LLC. **Address reprint requests and correspondence:** Dr Pugazhendhi Vijayaraman, Professor of Medicine, Geisinger Commonwealth School of Medicine, Geisinger Heart Institute, MC 36-10, 1000 E Mountain Blvd, Wilkes-Barre, PA 18711. E-mail address: pvijayaraman1@geisinger.edu.

https://doi.org/10.1016/j.hrcr.2020.08.010

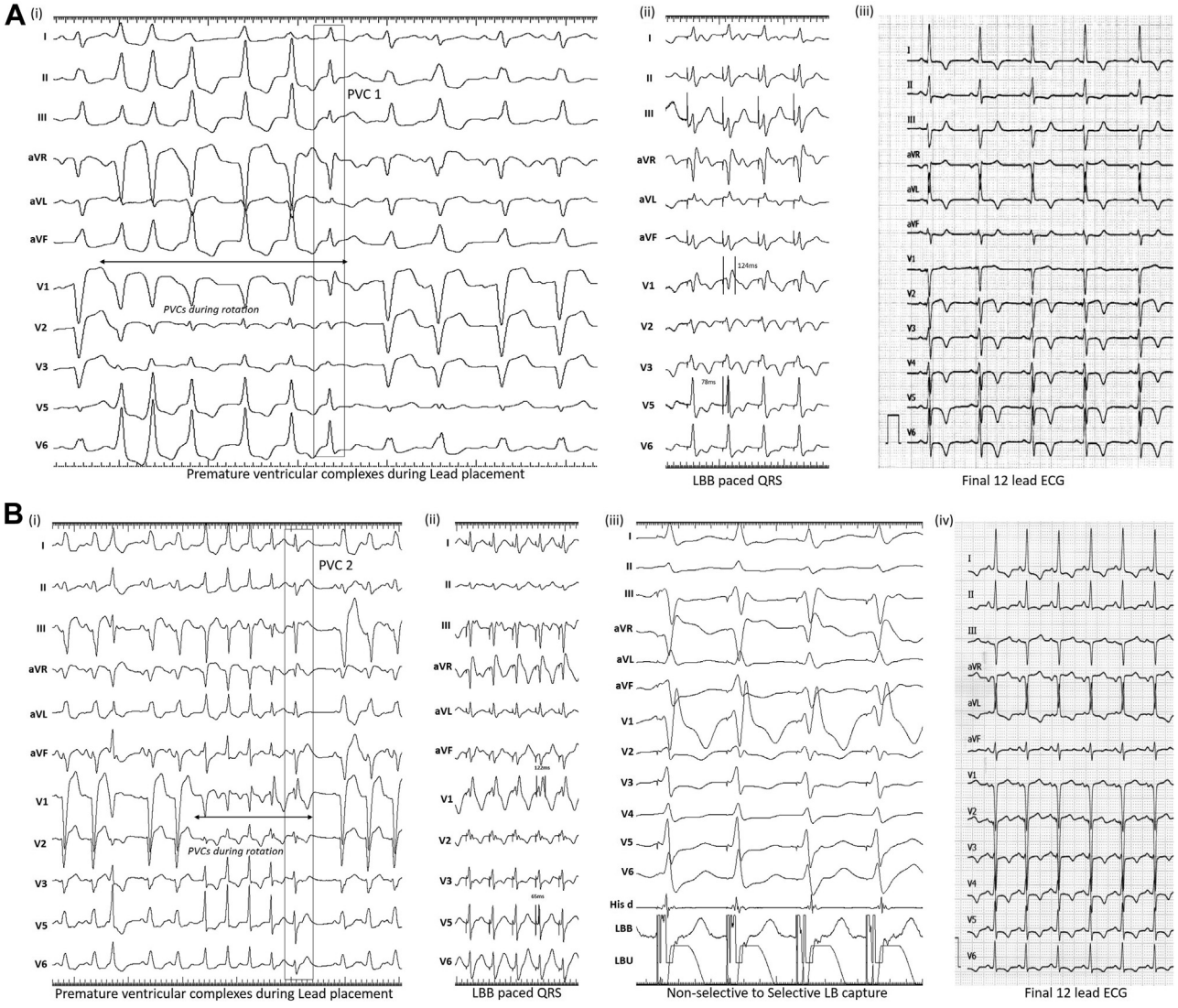

Figure 1 **A:** Left bundle branch pacing (LBBP) for nonischemic cardiomyopathy (NICM) with left bundle branch block (LBBB). (i) Premature ventricular contractions (PVCs) with changing morphology from QS to qR pattern (PVC1) in lead V_1 noted during rapid rotation. (ii) Left bundle branch (LBB) paced QRS mimicked PVC1 with duration of 124 ms and peak left ventricular activation time (pLVAT) of 78ms. (iii) Final 12-lead electrocardiography (ECG) after correcting right bundle branch delay by AV interval optimization (QRS duration 108 ms). **B:** LBBP for NICM with LBBB. (i) PVCs with changing morphology from QS to rSR pattern (PVC2) in lead V_1 noted during rapid rotation. (ii) LBB paced QRS morphology mimicked VES1 with duration of 122 ms and pLVAT of 65 ms. (iii) Nonselective (first 2 beats) to selective LBB capture (last 2 beats) at near threshold output. (iv) Final 12-lead ECG after RBB delay correction by optimizing the AV delay (QRS duration 98 ms). His d = distal His bundle electrogram; LBB = pacing lead electrogram bipolar; LBU = pacing lead electrogram unipolar.

morphology and discreet local ventricular electrogram at near threshold output (Figure 1B [iii]). Pacing threshold was 0.4 V at 0.5 ms and unipolar pacing impedance of 670 ohms. LBB paced QRS morphology mimicked PVC2 with duration of 122 ms and pLVAT in lead V_5 of 65 ms (Figure 1B [ii]). AV interval was optimized to correct the RBB delay (Figure 1B [iv]). Contrast angiography showed a lead depth of 10 mm.

Case 3

A 72-year-old man was referred for the management of permanent atrial fibrillation with uncontrolled ventricular rates and LV dysfunction. Echocardiography showed moderate mitral regurgitation with LV ejection fraction of 32% and IVS thickness of 10 mm. Atrioventricular junction (AVJ) ablation with physiological pacing option was recommended. LBBP was attempted as previously described. PVCs of changing morphology were noted while placing the lead deep inside the septum. Rotation was stopped immediately on observing PVC (PVC3) with narrow QRS duration and qR (RBB delay) in lead V_1 (Figure 2A). Nonselective to selective capture of LBB could be demonstrated at near threshold output (Figure 2D). LBB paced QRS mimicked PVC3 with duration of 124 ms and pLVAT of 65 ms (Figure 2B). The pacing threshold was 0.6 V at 0.5 ms pulse width and lead impedance of 730 ohms. LBB potential was recorded on the LBBP lead electrogram (LBB-ventricular interval of 25 ms, Figure 2C). AVJ ablation was completed

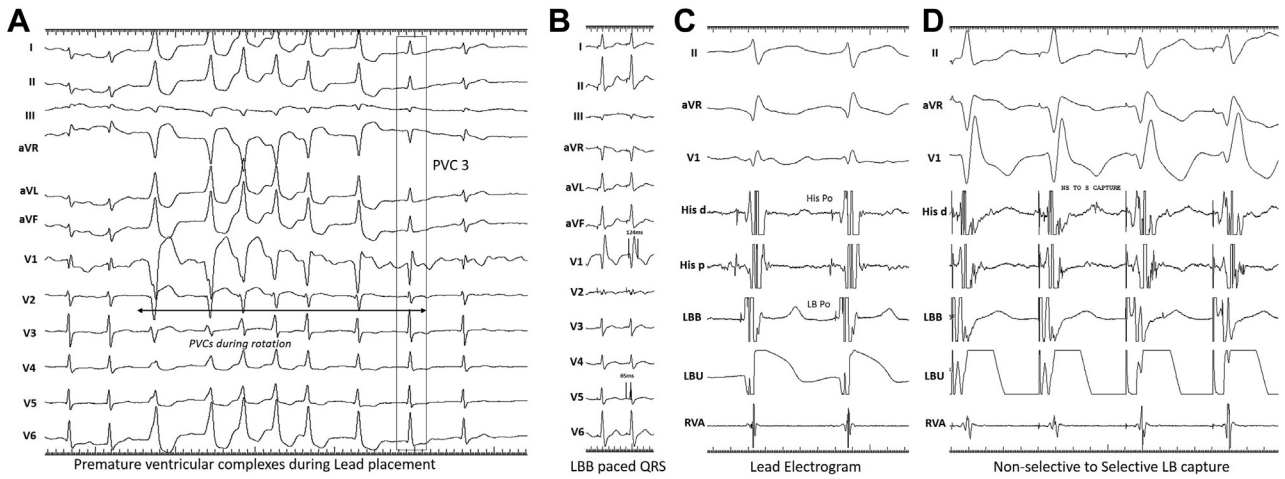

Figure 2 Left bundle branch pacing (LBBP) and atrioventricular junction ablation. **A:** Premature ventricular contractions (PVC) with changing morphology during lead rotation. **B:** Left bundle branch (LBB) paced QRS mimicked PVC3 with duration of 124 ms and peak left ventricular activation time 65 ms. **C:** Pacing lead electrogram (LBB) showing sharp LBB potentials (LB Po) preceding the local ventricular electrogram. **D:** Nonselective (first 2 beats) to selective (last 2 beats) capture of LBB. His d = distal His bundle electrogram; His p = proximal His bundle electrogram; His Po = His bundle potential; LBB = pacing lead electrogram bipolar; LBU = pacing lead electrogram unipolar; RVA = right ventricular electrogram.

using an irrigated-tip ablation catheter. Contrast angiography showed a lead depth of 9 mm.

Case 4

A 73-year-old woman with normal LV function (IVS thickness 11 mm) presented with symptomatic complete heart block. LBBP was performed using a 3830 SelectSecure lead and C315 His sheath (Medtronic). The pacing lead was positioned deep inside the septum by 4–5 rapid turns. PVCs with changing morphology were noted during lead advancement. Lead rotation was stopped immediately after observing narrow complex PVC (PVC4) with qR (RBB delay) pattern in lead V_1 (Figure 3A). Electrograms from the pacing lead demonstrated sharp left bundle potential (Figure 3C) preceding the ventricular electrogram (LB-ventricular interval of 20 ms). Pacing threshold was 0.4 V at 0.5 ms and lead impedance was 680 ohms. The paced QRS morphology mimicked the narrow PVC morphology (PVC4) with QRS duration of 114 ms with pLVAT in lead V_5 of 70 ms (Figure 3B). RBB delay was corrected by optimizing pacing output to allow anodal capture (Figure 3D). Contrast angiography showed a lead depth of 10 mm.

Discussion

LBBP is a promising alternative to HBP. Presence of RBB conduction delay pattern (qR in lead V_1) and demonstration of LBB potentials are often used as criteria for LBB capture.[2,3] LBB potentials may be demonstrable in 30%–80% of the study population at the time of implantation.[4,5] Transition in QRS morphology from nonselective to selective left bundle capture or nonselective to LV septal capture may be noted at near threshold outputs.[6] Rapid rotation of the pacing lead is necessary to achieve deep penetration of the interventricular septum. Perforation into the LV cavity can occur if

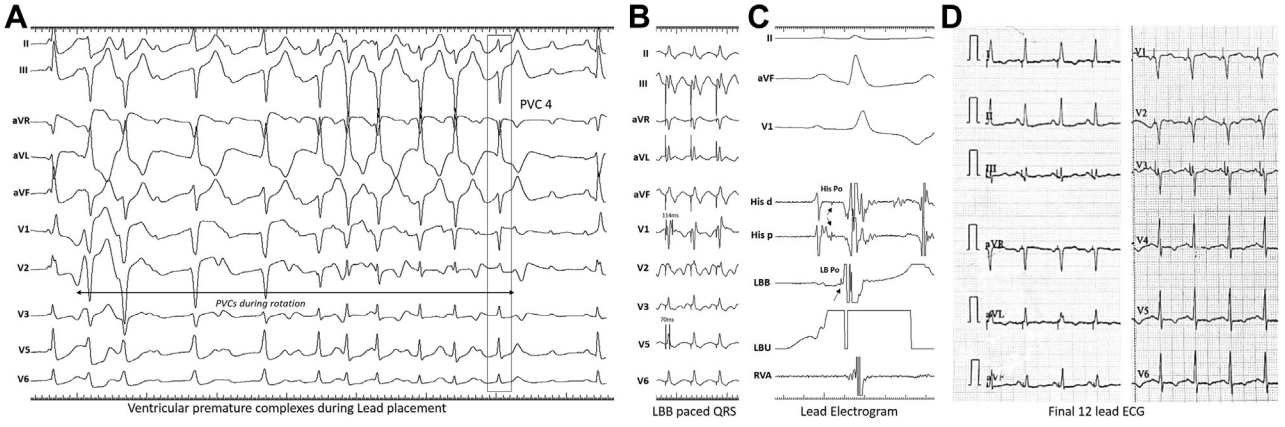

Figure 3 Left bundle branch pacing for complete heart block. **A:** Premature ventricular contractions (PVCs) during left bundle branch (LBB) lead placement. **B:** Paced QRS morphology mimicked PVC4 with duration of 114 ms and peak left ventricular activation time of 70 ms. **C:** Pacing lead electrogram showing sharp LBB potential (LB Po) preceding the local ventricular electrogram. **D:** Final 12-lead electrogram (ECG) after right bundle branch delay correction by anodal capture (QRS duration 100 ms). His d = distal His bundle electrogram; His p = proximal His bundle electrogram; His Po = His bundle potential; LBB = pacing lead electrogram bipolar; LBU = pacing lead electrogram unipolar; RVA = right ventricular electrogram.

the lead is advanced too rapidly, resulting in (1) fall in unipolar pacing impedance to <400 ohms, (2) rise in capture threshold, and (3) loss of current of injury in unipolar lead electrogram. PVCs are commonly noted while positioning the lead in the interventricular septum. The PVC morphology depends on the depth of the lead in the septum. We observed gradual change in morphology from wide QRS with QS morphology in lead V_1 to narrow QRS with RBB delay pattern (qR/rSR) as the lead penetrated the septum from the right ventricular side to the LBB area. In all 4 cases, rapid rotations were stopped as soon as PVCs with narrow QRS and RBB delay pattern were observed (PVC1, PVC2, PVC3, and PVC4). Paced QRS morphology matched the PVC morphology with short and constant pLVAT at differential pacing (high and low output). Though the pacing indications varied in these patients, PVC morphology predicted left bundle capture and guided in deciding the lead depth. LBB potentials were noted in 2 patients (complete heart block and AVJ ablation cases). It is possible to record LBB potentials in patients with LBBB during PVCs of RBB morphology if continuous recording can be performed during lead rotations. Lack of a revolving connector pin during lead rotations is a limitation with the current implant technique. Further rotations were avoided, preventing perforation of septum. Monitoring the change in PVC morphology and QRS duration during lead fixation would help in final positioning of the LBB pacing lead and confirming conduction system capture.

While deploying the lead deep inside the proximal septum, we monitored the 12-lead electrocardiogram for the appearance of PVCs. The morphology of the PVC was observed carefully, and the rotations were stopped immediately after getting RBB delay pattern in lead V_1 along with reduction in QRS duration. If the rotations were interrupted for some reason before getting the desired QRS pattern, a further few turns were given after checking the unipolar paced QRS morphology and pacing impedance to get RBB delay pattern. In our study cohort of 50 patients who had undergone successful LBBP, two-thirds of the patients (n = 34) showed PVCs during rapid lead deployment.[7] Excluding the patients with baseline LBBB, LBB potentials were noted in 75% of the patients who showed PVCs with changing morphology during lead deployment (21 of 28 patients). Lack of availability of the revolving connector pin prevented us from showing the potentials on the PVC with RBB delay pattern. Rapid rotations with lead deployment within 10 seconds usually resulted in runs of PVCs. The incidence of PVCs with changing morphology were infrequent if there was difficulty in rapid penetration of the septum where the lead deployment took more than 20 seconds. It is possible that Purkinje fibers are more sensitive to trauma induced by the pacing lead to trigger PVCs during implantation.

Since the initial description of LBBP, multiple studies have shown the safety and efficacy of left bundle branch pacing. Huang and colleagues[8] demonstrated 97% success rate in LBBP for nonischemic cardiomyopathy and LBBB along with significant improvement in LV ejection fraction at 1 year. A large retrospective multicenter study by Vijayaraman and colleagues[9] showed an 85% success rate in achieving cardiac resynchronization therapy by LBBP (277 out of 325 patients). Improvement in LVEF was noted in both ischemic and nonischemic cardiomyopathy and similarly in patients with LBBB and non-LBBB. Conduction system pacing combined with AV node ablation showed a high success rate in persistent atrial fibrillation patients with heart failure and implantable cardioverter-defibrillator indication.[10] This study also showed significant improvement in LV function and reduction in inappropriate shocks.

LBBP is emerging as a promising option to deliver physiological pacing. Though several criteria have been proposed to confirm capture of left bundle, prospective studies are necessary to validate. PVC-guided lead placement would help in final positioning of the lead and avoid septal perforation into the LV cavity.

References

1. Subzposh FA, Vijayaraman P. Long-term results of His bundle pacing. Card Electrophysiol Clin 2018;10:537–542.
2. Huang W, Chen X, Su L, et al. A beginner's guide to permanent left bundle branch pacing. Heart Rhythm 2019;16:1791–1796.
3. Vijayaraman P, Subzposh FA, Naperkowski A, et al. Prospective evaluation of feasibility, electrophysiologic and echocardiographic characteristics of left bundle branch area pacing. Heart Rhythm 2019;16:1774–1782.
4. Li X, Li H, Ma W, et al. Permanent left bundle branch area pacing for atrioventricular block: Feasibility, safety, and acute effect. Heart Rhythm 2019; 16:1766–1773.
5. Li Y, Chen K, Dai Y, et al. Left bundle branch pacing for symptomatic bradycardia: Implant success rate, safety, and pacing characteristics. Heart Rhythm 2019;16:1758–1765.
6. Vijayaraman P, Huang W. Atrioventricular block at the distal His bundle: Electrophysiological insights from left bundle branch pacing. HeartRhythm Case Rep 2019;5:233–236.
7. Ponnusamy SS, Muthu G, Kumar M, et al. Mid-term feasibility, safety and outcomes of left bundle branch pacing – Single center experience. J Interv Card Electrophysiol, https://doi.org/10.1007/s10840-020-00807-w. 2020.07.04.
8. Huang W, Wu S, Vijayaraman P, et al. Cardiac resynchronization therapy in patients with non-ischemic cardiomyopathy utilizing left bundle branch pacing. JACC Clin Electrophysiol 2020;6:849–858.
9. Vijayaraman P, Sundaram S, Cano O, et al. Left bundle branch area pacing for cardiac resynchronization therapy: results from International LBBAP Collaborative Study Group. JACCCEP 2020.
10. Wang S, Wu S, Xu L, et al. Feasibility and efficacy of His bundle pacing or left bundle pacing combined with AV node ablation in patients with persistent atrial fibrillation and implantable cardioverter-defibrillator therapy. J Am Heart Assoc 2019;17(8):e014253.

BRIEF REPORT

MAYO CLINIC

Status of Acute Myocardial Infarction in Southern India During COVID-19 Lockdown: A Multicentric Study

Ramachandran Meenakshisundaram, MBBS, MRCP, PhD, PGCert in HBE, FHEA; Subramanian Senthilkumaran, MD, PhD; Ponniah Thirumalaikolundusubramanian, MD; Melvin Joy, MSc; Narendra Nath Jena, MD; Ramalingam Vadivelu, MD; Shyamsundar Ayyasamy, MD; and V.P. Chandrasekaran, MD

Abstract

There has been a reduction in the reported cases of acute myocardial infarction (MI) across the globe during the outbreak of coronavirus disease 2019 (COVID-19) (severe acute respiratory distress syndrome coronavirus 2). An attempt was made to find out the number of acute MI cases treated during the COVID-19 lockdown period (April 2020) and highlight the possible reasons for the changes in the occurrence. A multicentric retrospective observational study was performed to collect the selected data from 12 private hospitals distributed in 4 cities—Madurai, Trichy (Thiruchirapalli), Erode, and Salem—of the Tamil Nadu state in southern India. There was a significant ($P<.001$) reduction in ST-segment elevation MI (STEMI), non-STEMI (NSTEMI), and total (STEMI and NSTEMI together) cases during the lockdown period (April 1 to 30, 2020) as compared with no-lockdown periods such as January and February 2020 and April 2019 and April 2018 in all cities, whereas the reduction was not significant for NSTEMI in Trichy when data for the lockdown period was compared with those for January and February 2020. Overall, there is a reduction in acute MI cases, which may be due to alterations in modifiable risk factors during the COVID-19 lockdown period. Hence, implementation of public education and polices on controlling modifiable risk factors is likely to pay dividends.

From the Manian Medical Centre, Erode, Tamil Nadu, India (R.M., S.S.); HCA Healthcare UK, HCA International Limited, London, UK (R.M.); Trichy SRM Medical College Hospital and Research Centre, Tiruchirappalli, Tamil Nadu, India (affiliated to the Tamil Nadu Dr. M.G.R. Medical University, Chennai) (P.T.); Christian Medical College, Vellore, Tamil Nadu, India (affiliated to the Tamil Nadu Dr. M.G.R. Medical University, Chennai) (M.J.); Meenakshi Mission Hospital and Research Centre, Madurai, Tamil Nadu, India (N.N.J.); Velammal Medical College Hospital and

Affiliations continued at the end of this article.

Because of the coronavirus disease 2019 (COVID-19) (severe acute respiratory syndrome coronavirus 2) pandemic, strict social containment measures were promoted in the form of lockdown in most of the countries. Although the health system is overwhelmed with COVID-19 cases across the globe, a change in the hospital admission pattern during the lockdown period has been reported.[1-4] The Government of India imposed a nationwide strict lockdown from March 25, 2020, with a nationwide curfew on March 22, 2020.[5] Hence, the present study was conducted to find out the number of acute myocardial infarction (MI) cases, which included ST-segment elevation MI (STEMI) and non-STEMI (NSTEMI) cases, treated during the lockdown period, to compare these cases with those in other months of 2020 before the lockdown as well as with those in the same month of previous years (2018 and 2019), and to highlight the possible reasons for these variations.

PATIENTS AND METHODS

We conducted a multicentric retrospective observational study across 12 private hospitals, which followed similar methods to collect the clinical data and adhere to Good Clinical Practice in the management of acute MI. These hospitals were located in different cities, namely, Madurai, Trichy (Thiruchirapalli), Erode, and Salem in the state of Tamil Nadu in southern India. The data on age, sex, and the category of acute MI (STEMI and NSTEMI) were collected from the records for

TABLE 1. City-wise Cases of Acute Myocardial Infarction and Emergency Department Attendance

Name of the city	No. of hospital(s)	Lockdown period			No-lockdown period											
					2020											
		Apr 2020			Feb			Jan			Apr 2019			Apr 2018		
		S	N	ET	S	N	ET	S	N	ET	S	N	ET	S	N	ET
Madurai	2	63	81	1416	155	203	2214	205	239	2786	243	239	2739	238	207	2088
Trichy	1	16	34	385	55	43	478	87	59	489	103	71	438	100	57	417
Erode	4	18	39	765	114	78	638	178	112	694	180	110	687	191	106	701
Salem	5	24	29	865	121	80	738	179	103	732	189	127	810	200	110	798
Total	*12*	*121*	*183*	*3431*	*445*	*404*	*4068*	*649*	*513*	*4701*	*715*	*547*	*4674*	*729*	*480*	*4004*

ET = total number of patients attended the emergency department; N = non– ST-segment elevation myocardial infarction; S = ST-segment elevation myocardial infarction.

January, February, and April 2020 as well as for April 2019 and April 2018. These data were classified as lockdown period (April 2020) and no-lockdown period (January and February 2020 and April 2019 and April 2018). Apart from that, the total number of cases presented to the emergency department of the respective hospitals was collected for the same period. The number of STEMI, NSTEMI, and total (STEMI and NSTEMI) cases treated during the COVID-19 lockdown period (April 2020) was compared with similar cases treated in the no-lockdown period by using the chi-square test. The 95% CI for the difference in proportion was calculated for each. A *P* value less than .05 was considered statistically significant. The statistical analysis was performed using R software version 4.0.0 (The R Foundation). Data for March 2020 were not considered, as they were a mixture for both no-lockdown and lockdown periods.

RESULTS

The median age of patients admitted during the lockdown and no-lockdown periods was 58 and 53 years, respectively. The sex ratio of male and female was 7:2, and there was no significant difference among them. Details of city-wise cases of acute MI and emergency department attendance are given in Table 1. The overall number of STEMI, NSTEMI, and total (STEMI and NSTEMI) cases treated during the COVID-19 lockdown period (April 2020) was compared with similar cases treated during the no-lockdown period of January and February 2020 and April 2019 and April 2018 independently of each. It was observed that cases treated during the COVID-19 lockdown period were significantly ($P<.001$) lower than those treated during the no-lockdown period irrespective of the months. The proportion of cases, *P* value, and 95% CI for the difference in proportion for STEMI, NSTEMI, and total (STEMI and NSTEMI) cases for each city and overall (all cities together) were calculated. The statistical data on acute MI cases treated during the COVID-19 lockdown and no-lockdown periods (city-wise and overall) are given in Table 2. The subanalysis for each city individually for STEMI, NSTEMI, and total cases treated during the COVID-19 lockdown period (April 2020) was significantly ($P<.001$) lower in Madurai, Erode, and Salem than that during the no-lockdown period. For Trichy, a significant reduction ($P<.001$) was noticed for STEMI and total cases during the lockdown period compared with the no-lockdown period whereas for NSTEMI cases the reduction was significant for only April 2020 compared with April 2019 and April 2018. When the NSTEMI data for April 2020 were compared with those for January and February 2020, the *P* value (95% CI) and difference in proportion were 0.153 (0.01 to 0.08) and 0.03 and 1.00 (0.04 to 0.04) and 0.002, respectively. Furthermore, when the statistical analysis was performed with pooled data for all cities for STEMI, NSTEMI, and total, there was a significant reduction in these cases (Table 2). The difference in proportion of acute MI cases treated during the COVID-19 lockdown and no-lockdown periods for each city is depicted in the Figure.

TABLE 2. Statistical Data on Acute Myocardial Infarction Cases Treated During COVID-19 Lockdown and No-Lockdown Periods (City-wise and Overall)

		STEMI				NSTEMI				Total (STEMI and NSTEMI)			
Variable	City name	p1	p2	95% CI	*P* value	p1	p2	95% CI	*P* value	p1	p2	95% CI	*P* value
STEMI (Apr 2020 vs Feb 2020)	Madurai	0.04	0.07	0.01-0.04	.002	0.06	0.09	0.02-0.05	<.001	0.10	0.16	0.04-0.08	<.001
STEMI (Apr 2020 vs Jan 2020)		0.04	0.07	0.01-0.04	<.001	0.06	0.09	0.01-0.05	.001	0.10	0.16	0.04-0.08	<.001
STEMI (Apr 2020 vs Apr 2019)		0.04	0.09	0.03-0.06	<.001	0.06	0.09	0.01-0.05	.001	0.10	0.18	0.05-0.10	<.001
STEMI (Apr 2020 vs Apr 2018)		0.04	0.11	0.05-0.09	<.001	0.06	0.10	0.02-0.06	<.001	0.10	0.21	0.09-0.14	<.001
STEMI (Apr 2020 vs Feb 2020)	Trichy	0.04	0.12	0.04-0.11	<.001	0.09	0.09	0.04-0.04	1.000	0.13	0.21	0.02-0.13	.005
STEMI (Apr 2020 vs Jan 2020)		0.04	0.18	0.09-0.18	<.001	0.09	0.12	0.01-0.08	.153	0.13	0.30	0.11-0.22	<.001
STEMI (Apr 2020 vs Apr 2019)		0.04	0.24	0.15-0.24	<.001	0.09	0.16	0.03-0.12	.002	0.13	0.40	0.21-0.33	<.001
STEMI (Apr 2020 vs Apr 2018)		0.04	0.24	0.15-0.25	<.001	0.09	0.14	0.002-0.09	.041	0.13	0.38	0.19-0.31	<.001
STEMI (Apr 2020 vs Feb 2020)	Erode	0.02	0.18	0.12-0.19	<.001	0.05	0.12	0.04-0.10	<0.001	0.07	0.30	0.18-0.27	<.001
STEMI (Apr 2020 vs Jan 2020)		0.02	0.26	0.20-0.27	<.001	0.05	0.16	0.08-0.14	<.001	0.07	0.42	0.30-0.39	<.001
STEMI (Apr 2020 vs Apr 2019)		0.02	0.26	0.20-0.27	<.001	0.05	0.16	0.08-0.14	<.001	0.07	0.42	0.30-0.39	<.001
STEMI (Apr 2020 vs Apr 2018)		0.02	0.27	0.21-0.28	<.001	0.05	0.15	0.07-0.13	<.001	0.07	0.42	0.31-0.39	<.001
STEMI (Apr 2020 vs Feb 2020)	Salem	0.03	0.16	0.11-0.17	<.001	0.03	0.11	0.05-0.10	<.001	0.06	0.27	0.17-0.25	<.001
STEMI (Apr 2020 vs Jan 2020)		0.03	0.24	0.18-0.25	<.001	0.03	0.14	0.08-0.14	<.001	0.06	0.39	0.28-0.36	<.001
STEMI (Apr 2020 vs Apr 2019)		0.03	0.23	0.17-0.24	<.001	0.03	0.16	0.09-0.15	<.001	0.06	0.39	0.29-0.37	<.001
STEMI (Apr 2020 vs Apr 2018)		0.03	0.25	0.19-0.26	<.001	0.03	0.14	0.08-0.13	<.001	0.06	0.39	0.29-0.37	<.001
STEMI (Apr 2020 vs Feb 2020)	Overall	0.04	0.11	0.06-0.09	<.001	0.05	0.10	0.03-0.06	<.001	0.09	0.21	0.10-0.14	<.001
STEMI (Apr 2020 vs Jan 2020)		0.04	0.14	0.09-0.11	<.001	0.05	0.11	0.04-0.07	<.001	0.09	0.25	0.14-0.17	<.001
STEMI (Apr 2020 vs Apr 2019)		0.04	0.15	0.11-0.13	<.001	0.05	0.12	0.05-0.08	<.001	0.09	0.27	0.17-0.20	<.001
STEMI (Apr 2020 vs Apr 2018)		0.04	0.18	0.13-0.16	<.001	0.05	0.12	0.05-0.08	<.001	0.09	0.30	0.20-0.23	<.001

COVID-19 = coronavirus disease 2019; NSTEMI = non–ST-segment elevation myocardial infarction; Overall = all cities together; p1 = proportion of cases treated during the COVID-19 lockdown period; p2 = proportion of cases treated in the no-lockdown period; STEMI = ST-segment elevation myocardial infarction; CI = confidence interval; Apr = April; Feb = February; Jan = January.

DISCUSSION

Cardiovascular disease is the major cause of mortality and morbidity across the globe. Although the burden of cardiovascular disease has declined in some regions, overall there was no change globally as reported in a multicentric prospective cohort study over the period from 1990 to 2015.[6] Risk factors for cardiovascular disease are already well known. Extreme temperature, change in weather condition, and air pollution have been found to be associated with an increased risk of MI.[7-9] The toxic effect of pollutants has been found to be higher during summer, thereby increasing the risk of cardiopulmonary diseases.[10,11] In Tamil Nadu, this study was conducted in the month of April, which is summer with daytime temperature generally above 30°C and nighttime temperature going down up to 25°C.

During the COVID-19 lockdown period, cases of injuries, infections, illnesses related to behavior, and so on, have reduced in private and government hospitals in the state of Tamil Nadu. In this study, we are limiting to acute MI only. From Table 1, it is clear that the number of cases treated for acute MI was almost consistent during the no-lockdown period of 2020 (January and February) as well as April 2019 and April 2018, whereas it was significantly lower in all the cities during the lockdown period. A similar significant reduction in MI admissions during the lockdown period was noted in recent publications.[1-4] Although the reasons remain unclear, we attribute various factors such as unwillingness to visit hospital owing to fear of COVID-19 infection[4,12]; reduced noise[13] and air pollution,[14,15] reduction in occupational stress in the susceptible population, and avoidance of travel; least or no exposure to tobacco smoke, alcohol, pollution, and junk foods; adherence to relaxation and recreation via audiovisual means, integration with family members, engaging in activities of interest, long hours of

Mayo Clin Proc Inn Qual Out ■ October 2020;4(5):506-510 ■ https://doi.org/10.1016/j.mayocpiqo.2020.06.010
www.mcpiqojournal.org

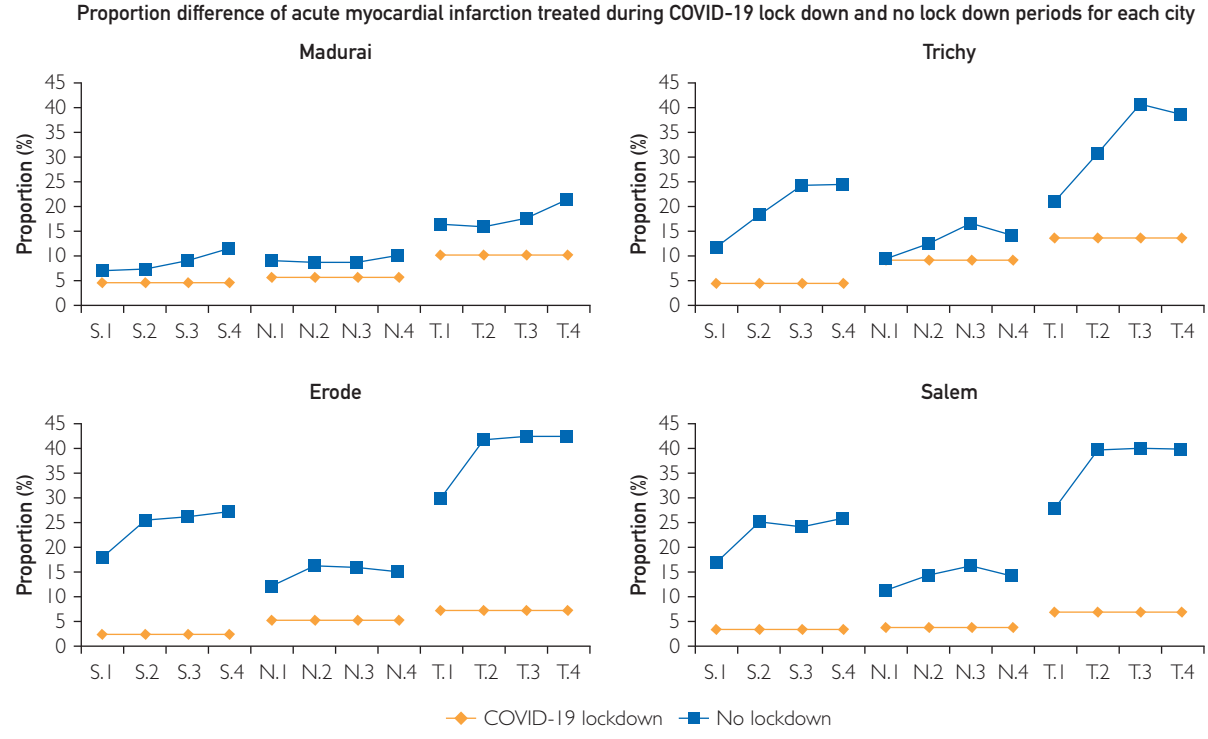

FIGURE. Difference in the proportion of acute myocardial infarction cases treated during the COVID-19 lockdown and no-lockdown periods for each city. The x-axis depicts diagnosis with period, and the y-axis denotes the difference in proportion. 1 = April 2020 vs February 2020; 2 = April 2020 vs January 2020; 3 = April 2020 vs April 2019; 4 = April 2020 vs April 2018; COVID-19 = coronavirus disease 2019; N = non–ST-segment elevation myocardial infarction; S = ST-segment elevation myocardial infarction; T = total (ST-segment elevation myocardial infarction and non–ST-segment elevation myocardial infarction).

sleep, and practicing exercise, yoga, and meditation; limiting to homemade food items, adoption to healthy lifestyle, and overall less physical and mental strain. Moreover, during the lockdown, the pollution index has significantly decreased in India[14] and many other nations,[15] which has a direct relationship with MI.

In summary, the reduction in the number of cases of acute MI during the lockdown period may be due to alterations in modifiable risk factors. Hence, implementation of public education and policies on controlling modifiable risk factors will pay dividends. However, we do not have a city-based registry for acute MI at the moment to state confidently on population-based MI or out-of-hospital deaths due to MI or missed MI due to avoidance of hospital by the public during this COVID-19 pandemic.[1,16] More studies from different cities are warranted to ascertain the changing epidemiology of illnesses during the pandemic and find out the health advantages of containment activities. During World War II, there was a dramatic reduction in mortality from vascular diseases,[17] which suggested a link for the low occurrence of certain diseases in extraordinary situations such as health crisis or war.

It is the time for the physicians to act in concert with clinical equipoise[18] and find out the reasons for the change in the epidemiology of various illnesses during the COVID-19 outbreak in an unprejudiced manner. These new findings likely pave ways for the prevention of illnesses and find out new methods toward the promotion of health. Also, it is mandatory to educate the public to seek medical attention for worrying symptoms and encourage them for adherence to safety precautions for COVID-19.[19] As the fear of

COVID-19 is a major deterrent for emergency visits, hospitals shall develop community-minded communications[12] to provide risk-free and reassuring environment for patients. The limitations of the study are retrospective and confining to a few selected centers located in a few cities.

CONCLUSION

The number of acute myocardial infarction cases was decreased during COVID-19 lockdown in our study population, as noted elsewhere. There are many reasons for the change in occurence including patient's deferral to seek medical attention because of fear of the infection of COVID-19. Hence, mandatory public health education and reassurance are required to prevent mortality from life-threatening illness. In addition, promotion of tele or virtual health consultation is required during such crisis. Also, reduction in the environmental risk factors may be a reason for the reduced occurence of MI and hence, policies on the environmental health are regulated and monitored periodically.

ACKNOWLEDGMENTS

Drs Jena, Vadivelu, Ayyasamy, and Chandrasekaran have equal contribution/authorship status.

Abbreviations and Acronyms: **COVID-19** = coronavirus disease 2019; **MI** = myocardial infarction; **NSTEMI** = non–ST-segment elevation myocardial infarction; **STEMI** = ST-segment elevation myocardial infarction

Affiliations (Continued from the first page of this article.): Research Institute, Madurai, Tamil Nadu, India (affiliated to The Tamil Nadu Dr. M.G.R. Medical University, Chennai) (R.V.); Apollo Specialty Hospitals, Tiruchirappalli, Tamil Nadu, India (S.A.); and Sri Gokulam Specialty Hospitals, Salem, Tamil Nadu, India (V.P.C.).

Potential Competing Interests: The authors report no competing interests.

Correspondence: Address to Ramachandran Meenakshisundaram, MBBS, MRCP, PhD, PGCert in HBE, FHEA, 47 Hurrell Dr, Harrow HA2 6DY, UK (rmsundarchandran@gmail.com; Twitter: @rmsundarchandra).

ORCID

Ramachandran Meenakshisundaram: https://orcid.org/0000-0002-1281-3346; Melvin Joy: https://orcid.org/0000-0001-9323-994X; Ramalingam Vadivelu: https://orcid.org/0000-0002-7195-3648

REFERENCES

1. De Filippo O, D'Ascenzo F, Angelini F, et al. Reduced rate of hospital admissions for ACS during Covid-19 outbreak in Northern Italy. *N Engl J Med*. 2020;383(1):88-89.
2. Garcia S, Albaghdadi MS, Meraj PM, et al. Reduction in ST-segment elevation cardiac catheterization laboratory activations in the United States during COVID-19 pandemic. *J Am Coll Cardiol*. 2020;75(22):2871-2872.
3. Rodríguez-Leor O, Cid-Álvarez B, Ojeda S, et al. Impacto de la pandemia de COVID-19 sobre la actividad asistencial en cardiología intervencionista en España. *REC Interv Cardiol*. 2020;2:82-89.
4. Rangé G, Hakim R, Motreff P. Where have the ST-segment elevation myocardial infarctions gone during COVID-19 lockdown? *Eur Hear J Qual Care Clin Outcomes*. 2020;6(3):223-224.
5. The Lancet. India under COVID-19 lockdown. *Lancet*. 2020;395(10233):1315.
6. Roth GA, Johnson C, Abajobir A, et al. Global, regional, and national burden of cardiovascular diseases for 10 causes, 1990 to 2015. *J Am Coll Cardiol*. 2017;70(1):1-25.
7. Guo S, Niu Y, Cheng Y, et al. Association between ambient temperature and daily emergency hospitalizations for acute coronary syndrome in Yancheng, China. *Environ Sci Pollut Res Int*. 2020;27(4):3885-3891.
8. Sharif Nia H, Chan YH, Froelicher ES, et al. Weather fluctuations: predictive factors in the prevalence of acute coronary syndrome. *Heal Promot Perspect*. 2019;9(2):123-130.
9. Kuźma Ł, Pogorzelski S, Struniawski K, Dobrzycki S, Bachórzewska-Gajewska H. Evaluation of the influence of air pollution on the number of hospital admissions for acute coronary syndrome in elderly patients. *Pol Arch Intern Med*. 2019;130(1):38-46.
10. Guarnieri M, Balmes JR. Outdoor air pollution and asthma. *Lancet*. 2014;383(9928):1581-1592.
11. Loughnan ME, Nicholls N, Tapper NJ. The effects of summer temperature, age and socioeconomic circumstance on acute myocardial infarction admissions in Melbourne, Australia. *Int J Health Geogr*. 2010;9:41.
12. Wong LE, Hawkins JE, Langness S, Murrell KL, Iris P, Sammann A. Where are all the patients? Addressing Covid-19 fear to encourage sick patients to seek emergency care [published online ahead of print May 14, 2020]. *NEJM Catal*. https://doi.org/10.1056/CAT.20.0193.
13. Münzel T, Schmidt FP, Steven S, Herzog J, Daiber A, Sørensen M. Environmental noise and the cardiovascular system. *J Am Coll Cardiol*. 2018;71(6):688-697.
14. NASA. European Space Agency data show drop in air pollution in india during COVID-19 lockdown. Firstpost website. https://www.firstpost.com/tech/science/nasa-european-space-agency-data-show-drop-in-air-pollution-in-india-during-covid-19-lockdown-8304391.html. Accessed May 8, 2020.
15. Muhammad S, Long X, Salman M. COVID-19 pandemic and environmental pollution: a blessing in disguise? *Sci Total Environ*. 2020;728:138820.
16. Baldi E, Sechi GM, Mare C, et al. Out-of-hospital cardiac arrest during the Covid-19 outbreak in Italy. *N Engl J Med*. 2020;383(5):496-498.
17. Strøm A, Jensen RA. Mortality from circulatory diseases in Norway. *Lancet*. 1951;257(6653):528.
18. Zagury-Orly I, Schwartzstein RM. Covid-19—a reminder to reason. *N Engl J Med*. 2020;383(3):e12.
19. Finset A, Bosworth H, Butow P, et al. Effective health communication—a key factor in fighting the COVID-19 pandemic. *Patient Educ Couns*. 2020;103(5):873-876.

Indian Pacing and Electrophysiology Journal 20 (2020) 237–242

Contents lists available at ScienceDirect

Indian Pacing and Electrophysiology Journal

journal homepage: www.elsevier.com/locate/IPEJ

Practice Guidelines

Acute hemodynamics of cardiac sympathetic denervation

Kunal Sinkar, Avishek Bagchi*, Ankit Mahajan, Ramalingam Vadivelu, Meera Venkatraman, Reshma Motwani, Sanjeev Vichare, Suresh Joshi, Dinesh Parikh, Jude Vaz, Yash Lokhandwala

Holy Family Hospital, Bandra West, Mumbai, 400050, India

ARTICLE INFO

Article history:
Received 18 April 2020
Received in revised form
2 June 2020
Accepted 11 June 2020
Available online 14 June 2020

Keywords:
ventricular tachycardia
Sympathectomy
Blood pressure

ABSTRACT

Introduction: We aimed to study the immediate hemodynamic effects of thoracoscopic bilateral cardiac sympathetic denervation (CSD) for recurrent ventricular tachycardia (VT) or VT storm.
Method: We studied a group of 18 adults who underwent bilateral thoracoscopic CSD; the blood pressure (BP) and Heart Rate (HR) were continuously monitored during the surgery and up to 6 h post-operatively.
Results: Immediately on removal of the sympathetic ganglia, the patients had a drop in both the systolic (110 mm Hg to 95.8 mm Hg, $p < 0.001$) and diastolic BP (69.4 mm Hg to65 mm Hg, $p = 0.007$) along with a drop in the HR (81.6 bpm to 61.2 bpm, $p < 0.001$).At 6 h after CSD, the systolic and diastolic BP did not recover significantly, while there was recovery in HR (61.2 bpm to 66 bpm, $p = 0.02$). There was no significant difference between those with and without left ventricular (LV) systolic dysfunction.
Conclusion: The acute hemodynamic changes during the perioperative period of CSD are significant but not serious. Awareness of this is useful for peri-operative management.

1. Introduction

The treatment of ventricular arrhythmias has been rapidly evolving over the past few decades. Starting with antiarrhythmic drugs, followed by defibrillation and implantable cardioverter-defibrillators (ICDs) and subsequent development of two dimensional and three-dimensional cardiac mapping and ablations, one can trace the encouraging journey we have had in the management of these complex patients.

A recent addition to the armamentarium against ventricular arrhythmias is thoracoscopic cardiac sympathetic denervation (CSD). Though CSD had traditionally been used as a treatment for refractory angina with good results [1–3], its antiarrhythmic potential has been explored only over the last few years. Beginning with a few isolated case reports [4,5], we now have several studies making a case to consider CSD for resistant ventricular arrhythmias [6–15].

Bilateral CSD from T1-T4 ganglia abolishes most of the sympathetic inputs to the heart. Since it compares with acute high dose complete beta blockade, there is a theoretical possibility of acute drop in blood preesure (BP) and heart rate (HR). These acute hemodynamic effects of bilateral CSD have been documented in few isolated case reports [16], but no substantial study has yet looked specifically for this effect in the intra-operative and immediate post-operative periods. This particular hemodynamic effect, though of smaller magnitude, has been observed in earlier studies where thoracic sympathectomy was performed for palmar hyperhidrosis and facial blushing [17–26]. This might have been mainly due to the fact that the stellate ganglion was not resected in these cases.

We aimed to study the acute hemodynamic effects of thoracoscopic bilateral CSD in a group of patients with recurrent refractory ventricular arrhythmias. We expected that the observations would help future perioperative management.

2. Method

All consecutive adult patients taken for CSD in Holy Family Hospital for recurrent ventricular tachycardia (VT) or VT storm between the time period of November 2018 to December 2019 were included in this study. VT storm was defined as ≥3 episodes of sustained VT, ventricular fibrillation (VF), or appropriate shocks from an ICD within 24 h [27]. Patients were taken up for CSD if they had pleomorphic VT (monomorphic VTs of different morphologies)

* Corresponding author.
E-mail address: avi25986@gmail.com (A. Bagchi).
Peer review under responsibility of Indian Heart Rhythm Society.

https://doi.org/10.1016/j.ipej.2020.06.006

Table 1
Baseline characteristics (n = 18).

Characteristics			Percent
Age (years ± SD)		48.67 ± 15.51	…. .
Gender	Male	15	83.3
	Female	3	16.7
Hypertension	Yes	3	16.7
	No	15	83.3
Diabetes	Yes	3	16.7
	No	15	83.3
Hyperlipidemia	Yes	2	11.1
	No	16	88.9
Primary Diagnosis	Old MI	6	33.3
	DCMP	5	27.8
	CPVT	1	5.6
	Myocarditis	2	11.1
	Sarcoidosis	1	5.6
	HCM	1	5.6
	ARVC	1	5.6
	Muscular dystrophy	1	5.6
Left ventricular ejection fraction (LVEF)	Mild dysfunction (LVEF 0.45–0.54)	1	5.6
	Moderate dysfunction (LVEF 0.3–0.44)	6	33.3
	Severe dysfunction (LVEF < 0.3)	11	61.1
NYHA (New York Heart Association) Class	I	3	16.7
	II	6	333
	III	6	33.3
	IV	3	16.7
Ventricular Tachycardia (VT) Morphologies	1	1	5.6
	2	2	11.1
	≥3	15	83.3

(MI : Myocardial Infarction; DCMP: Dilated cardiomyopathy; CPVT : catecholaminergic polymorhic VT;HCM: Hypertrophic Cardiomyopathy; ARVC: Arrhythmogenic right ventricular dysplasia)

or if they had at least one failed attempt or recurrence after at least one attempt of radiofrequency ablation for monomorphic VT.

Old myocardial infarction (MI), dilated cardiomyopathy (DCMP), catecholaminergic polymorphic ventricular tachycardia (CPVT), sarcoidosis, old myocarditis, hypertrophic cardiomyopathy (HCM), muscular dystrophy and arrhythmogenic right ventricular cardiomyopathy (ARVC) were the underlying substrates.

All patients underwent video assisted thoracoscopic surgery (VATS) guided bilateral upper thoracic sympathectomy. All procedures were performed under general anaesthesia. In patients with ICDs, therapies were turned off and the lower rate was set at 40/min. Three 1.5 cm incisions were made on each side at a time: fourth intercostal space in the mid-axillary line, second intercostal space in the mid-clavicular line and 2 cm further laterally. The sympathetic chain behind the parietal pleura was identified and the lower one-half to one-third of the stellate ganglion, as well as the thoracic ganglia at T2 to T4, were cauterized and excised. Specimens were sent for histological confirmation. After CSD, the presence of ganglionic tissue was confirmed by pathologist in all cases, using routine histopathology sections with H and E stain.

All the patients had arterial line put in one radial artery before the surgery and blood pressure and heart rate measured and noted invasively prior to shifting to the operation theatre. During the surgery, BP and HR were continuously monitored and the lowest values noted after removal of the ganglia intra-operatively were considered for analysis. After 6 h, intraarterial BP and HR were again noted and considered for analysis.

3. Statistics

Continuous variables were assessed as means with standard deviations (SDs) and categorical variables as percentages. Systolic BP (SBP), diastolic BP (DBP) and HR were compared both between preoperative state and intra-operative state and between intra-operative state and post-operative state by means of multiple paired t-tests. To compare the acute changes in BP and HR across various groups based on presence or absence of severe left ventricular (LV) dysfunction, we used independent student's t-test. The significance level adopted in the statistical analyses was 0.05. All statistical analyses were performed with the SPSS software, version 23.0(SPSS Inc. Chicago, IL, USA).

4. Results

The study involved a group of 18 patients. Patient data are summarized in Table 1. The age varied from 21 year to 78 years with a mean of 48.7 ± 15.5 years. The baseline parameters are described in Table 1. The group was very heterogenous as regards the underlying substrate, with old myocardial infarction, dilated cardiomyopathy and myocarditis being the major categories.

As regards the VT characteristics, most (17/18, 94%) patients had

Table 2
Treatment modalities used prior to surgery (n = 18).

Characteristics		N	%
Anti-Arrhythmics	Amiodarone	1	5.6
	Beta-blockers	1	5.6
	Amiodarone and beta-blockers	8	44.4
	Amiodarone, phenytoin and beta blockers	4	22.2
	Amiodarone, beta blockers and mexiletine	1	5.6
	Amiodarone and sotalol	1	5.6
	Amiodarone, sotalol and phenytoin	1	5.6
	Sotalol and phenytoin	1	5.6
ICD	No ICD	2	11.1
	Single chamber ICD	11	61.1
	Dual chamber ICD	5	27.8
VT Ablations	0	13	72.2
	1	4	22.2
	2	1	5.6
Revascularization	None	15	83.3
	Old Angioplasty	1	5.6
	Old Bypass Surgery	2	11.1

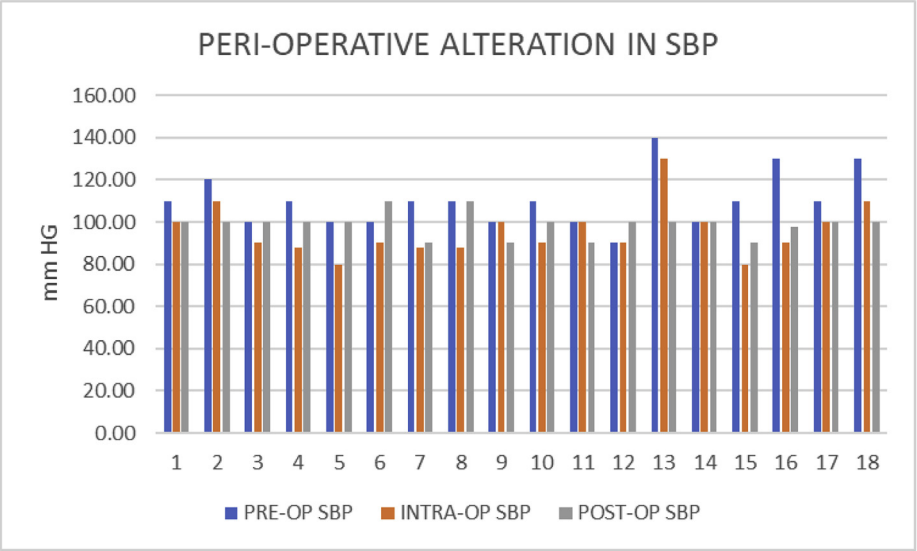

Fig. 1. Peri-operative alteration of SBP(n = 18).

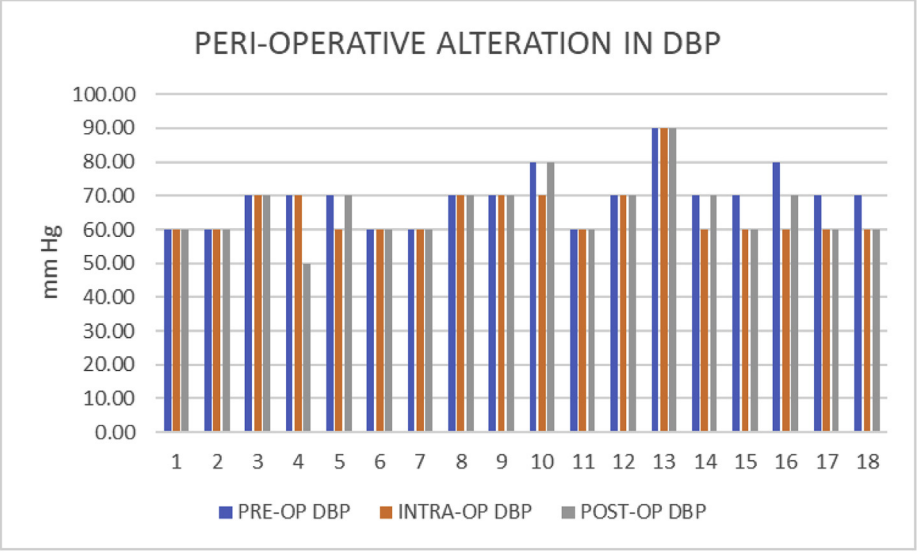

Fig. 2. Peri-operative alteration of DBP (n = 18).

pleomorphic VTs. Also, they were on maximum tolerated dosage of anti-arrhythmic drugs, with 16/18 (88.9) % of patients on two or more drugs. Furthermore, 16/18 (88.9%) of patients had ICDs and were receiving appropriate therapies. A few (5/18) patients had undergone radiofrequency (RF) ablation. The details of the anti-arrhythmic drugs and therapies are shown in Table 2. The patients with LV dysfunction were on optimal guideline directed medical therapy including beta blockers, angiotensin converting enzyme inhibitors or angiotensin receptor blockers, diuretics and spironolactone; these therapies were continued perioperatively withlast dose being given 8 h prior tothe surgery.

The patients had significant hemodynamic alterations in the intra-operative period (Figs. 1–3). Immediately on removal of the ganglia, the patients had a significant drop in both the systolic BP and diastolic BP along with a significant drop in the HR (shown in Table 3). No patient needed pacing. Patients mostly had sinus bradycardia, with some patients having intermittent junctional rhythm initially after removing the stellate ganglia which subsequently recovered to sinus rhythm in all cases.

We did not find significant difference in acute BP and HR responses intra-operatively between patients with and without severe LV dysfunction (LV Ejection Fraction <0.3 and ≥ 0.3 respectively) as displayed in Table 4.

When the post-operative hemodynamic parameters were compared with those intra-operatively, we found that there was increase in the HR but no significant increase in the systolic BP or diastolic BP (Table 5).

5. Discussion

This study had two objectives: i) To see the BP and HR changes, for which BP and heart rate (HR) were continuously monitored, and the lowest values noted after removal of the ganglia intra-operatively were considered for analysis. ii) From a management

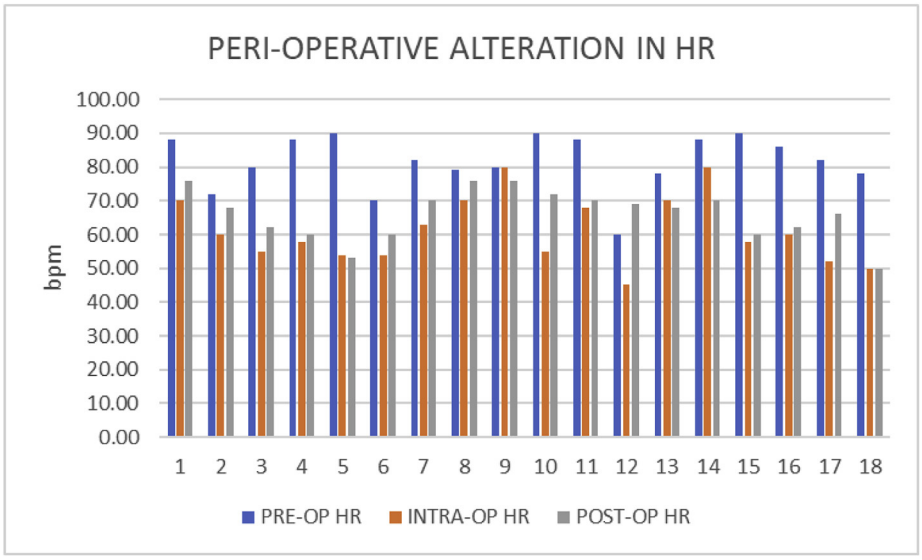

Fig. 3. Peri-operative alteration of HR (n = 18).

Table 3
Intra-operative hemodynamic alterations (n = 18).

Parameter	Time	Values	p Value (paired *t*-test)
Systolic BP (mm Hg)	Pre-operative	110 ± 12.8	<0.001
	Intra-operative	95.8 ± 12.2	
Diastolic BP (mm Hg)	Pre-operative	69.4 ± 8	0.007
	Intra-operative	65 ± 7.9	
HR (bpm)	Pre-operative	81.2 ± 8.1	<0.001
	Intra-operative	61.2 ± 9.9	

Table 4
Intra-operative hemodynamic alteration according to LVEF (n = 18).

	LVEF	n	Mean ± SD	p value (*t*-test)
Pre-operative systolic BP	<0.3	11	105.5 ± 8.2	0.06
	≥0.3	7	117.1 ± 16	
Drop in systolic BP	<0.3	11	11.5 ± 9	0.25
	≥0.3	7	18.6 ± 13.5	
Pre-operative Diastolic BP	<0.3	11	67.3 ± 4.7	0.25
	≥0.3	7	72.9 ± 11.1	
Drop in Diastolic BP	<0.3	11	2.7 ± 4.7	0.20
	≥0.3	7	7.1 ± 7.6	
Pre-operative HR	<0.3	11	80.8 ± 8.7	0.61
	≥0.3	7	82.9 ± 7.6	
Drop in HR	<0.3	11	18.4 ± 11	0.30
	≥0.3	7	23.6 ± 9.5	

perspective, in our initial CSD procedures we sometimes had sudden drop in HR and BP and the surgical team would be taken unawares. CSD is undertaken by very few centres even now. Hence, in this study we mentioned the lowest values to help guide other emerging groups performing CSD about the problems that can occur.

In our study, the patients were predominantly middle-aged and there was a marked (15/18) male preponderance. The substrates were heterogeneous and except for 1 patient with CPVT, all had structural heart disease. They were refractory to several modalities of treatment, with most having been tried on at least a combination 2 anti-arrhythmic drugs. Only 1 patient had a single VT morphology, while of the remaining 17 patients, 15 had at least 3 different VTs. A clear underlying infarct scar was present in only 6 patients. Thus, it was not surprising that only 5 patients had undergone RF ablation attempts prior to CSD.

The cardiac autonomic nervous system (NS) has both sympathetic and parasympathetic arms. The sympathetic cardiac NS comprises of the brain stem, the spinal cord, the dorsal root ganglia, the paravertebral sympathetic ganglia and the mediastinal cardiac plexus. Sympathetic preganglionic neurons destined for heart have their cell-bodies in the intermediolateral column of spinal cord and they synapse with the postganglionic neurons located in the lower cervical and upper thoracic paravertebral ganglia. The lowest cervical ganglion (C8) and the highest thoracic ganglion (T1) are generally fused bilaterally to constitute the left and the right stellate ganglia. The stellate ganglia convey a large amount of cardiac sympathetic postganglionic fibres. The remaining are provided by T2-4 paravertebral ganglia [26].These ganglia receive inputs from multiple spinal levels, process those and finally deliver output to the heart via the post-ganglionic neurons. Nor-epinephrine is the final neurotransmitter of these post-ganglionic neurons. The cardiac feedback to the autonomic NS is carried via these post-ganglionic neurons to the spinal cord and brainstem [28].This sympathetic NS is concerned with the so called “fight or flight” response and is the main target for treating tachyarrhythmias.

The parasympathetic NS of the heart mainly comprises of the vagal nerves. The preganglionic cell bodies are located in the medullaoblongatawhile the postganglionic cell bodies are located in the inferior ganglia of the vagus nerves, the cardiac plexus at the base of the heart, around the aorta in front of the tracheal bifurcation and in the atrial walls [29]. The parasympathetic NS is not responsible for tachyarrhythmias.

The cardiac sympathetic NS plays a key role in ventricular arrhythmias and is a potential target for treatment of resistant arrhythmias. The mechanism behind the benefit of CSD is likely related to disruption of both afferent as well as efferent sympathetic fibres [30–34]. However, sudden CSD is supposed to have extensive effects on multiple components of the cardiovascular system. Kingma et al. [19] studied the hemodynamic response on removal of the upper thoracic ganglia for the treatment of palmar hyperhidrosis. They showed a drop in mean HR in sitting position and a decrease in total peripheral resistance and BP in both sitting and standing positions. However, this study compared the pre-operative readings with those at four weeks after the surgery. Similar response has been documented by Papa et al. [17], who

Table 5
Comparison of intra-operative and post-operative (at 6 h) hemodynamic parameters (n = 18).

Parameter	Time	Values	p Value (paired *t*-test)
Systolic BP (mm Hg)	Intra-operative	95.8 ± 12.2	0.354
	Post-operative	98.8 ± 5.8	
Diastolic BP (mm Hg)	Intra-operative	65 ± 7.9	0.495
	Post-operative	66.1 ± 9.2	
HR (bpm)	Intra-operative	61.2 ± 9.9	0.020
	Post-operative	66 ± 7.5	

found an acute drop in HR immediately after sectioning of T2 and T3 ganglia of either side in a group of 10 patients. In a patient population of 29 patients they have demonstrated a significant drop in systolic BP, diastolic BP and HR both at rest and on exercise after a period of one month after the surgery. There are also a few older animal and human studies analysing the hemodynamic response of unilateral and bilateral upper thoracic sympathetic denervation [32–37]. They demonstrated that right and left thoracic sympathetic denervation may produce opposite effects on cardiac arrhythmias in experimental animals and in humans, with left sided sympathectomy producing more drop in BP, shortening of QTc and decrease in HR. However, none of these studies had removal of the stellate ganglion done and hence they were incomplete CSD. Song et al. [38] have shown no significant effect on heart rate or blood pressure immediately on bilateral stellate ganglia block; in fact, a subgroup of their patients has shown vagal blockade and increase in heart rate and blood pressure acutely. However, their study was a study of percutaneous stellate ganglia block with lignocaine and there is no study available till date looking at the immediate hemodynamic response of the surgical complete bilateral CSD.

In our 'learning curve' of CSD (prior to this study), there were instances of sudden marked drop in heart rate and BP, needing chronotropic drugs/increase in pacing rate and inotropes/vasopressors. However, now our anaesthesiologists and surgeons have learnt to anticipate and avoid these situations. In the present study, there was a significant acute hemodynamic alteration across the study population. Mostly patients were in sinus bradycardia, with few minutes of junctional rhythm seen intermittently. These acute hemodynamic changes were similar in patients with and without LV dysfunction. This finding is interesting and needs to be further evaluated in a large group of patients.

Subsequently, systolic and diastolic BP gradually started to increase, but did not show significant change in the immediate post-op period. However, the HR showed significant recovery in the immediate post-op period. Overall, our study adds to the currently available literature on CSD. It helps care givers to anticipate and deal with such issues during the peri-operative period.

6. Conclusion

Ours is the first study specifically aimed at assessing immediate and early post-operative hemodynamic response of bilateral complete CSD. We validated each sympathectomy with histopathology. Immediately after CSD, there was a drop in systolic BP, diastolic BP and HR. At 6 h after CSD, there was some recovery in HR. There was no significant difference between those with and without LV systolic dysfunction.

Declaration of competing interest

None.

References

[1] François-Franck C. Signification physiologique de la resection du sympathetique dans la maladie de Basedow, l'epilepsie, l'idiotie et de glaucome. Bull Acad Med 1899;41:565.
[2] Jonnesco T. Traitement chirurgical de l'angine de poitrine par la résection du sympathique cervico-thoracique. Presse Med 1921;20:221–30.
[3] Leriche R, Fontaine R. The surgical treatment of angina pectoris: what it is and what it should be. Am Heart J 1928;3:649–71.
[4] Estes Jr EH, Izlar Jr HL. Recurrent ventricular tachycardia. A case successfully treated by bilateral cardiac sympathectomy. Am J Med 1961;31:493–7.
[5] Zipes DP, Festoff B, Schaal SF, Cox C, Sealy WC, Wallace AG. Treatment of ventricular arrhythmia by permanent atrial pacemaker and cardiac sympathectomy. Ann Intern Med 1968;68:591–7.
[6] Schwartz PJ, Priori SG, Cerrone M, et al. Left cardiac sympathetic denervation in the management of high-risk patients affected by the long QT syndrome. Circulation 2004;109:1826–33.
[7] Wilde AAM, Bhuiyan ZA, Crotti L, et al. Left cardiac sympathetic denervation for catecholaminergic polymorphic ventricular tachycardia. N Engl J Med 2008;358:2024–9.
[8] Ajijola AO, Vaseghi M, Mahajan A, Shivkumar K. Bilateral cardiac sympathetic denervation: why, who and when. Expert Rev Cardiovasc Ther 2012;10(8):947–9.
[9] Hofferberth SC, Cecchin F, Loberman D, Fynn-Thompson F. Left thoracoscopic sympathectomy for cardiac denervation in patients with life-threatening ventricular arrhythmias. J Thorac Cardiovasc Surg 2014;147(1):404–11.
[10] Te Riele AS, Ajijola OA, Shivkumar K, Tandri H. Role of bilateral sympathectomy in the treatment of refractory ventricular arrhythmias in arrhythmogenic right ventricular dysplasia/cardiomyopathy. Circ Arrhythm Electrophysiol 2016;9(4):e003713.
[11] Cho Y. Left cardiac sympathetic denervation: an important treatment option for patients with hereditary ventricular arrhythmias. J Arrhythmia 2016;32(5):340–3.
[12] Vaseghi M, Gima J, Kanaan C, Ajijola OA, Marmureanu A, Mahajan A, Shivkumar K. Cardiac sympathetic denervation in patients with refractory ventricular arrhythmias or electrical storm: intermediate and long-term follow-up. Heart Rhythm 2014;11(3):360–6.
[13] Vaseghi M, Barwad P, Corrales FJ, Tandri H, Mathuria N, Shah R, Sorg JM, Gima J, Mandal K, Morales LC, Lokhandwala Y. Cardiac sympathetic denervation for refractory ventricular arrhythmias. J Am Coll Cardiol 2017;69(25):3070–80.
[14] Richardson T, Lugo R, Saavedra P, Crossley G, Clair W, Shen S, Estrada JC, Montgomery J, Shoemaker MB, Ellis C, Michaud GF. Cardiac sympathectomy for the management of ventricular arrhythmias refractory to catheter ablation. Heart Rhythm 2018;15(1):56–62.
[15] Téllez LJ, Garzón JC, Vinck EE, Castellanos JD. Video-assisted thoracoscopic cardiac denervation of refractory ventricular arrhythmias and electrical storms: a single-center series. J Cardiothorac Surg 2019;14:17.
[16] Lee LS, Lin CC, Ng SM, Au CF. The haemodynamic effect of thoracoscopic cardiac sympathectomy. Eur J Surg Suppl 1998;(580):37–8.
[17] Papa MZ, Bass A, Schneiderman J, Drori Y, Tucker E, Adar R. Cardiovascular changes after bilateral upper dorsal sympathectomy. Short- and long-term effects. Ann Surg 1986;204(6):715–8.
[18] Drott C, Claes G, Göthberg G, Paszkowski P. Cardiac effects of endoscopic electrocautery of the upper thoracic sympathetic chain. Eur J Surg 1994;160:65–70.
[19] Kingma R, TenVoorde BJ, Scheffer GJ, Karemaker JM, Mackaay AJ, Wesseling KH, de Lange JJ. Thoracic sympathectomy: effects on hemodynamics and baroreflex control. Clin Auton Res 2002 Feb;12(1):35–42.
[20] Schwartz PJ. The rationale and role of left stellectomy for the prevention of malignant arrhythmias. Ann NY Acad Sci 1984;427:199–221.
[21] Malliani A, Schwartz PJ, Zanchetti A. Neural mechanisms in life threatening arrhythmias. Am Heart J 1980;100:705–15.
[22] Schwartz PJ, Stone HL. Effects of unilateral stellectomy upon cardiac performance during exercise in dogs. Canc Res 1979;44:637–45.
[23] Austoni P, Rosati R, Gregorini L, et al. Effects of stellectomy on exercise-induced Q-T changes in man. Circulation 1977;56(suppl III):184.
[24] Austoni P, Rosati R, Gregorini L, et al. Stellectomy and exercise in man. Am J Cardiol 1979;43:399.
[25] Schwartz PJ, Stone HL, Brown AM. Effects of unilateral stellate ganglion blockade on the arrhythmias associated with coronary occlusion. Am Heart J 1976;92:589–99.
[26] Dusi V, De Ferrari GM, Pugliese L, Schwartz PJ. Cardiac sympathetic denervation in channelopathies. Front Cardiovasc Med 2019;6:27.
[27] Al-Khatib SM, Stevenson WG, Ackerman MJ, et al. AHA/ACC/HRS guideline for management of patients with ventricular arrhythmias and the prevention of sudden cardiac death: executive summary: a report of the American college of cardiology/American heart association task force on clinical practice guidelines and the heart rhythm society. Heart Rhythm 2017;15(10):e190–252. 2018 Oct.
[28] Kapa S, DeSimone CV, Asirvatham SJ. Innervation of the heart: an invisible grid within a black box. Trends Cardiovasc Med 2016 Apr;26(3):245–57.
[29] Battipaglia I, Lanza GA. The autonomic nervous system of the heart. In: Slart R, Tio R, Elsinga P, Schwaiger M, editors. Autonomic innervation of the heart.

Berlin, Heidelberg: Springer; 2015.
[30] Irie T, Yamakawa K, Hamon D, Nakamura K, Shivkumar K, Vaseghi M. Cardiac sympathetic innervation via the middle cervical and stellate ganglia and anti-arrhythmic mechanism of bilateral stellectomy. Am J Physiol Heart Circ Physiol 2017;312:H392–405.
[31] Khalsa SS, Shahabi L, Ajijola OA, Bystritsky A, Naliboff BD, Shivkumar K. Synergistic application of cardiac sympathetic decentralization and comprehensive psychiatric treatment in the management of anxiety and electrical storm. Front Integr Neurosci 2014;7:98.
[32] Malliani A, Lombardi F, Pagani M, Recordati G, Schwartz PJ. Spinal sympathetic reflexes in the cat and the pathogenesis of arterial hypertension. Clin Sci Mol Med Suppl 1975;2. 259s–60s.
[33] Malliani A, Recordati G, Schwartz PJ. Nervous activity of afferent cardiac sympathetic fibres with atrial and ventricular endings. J Physiol 1973;229:457–69.
[34] Schwartz PJ, Foreman RD, Stone HL, Brown AM. Effect of dorsal root section on the arrhythmias associated with coronary occlusion. Am J Physiol 1976;231:923–8.
[35] Masood SA, Kazmouz S, Heydemann P, Li H, Kenny D. Under-recognition of low blood pressure readings in patients with duchenne muscular dystrophy. Pediatr Cardiol 2015;36(7):1489–94.
[36] Marui Fabiane RRH, Bianco HT, Bombig MTN, et al. Behavior of blood pressure variables in children and adolescents with duchenne muscular dystrophy. Arq Bras Cardiol 2018 June;110(6):551–7.
[37] Johnson JN, Harris KM, Moir C, et al. Left cardiac sympathetic denervation in a pediatric patient with hypertrophic cardiomyopathy and recurrent ventricular fibrillation. Heart Rhythm 2011 Oct;8(10):1591–4.
[38] Song JG, Hwang GS, Lee EH, et al. Effects of bilateral stellate ganglion block on autonomic cardiovascular regulation. Circ J 2009;73(10):1909-13.

Title Page

Narrow QRS tachycardia with atrial and ventricular cycle length wobbling – What is the mechanism?

Author Details

Corresponding Author:

1. Dr. Shunmuga Sundaram Ponnusamy MD., DM., PDF (EP)., CEPS

   Assistant Professor, Department of Cardiology

   Velammal Medical college hospital and research institute

   Madurai, Tamilnadu, India

Additional Authors:

2. Dr. Vidhya Ganesan MBBS., MD.,

   Associate professor, Department of Microbiology

   Velammal Medical College hospital and research institute

   Madurai, Tamilnadu, India

Address for correspondence

Dr P. Shunmuga Sundaram MD., DM., PDF (EP)., CEPS

Assistant Professor, Department of Cardiology

Velammal Village, Airport ring road

Velammal Medical college hospital and research institute

Madurai – 625009

Mobile no: +919444712846

Email id: shunmuga.pgi@gmail.com

This article has been accepted for publication and undergone full peer review but has not been through the copyediting, typesetting, pagination and proofreading process, which may lead to differences between this version and the Version of Record. Please cite this article as doi: 10.1111/pace.13994.

Word Counts: 1164 words

Short title: An irregular narrow QRS tachycardia

Keywords: Narrow QRS tachycardia, Ablation, His bundle electrogram

Financial Source

No funding or financial sources received for this study

We have no conflicts of interest to disclose.

Narrow QRS tachycardia with atrial and ventricular cycle length wobbling – What is the mechanism?

Case Presentation

A 41 years old lady presented to us with drug refractory narrow QRS tachycardia. Echocardiography revealed normal left ventricular systolic function. 12 lead electrocardiography (ECG) showed long RP (RP>PR) narrow QRS tachycardia. Radiofrequency catheter ablation was performed after obtaining informed consent. Intracardiac electrograms and 12 lead ECG were continuously monitored using Workmate Claris system (Abbott, Plymouth, MN). Upper limb Venous angiography showed dilated coronary sinus with left sided superior vena cava. Basal AH and HV intervals were 85ms and 44ms respectively. Patient had spontaneously inducible tachycardia (Fig 1B) which could be terminated by intravenous adenosine. ECG showed narrow QRS tachycardia with variation in both atrial and ventricular cycle length (Fig 1A). Intracardiac electrogram during tachycardia showed variation in H-H, A-A, V-V and HA intervals (Fig 2)

1. What is the mechanism of the tachycardia onset?
2. What is the substrate for re-entry?

3. What could be the reason for the variation in A-A, H-H, H-A and V-V intervals?

Discussion:

12 lead ECG showed narrow QRS tachycardia with retrograde VA wenckebaching ruling out atrium as a part of the circuit. Variation in both A-A and V-V intervals were noted though the atrial activation pattern remained the same (Fig 1B and Fig 2A). As we could rule out atrium as a part of the circuit, atrial tachycardia (AT) and AV-reciprocating tachycardia were excluded. Intracardiac electrogram showed an interesting phenomenon during tachycardia initiation (Fig 1B). The second sinus atrial impulse produced two QRS complexes followed by continuation of tachycardia. This would confirm the presence of dual AV node physiology (1:2 AV response) with antegrade fast pathway (FP) conduction producing the first QRS and antegrade slow pathway (S1) producing the second QRS. Since the next VA interval was long the retrograde limb of the circuit must be another slow pathway (S2) as S1 could not be immediately activated retrogradely, confirming the involvement of multiple slow pathways in the tachycardia circuit. A tachycardia initiated by 1:2 AV response with retrograde long VA interval would require two different slow pathways (initial antegrade activation of FP and S1 during 1:2 response followed by retrograde S2 activation to produce long VA interval). Other important features to be considered in making the diagnosis were response to adenosine, concentric fixed atrial activation pattern in spite of the varying A-A interval (fig 2A) and fixed HV interval (44ms) during tachycardia. All these features would favor a diagnosis of atypical slow-slow AV nodal re-entrant tachycardia (AVNRT) in this case.

The possibility of automatic junctional tachycardia was excluded based on response to premature atrial extra-stimuli and intravenous adenosine. Intracardiac electrogram showed variation in A-A, V-V, H-H and HA intervals. Atypical AVNRT of slow – slow type with decremental conduction of upper common pathway (UCP) could explain the variation in A-A and H-A intervals (Fig 3A, B and C). The H-H and V-V interval variations could be due to decremental conduction in the

same slow pathway, lower common pathway or presence of multiple antegrade pathways. We propose a probable circuit with the presence of multiple slow pathways as below

(a) Three slow pathways with different electrophysiological properties
(b) Initial re-entry between slow pathway-1 (S1-antegrade) and slow pathway-2 (S2-retrograde) at a cycle length of 410ms with concealed conduction into slow pathway-3 (S3) and decremental conduction in upper common pathway (fig 3A)
(c) Decremental conduction of S1 resulting in gradual prolongation of H-H interval followed by block which favored the transient re-entry between S3 (antegrade) and S2 (retrograde) (cycle length 379ms) and subsequent resumption of S1 conduction (fig 3B & C)

The possibility of two antegrade slow pathway conduction has been described previously as a cause for cycle length alteration during AVNRT[1]. Multiple slow pathways are required for the initiation of re-entrant tachycardia after 1:2 AV response which otherwise would not have induced. In our patient the cycle length alteration was noted in both atrial (A-A) and ventricular (V-V) intervals. This could be explained by a rare combination of decremental conduction in both upper common pathway and antegradely conducting slow pathway (S1). The second pathway (S2) has different electrophysiological properties (conduction velocity and refractory period) as evidenced by the intracardiac electrogram and it is unlikely to be a fast pathway as the HA interval is long. The fourth beat in the figure 2C has slightly longer cycle length (422ms) due to concealed conduction of previous impulse into S1. These findings emphasize the fact that both atrium and the ventricle are not the part of circuit in AVNRT. Electroanatomic mapping (ENSITE Velocity, Abbott, Plymouth, MN) confirmed earliest atrial activation at coronary sinus ostium (fig 2B) Slow pathway was ablated (medium curve catheter; 60W, 60^{o}C) which rendered the tachycardia non-inducible. Since there were three slow pathways involved in this patient, this rare variety could be labelled as ‘atypical slow-slow-slow AVNRT’.

The mechanism of re-entry in typical as well as atypical AVNRT remains elusive[2]. There has been electrophysiologic evidence of multiple superior atrial inputs to the AV node[3] that could explain multiple sites of early atrial activation during tachycardia. Cycle length alternans can occur during AVNRT due to either antegrade conduction via two slow pathways or junctional bigeminism[4]. The decremental conduction properties of antegrade slow pathway (S1) and upper common pathway were the reasons for variation in A-A, H-H, H-A and V-V intervals in our case of atypical slow-slow-slow AVNRT.

References

1. Maury P, Raczka F, Piot C, Davy JM. QRS and cycle length alternans during paroxysmal supraventricular tachycardia: What is the mechanism? J Cardiovasc Electrophysiol 2002;13:92-3
2. Katritsis DG, Camm AJ. Atriovenricular nodal reentrant tachycardia. Circulation 2010;122:831-40.
3. Wu J, Wu J, Olgin J, Miller JM, Zipes DP. Mechanisms underlying the reentrant circuit of atrioventricular nodal re-entrant tachycardia in isolated canine atrioventricular nodal preparation using optical mapping. Circ Res 2001;88:1189-95.
4. Surawicz B, Fisch C. Cardiac Alternans: Diverse mechanisms and clinical manifestations. J Am Coll Cardiol 1992;20:483-499

Figure Legends

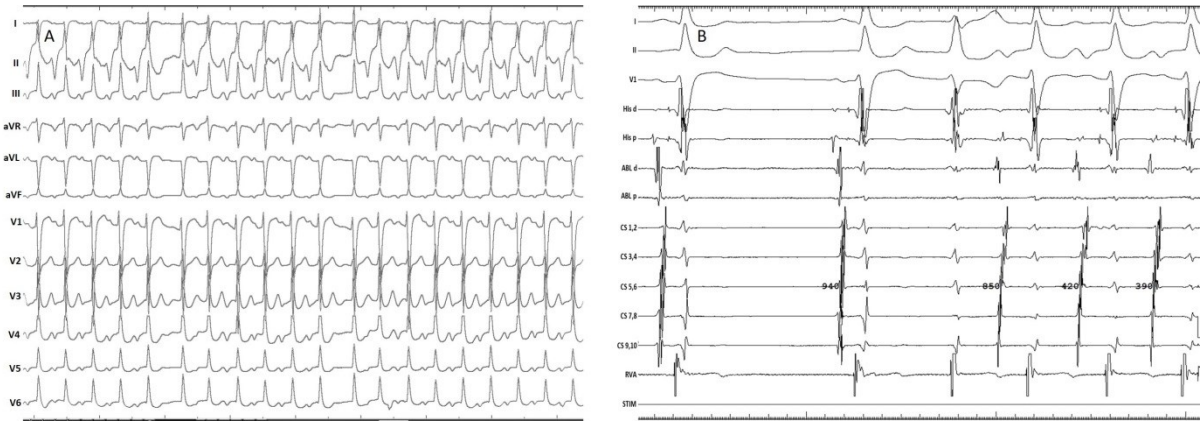

Fig 1: A -12 lead ECG showing narrow QRS tachycardia with varying RP interval. B – Electrogram showing the spontaneous initiation of tachycardia. Single sinus atrial impulse (second beat) has got conducted through both fast and slow pathways to produce 1:2 AV response followed by initiation of tachycardia. His d and His p – His electrograms – distal and proximal, ABL d and P – Ablation catheter distal and proximal, CS 1-10 – Coronary sinus electrograms, RVA – RV apex electrogram

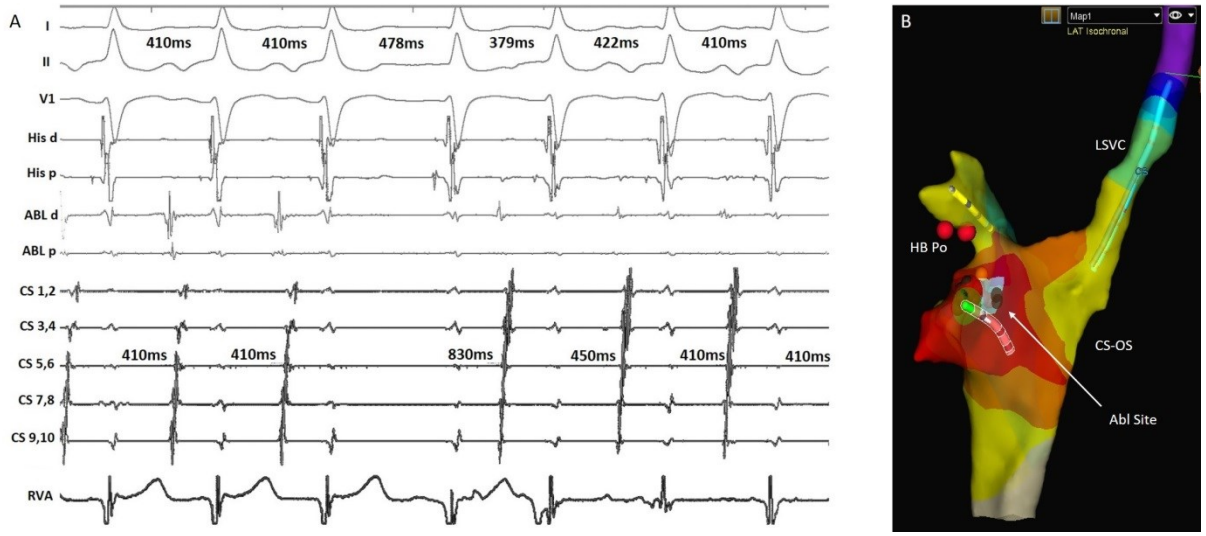

Fig 2: A – Intracardiac electrogram showing variation in A-A, H-H, H-A and V-V intervals due to decremental conduction in upper common pathway and antegrade slow pathway (S1). B- Electroanatomic map showing dilated coronary sinus ostium (CS-OS) with left SVC (LSVC) and the site of earliest atrial activation (white spot). His d and His p – His electrograms – distal and proximal, ABL d and P – Ablation catheter distal and proximal, CS 1-10 – Coronary sinus electrograms, RVA– RV apex electrogram, His po- His potential

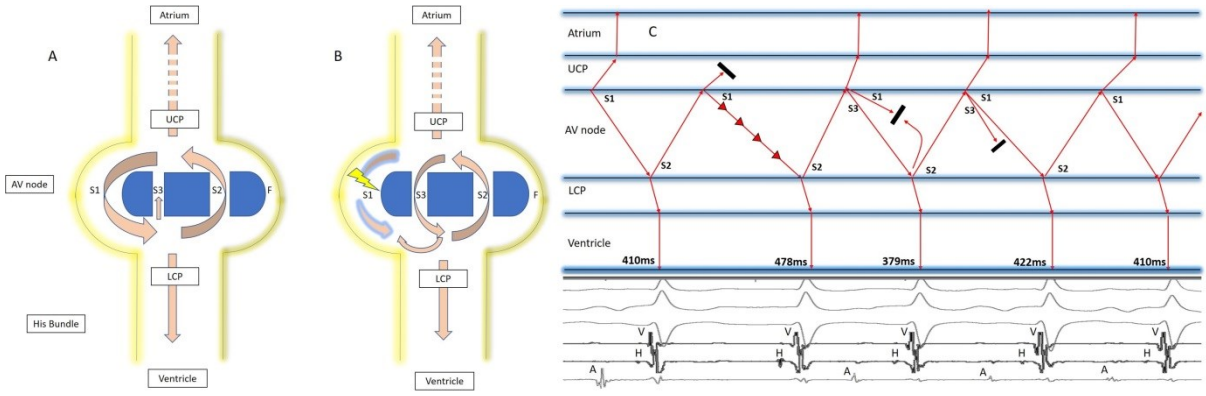

Fig 3: A – Atypical slow- slow AVNRT with re-entry between S1 and S2 with concealed conduction into S3. Upper common pathway showed decremental conduction. B – Transient block in S1 due to decremental conduction favored re-entry between S3 and S2 with concealed conduction into S1. C – Ladder diagram showing the same phenomenon. The decremental conduction in S1 prolonged H-H/V-V interval from 410ms to 478ms. S3 could conduct in the next beat with H-H interval of 379ms as S1 was transiently blocked. In the subsequent beat S1 conduction resumed with minimal prolongation of H-H interval due to concealed conduction. Atrial conduction occurred decrementally through upper common pathway (UCP). S1,2,3 – slow pathways 1,2 and 3, F – fast pathway, LCP -Lower common pathway

J Innov Cardiac Rhythm Manage. 2020;11(9):4242–4245

The Journal of Innovations in Cardiac Rhythm Management™

DOI: 10.19102/icrm.2020.1100902

CATHETER ABLATION

PEDIATRIC ELECTROPHYSIOLOGY

CASE REPORT

Catheter Ablation of Pediatric Atrioventricular Nodal Re-entrant Tachycardia

SHUNMUGA SUNDARAM PONNUSAMY, MD, DM, PDF (EP), CEPS,[1] GIRIDHAR MUTHU, MD, DM,[1] and VIJESH ANAND, MBBS, MD[1]

[1]*Department of Cardiology, Velammal Medical College Hospital and Research Institute, Madurai, Tamil Nadu, India*

ABSTRACT. *Catheter ablation is considered as the standard treatment for all patients with symptomatic drug-refractory tachyarrhythmia. The safety and efficacy of the procedure in the adult population is well-established. Due to the small size of the patient and difficulty in attaining venous access, infants are rarely subjected to radiofrequency ablation. Here, we report a case of drug-refractory AV nodal re-entrant tachycardia in a two-year-old child. Radiofrequency ablation was performed with a 5-Fr sized medium-curve ablation catheter deployed at the slow pathway region where a fractionated A-wave with slow-pathway potential was recorded. After ablation, no recurrence of SVT at the end of 12 months of follow-up was observed.*

KEYWORDS. *AVNRT, pediatric arrhythmia, radiofrequency ablation.*

ISSN 2156-3977 (print)
ISSN 2156-3993 (online)

Introduction

Although catheter ablation for cardiac arrhythmia has been performed in adult populations since the early 1980s, ablation for cardiac arrythmias in the pediatric population was not attempted until the early 1990s.[1,2] Supraventricular tachycardias (SVTs) are the most commonly encountered substrates, among which, those related to the accessory pathway account for 75% of cases in older children and 95% of cases among infants. Atrioventricular (AV) node reentrant tachycardia (AVNRT) is a less frequent (12%) occurrence.[3,4] Most of these arrhythmias respond to medical management and catheter ablation is reserved for drug-refractory cases only. Cryoablation is the preferred modality for infants and young children as it reduces the risk of AV blockage. Herewith, we report the case of a two-year-old child with drug-refractory AVNRT with repeated hospitalization for the arrhythmia who was subsequently treated by radiofrequency (RF) ablation.

The authors report no conflicts of interest for the published content. Address correspondence to: Dr. Shunmuga Sundaram Ponnusamy, MD, DM, PDF (EP), CEPS, Department of Cardiology Velammal Medical College Hospital and Research Institute, Velammal Village, Airport Ring Road, Madurai 625009, Tamil Nadu, India.
Email: shunmuga.pgi@gmail.com.

Case report

A two-year-old child weighing 10 kg was referred for catheter ablation for drug-refractory SVT. Her mother reported a history of frequent hospitalizations despite maximal doses of oral verapamil and β-blocker medication. Electrocardiography (ECG) during sinus rhythm did not show pre-excitation. Echocardiography ruled out structural heart disease. A narrow QRS tachycardia at the rate of 260 bpm was documented during an SVT episode **(Figure 1)**. In view of recurrent hospitalization despite maximal medical management, an option of catheter ablation was discussed. Informed consent was obtained in view of the nonavailability of cryoablation and the risk of AV blockage.

RF ablation was performed under intravenous sedation. Twelve-lead ECG and intracardiac electrograms were continuously recorded using an electrophysiology system (Abbott Laboratories, Chicago, IL, USA). Venous access was obtained from both the right femoral vein and the left femoral vein. Baseline sinus rhythm showed normal AH (94 ms) and HV (39 ms) intervals **(Figure 2A)**. Tachycardia could be easily induced by programmed atrial stimulation at 400 ms (S1), 350 ms (S2), and 230 ms (S3) with an AH jump. The tachycardia cycle length was 230 ms and coronary sinus electrograms showed a concentric atrial

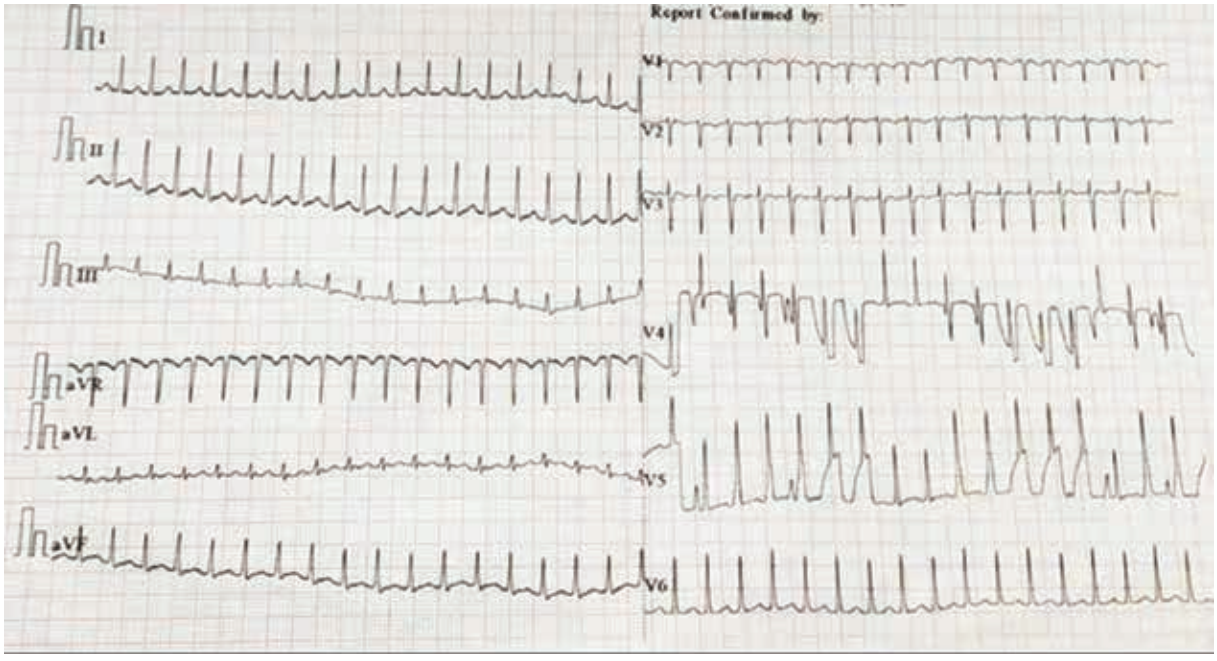

Figure 1: ECG taken during tachycardia showed a regular narrow QRS tachycardia with a pseudo–S-wave in lead II and pseudo–R-wave in lead aVR suggestive of AVNRT.

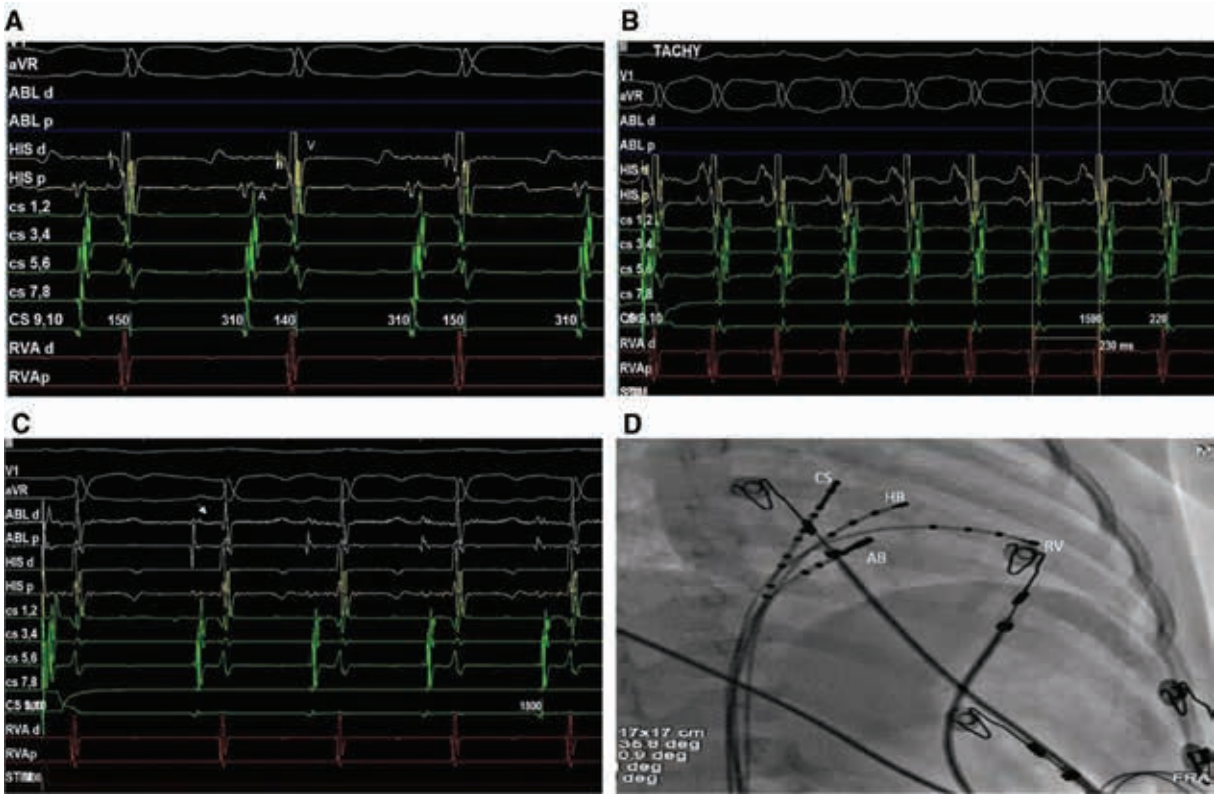

Figure 2: A: Baseline AH and HV intervals were 94 ms and 39 ms. **B**: AVNRT with a cycle length of 230 ms with a concentric activation pattern in the coronary sinus. **C:** Ablation catheter showing a fractionated atrial signal with slow-pathway potential (white arrowhead). **D:** Ablation catheter at the anterior margin of the coronary sinus in the right anterior oblique fluoroscopy view. CS: coronary sinus; HB: His bundle; AB: ablation catheter; RV: right ventricle.

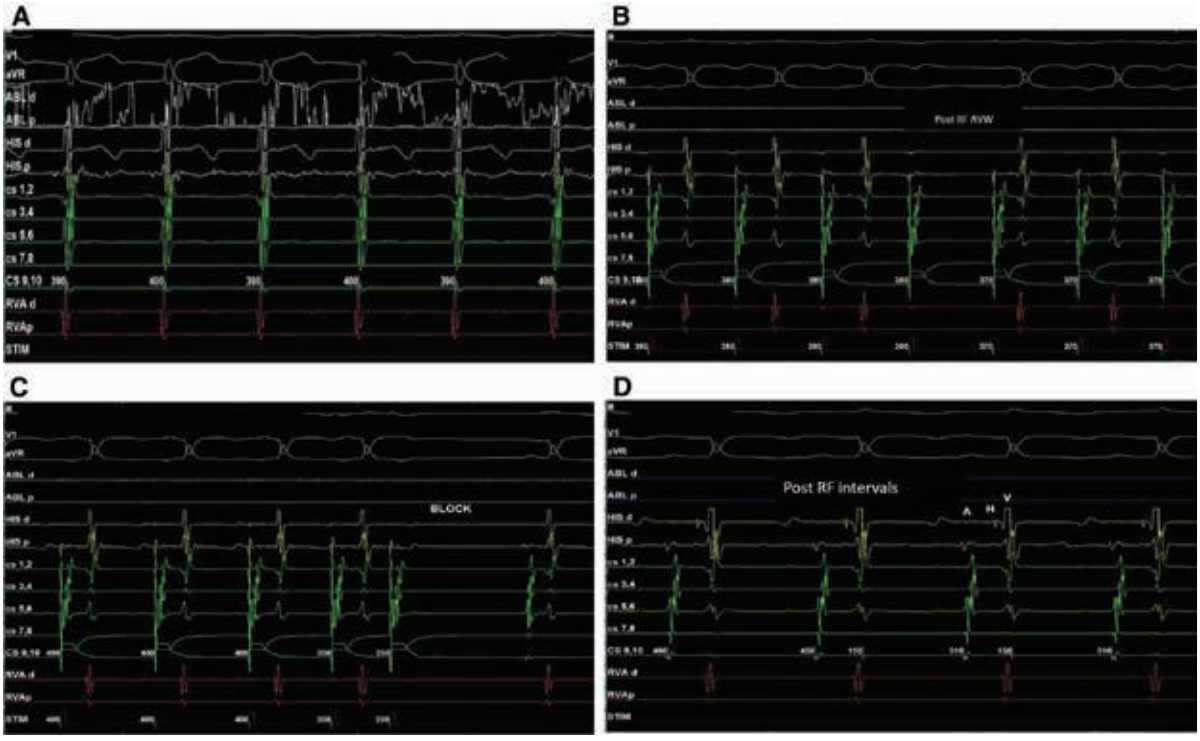

Figure 3: A: Junctional rhythm during RF ablation at a 400-ms cycle length. **B:** Post-RF ablation incremental atrial pacing showed Wenckebaching at a 380-ms cycle length. **C:** Programmed atrial stimulation showed AH block at 400 ms (S1), 350 ms (S2), and 250 ms (S3). **D:** Postablation AV-nodal conduction remained intact with AH and HV intervals of 94 ms and 40 ms.

activation pattern **(Figure 2B)**. The ventricular entrainment protocol confirmed AVNRT.

Ablation at the posterior part of Koch's triangle with a fractionated atrial signal with slow-pathway potential **(Figures 2C and 2D)** using a 5-French (Fr) medium-curve RF ablation catheter (Abbott Laboratories, Chicago, IL, USA) resulted in good junctional rhythm at the 400-ms cycle length (30 W power gradually increased to 50 W, temperature of 50°C for 60 seconds) **(Figure 3A)**. The total fluoroscopy time was five minutes and the procedure lasted for 30 minutes. Postablation tachycardia could not be induced despite an aggressive induction protocol. Incremental atrial pacing showed AV Wenckebaching at a 380-ms cycle length, confirming the elimination of slow-pathway conduction **(Figure 3B)**. Fast-pathway conduction remained intact as programmed atrial stimulation revealed AH block at 400 ms (S1), 350 ms (S2), and 250 ms (S3) **(Figure 3C)**. The AH and HV intervals after ablation were 94 ms and 40 ms, respectively **(Figure 3D)**. The child was discharged the next day without any complications and remained symptom-free at 12 months after the procedure.

Discussion

Drug-refractory SVTs are rare during childhood. The most common arrhythmias are accessory pathway–mediated AVNRT. Although there are several reports of successful ablation of orthodromic AV-reciprocating tachycardia in infants, AVNRT is rare. Our case is unique in that the AVNRT was drug-refractory despite optimal therapy and RF ablation was performed instead of cryoablation. Two major challenges exist with this protocol: (1) obtaining venous access and (2) avoiding causing injury to the AV node while ablating the slow pathway. In this present case, we restricted our venous access to the femoral vein (two punctures on each side, using a 4-Fr quadripolar catheter and a 5-Fr ablation catheter). Venous Doppler imaging was performed before discharge and ruled out venous thrombosis. To avoid AV nodal block during ablation, it was deemed safe to target fractionated atrial signals with an AV ratio of 1:10 **(Figure 2C)** and to stop ablating when there existed a fast junctional rhythm at a cycle length of less than 300 ms.

AVNRT is the second most-encountered SVT in the pediatric population. The AV node consists of two pathways: the fast pathway, which is composed of transitional cells in the region extending from the compact node to the anterior aspect of Koch's triangle, and a slow pathway composed of a deeper inferoposterior extension.[5] AVNRT can be safely cured by slow-pathway modification in the posterior aspect of Koch's triangle. Cryoablation is the modality of choice in infants and children as it can reduce the incidence of AV block. However, we had to employ RF energy as cryoablation is not yet available in our region.

The most common challenge that we come across in the pediatric population is the small size of the heart and the

varied anatomy associated with congenital heart diseases.[6] The varied intracardiac and venous anatomy often makes it difficult to ablate in this population. In many centers, the procedures are modified with the usage of fewer catheters than in the adult population and the adoption of transesophageal catheters to pace the left atrium and 4-Fr ablation catheters to avoid vascular complications. The reported complications during pediatric RF ablation include complete heart block and thrombus formation. Cardiac perforation and death are rare complications and are more frequent in correlation with smaller patient sizes and left-sided procedures. Blaufox et al.[7] showed the feasibility of catheter ablation for cardiac arrhythmias in small children weighing less than 15 kg. Of 268 RF catheter ablation procedures, 18 were performed in 14 patients weighing less than 15 kg. Orthodromic AVRT was noted in nine patients, atrial tachycardia was seen in one patient, and ventricular tachycardia was found in four patients. The complications reported included pericardial effusion, mitral regurgitation, and myocardial infarction. In the AVRT subgroup, the indexed total application time trended higher during complicated as compared with during uncomplicated procedures (40.6 versus 6.6 s/kg). The authors concluded that RF ablation can be successful in small children; however, complications appear to be related to the RF dose indexed for body size. Elsewhere, the MAP-IT registry[8] highlighted the safety of pediatric ablation with a significant reduction in radiation exposure among the 1,417 procedures done. Cryoablation was performed in one-quarter of the cases. Two percent of the patients were younger than three years of age and their success rate and complications were not different from those of older patients.

Despite all these challenges and complications, however, catheter ablation for AVNRT is a safe procedure in the pediatric population when performed by experienced hands.

Conclusion

AVNRT is the second most common variety of SVT in children. Drug therapy remains the first option for treating pediatric arrhythmias. In rare instances where drugs are not effective in controlling the arrhythmia, RF catheter ablation can be safely performed while safeguarding the AV node. Although single case results cannot be extrapolated to the general population, further studies could provide additional insights and confirm the safety of RF ablation in toddlers.

References

1. Van Hare GF, Velvis H, Langberg JJ. Successful transcatheter ablation of congenital junction ectopic tachycardia in a ten-month-old infant using radiofrequency energy. *Pacing Clin Electrophysiol*. 1990;13(6):730–735.
2. Tanel RE, Walsh EP, Triedman JK, Epstein MR, Bergau DM, Saul JP. Five-year experience with radiofrequency catheter ablation: implications for management of arrhythmias in pediatric and young adult patients. *J Pediatr*. 1997;131(6):878–887.
3. Kugler JD, Danford DA, Houston KA, Felix G; Pediatric Radiofrequency Ablation Registry of the Pediatric Radiofrequency Ablation Registry of the Pediatric Electrophysiology Society. Pediatric radiofrequency catheter ablation registry success, fluoroscopy time, and complication rate for supraventricular tachycardia: comparison of early and recent eras. *J Cardiovasc Electrophysiol*. 2002;13(4):336–341.
4. Van Hare GF, Javitz H, Carmelli D, et al. Prospective assessment after pediatric cardiac ablation: recurrence at 1 year after initially successful ablation of supraventricular tachycardia. *Heart Rhythm*. 2004;1(2):188–196.
5. Cohen MI, Wieand TS, Rhodes LA, Vetter VL. Electrophysiologic properties of the atrioventricular node in pediatric patients. *J Am Coll Cardiol*. 1997;29(2):403–407.
6. Silka MJ, Halperin BD, Hardy BG, McAnulty JH, Kron J. Safety and efficacy of radiofrequency modification of slow pathway conduction in children less than 10 years of age with atrioventricular node reentrant tachycardia. *Am J Cardiol*. 1997;80(10):1364–1367.
7. Blaufox AD, Paul T, Saul JP. Radiofrequency catheter ablation in small children: relationship of complications to application dose. *Pacing Clin Electrophysiol*. 2004;27(2):224–229.
8. Dubin AM, Jorgensen NW, Radbill AE, et al. What have we learned in the last 20 years? A comparison of modern era paediatric and congenital catheter ablation registry to prior paediatric ablation registries. *Heart Rhythm*. 2019;16(1):57–63.

RESEARCH PAPER

Arrhythmia in Children and Adolescents and Outcome of Radiofrequency Ablation for Tachyarrhythmias - A Single Center Experience Over 16 Years

DEBABRATA BERA[1], VADIVELU RAMALINGAM[1], CHETAN RATHI[2], RAJEEV SHARMA[1], NEETA BACHANI[2] AND YASH LOKHANDWALA[1]

From Departments of [1]Electrophysiology and [2]Cardiology, Holy Family Hospital, Mumbai, India.

Correspondence to: Dr Debabrata Bera, Holy Family Hospital, Hill Road, Bandra(West), Mumbai 400050,India. debabratabera81@gmail.com
Submitted: October 14, 2019; Initial review: November 20, 2019; Accepted: April 9, 2020.

Objectives: Radiofrequency (RF) ablation for tachycardia in children poses challenges in view of slender veins and delicate cardiac structures in close proximity. **Methods**: We reviewed hospital records for patients below 18 years,who underwent RF ablation from August, 2001 to February, 2017 at a single hospital. **Results**: Among 214 patients (134 males, age12.5 (4.6) years), there were 221 tachycardia substrates: accessory pathways in 85 patients (39%), AV nodal re-entrant tachycardia in 79 patients (36%), ventricular tachycardia in 28 patients (13%) and atrial tachycardia in 21 patients (9.6%).The overall success rate of RF ablation was 95% (204/214). Success rate in those younger than 6 years was similar to those in older age groups.There were no major complication. **Conclusion**: RF ablation below 18 years of age has a high success rates and low complications.

Keywords: *Catheter ablation, Management, Outcome, Supraventricular tachycardia*.

Published online: **June 12, 2020;** ***PII:*****S097475591600200**

Catheter ablation in children using radiofrequency (RF) energy has been in vogue since 1989 [1]. Radiofrequency ablation ensures a permanent cure of arrhythmias and hence, is the preferred treatment in the vast majority. Previous registries have demonstrated that RF ablation can safely and effectively be performed in children [2,3]. However, patients weighing less than 15 kg have been identified as being at greater risk for complications [2,3]. Though medical therapy is an alternative option, it has its own limitations [5]. The experience from India on RF ablation is also limited [4], due to a lack of widespread availability, lack of expertise, and fear of complications in children, though rare [6].

We have been using conventional RF ablation techniques in the pediatric age group since the last two decades. We conducted a retrospective study of patients aged up to 18 years and analyzed them for the tachycardia substrates, success and complications.

METHODS

The patients were categorized into three groups according to age: Groups A (younger than six year), B (aged 6-12 years) and C (older than 12 years). General anesthesia was required for the procedure for majority of children in Groups A and B; midazolam, propofol, fentanyl and sevoflurane were the drugs used. For Group C, local anesthesia and sedation were used.

All anti-arrhythmic drugs were suspended for a duration of at least four half-lives before the procedure. For AVNRT (Atrioventricular nodal re-entrant tachycardia) and right-sided accessory pathways (APs), three venous punctures were sufficient – for coronary sinus (CS), His bundle and a roving catheter. For left sided APs, two femoral venous accesses and one femoral arterial route were employed. The sheaths used ranged from 4F to 7F caliber. Unfractionated heparin was used for all cases (50 units/ kg for venous route and 100 units/kg for arterial route).

When the arrhythmia was not induced at baseline, intravenous isoprenaline was administered (1-2 μg/min). Atropine (according to bodyweight) was used when isoprenaline failed. Fluoroscopy time and procedure time were noted. The RF energy output, length of application and temperature were individually titrated. After ablation, 30-45 minute waiting period was kept along with isoprenaline and atropine for re-induction.

Acute success of RF ablation was defined as failure to induce causal arrhythmia after application of adequate number of RF energies. Failure was defined when tachycardia remained inducible at the end of the procedure.

There were two subsets, *viz.* unable to ablate the tachycardia source/circuit, or unable to deliver RF energy due to apprehension of complication or due to mechanical stunning of the pathway. Relapses/recurrence was defined as recurrence of same clinical arrhythmia after acute success of RF ablation.

Follow-up was done by reviewing the patients' medical records, outpatient visits and telephonic conversation. Follow-up period varied from 2-16 years.

Statistical analyses: The SPSS software was used for database organization and statistical calculations. The discrete variables were compared using Chi-square test, considering *P* value below 0.05 as significant.

RESULTS

A total of 2980 cases underwent the procedure during study period – 229 (8%) were performed in patients aged younger than 18 years [mean (SD) age, 12.5 (4.6) year]. In 11 patients the data was incomplete; and another 4 patients did not have inducible tachycardia.Finally, data of 214 children (62% males) undergoing RF ablation were analyzed for this study.

Table I Tachycardia Substrates in Children Undergoing Radiofrequency Ablation (*N*=211)*

	≤6y (n=33)	*7-12 y (n=53)*	*13-18 y (n=135)*
Males	18	32	84
LVEF, %#	70 (9)	67 (9)	65 (10)
Upfront ablation			
Parental preference	1	5	22
Tachycardiomyopathy	1	1	2
AVNRT	8	22	49
Manifest AP (WPW)	14	15	31
Concealed AP	2	11	16
Atrial tachycardia	5	5	11
Fascicular VT	1	0	17
Outflow VT	3	0	7
Miscellaneous	0	0	4

**211 substrates in 214 children; #mean (SD); LVEF: Left ventricular ejection fraction; AVNRT: Atrioventricular nodal reentrant tachycardia; WPW: Wolff-Parkinson-White syndrome, AP: Accessory pathway; VT: Ventricular tachycardia.*

These 214 patients had a total of 211 arrhythmia substrates. The commonest tachycardias found were APs in 85 (39 %) and AVNRT in 79 (36 %) patients. The most common arrhythmia with APs was orthodromic atrio ventricular re-entrant tachycardia (AVRT) followed by antidromic tachycardia (ADT) and pre-excited atrial fibrillation. Ventricular tachycardia was found in 28 patients (13 %), and atrial tachycardia (AT) in 21 patients (9.6%). Three patients had automatic junctional tachycardia and one patient had atrial flutter (previous surgery for atrial septal defect). Four patients had multiple tachycardia mechanisms and three patients had multiple APs.

We categorized them age-wise into three subgroups (***Table* I**). In younger children, AP was the most common mechanism, but above 12 years, AVNRT emerged as the most common tachycardia mechanism. Fascicular VT was by far commoner in Group C. Among the 85 patients with APs, we detected 89 APs; of them there were nine right free wall Mahaim-like (atrio-fascicular) APs with antidromic tachycardia. Other than these, only two other patients had antidromic tachycardia, one of whom also had associated orthodromic AVRT. The left lateral location was the commonest (31/89, 35%). Left sided APs were more common in concealed APs (18/29, 62%) than in WPW group (13/60, 21%, $P<0.001$).

The overall immediate success rate **(*Table* II)** was 95% (204/214). For AVNRT, 98.7% (78/79) were ablated by slow pathway modification. Among the APs, immediate success rate was 96.4% (82/85); failure was most commonly seen in Ebstein anomaly and with Mahaim-like pathways (***Web Table* I**).The success rates in the three groups were similar. There were no major or minor

Table II Success Rate of Radiofrequency Ablation in Children With Tachyarrhythmia

	Total	*Success*	*Fluoroscopy time (min)**	*Mean procedure time (min)*	*No. of RF lesions**	*Maximum temperature* (°C)
AVNRT	79	78	10.9 (5.9)	78	4.7 (2.5)	60
Accessory pathway (AVRT)	85	82	14.6 (7.1)	90	5.1 (3.3)	55-60
Atrial tachycardia	21	19	19.3 (10.2)	117	4.3 (2.0)	50-60
Outflow tract VT	10	10	17.5 (13.3)	103	5.9 (3.1)	60
Fascicular VT	18	15	21.1 (11.1)	130	6.5 (2.5)	50-60
Miscellaneous	4	3	15 (7.2)	90	3.5 (2.2)	60

**Values are expressed as mean (SD); AVNRT: Atrioventricular nodal re-entrant tachycardia; VT: Ventricular tachycardia.*

WHAT THIS STUDY ADDS?

- Ablation in children using conventional radiofreauency energy was safe and effective, with similar success rate among those younger or older than six years.

complication. The recurrence rate was 2.9 % (6/205); 2 had AVNRT, 3 had APs and 1 had AT.

We sub-categorized those who had prolonged procedures, arbitrarily defined more than two hours. There were seven such patients; three had atrial tachycardia, three had APs and one had VT. Five of them required left sided ablation; all these procedures were finally successful.

Among patients undergoing the procedures, six had congenital heart disease (three had atrial septal defect, two had Ebstein's anomaly and one had ventricular septal defect). Four more patients had tachycardiomyopathy, among whom three had incessant AT.

DISCUSSION

We found AVRT to be the most common tachycardia below six years; above this age, AVNRT and AVRT were comparable.This is in contrast to older studies [6], which found that accessory pathway was the most prevalent finding between age range of 2-18 years, with AVRT in 65%, AVNRT in 30%, ventricular tachycardia in 4%, and atrial tachycardia in 0.7%.

Previous report shave demonstrated that RF ablation can safely and effectively be performed in pediatric patients [2-4,6]. After 1-16 year follow up, the overall success rate was also higher than older studies [1]. With the advent of cryoablation, studies revealed, AV block was less with cryoablation, though recurrence was significantly higher [7]. We have performed only conventional RF for all age groups as cryoablation was unavailable at our center. Van Hare, *et al*. [1] reported a success rate of 95.7% with RF ablation in AVRT and AVNRT in pediatric patients. Simao, *et al*. [8] reported slightly lower success rate of 91.7% in AVNRT and 83.5% for APs. Our study is in concordance with these previous results [2-6]. Our study revealed better immediate success rate of 95% and recur-rence rate of only 2.9%. After successful ablation we could withdraw anti-arrhythmic drugs and the majority remained asymptomatic without recurrence.

In our cohort, infants were few and hence we did not compare or analyze the results separately. A unique finding in our study was higher incidence of Mahaim (atriofascicular) pathways (9/89, 10%). Compared to reports of only 3% of accessory pathways [9]. Another unusual finding in our study was that idiopathic VT comprised a significant proportion (12.9 % of all tachycardias), where we had a good success rate (25/28, 89%). A study [10] comparing RF ablation in neonates and children between 1 and 18 months of age, found that neonates had significantly higher structural heart disease and yet the success rate and complications were surprisingly similar in both subsets. The comparable success rates in our cohort could partially be due to the fact that ablations in smaller children are more likely to be attempted by more experienced pediatric electro-physiologists and experience has been shown to be an important factor in successful pediatric RF ablation procedures [11].

This was a hospital-based retrospective analysis and suffers from the risk of bias and lack of generalizability. Infants and very small children were avoided unless pressing indications, hence these were few subjects in that age range.We did not have cryoablation, hence comparison was not possible between RF and cryoablation.

We believe RF ablation can be considered for pediatric arrhythmias, especially when they are recurrent and in children above 5 years of age. Whether RF ablation can be a primary treatment modality for young children is still a debatable issue,this can perhaps be addressed by more data from other Indian centers.

Ethical clearance: Institutional ethical committee of Holy Family Hospital; ECR/196/INST/MH/2013/RR-16, dated September 14, 2019.
Contributors: DB: analysed data and drafted the manuscript; VV:collection of data, designing study; CR: manuscript scrutiny and helped in data analysis; RS: helped in writing the manuscript and develop images; NB: performed echocardiography for majority of the patients and helped in data analysis; YL: concept of the study, supervised cognitive and behavioral assessments, supervised manuscript preparation.
Funding: None; *Competing interest*: None stated.

REFERENCES

1. Van Hare GF, Lesh MD, Scheinman M, Langberg JJ. Percutaneous radiofrequency catheter ablation for supraventricular arrhythmias in children. J Am Coll Cardiol. 1991;17:1613-20.
2. Kugler JD, Danford DA, Deal BJ, Gillette PC, Perry JC, Silka MJ, *et al*. Radiofrequency catheter ablation for tachyarrhythmias in children and adolescents. New England J Med. 1994;330:1481-7.

3. Kugler JD, Danford DA, Houston K, Felix G. Radiofrequency catheter ablation for paroxysmal supraventricular tachycardia in children and adolescents without structural heart disease. Am J Cardiol. 1997;804: 1438-43.
4. Vora A, Lokhandwala Y, Sheth C, Dalvi B. Radiofrequency ablation in an infant with recurrent supraventricular tachy-cardia and cyanosis. Ann Pediatr Cardio.2009; 2:156-8.
5. Maragnès P, Tipple M, Fournier A. Effectiveness of oral sotalol for treatment of pediatric arrhythmias. Am J Cardiol. 1992;69:751-54.
6. Kim YH, Park H-S, Hyun MC, Kim Y-N. Pediatric tachyarrhythmia and radiofrequency catheter ablation: Results from 1993 to 2011. Korean Circulation J. 2012;42: 735-40.
7. Avari J, Jay K, Rhee E. Experience and results during transition from radiofrequency ablation to cryoablation for treatment of pediatric atrioventricular nodal reentrant tachycardia. Pacing Clinical Electrophysiol.2008;31:454-60.
8. Simao MF, Rios MN, Leiria TL, Kruse ML, Pires LM, Sant Anna RT, *et al*. Electrophysiological studies and radiofrequency ablations in children and adolescents with arrhythmia. Arq Bras Cardiol.2015;104:53-7.
9. Miller JM, Olgin JE. Catheter ablation of free-wall accessory pathways and 'Mahaim' fibers. *In*: Zipes DP, Haissaguere M, editors. Catheter ablation of cardiac arrhythmias. 2nd edition. Armonk, NY: Futura, 2002 :277-303.
10. Blaufox AD, Felix GL, Saul JP. Pediatric catheter ablation registry radiofrequency catheter ablation in infants and dd18 months old: When is it done and how do they fare? Short-term data from the pediatric ablation registry. Circulation. 2001; 104:2803-8.
11. Danford D, Kugler J, Deal B, Case C, Friedman R, Saul J, *et al*. The learning curve for radiofrequency ablation of tachyarrhythmias in pediatric patients. Am J Cardiol. 1995;75:587-90.

Web Table I Details of Children With Failed Ablations (*N*=10)

Age, y	*Diagnosis*	*Cause of failure*
14	WPW/Left lateral AP	Broad pathway, Epicardial location*
13	Junctional tachycardia	Proximity to AV node#
10	AVNRT	Proximity to AV node#
04	AT (right atrial)	Remained inducible*
16	AT (right superior pulmonary vein)	Remained inducible*
14	Fascicular (upper septal) VT	Proximity to his bundle#
15	Fascicular (upper septal) VT	Proximity to his bundle#
14	Ebstein's anomaly	Broad AP, could not be ablated completely*
14	Mahaim atrio-fascicular accessory pathway	Stunned by catheter contact and then could not be mapped#

*Cause of failure: *Unable to ablate the tachycardia source/circuit; #Unable to deliver RF energy due to apprehension of complication or due to mechanical stunning of the pathway; AVNRT: Atrioventricular nodal re-entrant tachycardia, AP: Accessory pathway, AT: Atrial tachycardia, WPW: Wolff-Parkinson-White syndrome, VT: Ventricular tachycardia.*

The Egyptian Heart Journal

RESEARCH Open Access

Association of culprit lesion plaque characteristics with flow restoration post-fibrinolysis in ST-segment elevation myocardial infarction: an intravascular ultrasound-virtual histology study

Raghavendra Rao K[1], Sreenivas Reddy[1*], Jeet Ram Kashyap[1], Vadivelu Ramalingam[1], Debabrata Dash[1], Vikas Kadiyala[1], Suraj Kumar[1], Hithesh Reddy[1], Jaspreet Kaur[1], Ashok Kumar[2], Naindeep Kaur[1] and Anish Gupta[1]

Abstract

Background: Not every patient achieves normal coronary flow following fibrinolysis in STEMI (ST-segment elevation myocardial infarction). The culprit lesion plaque characteristics play a prominent role in the coronary flow before and during percutaneous coronary intervention. The main purpose was to determine the culprit lesion plaque features by virtual histology-intravascular ultrasound (VH-IVUS) in patients with STEMI following fibrinolysis in relation to baseline coronary angiogram TIMI (thrombolysis in myocardial infarction) flow. Pre-intervention IVUS was undertaken in 61 patients with STEMI after successful fibrinolysis. After the coronary angiogram, they were separated into the TIMI1–2 flow group (n = 31) and TIMI 3 flow group (n = 30). Culprit lesion plaque composition was evaluated by VH-IVUS.

Results: On gray-scale IVUS, the lesion external elastic membrane cross-sectional area (EEM CSA) was significantly higher in the TIMI 1–2 groups as compared to the TIMI 3 group (15.71 ± 3.73 mm^2 vs 13.91 ± 2.94 mm^2, $p = 0.041$) with no significant difference in plaque burden (82.42% vs. 81.65%, $p = 0.306$) and plaque volume (108.3 mm^3 vs. 94.3 mm^3, $p = 0.194$). On VH-IVUS, at the minimal luminal area site (MLS), the fibrous area (5.83 mm^2 vs. 4.37 mm^2, $p = 0.024$), necrotic core (NC) area (0.95 mm^2 vs. 0.59 mm^2, $p < 0.001$), and NC percentage (11% vs. 7.1%, $p = 0.024$) were higher in the TIMI 1–2 groups in contrast to the TIMI 3 group. The absolute necrotic core (NC) volume (8.3 mm^3 vs. 3.65 mm^3, $p < 0.001$) and NC percentage (9.3% vs. 6.0%, $p = 0.007$) were significantly higher in the TIMI 1–2 groups as compared to the TIMI 3 group. Absolute dense calcium (DC) volume was higher in TIMI 1–2 groups with a trend towards significance (1.0 mm^3 vs.0.75 mm^3, $p = 0.051$). In multivariate analysis, absolute NC volume was the only independent predictor of TIMI 1–2 flow (odds ratio = 1.561; 95% CI 1.202–2.026, $p = 0.001$). Receiver operating characteristic curves showed absolute NC volume has best diagnostic accuracy (AUC = 0.816, $p < 0.001$) to predict TIMI 1–2 flow with an optimal cutoff value of 4.5 mm^3 with sensitivity and specificity of 79% and 61%, respectively.

(Continued on next page)

* Correspondence: reddycardio2911@gmail.com
[1]Department of Cardiology, Government Medical College and Hospital, Sector 32, Chandigarh 160030, India
Full list of author information is available at the end of the article

(Continued from previous page)
Conclusions: This study exemplifies that the necrotic core component of the culprit lesion plaque in STEMI is associated with the coronary flow after fibrinolysis. The absolute necrotic core volume is a key determinant of flow restoration post-fibrinolysis and aids in prognostication of less than TIMI 3 flow.

Keywords: ST-segment elevation myocardial infarction, Fibrinolysis, Intravascular ultrasound, Virtual histology-intravascular ultrasound, Necrotic core, TIMI flow

Background

Cardiovascular disease (CVD) afflicts the entire world and is the prominent cause of mortality in developing countries accounting for 80% of all cardiovascular-related deaths [1]. ST-segment elevation myocardial infarction (STEMI) is associated with significant morbidity and mortality. Timely and adequate reperfusion has been undoubtedly proven to be beneficial. Primary percutaneous coronary intervention (PPCI) achieves reperfusion with few complications as compared to thrombolysis and is considered the standard therapy [2–4]. However, as compared to the developed countries, the developing countries face a huge gap in the STEMI care due to limited health care infrastructure, financial constraints, poor accessibility, or non-availability, making fibrinolysis a reasonable alternative to PPCI [5–8]. The finding of less than TIMI 3 flow in the culprit vessel after fibrinolysis is in consonance with higher rates of complications such as recurrent ischemia, heart failure, and diminished salvage of myocardium which are linked to increased mortality [9], whereas the existence of TIMI 3 flow prior to primary PCI is known to improve early and late survival with favorable long-term outcomes [10, 11]. Even after fibrinolysis, a sizeable proportion of patients fails to achieve TIMI 3 flow on coronary angiography [12].

Intravascular ultrasound (IVUS) is a pivotal tool for the quantitative and qualitative assessment of the coronary atherosclerosis. Virtual histology IVUS (VH-IVUS) provides additional quantitative information on the plaque composition and characterizes atherosclerotic plaque phenotypes with an excellent correlation with histopathological examination with high predictive accuracies varying from 87.1 to 96.5% [13, 14].

Aim of the work

The purpose of the study was to demonstrate the culprit lesion plaque traits in subjects with STEMI following fibrinolysis in relation to TIMI flow on coronary angiogram.

a) Comparison of culprit lesion plaque composition by VH-IVUS in patients with TIMI 3 versus TIMI 1–2 flow in STEMI patients post fibrinolysis.

b) Identifying VH-IVUS predictors of TIMI 1–2 flow.

Methods

Study population

Between June 2017 and November 2019, a total of 495 patients with the acute coronary syndrome (ACS) to the tertiary care center were screened as part of IVUS in ACS study. A total of 342 patients were diagnosed with STEMI, of which 61 patients underwent successful fibrinolysis (ST-segment resolution by ≥ 50% from baseline elevation within 90 min and remission of clinical symptoms) and referred for coronary angiogram were included. ST-segment elevation myocardial infarction (STEMI) was determined by continuous chest pain lasting > 30 min, a new ST-segment elevation ≥ 2 mm on at least 2 contiguous electrocardiogram leads and with a rise in troponins or creatine kinase-myocardial band (CK-MB) > 3 times normal value. The identification of the culprit vessel and lesion was based on electrocardiographic changes, echocardiogram findings, and angiographic lesion morphology.

Patients with unstable angina, non-ST-segment elevation myocardial infarction (NSTEMI), severe renal dysfunction (creatinine clearance < 30 ml/minute), coronary vessels not feasible for IVUS imaging, unstable hemodynamics, Killip class III/IV, prior history of angioplasty or coronary bypass surgery, and unwilling to give consent were excluded. A written informed consent was obtained from all the patients prior to the study initiation and was approved by the Institutional Ethics Committee. All patients underwent peripheral blood examination for hemogram, renal function tests, total cholesterol along with fractions, and CK-MB levels. All the procedures were performed in conformity with the Good Clinical Practice (GCP) principles as mentioned in the Declaration of Helsinki.

Interventional procedures

The coronary angiogram and percutaneous coronary intervention were performed either from radial or femoral routes after preloading with aspirin, clopidogrel or prasugrel or ticagrelor in standard doses. Unfractionated heparin was administered intravenously at a dose of 70–100 U/kg and titration made to achieve targeted activated clotting time 250–300 s during the PCI procedure. IVUS imaging was undertaken immediately after the coronary angiogram following the administration of

200–300 mcg of intracoronary nitroglycerine using a 20-MHz, 2.9 French, Eagle Eye® Platinum RX digital IVUS catheter (Eagle Eye, Philips Volcano, San Diego, CA, USA). IVUS catheter advanced 15 mm distal to the lesion and pull back taken till the aorto-ostial junction with a motorized automatic pullback system (R-100 pull back, Volcano) at a constant speed of 0.5 mm/s before any balloon pre-dilatation.

Angiographic analysis

A cine frame rate of 15/s was adopted for performing coronary angiography and PCI. A computerized software Medis Q Angio® XA 7.3 (Medis Medical Imaging Systems, Leiden, the Netherlands) was utilized for analysis of the baseline coronary angiograms by two independent observers (VK and JRK) blinded to patient clinical data. After analyzing the baseline coronary angiograms, two groups constituted the TIMI 3 flow group and TIMI 1–2 flow groups. For the objective assessment of coronary flow, corrected thrombolysis in myocardial infarction frame count (CTFC) was utilized and cine frame count calculated by multiplication of 30 and divided by 15 to be reported as standard methods [15]. Thrombus grading from 0 to 5 as described by Gibson et al. [16] and the coronary collaterals grading by Rentrop et al. were estimated [17].

Gray-scale and virtual histology-IVUS analysis

The IVUS images obtained were recorded in digital media and archived in a DVD-ROM for offline analysis. Independent observers unbeknownst of patient characteristics or angiograms (HR and SK) undertook the analysis. The IVUS measurements and analysis were conducted in congruence with current standard methods [18]. An Echoplaque 4.3.12J computerized software (Indec Medical Systems, Inc., Santa Clara, CA, USA) was used for the analysis. The culprit lesion considered was the smallest lumen site. The image slices situated within 10 mm on either side of the lesion were the proximal and distal reference sites with the least plaque burden and no major side branch. The software automatically detects the lumen and media-adventitia interface. Manual correction if required to be confirmed and the calculated results are displayed. External elastic membrane (EEM) and lumen cross-sectional areas (CSA) were measured. Plaque and media (P&M) CSA was calculated as EEM minus lumen CSA. Plaque burden calculation was made as plaque and media CSA/EEM CSA multiplied by 100. The lesion was considered as the image slice site with the smallest lumen CSA along with the largest EEM and P&M CSA. The ratio between lesion site EEM CSA and mean of the proximal and distal reference EEM CSA was the remodeling index. Positive remodeling and negative remodeling were remodeling index > 1.05 and < 0.95, respectively [19]. A cross-sectional analysis was carried out at the minimal lumen area site. Volumetric analysis was executed over a 10-mm vascular segment with minimal luminal area site considered as center and calculations made by Simpson's rule. Virtual histology analysis images exhibit four major tissue components to be displayed: fibrous as green, fibrofatty as yellow-green, dense calcium as white, and necrotic core as red. The measurements were expressed in terms of percentage of plaque area/volumes or as absolute units. The TCFA (thin-cap fibroatheroma) was contemplated when a lesion fulfilled the said criteria in at least 3 consecutive images slices (a) confluent necrotic core ≥ 10% of plaque area in direct contact with the lumen (b) subtending an arc > 30° necrotic core (c) plaque burden of ≥ 40% [20].

Assessment of reproducibility

Intraobserver variability was assessed by analyzing a set of IVUS pullbacks twice by the same person at an interval of 3 months. The corresponding intra-class correlation coefficient (ICC) for repeated measurement was 0.81 (95% confidence interval 0.68–0.89) for lumen measurements and 0.91 (95% confidence interval 0.85–0.94) for volumes. The intraclass correlation coefficient for interobserver variability was 0.87 (95% confidence interval 0.74–0.93) for lumen measurements and 0.94 (95% confidence interval 0.88–0.97) for volume, suggestive of acceptable concordance.

Statistical analysis

A SPSS version 23.0 (SPSS, Inc., Chicago, Illinois) utilized for statistical analysis. Categorical data was presented as percentages (%) and frequencies. Continuous variables were evaluated using Shapiro-Wilk test and reported as mean with standard deviation when distributed normally and median with the 25th and 75th percentiles if skewed distribution. Bivariate analysis was done to determine associations of categorical variables within the two study groups using chi-squared test/Fisher's exact test as appropriate, and for continuous variables, we used independent t test/Mann-Whitney U test. Variables that were significant ($p < 0.05$) in the bivariate analysis were considered for multivariate analysis. We performed backward stepwise logistic regression with entry p value as 0.20 and exit p value as 0.05. The model performance was judged by Cox and Snell R^2 and classification accuracy. A p value < 0.05 was considered for statistical significance for the analyses.

Results

Patient clinical characteristics

The study comprised 61 patients for analysis. All patients received fibrinolytic therapy, and on coronary

angiogram, TIMI 3 flow was seen in 30 patients (49.1%), TIMI 2 was noted in 25 (40.9%), and TIMI 1 was observed in 6 (9.8%). The patient clinical characteristics at baseline are listed in Table 1. No difference was observed in age, hypertension, diabetes mellitus, smoking, and family history of premature coronary artery disease among the groups. Likewise, no significance was discerned in fibrinolytic agents use, symptom onset to fibrinolysis time, fibrinolysis to PCI time, and glycoprotein IIb/IIIa inhibitors use between the groups. Blood parameters such as hemoglobin, creatinine, lipids, and creatine kinase-MB were comparable among the groups. Left ventricular ejection fraction on echocardiogram was lower in the TIMI 1–2 groups in comparison to the TIMI 3 group (40.25 ± 6.34% vs 43.40 ± 4.28 %; $p = 0.027$).

Coronary angiographic and intervention procedural features

Angiographic traits and findings are listed in Table 2. The corrected TIMI frame count (CTFC) was significantly higher in the TIMI 1–2 groups as compared to the TIMI 3 group at baseline coronary angiogram (50.58 vs. 34.0; $p < 0.001$). On coronary angiography, the number of diseased vessels, ACC/AHA lesion type, TIMI thrombus grading, and collateral flow grades were comparable among the

Table 1 Baseline characteristics of the patients ($n = 61$)

Variables	TIMI flow 3 ($n = 30$)	TIMI flow 1–2 ($n = 31$)	p value
Age (years)	54.63 ± 8.98	57.10 ± 14.13	0.419
Male, *n* (%)	26 (86.7%)	26 (83.9%)	1.000
Hypertension, *n* (%)	5 (16.7%)	11 (35.5%)	0.095
Diabetes mellitus, *n* (%)	6 (20%)	7 (22.6%)	0.806
Smoking, *n* (%)	17 (56.7%)	12 (38.7%)	0.160
Family history of CAD, *n* (%)	3 (10%)	3 (9.7%)	1.000
BMI (kg/m^2)	25.4 ± 4.17	25.10 ± 3.04	0.753
BSA (m^2)	1.74 ± 0.13	1.74 ± 0.12	0.891
Symptom to thrombolysis time (hours)	4.77 ± 1.60	4.67 ± 1.47	0.809
Thrombolysis to PCI time (hours)	16.03 ± 1.37	15.71 ± 1.40	0.377
Hemoglobin (g/dL)	13.19 ± 1.85	13.31 ± 2.06	0.822
Creatinine (mg/dL)	1.1 ± 0.17	1.07 ± 0.18	0.485
Total cholesterol (mg/dL)	152.1 ± 52.85	139 ± 30.16	0.262
Triglycerides (mg/dL)	134.1 ± 47.18	119.2 ± 40.82	0.208
LDL-cholesterol (mg/dL)	100.8 ± 54.47	86.6 ± 33.42	0.247
HDL-cholesterol (mg/dL)	38.18 ± 9.05	38.84 ± 11.74	0.814
CK-MB (IU/l)	40 (36.25–53)	37 (31 − 97.75)	0.852
Ejection fraction, (%)	43.40 ± 4.28	40.25 ± 6.34	0.027
Thrombolysis, *n* (%)			0.656
Streptokinase	24 (80%)	22 (71%)	
Reteplase	6 (20%)	8 (25.8%)	
Tenecteplase	0 (0%)	1 (3.2%)	
GP IIb-IIIa inhibitor use, *n* (%)	11 (36.7%)	10 (32.3%)	0.717
Medications at admission (%)			
Antiplatelets (%)	2 (6.6%)	3 (9.6%)	1.000
Statins (%)	3 (10%)	4 (12.9%)	1.000
Beta blockers (%)	2 (6.6%)	5 (16.1%)	0.425
ACE I/ARBs (%)	4 (13.3%)	5 (16.1%)	1.000
OHAs (%)	3 (10%)	5 (16.1%)	0.707
Insulin (%)	2 (6.6%)	1 (3.2%)	0.612

Data are presented as mean ± SD, median (interquartile range), or *n* (%)

CAD coronary artery disease, *BMI* body mass index, *BSA* body surface area, *PCI* percutaneous coronary intervention, *LDL* low-density lipoprotein, *HDL* high-density lipoprotein, *CK-MB* creatine kinase-myocardial band (IU/l), *ACE I* angiotensin-converting-enzyme inhibitors, *ARB* angiotensin receptor blockers, *OHA* oral hypoglycemic agents

Table 2 Angiographic characteristics and procedure findings (n = 61)

Variables	TIMI flow 3 (n = 30)	TIMI flow 1–2 (n = 31)	p value
Culprit vessel, *n* (%)			< 0.001
LAD	13 (43.3%)	28 (90.3%)	
LCX	4 (13.3%)	1 (3.2%)	
RCA	13 (43.3%)	2 (6.5%)	
Diseased vessels, *n* (%)			
SVD	17 (56.7%)	21 (67.7%)	0.372
DVD	11 (36.7%)	6 (19.4%)	0.132
TVD	2 (6.7%)	4 (12.9%)	0.671
ACC/AHA Lesion type, *n* (%)			0.350
Type A	14 (46.7%)	13 (41.9%)	
Type B_1	9 (30%)	10 (32.3%)	
Type B_2	3 (10%)	7 (22.6%)	
Type C	4 (13.3%)	1 (3.2%)	
Baseline TIMI flow grade, *n* (%)			< 0.001
1	0 (0%)	6 (19.4%)	
2	0 (0%)	25 (80.6%)	
3	30 (100%)	0 (0%)	
Collateral flow grade (Rentrop), *n* (%)			1.000
0	30 (100%)	30 (96.8%)	
1	0 (0%)	0 (0%)	
2	0 (0%)	1 (3.2%)	
3	0 (0%)	0 (0%)	
TIMI Thrombus grading, *n* (%)			0.662
0	27 (90%)	24 (77.4%)	
1	2 (6.7%)	5 (16.1%)	
2	0 (0%)	0 (0%)	
3	1 (3.3%)	1 (3.2%)	
4	0 (0%)	1 (3.2%)	
5	0 (0%)	0 (0%)	
CTFC (baseline angiogram)	34 (28.82–42)	50.58 (44.7–61.17)	< 0.001
Quantitative coronary angiography data			
Obstruction diameter (mm)	0.86 (0.73–1.19)	0.95 (0.73–1.31)	0.549
Reference diameter (mm)	2.55 ± 0.38	2.56 ± 0.55	0.967
Diameter stenosis (%)	62.20 ± 10.15	59.40 ± 15.25	0.404
Area stenosis (%)	85.62 (78.58–91.32)	86.51 (70.29–91.07)	0.399

Data are presented as mean ± SD, median (interquartile range), or *n* (%)
LAD left anterior descending coronary artery, *LCX* left circumflex coronary artery, *RCA* right coronary artery, *SVD* single-vessel disease, *DVD* double vessel disease, *TVD* triple vessel disease, *TIMI* thrombolysis in myocardial infarction, *CTFC* corrected thrombolysis in myocardial infarction frame count, *PCI* percutaneous coronary intervention

groups. The culprit vessel was LAD in the majority of patients in the TIMI 1–2 group in contrast to the TIMI 3 group (90.3% vs. 43.3%; p < 0.001). Quantitative coronary angiography (QCA) analysis between the groups was comparable with no statistically significant difference.

Gray-scale and VH-IVUS findings

The gray-scale IVUS findings are shown in Table 3. The lesion length exhibited no significance between the groups. The estimated values in proximal and distal reference sites were no different in the groups except for the distal reference plaque burden which was higher in

Table 3 Gray-scale IVUS findings (n = 61)

Variables	TIMI flow 3 (n = 30)	TIMI flow 1–2 (n = 31)	p value
IVUS lesion length (mm)	28.95 (19.40–39.62)	25.20 (19.70–31.90)	0.299
Proximal reference			
Lumen CSA (mm^2)	8.65 (7.68–9.89)	9.86 (6.86–11.50)	0.328
EEM CSA (mm^2)	13.21 (12.03–15.76)	15.65 (11.68–18.31)	0.124
Plaque burden (%)	33.28 (27.37–38.11)	36.11 (28.37–38.74)	0.585
Distal reference			
Lumen CSA (mm^2)	5.95 ± 1.93	5.36 ± 1.65	0.212
EEM CSA (mm^2)	9.21 (6.13–11.49)	8.48 (6.43–11.56)	0.828
Plaque burden (%)	31.40 (26.93–37.27)	36.92 (33–39.91)	0.027
Average/Mean Lumen CSA (mm^2)	7.32 (6.39–8.80)	7.30 (5.60–8.59)	0.725
Average/Mean EEM CSA (mm^2)	10.95 (9.61–13.31)	12.36 (8.87–14.93)	0.213
Lesion measurements			
Lesion minimum luminal diameter (mm)	1.56 (1.5–1.63)	1.57 (1.51–1.68)	0.436
Lesion maximum luminal diameter (mm)	2.0 (1.82–2.22)	2.06 (1.82–2.25)	0.670
Lesion Lumen CSA (mm^2)	2.43 (2.15–2.71)	2.45 (2.11–2.87)	0.363
Lesion EEM CSA (mm^2)	13.91 ± 2.94	15.71 ± 3.73	0.041
Lesion (P + M) CSA (mm^2)	11.45 ± 2.85	13.13 ± 3.66	0.050
Lesion lumen area stenosis (%)	67.30 (60.39–71.18)	66.14 (55.12–71.57)	0.658
Lesion plaque burden (%)	81.65 (79.98–84.01)	82.42 (80.68–85.77)	0.306
Plaque volume (mm^3)	94.3 (72.22–120.22)	108.3 (94.10–120.20)	0.194
Remodeling index	1.21 (1.06–1.42)	1.22 (1.03–1.50)	0.946

Data are presented as mean ± SD, median (interquartile range), or n (%)
IVUS intravascular ultrasound, *EEM CSA* external elastic membrane cross-sectional area, *P + M* plaque plus media

the TIMI 1 or 2 group (36.92% vs. 31.4%; p = 0.027). Similarly, the gray-scale IVUS measurements at the minimal luminal area site (MLS) were comparable except for the lesion EEM CSA being higher in TIMI 1–2 groups in comparison to the TIMI 3 group (lesion EEM CSA: 15.71 ± 3.73 mm^2 vs. 13.91 ± 2.94 mm^2, p = 0.041). The remodeling index revealed no statistical difference (1.21 vs. 1.22; p = 0.946).

The VH-IVUS results are displayed in Figs. 1 and 2. At the minimal luminal area site (MLS), fibrous area, necrotic core area, and necrotic core percentage were notably higher in the TIMI 1–2 groups as compared to the TIMI 3 group (fibrous area: 5.83 mm^2 vs. 4.37 mm^2, p = 0.024; NC area: 0.95 mm^2 vs. 0.59 mm^2, p < 0.001, and NC percentage 11.0% vs. 7.1%, p = 0.024, respectively). Similarly, the absolute necrotic core volume and necrotic core percentage were significantly higher in the TIMI 1–2 groups in comparison to the TIMI 3 group (absolute NC volume: 8.3 mm^3 vs. 3.65 mm^3, p < 0.001; NC percentage: 9.3% vs. 6.0%, p = 0.007, respectively). Correlation of the absolute necrotic core volume and relative necrotic core percentage with the TIMI flow grades is depicted in Fig. 3. The occurrence of TCFA either single or multiple did not differ between the two groups (single TCFA: 29.0% vs. 20.7%, p = 0.462 and multiple TCFAs: 12.9% vs. 3.4%, p = 0.355, respectively).

Predictors and determinants of TIMI flow grade

The variables with significant values in the bivariate analysis were subjected further for multivariate analysis. We performed backward stepwise logistic regression and the model summary statistics, Cox and Snell R^2 was 0.303, and Nagelkerke R^2 was 0.404. The prediction accuracy for this model was 72.2%, and the overall model was significant with a p < 0.001. The variables taken for multivariate analysis were distal reference plaque burden, lesion EEM CSA, fibrous area at MLS, necrotic core area at MLS, necrotic core percentage at MLS, and necrotic core volume. On multivariate analysis, the absolute NC volume was found to be the only independent predictor of TIMI 1–2 flow post fibrinolysis in STEMI patients (odds ratio = 1.561; 95% CI 1.202–2.026, p = 0.001).

Receiver operating characteristic (ROC) curve analyses were undertaken to single out the gray-scale IVUS (distal reference plaque burden, lesion EEM CSA) and VH-IVUS (fibrous area at MLS, necrotic core area at MLS, necrotic core percentage at MLS, and absolute necrotic core volume) parameters that could assist differentiating cases of TIMI 1–2 flow from TIMI 3 flow post fibrinolysis in STEMI (Fig. 4). The absolute necrotic core volume had the best predictive value (AUC = 0.816, p < 0.001) for TIMI 1–2 flow post fibrinolysis, and the best cutoff value to predict TIMI 1 or 2 flow was > 4.5 mm^3 with a sensitivity and specificity of 79% and 61%, respectively.

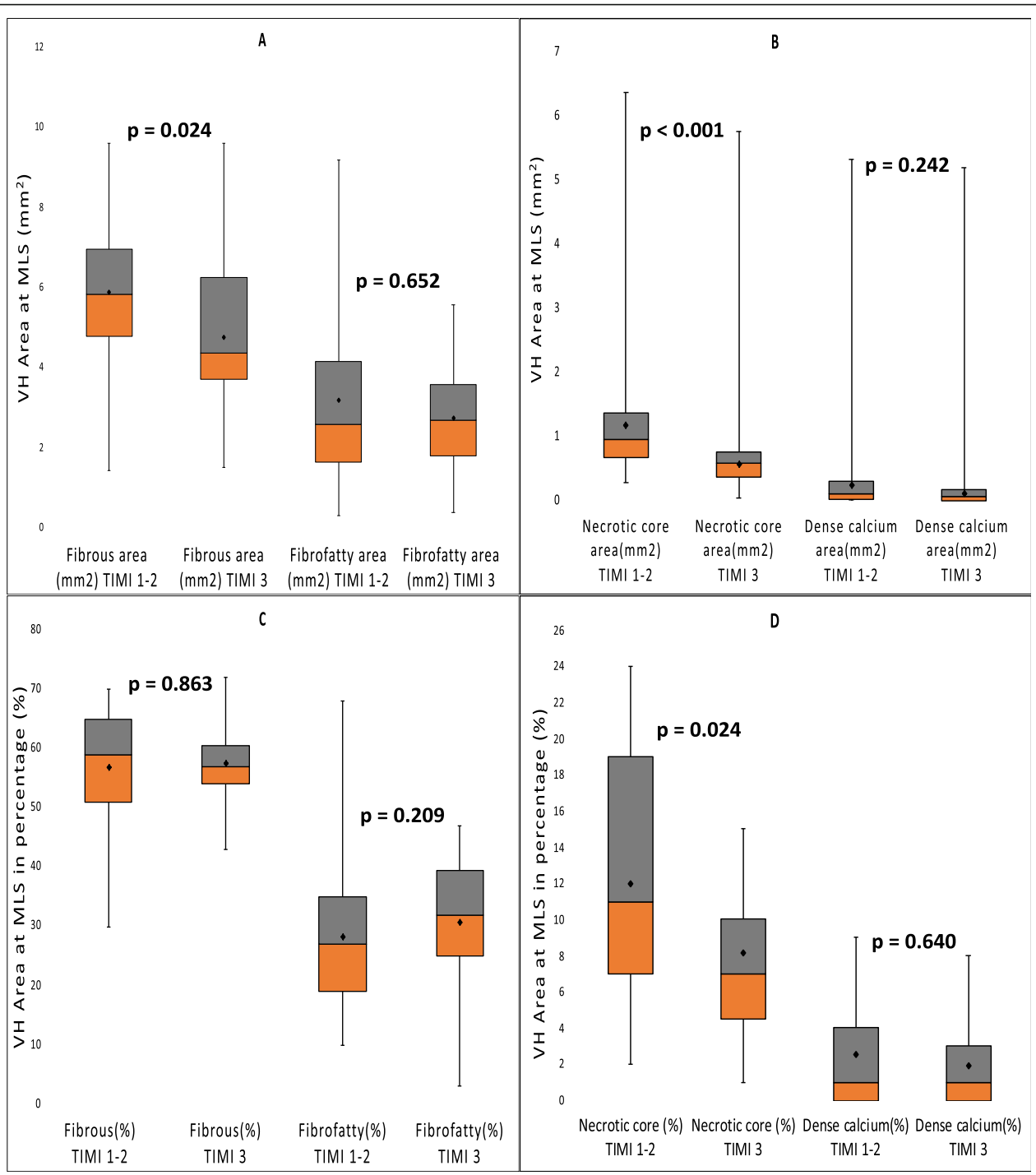

Fig. 1 The virtual histology plaque components in TIMI 1–2 and TIMI 3 groups at the minimum lumen area site (MLS). **a**, **b** The absolute plaque components and **c**, **d** the relative plaque components at the MLS

Discussion

The main findings of the current study are as follows: (i) the necrotic core component of plaque in culprit lesion in patients with STEMI after successful fibrinolysis is strongly associated with the extent of flow restoration in the culprit artery. (ii) The necrotic core volume was the only independent predictor of TIMI 1–2 flow post fibrinolysis in STEMI patients.

Atherosclerosis is a continuous process developing in arterial wall lesions with progressive accumulation of cholesterol-rich lipid deposits along with the inflammatory response [21]. The patients with ACS presents with

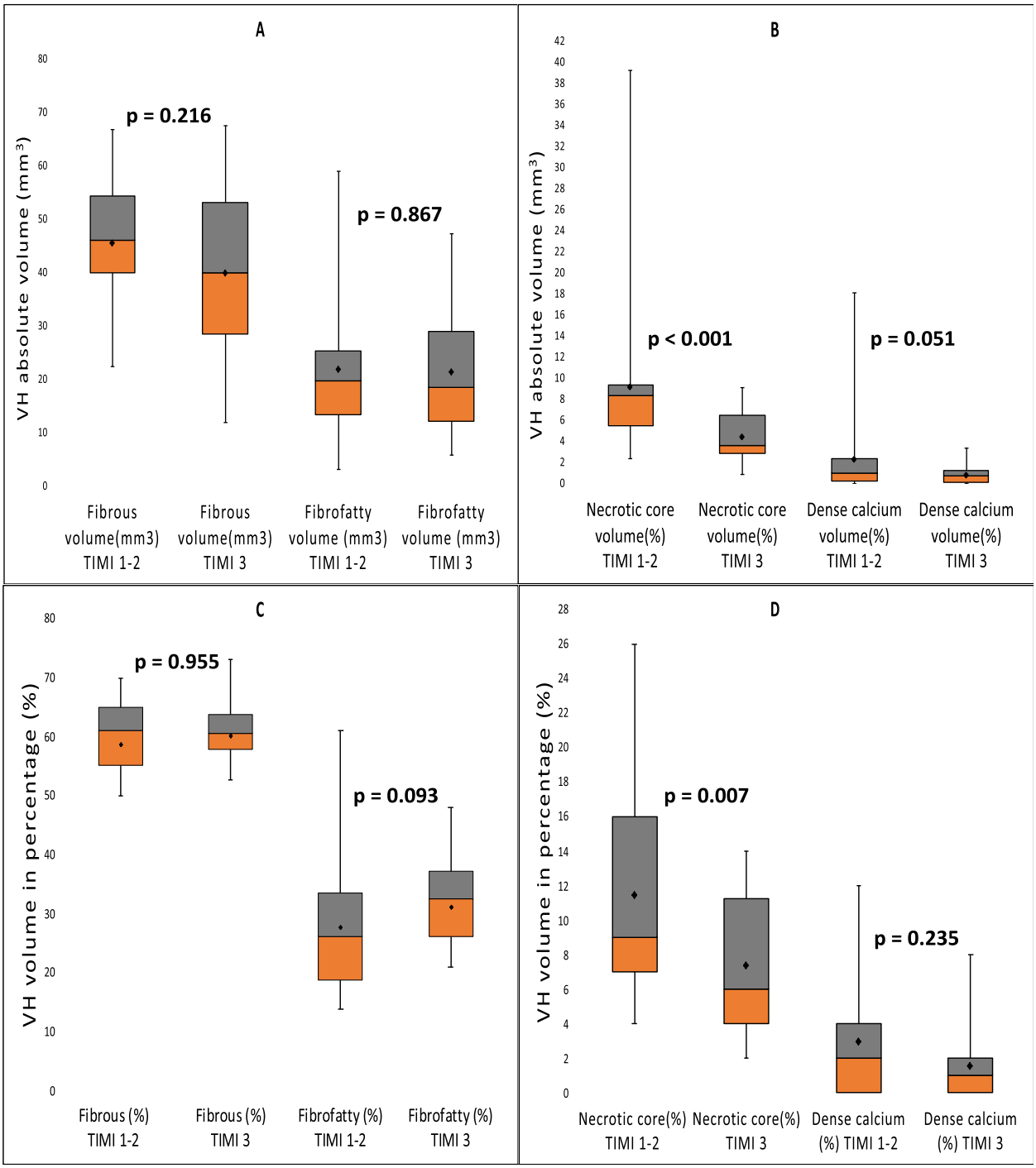

Fig. 2 The virtual histology plaque components in TIMI 1–2 and TIMI 3 groups over the segment. **a**, **b** The absolute volumes of the plaque components and **c**, **d** the relative plaque components

a varied spectrum in terms of clinical presentations, intracoronary imaging, and pathological findings [22]. Autopsy series in patients with sudden cardiac death have shown the frequency of coronary thrombus in 60% with underlying etiology detected to be plaque rupture (50–60%), plaque erosion (30–35%), and calcified nodule (2–7%) [23]. Similarly in vivo studies in ACS and STEMI using various intracoronary imaging modalities have shown the incidence of plaque rupture varying from 44 to 73% and plaque erosion in 27–44% [22].

Plaque rupture tends to occur at the weak and thinnest portion of the fibrous cap with maximum

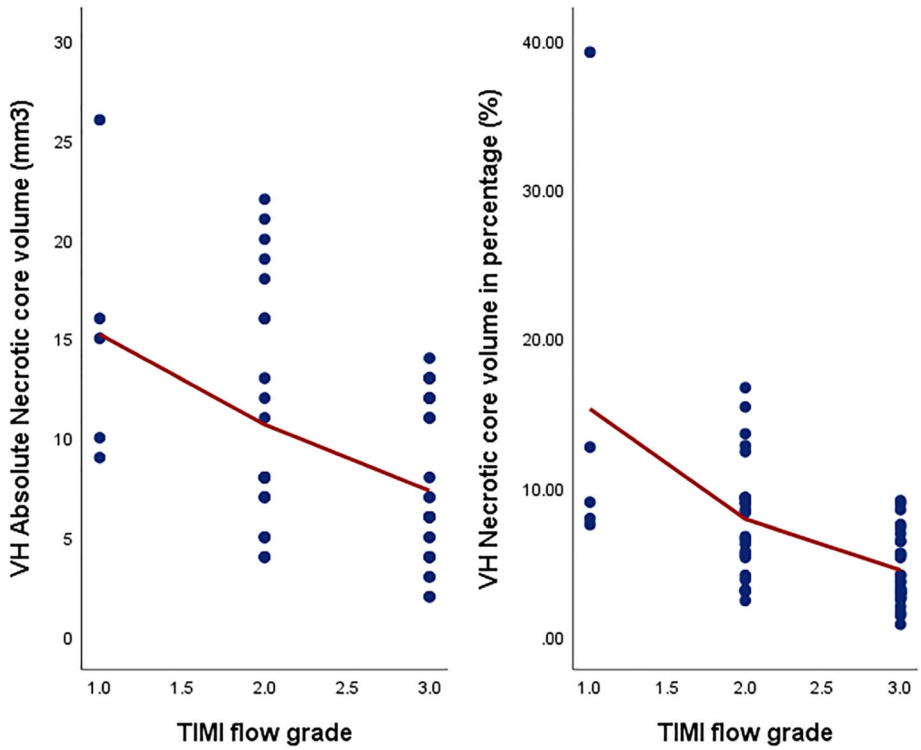

Fig. 3 Absolute necrotic core volume (left panel) and relative necrotic core percentage (right panel) in the culprit plaque, according to the post-fibrinolysis TIMI flow grade

infiltration of macrophage foam cells. The activated macrophages secrete proteolytic enzymes such as plasminogen activators, cathepsins, and matrix metalloproteinases (MMPs). Thinning of the fibrous cap involves a gradual loss of smooth muscle cells (SMCs) and degradation of collagen matrix by the infiltrating macrophages [24]. Intraplaque hemorrhage arises from vasa vasorum that infiltrates the plaque from the adventitia in response to the hypoxic environment and plays an important role in plaque vulnerability [25]. Further, it promotes inflammation and increases the level of free cholesterol leading to plaque progression and rapid necrotic core expansion leading to rupture [24, 26, 27]. The rupture of the fibrous cap exposes the lipids and tissue factors in the necrotic core to the thrombogenic factors of bloodstream [28].

Pathological studies with 2 to 3 mm interval sections revealed plaque ruptures to be frequently situated at a severely narrowed site or distal to it [24, 29, 30]. The site of plaque rupture in STEMI is usually not at the severe stenosis but is proximal to the narrowest portion. Plaque ruptures occur predominantly in the vicinity of the maximum necrotic core site and tend to be proximal to the maximum plaque burden and minimum lumen area sites. The ruptures occurred at the maximum necrotic core sites in 26% and either proximal (44%) or distal (30%) to it in the remaining 74% suggesting that the longitudinal shoulder of the maximum necrotic core site is the weakest point for plaque rupture [31]. Few other studies also have shown that the maximum necrotic core site is located proximal to the severe most stenosis [32, 33]. Therefore, the above data suggests that the analysis of the most diseased segment in and around the lesion provides useful information regarding the events linked to plaque rupture.

Autopsy series, in sudden coronary death patients revealed higher necrotic core content in culprit plaque and rupture-prone plaques [34]. The necrotic core content of the culprit lesion tends to be significantly higher in ACS as compared to stable angina and is considered as a marker of plaque vulnerability [35, 36]. Plaque rupture or erosion leads to the exposure of the necrotic core contents into the blood circulation causing activation of tissue factor and coagulation cascade, subsequently culminating into coronary thrombosis and ACS. Further, the embolization of the gruel necrotic core components along with thrombi distally leads to clogging of microcirculation potentiating coronary slow flow [37, 38].

On the gray-scale IVUS analysis, a larger plaque burden has been identified as a predictor and discriminator of coronary slow flow in ACS undergoing PCI [39, 40]. However, in our study, the plaque burden was comparable between both groups. Coronary artery remodeling is a vascular responsive phenomenon varying from positive remodeling

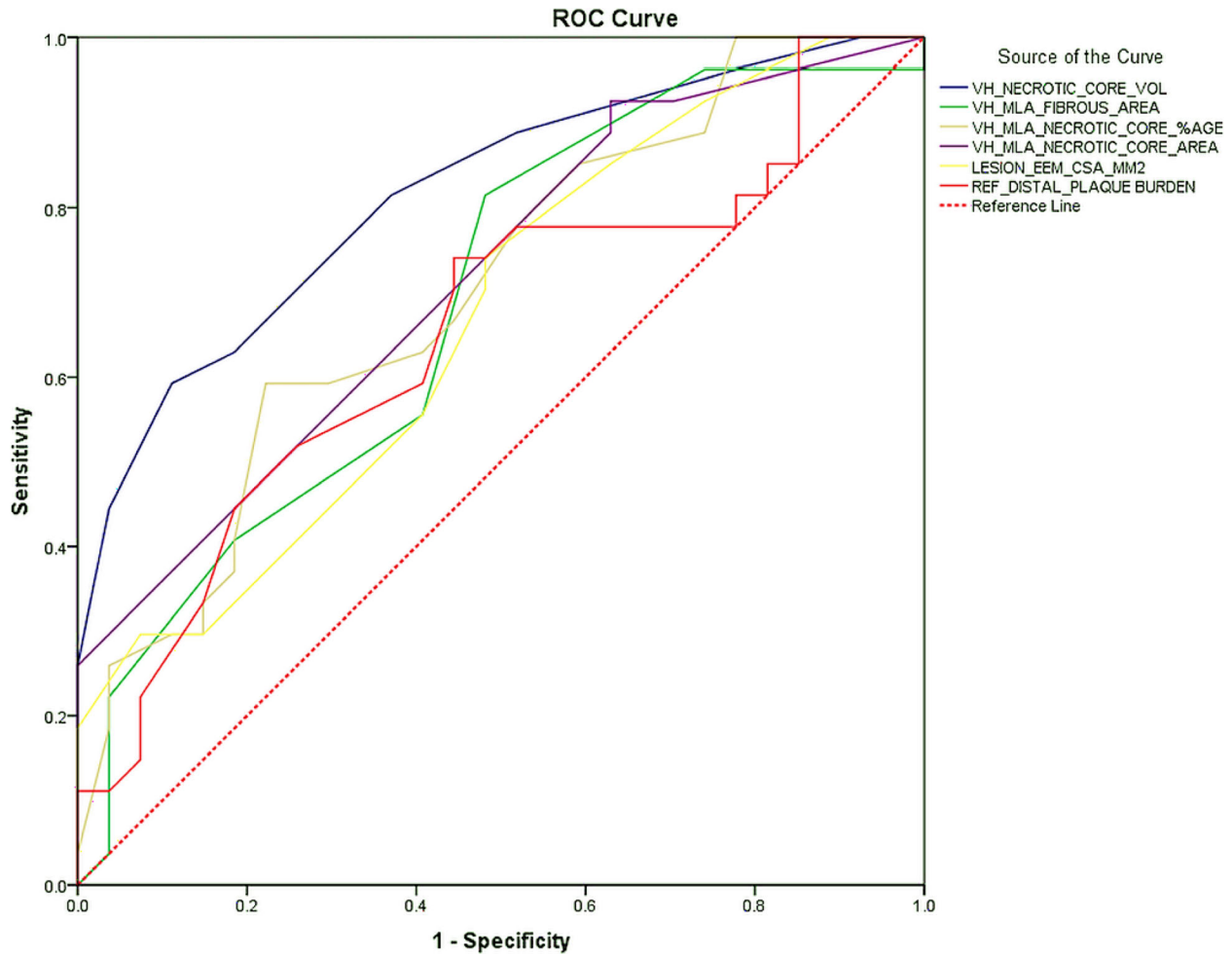

Fig. 4 Receiver operating characteristic (ROC) curves of the gray-scale and VH-IVUS parameters for the determinants of TIMI 1–2 flow

frequently observed in ACS to negative remodeling associated with stable angina [41, 42]. Positive remodeling, a marker of plaque vulnerability, with its high lipid content and macrophage count is a potential risk factor for slow flow after primary PCI and subsequent cardiac enzyme elevation [43, 44]. In our study, positive remodeling was observed in both groups with no difference.

On virtual histology, the necrotic core comprises cholesterol crystals, lipid-laden foam cells, microcalcifications, and microhemorrhages. The substantial increase of these elements noted in STEMI with plaque rupture when embolized to distal coronary microcirculation contributes to slow flow [13, 14, 45]. Giannopoulos et al. showed that the relative necrotic core percentage by VH-IVUS in culprit lesions with STEMI are linked to coronary flow restoration following thrombolysis and was significantly higher in patients with TIMI flow grades 1–2 [46]. In line with the above findings, the present study also showed a higher relative necrotic core percentage. Additionally, we also demonstrated that the absolute necrotic core volume to be higher in the TIMI 1–2 groups, a finding not observed previously [46]. Souza et al. on tissue characterization by iMAP in culprit lesions with STEMI after fibrinolysis revealed a predominance of necrotic core component demonstrating greater plaque vulnerability and instability [47]. Studies involving optical coherence tomography (OCT) in individuals presenting with ACS and STEMI have identified lipid-rich plaque content as an important risk factor for coronary slow flow after stent deployment and also a predictor of blood flow restoration after fibrinolysis for STEMI [38, 40, 48].

Coronary calcification in general indicates a long-standing atherosclerotic disease and its extent correlates with atherosclerotic plaque burden [49, 50]. The inflammatory mediators and lipid content within atherosclerotic plaque induce osteogenic differentiation of vascular smooth muscle cells resulting in atherosclerotic intimal calcification in the vessel wall [51, 52]. The effect of calcification on future coronary events appears to be biphasic

with spotty and superficial calcification being more vulnerable for plaque rupture leading to acute coronary syndrome. On the contrary, large calcium deposits were seen more frequently in stable angina pectoris suggesting that as the calcified plaques coalesce, the interface area decrease, and mechanical stability of the plaque increases [49, 52–55]. Calcification also contributes to the slow flow phenomenon after plaque rupture by distal embolization. However, previous studies have shown that dense calcium on VH-IVUS did not contribute to coronary slow flow post-fibrinolysis [46, 47]. Although in our study the dense calcium was high in the TIMI 1–2 groups, it failed to reach the statistical significance and this further substantiates the existing literature.

Study limitations

Firstly, the study was a single-center prospective observational study with the inclusion of a relatively small sample size. However, the study achieved a statistical significance to demonstrate the difference in the plaque phenotypes. Secondly, an important drawback of VH-IVUS is the inherent and inappropriate classification of thrombus as fibrous/fibrofatty phenotype. The effect of this was minimal as no difference was evident in either the fibrous or fibrofatty component over the analyzed segment among the studied groups. Further presence of thrombus underestimates the incidence of TCFAs. A long-term clinical follow-up for outcomes is warranted in these subsets.

Conclusion

The necrotic core content of the plaque in culprit lesions in patients with STEMI as assessed by VH-IVUS determines the adequacy of flow restoration after fibrinolysis. Our study demonstrates that absolute necrotic core volume was the only independent predictor of flow restoration following fibrinolysis in STEMI. The identification of increased necrotic volume as demonstrated helps in the management and prognosis of patients who might end up with less than normal coronary flow or slow flow.

Abbreviations

ACS: Acute coronary syndrome; CVD: Cardiovascular disease; CK-MB: Creatine kinase-myocardial band; CTFC: Corrected thrombolysis in myocardial infarction frame count; CSA: Cross-sectional area; DC: Dense calcium; EEM: External elastic membrane; EEM CSA: External elastic membrane cross-sectional area; IVUS: Intravascular ultrasound; MMPs: Matrix metalloproteinases; MLS: Minimal luminal area site; NC: Necrotic core; NSTEMI: Non-ST-segment elevation myocardial infarction; OCT: Optical coherence tomography; P&M CSA: Plaque and media cross-sectional area; PPCI: Primary percutaneous coronary intervention; QCA: Quantitative coronary angiography; ROC: Receiver operating characteristic; SMCs: Smooth muscle cells; STEMI: ST-segment elevation myocardial infarction; TIMI: Thrombolysis in myocardial infarction; TCFA: Thin-cap fibroatheroma; VH-IVUS: Virtual histology intravascular ultrasound

Acknowledgements

We thank the secretarial assistance of Mrs. Deepika and Mr. Jeevan Lal.

Authors' contributions

SR designed the study, helped in the data collection, participated in the coordination, performed the statistical analysis, wrote the paper, and finalized the final draft of the manuscript. RRK, VR, and JK participated in the data collection, literature reviewing, writing the paper, and statistical analysis. JRK, VK, HR, and SK contributed to the data collection. DD, AK, NK, and AG helped in preparing the manuscript. The authors have read and approved the final submitted manuscript.

Funding

None

Availability of data and materials

All data used and analyzed in the current study were available in the institute. These data are available from the corresponding author on reasonable request.

Ethics approval and consent to participate

The study was approved by the Institutional Ethics Committee of the Government Medical College and Hospital, reference number IEC/2017/12 dated 04.05.17. All procedures performed in the study involving human participants were in accordance with the ethical standards of the institutional and/or national research committee and with the 1964 Helsinki Declaration and its later amendments or comparable ethical standards. A written informed consent was obtained from all individual participants prior to their inclusion in the study.

Consent for publication

Not applicable

Competing interests

The authors declare that they have no competing interests.

Author details

[1]Department of Cardiology, Government Medical College and Hospital, Sector 32, Chandigarh 160030, India. [2]Department of Neurology, Post Graduate Institute of Medical Education and Research (PGIMER), Chandigarh 160012, India.

Received: 17 September 2020 Accepted: 27 November 2020
Published online: 09 December 2020

References

1. Gersh BJ, Sliwa K, Mayosi BM, Yusuf S (2010) Novel therapeutic concepts: the epidemic of cardiovascular disease in the developing world: global implications. Eur Heart J. 31(6):642–648
2. Subban V, Lakshmanan A, Victor SM, Pakshirajan B, Udayakumaran K, Gnanaraj A et al (2014) Outcome of primary PCI - an Indian tertiary care center experience. Indian Heart J. 66(1):25–30
3. Alexander T, Mehta S, Mullasari A, Nallamothu BK (2012) Systems of care for ST-elevation myocardial infarction in India. Heart. 98(1):15–17
4. Keeley EC, Boura JA, Grines CL (2003) Primary angioplasty versus intravenous thrombolytic therapy for acute myocardial infarction: a quantitative review of 23 randomised trials. Lancet. 361(9351):13–20
5. Alexander T, Mullasari AS, Kaifoszova Z, Khot UN, Nallamothu B, Ramana RG et al (2015) Framework for a National STEMI Program: consensus document developed by STEMI INDIA, Cardiological Society of India and Association Physicians of India. Indian Heart J. 67(5):497–502
6. Xavier D, Pais P, Devereaux PJ, Xie C, Prabhakaran D, Reddy KS et al (2008) Treatment and outcomes of acute coronary syndromes in India (CREATE): a prospective analysis of registry data. Lancet. 371(9622):1435–1442
7. Negi PC, Merwaha R, Panday D, Chauhan V, Guleri R (2016) Multicenter HP ACS Registry. Indian Heart J. 68(2):118–127
8. Mohanan PP, Mathew R, Harikrishnan S, Krishnan MN, Zachariah G, Joseph J et al (2013) Presentation, management, and outcomes of 25 748 acute coronary syndrome admissions in Kerala, India: results from the Kerala ACS Registry. Eur Heart J. 34(2):121–129

9. Lincoff AM, Topol EJ, Califf RM, Sigmon KN, Lee KL, Ohman EM et al (1995) Significance of a coronary artery with thrombolysis in myocardial infarction grade 2 flow "patency" (outcome in the thrombolysis and angioplasty in myocardial infarction trials). Thrombolysis and Angioplasty in Myocardial Infarction Study Group. Am J Cardiol. 75(14):871–876
10. Stone GW, Cox D, Garcia E, Brodie BR, Morice MC, Griffin J et al (2001) Normal flow (TIMI-3) before mechanical reperfusion therapy is an independent determinant of survival in acute myocardial infarction: analysis from the primary angioplasty in myocardial infarction trials. Circulation. 104(6):636–641
11. Zeymer U, Huber K, Fu Y, Ross A, Granger C, Goldstein P et al (2012) Impact of TIMI 3 patency before primary percutaneous coronary intervention for ST-elevation myocardial infarction on clinical outcome: results from the ASSENT-4 PCI study. Eur Heart J Acute Cardiovasc Care. 1(2):136–142
12. Barbagelata NA, Granger CB, Oqueli E, Suarez LD, Borruel M, Topol EJ et al (1997) TIMI grade 3 flow and reocclusion after intravenous thrombolytic therapy: a pooled analysis. Am Heart J. 133(3):273–282
13. Hong YJ, Jeong MH, Choi YH, Ko JS, Lee MG, Kang WY et al (2011) Impact of plaque components on no-reflow phenomenon after stent deployment in patients with acute coronary syndrome: a virtual histology-intravascular ultrasound analysis. Eur Heart J. 32(16):2059–2066
14. Nasu K, Tsuchikane E, Katoh O, Vince DG, Virmani R, Surmely JF et al (2006) Accuracy of in vivo coronary plaque morphology assessment: a validation study of in vivo virtual histology compared with in vitro histopathology. J Am Coll Cardiol. 47(12):2405–2412
15. Gibson CM, Cannon CP, Daley WL, Dodge JT Jr, Alexander B Jr, Marble SJ et al (1996) TIMI frame count: a quantitative method of assessing coronary artery flow. Circulation. 93(5):879–888
16. Gibson CM, de Lemos JA, Murphy SA, Marble SJ, McCabe CH, Cannon CP et al (2001) Combination therapy with abciximab reduces angiographically evident thrombus in acute myocardial infarction: a TIMI 14 substudy. Circulation. 103(21):2550–2554
17. Rentrop KP, Cohen M, Blanke H, Phillips RA (1985) Changes in collateral channel filling immediately after controlled coronary artery occlusion by an angioplasty balloon in human subjects. J Am Coll Cardiol. 5(3):587–592
18. Mintz GS, Nissen SE, Anderson WD, Bailey SR, Erbel R, Fitzgerald PJ et al (2001) American College of Cardiology Clinical Expert Consensus Document on Standards for Acquisition, Measurement and Reporting of Intravascular Ultrasound Studies (IVUS). A report of the American College of Cardiology Task Force on Clinical Expert Consensus Documents. J Am Coll Cardiol. 37(5):1478–1492
19. Rodriguez-Granillo GA, Serruys PW, Garcia-Garcia HM, Aoki J, Valgimigli M, van Mieghem CA et al (2006) Coronary artery remodelling is related to plaque composition. Heart. 92(3):388–391
20. Maehara A, Cristea E, Mintz GS, Lansky AJ, Dressler O, Biro S et al (2012) Definitions and methodology for the grayscale and radiofrequency intravascular ultrasound and coronary angiographic analyses. JACC Cardiovasc Imaging. 5(3 Suppl):S1–S9
21. Insull W Jr (2009) The pathology of atherosclerosis: plaque development and plaque responses to medical treatment. Am J Med. 122(1 Suppl):S3–S14
22. Partida RA, Libby P, Crea F, Jang IK (2018) Plaque erosion: a new in vivo diagnosis and a potential major shift in the management of patients with acute coronary syndromes. Eur Heart J. 39(22):2070–2076
23. Virmani R, Burke AP, Farb A, Kolodgie FD (2006) Pathology of the vulnerable plaque. J Am Coll Cardiol. 47(8 Suppl):C13–C18
24. Bentzon JF, Otsuka F, Virmani R, Falk E (2014) Mechanisms of plaque formation and rupture. Circ Res. 114(12):1852–1866
25. Finn AV, Nakano M, Narula J, Kolodgie FD, Virmani R (2010) Concept of vulnerable/unstable plaque. Arterioscler Thromb Vasc Biol. 30(7):1282–1292
26. Kolodgie FD, Gold HK, Burke AP, Fowler DR, Kruth HS, Weber DK et al (2003) Intraplaque hemorrhage and progression of coronary atheroma. N Engl J Med. 349(24):2316–2325
27. Toutouzas K, Benetos G, Karanasos A, Chatzizisis YS, Giannopoulos AA, Tousoulis D (2015) Vulnerable plaque imaging: updates on new pathobiological mechanisms. Eur Heart J. 36(45):3147–3154
28. Otsuka F, Yasuda S, Noguchi T, Ishibashi-Ueda H (2016) Pathology of coronary atherosclerosis and thrombosis. Cardiovasc Diagn Ther. 6(4):396–408
29. Falk E, Shah PK, Fuster V (1995) Coronary plaque disruption. Circulation. 92(3):657–671
30. Alfonso F, Virmani R (2011) New morphological insights on coronary plaque rupture: bridging the gap from anatomy to clinical presentation? JACC Cardiovasc Interv. 4(1):83–86
31. Zheng G, Li Y, Takayama T, Nishida T, Sudo M, Haruta H et al (2016) The spatial distribution of plaque vulnerabilities in patients with acute myocardial infarction. PLoS One. 11(3):e0152825
32. de Graaf MA, van Velzen JE, de Graaf FR, Schuijf JD, Dijkstra J, Bax JJ et al (2013) The maximum necrotic core area is most often located proximally to the site of most severe narrowing: a virtual histology intravascular ultrasound study. Heart Vessels. 28(2):166–172
33. Kaple RK, Maehara A, Sano K, Missel E, Castellanos C, Tsujita K et al (2009) The axial distribution of lesion-site atherosclerotic plaque components: an in vivo volumetric intravascular ultrasound radio-frequency analysis of lumen stenosis, necrotic core and vessel remodeling. Ultrasound Med Biol. 35(4):550–557
34. Virmani R, Kolodgie FD, Burke AP, Farb A, Schwartz SM (2000) Lessons from sudden coronary death: a comprehensive morphological classification scheme for atherosclerotic lesions. Arterioscler Thromb Vasc Biol. 20(5): 1262–1275
35. Ivanovic M, Rancic M, Rdzanek A, Filipjak KJ, Opolski G, Cvetanovic J (2013) Virtual histology study of atherosclerotic plaque composition in patients with stable angina and acute phase of acute coronary syndromes without ST segment elevation. Srp Arh Celok Lek. 141(5-6):308–314
36. Hong MK, Mintz GS, Lee CW, Suh J, Kim JH, Park DW et al (2007) Comparison of virtual histology to intravascular ultrasound of culprit coronary lesions in acute coronary syndrome and target coronary lesions in stable angina pectoris. Am J Cardiol. 100(6):953–959
37. Badimon L, Vilahur G (2014) Thrombosis formation on atherosclerotic lesions and plaque rupture. J Intern Med. 276(6):618–632
38. Kotani J, Nanto S, Mintz GS, Kitakaze M, Ohara T, Morozumi T et al (2002) Plaque gruel of atheromatous coronary lesion may contribute to the no-reflow phenomenon in patients with acute coronary syndrome. Circulation. 106(13):1672–1677
39. Iijima R, Shinji H, Ikeda N, Itaya H, Makino K, Funatsu A et al (2006) Comparison of coronary arterial finding by intravascular ultrasound in patients with "transient no-reflow" versus "reflow" during percutaneous coronary intervention in acute coronary syndrome. Am J Cardiol. 97(1):29–33
40. Soeda T, Higuma T, Abe N, Yamada M, Yokoyama H, Shibutani S et al (2017) Morphological predictors for no reflow phenomenon after primary percutaneous coronary intervention in patients with ST-segment elevation myocardial infarction caused by plaque rupture. Eur Heart J Cardiovasc Imaging. 18(1):103–110
41. Schoenhagen P, Ziada KM, Kapadia SR, Crowe TD, Nissen SE, Tuzcu EM. Extent and direction of arterial remodeling in stable versus unstable coronary syndromes: an intravascular ultrasound study. Circulation. 2000; 101(6):598-603.
42. Hong YJ, Jeong MH, Choi YH, Ko JS, Lee MG, Kang WY et al (2009) Positive remodeling is associated with more plaque vulnerability and higher frequency of plaque prolapse accompanied with post-procedural cardiac enzyme elevation compared with intermediate/negative remodeling in patients with acute myocardial infarction. J Cardiol. 53(2):278–287
43. Varnava AM, Mills PG, Davies MJ (2002) Relationship between coronary artery remodeling and plaque vulnerability. Circulation. 105(8):939–943
44. Watanabe T, Nanto S, Uematsu M, Ohara T, Morozumi T, Kotani J et al (2003) Prediction of no-reflow phenomenon after successful percutaneous coronary intervention in patients with acute myocardial infarction: intravascular ultrasound findings. Circ J. 67(8):667–671
45. Reddy S, Rao KR, Kashyap JR, Kadiyala V, Reddy H, Malhotra S et al (2020) Impact of plaque burden and composition on coronary slow flow in ST-segment elevation myocardial infarction undergoing percutaneous coronary intervention: intravascular ultrasound and virtual histology analysis. Acta Cardiol.:1–11
46. Giannopoulos G, Pappas L, Synetos A, Hahalis G, Raisakis K, Papadimitriou C et al (2014) Association of virtual histology characteristics of the culprit plaque with post-fibrinolysis flow restoration in ST-elevation myocardial infarction. Int J Cardiol. 174(3):678–682
47. CFd S, Maehara A, Lima E, LdFC G, Carvalho AC, CMR A et al (2014) Morphological and tissue characterization of culprit lesions in patients with ST-segment elevation myocardial infarction after thrombolytic therapy. Analysis with Gray scale Intravascular Ultrasound and iMAP^{TM} Technology. Rev Bras Cardiol Invasiva 22(3):225–232

48. Toutouzas K, Tsiamis E, Karanasos A, Drakopoulou M, Synetos A, Tsioufis C et al (2010) Morphological characteristics of culprit atheromatic plaque are associated with coronary flow after thrombolytic therapy: new implications of optical coherence tomography from a multicenter study. JACC Cardiovasc Interv. 3(5):507–514
49. Ehara S, Kobayashi Y, Yoshiyama M, Shimada K, Shimada Y, Fukuda D et al (2004) Spotty calcification typifies the culprit plaque in patients with acute myocardial infarction: an intravascular ultrasound study. Circulation. 110(22):3424–3429
50. Sangiorgi G, Rumberger JA, Severson A, Edwards WD, Gregoire J, Fitzpatrick LA et al (1998) Arterial calcification and not lumen stenosis is highly correlated with atherosclerotic plaque burden in humans: a histologic study of 723 coronary artery segments using nondecalcifying methodology. J Am Coll Cardiol. 31(1):126–133
51. Madhavan MV, Tarigopula M, Mintz GS, Maehara A, Stone GW, Genereux P (2014) Coronary artery calcification: pathogenesis and prognostic implications. J Am Coll Cardiol. 63(17):1703–1714
52. Abedin M, Tintut Y, Demer LL (2004) Vascular calcification: mechanisms and clinical ramifications. Arterioscler Thromb Vasc Biol. 24(7):1161–1170
53. Mizukoshi M, Kubo T, Takarada S, Kitabata H, Ino Y, Tanimoto T et al (2013) Coronary superficial and spotty calcium deposits in culprit coronary lesions of acute coronary syndrome as determined by optical coherence tomography. Am J Cardiol. 112(1):34–40
54. Ehara S, Kobayashi Y, Yoshiyama M, Ueda M, Yoshikawa J (2006) Coronary artery calcification revisited. J Atheroscler Thromb. 13(1):31–37
55. Sakaguchi M, Hasegawa T, Ehara S, Matsumoto K, Mizutani K, Iguchi T et al (2016) New insights into spotty calcification and plaque rupture in acute coronary syndrome: an optical coherence tomography study. Heart Vessels. 31(12):1915–1922

Publisher's Note

Indian Pacing and Electrophysiology Journal 20 (2020) 78–80

Contents lists available at ScienceDirect

Indian Pacing and Electrophysiology Journal

journal homepage: www.elsevier.com/locate/IPEJ

Selective left bundle branch pacing for pediatric complete heart block

Shunmuga Sundaram Ponnusamy*, Giridhar Muthu, Dasarath Bopanna

Department of Cardiology, Velammal Medical College Hospital and Research Institute, Madurai, India

ARTICLE INFO

Article history:
Received 28 October 2019
Received in revised form
15 December 2019
Accepted 15 December 2019
Available online 19 December 2019

Keywords:
Congenital CHB
Physiological pacing
Left bundle pacing
Left ventricular activation time
LV synchrony

ABSTRACT

Traditionally Right Ventricle has been the preferred site of pacing for the management of symptomatic brady-arrhythmias. The deleterious effect of chronic RV pacing has been shown by several studies. This has generated interest into a novel pacing strategy called physiological pacing wherein the His bundle or the left bundle is paced directly with 4.1 F pacing lead. Herewith we are reporting a case of congenital complete heart block in a 13-year-old child for whom selective left bundle branch pacing was done. This physiological pacing will ensure a synchronized contraction of the ventricles thereby avoiding the deleterious effect of RV pacing.

1. Introduction

Congenital complete heart block can manifest at any age. As per ACC/AHA guidelines any symptomatic complete heart block needs permanent pacemaker implantation. Long term effects of chronic right ventricular pacing are well known which includes atrial arrhythmias, left ventricular dysfunction and recurrent heart failure [1]. Since these are young patients who need pacing for a long time it is good to look for alternative sites other than routine right ventricular apex. With recent developments in the field of physiological pacing it is better to consider this modality of pacing for young patients who need long term pacing. Several studies have confirmed the beneficial effect of permanent his bundle pacing (HBP). But there are certain limitations with HBP – high threshold, early battery depletion and risk of lead revision due to rise in threshold/dislodgement [2]. Selective left bundle pacing can overcome these limitation as it provides excellent threshold with good lead stability [3].

2. Case report

A 13 years old female child came to us for the management of bradycardia with recurrent presyncope. On examination she was diagnosed to have congenital complete heart block. Electrocardiography showed atrio-ventricular (AV) dissociation with ventricular rate of 40 beats per minute (QRS duration 80 ms) (Fig. 1). Echocardiography showed mildly dilated Right atrium and ventricle with normal LV systolic function. 24 hours Holter monitoring showed minimum heart rate of around 35 beats per minute. Since she was symptomatic she was planned for permanent pacemaker implantation. In view of young age and requirement of long term pacing an option of physiological pacing was given.

After obtaining informed consent procedure was done under intravenous sedation. Twelve lead electrocardiography and intracardiac electrograms were continuously recorded using St Jude electrophysiology system. A quadripolar (St Jude Medical) catheter was placed via right femoral vein access to get His bundle signals. Baseline study showed AV dissociation with AH block. HV interval was 37 ms (Fig. 2A). After obtaining two separate extra thoracic left subclavian venous puncture C315 His Sheath (Medtronic, Mineapolis, MN) was used to map left bundle area. The lumen less 4.1 F 3830 Selectsecure lead (Medtronic, Mineapolis, MN) was introduced and unipolar mapping was done with the help of EP system. At a region 1 cm below the distal end of the His bundle catheter unipolar pacing showed “W” pattern. The lead was rotated rapidly for 4 turns to get deep into the septum. Pacing there showed typical right bundle branch delay with QRS duration of 97 ms. The paced left ventricular activation time (LVAT in lead V5) was 51 ms (Fig. 2B). Pacing from high output to low output showed non-selective to selective left bundle capture. Native rhythm showed sharp left bundle potential preceding local Ventricular electrogram

* Corresponding author.
E-mail address: shunmuga.pgi@gmail.com (S.S. Ponnusamy).
Peer review under responsibility of Indian Heart Rhythm Society.

https://doi.org/10.1016/j.ipej.2019.12.012

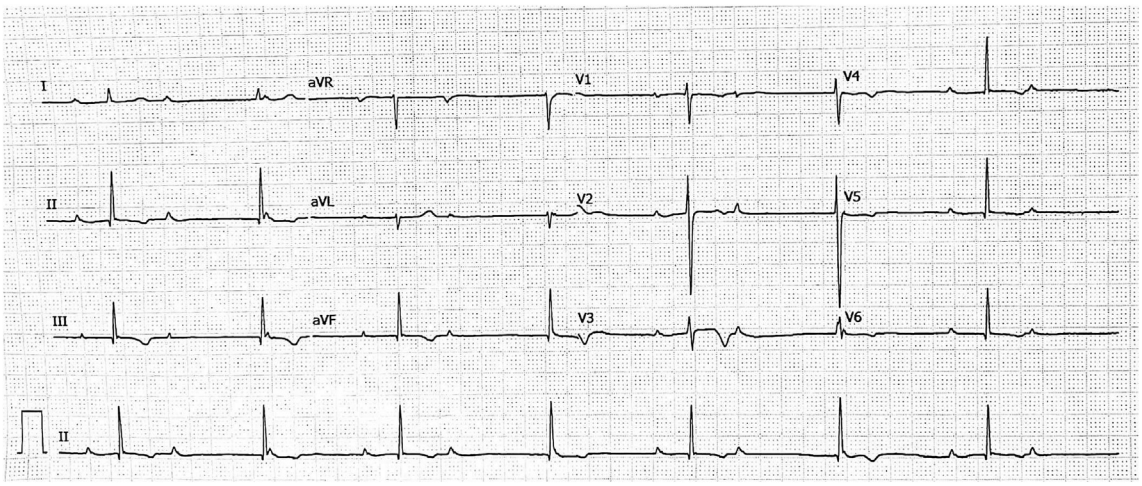

Fig. 1. Baseline ECG showing complete heart block with narrow QRS escape.

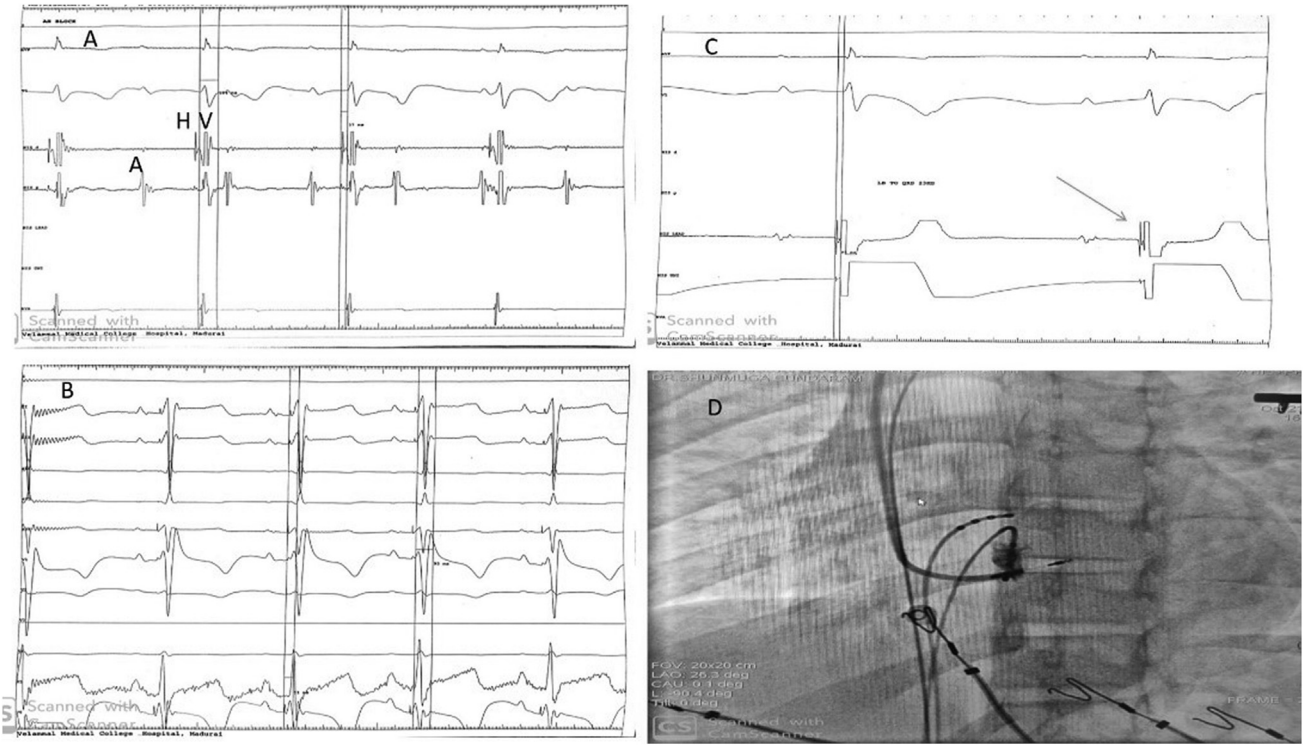

Fig. 2. A) Baseline intracardiac electrogram showing AH bock with normal HV interval. B) Left bundle branch paced QRS duration of 97 ms and LVAT of 51 ms. C) 3830 Selectsecure lead electrogram showing giant left bundle potential with LBP to QRS duration of 23 ms. D) Sheath angiography in LAO view showing the depth of the lead (~9mm).

(Fig. 2C). The left bundle to local ventricular electrogram interval was 23 ms. All features favored selective left bundle capture. The local R wave was 10 mV and pacing threshold was 0.3V at 0.6 ms pulse width. Sheath angiography was taken in Left anterior oblique (LAO) view which showed a lead depth of around 9 mm (Fig. 2D). Subsequently atrial lead was placed at right atrial appendage. Both the leads were connected to a dual chamber Medtronic pulse generator. Final paced ECG showed right bundle branch delay pattern with QRS duration of 96ms (Fig. 3). Patient recovered well and discharged on the 4th post procedure day.

3. Discussion

Cardiac pacing remains the definitive therapy for symptomatic bradyarrhythmias. Since chronic RV pacing has produced significant hemodynamic problems alternative pacing sites were considered which includes right ventricular septum, Right ventricular outflow tract and left ventricle. Eventually the concept of permanent his bundle pacing was described by Desmukh et al. [4]. Subsequently with further insights into the anatomy of the conduction system selective pacing of the left bundle branch was attempted by Huang et al. [3]. Since the lead is placed deep into the interventricular septum the pacing parameters are good with good lead stability.

Selective left bundle pacing can be done to treat any symptomatic brady-arrhythmia. 3830 Medtronic selectsecure MRI lead is used and it is guided deep into the septum with the help of C315 sheath. The paced QRS morphology and pacing impedance should

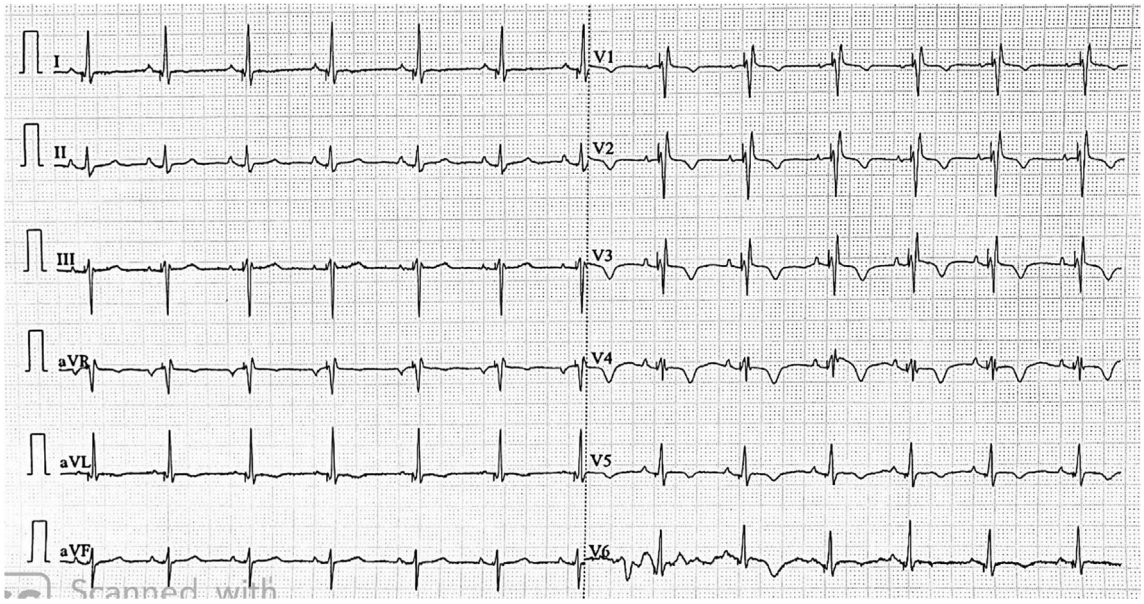

Fig. 3. Final selective left bundle branch paced QRS showing right bundle branch delay pattern with duration of 96 ms.

be monitored as the lead goes into the septum to avoid perforation. With excellent pacing parameters, this modality is considered as an alternative to cardiac resynchronization therapy for patients with dilated cardiomyopathy with left bundle branch block and LV dysfunction. Studies have shown promising results with significant improvement in NYHA functional class and LV ejection fraction [5].

Any patient requiring pacing for more than 40% are at risk of developing chronic RV pacing related complication. Congenital complete heart block is a specific subset of patients who require long term pacing from the early part of their life. Hence physiological pacing must be considered in this subset, it can be either His bundle pacing or left bundle branch pacing. This is going to activate normal cardiac conduction system and provide synchronized contraction of ventricles. With further insights from randomized controlled trials, physiological pacing (His bundle/Left bundle) might come as an effective alternative to cardiac resynchronization therapy in non-ischemic dilated cardiomyopathy patients.

Declaration of competing interest

We have no conflicts of interest to disclose.

References

[1] Wilkoff BL, Cook JR, et al. Dual chamber pacing or ventricular backup pacing in patients with an implantable defibrillator – the Dual Chamber and VVI implantable defibrillator (DAVID) Trial. J Am Med Assoc 2002;288:3115–23.
[2] Huang W, Su L, Wu S, et al. Long term outcomes of his bundle pacing in patients with heart failure with left bundle branch block. Heart 2019 Jan;105(2):137–43.
[3] Huang W, Su L, Wu S, et al. A novel pacing strategy with low and stable output: pacing the left bundle branch immediately beyond the conduction block. Can J Cardiol 2017;33(12):1731–6.
[4] Desmukh P, Casavant DA, et al. Permanent direct his bundle pacing: a novel approach to cardiac pacing in patients with hormal his purkinje activation. Circulation 2000;101(8):869–77.
[5] Zhang Weiwei, Huang Jingjuan, et al. Cardiac resynchronization therapy by left bundle branch area pacing in heart failure patients with left bundle branch block. Heart Rhythm 2019. Sep 9. pii: S1547 – 5271 (Epub ahead of print).